Measurement and mechanisms of complement-induced neutrophil dysfunction

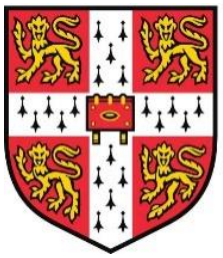

UNIVERSITY OF CAMBRIDGE

This dissertation is submitted for the degree of Doctor of Philosophy

Alexander James Telfer Wood

Emmanuel College

November 2018

Abstract: Measurement and mechanisms of complement-induced neutrophil dysfunction

Dr Alexander JT Wood

Critical illness is an aetiologically and clinically heterogeneous syndrome that is characterised by organ failure and immune dysfunction. Mortality in critically ill patients is driven by inflammation-associated organ damage and a profound vulnerability to nosocomial infection. Both factors are influenced by the complement protein C5a, released by unbridled activation of the complement system during critical illness. C5a suppresses antimicrobial functions of key immune cells, in particular the neutrophil, and this suppression has been shown to be associated with poorer outcomes amongst critically ill adults. The intracellular signalling pathways which mediate C5a-induced neutrophil dysfunction are incompletely understood, and scalable tools with which to assess immune cell dysfunction in patients are lacking. This thesis aimed to develop tools with which to assess neutrophil function and delineate intracellular signalling pathways driving C5a-induced impairment.

Neutrophils were isolated from healthy volunteer blood and functions (priming, phagocytosis and reactive oxygen species production) were assessed using light microscopy, confocal microscopy and flow cytometry. A new assay was developed using an Attune Nxt™ acoustic focusing cytometer (Life Technologies) which allowed the rapid assessment of multiple neutrophil functions in small samples of unlysed, minimally-manipulated human whole blood. Complete proteomes and phosphoproteomes of phagocytosing neutrophils were obtained from four healthy donors pre-treated with C5a or vehicle control.

Several key insights were gained from this work and are summarised here. Firstly, C5a was found to induce a prolonged (greater than seven hours) impairment of neutrophil phagocytosis. This defect was found to be preventable by previous or concurrent phagocytosis, indicating common signalling mechanisms. Secondly, a novel assay was developed which allows the rapid assessment of multiple neutrophil functions in less than2 mL of whole blood, and this assay can feasibly be applied in clinical settings. Thirdly, cell-surface expression of the C5a receptor was found to be markedly decreased during phagocytosis, and this decrease was not mediated by protease activity. Finally, unbiased proteomics quantified 4859 proteins and 2712 phosphoproteins respectively. This quantification is the deepest profile of the human neutrophil proteome published to date, and has revealed novel insights into the mechanisms of C5a-induced neutrophil dysfunction and phagocytosis.

Declaration

This dissertation is the result of my own work and includes nothing which is the outcome of work done in collaboration except as declared in the Preface and specified in the text. I thank Dr Arlette Vassallo, Dr Andrew Conway Morris and Carmelo Zinnato for their assistance in generating data presented in this thesis. Their specific contributions have been acknowledged in the relevant Results sections and figure legends. I have published sections of Chapter I as a first-author review article in the European Journal of Clinical Investigation, the citation for which is listed in Appendices.

This dissertation is not substantially the same as any that I have submitted, or, is being concurrently submitted for a degree or diploma or other qualification at the University of Cambridge or any other University or similar institution except as declared in the Preface and specified in the text. I further state that no substantial part of my dissertation has already been submitted, or, is being concurrently submitted for any such degree, diploma or other qualification at the University of Cambridge or any other University or similar institution except as declared in the Preface and specified in the text. It does not exceed the prescribed word limit set by the Degree Committee of the Department of Medicine.

Alexander JT Wood
5th November 2018

Acknowledgements

Dark. Cold. Wet. A classic Cambridge day in December. I found myself peering down a microscope at hundreds, perhaps even thousands, of notoriously pernicious and irritable cells I now confidently call neutrophils. My task? Count the number of yeast balls inside *each* and *every* one. It was on that day I wondered what on earth had motivated me to leave a great job, in a warm country, and come to the UK. It was a good thing I did though; my mind has been opened to a whole new world of possibilities and I've met some fantastic people, some of whom I would like to thank below.

Firstly, I must thank the staff of the NIHR Cambridge BRC Cell Phenotyping Hub, specifically Esther Perez Garcia, Natalia Savinykh, Simon McCallum and Alex Hatton for their invaluable assistance and patience in training me to use flow cytometers and confocal microscopes. Marie Ruchaud-Sparagano, Jonathon Scott and John Simpson at the University of Newcastle provided invaluable assistance and advice in establishing assays of phagocytosis, especially when they weren't working! I'd like to acknowledge Karen Anderson at the Babraham Institute for her assistance with PtdIns(3,4,5)P_3 assays, and Arlette Vassallo, Carmelo Zinnato and Andrew Conway Morris for their assistance in collecting data presented during this thesis. The phosphoproteomics dataset would not have been possible without the care, skill and attention to detail provided by Clive D'Santos, Carmen Gonzalez Tejedo and Kamal Kishore of CRUK-CI, to whom I am very grateful.

Laboratories are made by those in them, and I feel the following people made ours one of the best: thank you Ben (Dunny) Dunmore, Alexi Crosby, Andy Cowburn, Rowena Jones, Al Jubb, Simon Lambden, Sarah Chantler and Andrew Savage for making the lab a great place to be. I thank Charlotte Summers for her kindness, insight and honesty. I also wish to thank the blood donors and patients who contributed to my work, along with the Gates Cambridge Trust for making this possible. Arlette, Katharine and Eleo are my mates, my 'dahlings', my Misfit Toys. I will miss them most of all, though I'm sure it won't be for too long.

I landed in Cambridge with the best team of supervisors anyone could ever wish for. David and Edwin made me feel welcome, plied me with food and wine, and challenged me to do my very best science, which started from a low baseline, but improved significantly! Andy Conway Morris has been supportive, responsive and has gone over and above in every possible way to make my PhD happen, and I honestly could not be more grateful. Here's hoping I'm the first of many students to come! I wouldn't have made it to Cambridge without Mum and Dad who gave me every opportunity to succeed; thanks to you both. Lastly, I wish to thank my partner Lucy, for understanding neutrophils and understanding me. I couldn't have done it without you.

Contents

Figures

Tables

Abbreviations

Abbreviation	Definition
95 % CI	95 % confidence interval
AF	AlexaFluor
AGC	Automatic gain control
APACHE II	Acute Physiology and Chronic Health Evaluation II
ARDS	Acute respiratory distress syndrome
AS	Autologous serum
ATP	Adenosine triphosphate
bRP	Basic pH reversed-phase fractionation
BV	Brilliant Violet™
C5a	Complement component C5a
C5aR	Complement component C5a receptor (also known as CD88)
C5aR1, CD88	C5a receptor 1, also known as cluster of differentiation molecule 88
C5aR2, C5L2, GPR77	C5a receptor 2, also known as G-protein coupled receptor 77
camp	Cyclic adenosine monophosphate
CDxx	Cluster of differentiation molecule XX
CFU	Colony forming unit
CID	Collision-induced dissociation
CLP	Caecal ligation and puncture
CORD	Critical illness-induced organ dysfunction
CR3	Complement receptor 3 (also known as CD11b/CD18 and MAC1)
CRISPR	Clustered regularly interspaced short palindromic repeats
CRUK-CI	Cancer Research UK, Cambridge Institute
CXCLxx	C-X-C motif chemokine ligand XX
CXCRxx	C-X-C motif chemokine receptor XX
DAMP	Damage associated molecular pattern
DAPI	4',6-diamidino-2-phenylindole
dH_2O	Deionised water
DIC	Disseminated intravascular coagulopathy
DMSO	Dimethyl sulfoxide
DPI	Diphenyleneiodonium chloride
EDTA	Ethylenediaminetetraacetic acid
ERK	Extracellular signal related kinase
ESCRT	Endosomal sorting complex required for transport
FDR	False discovery rate
fMLP	N-formylmethionyl-leucyl-phenylalanine
FWHM	Full width half maximum
GAP	GTPase-activating protein
G-CSF	Granulocyte colony stimulating factor
GEF	Guanosine nucleotide exchange factor
GM-CSF	Granulocyte-macrophage colony stimulating factor
GPCR	G protein-coupled receptor
GTPase	Guanosine triphosphatase
H2O2	Hydrogen peroxide

HCD	High energy collision-induced dissociation
HLA-DR	Human leukocyte antigen D-related
HMGB1	High mobility group box 1
ICAMxx	Intercellular adhesion molecule XX
ICU	Intensive care unit
IL-xx	Interleukin-XX
IMDM	Iscove's modified Dulbecco's medium
IQR	Interquartile range
ITU	Intensive therapy unit
LB	Luria-Bertani
LC-MS/MS	Liquid chromatography and tandem mass spectrometry
LMNB1	Lamin B1
LPS	Lipopolysaccharide
MAC	Membrane attack complex
MAPK	Mitogen activated protein kinase
MASP	Mannose binding lectin-associated serine protease
MBL	Mannose binding lectin
MDSC	Myeloid-derived suppressor cell
MD-x	Myeloid differentiation factor-x
MFI	Median fluorescence intensity
MLCP	Myosin light chain phosphatase
MODS	Multi-organ dysfunction syndrome
MOI	Multiplicity of infection
MSSA	Methicillin sensitive staphylococcus aureus
MTT	3-[4,5-dimethylthiazol-2-yl]-2,5-diphenyltetrazolium bromide
NADPH	Nicotinamide adenine dinucleotide phosphate
NCE	Normalized collision energy
NET	Neutrophil extracellular trap
NF-κB	Nuclear factor kappa-beta
NHE1	Sodium/hydrogen exchanger 1
NOX2	NADPH-oxidase complex 2
PAMP	Pathogen associated molecular pattern
PBMC	Peripheral blood mononuclear cell
PBS	Dulbecco's phosphate buffered saline
PE	Phycoerythrin
PI	Phagocytic index
PtdIns(3,4,5)P_3, PIP3	Phosphatidylinositol 3,4,5 trisphosphate
PtdIns3P, PI3P	Phosphatidylinositol-3-phosphate
PI3K-X	Phosphoinositide-3-kinase-X
PI3P	Phosphatidylinositol-3-phosphate
PICD	Phagocytosis induced cell death
PIK3C2α	Phosphatidylinositol 4-phosphate 3-kinase C2 domain-containing subunit alpha
PIKFYVE	1-phosphatidylinositol-3-phosphate 5-kinase
PKB	Protein kinase B
PKC	Protein kinase C

PLC	Phospholipase C
PMN	Polymorphonuclear cells (neutrophils)
PRR	Pattern recognition receptor
PTEN	Phosphatase and tensin homolog
PTM	Post-translational modification
PVDF	Polyvinylidene difluoride
RAB7A	Ras-related protein 7a
RAGE	Receptor for advanced glycosylation products
RFU	Relative fluorescence units
ROCK	Rho-associated, coiled-coil-containing protein kinase 1
ROS	Reactive oxygen species
rTEM	Reverse transendothelial migration
SAPS	Simplified Acute Physiology Score
SDF-1α	Stromal-derived factor 1-α
SDS	Sodium dodecyl sulfate
SDS-PAGE	Sodium dodecyl sulfate-polyacrylamide gel electrophoresis
SEM	Standard error of the mean
SIRS	Systemic inflammatory response syndrome
SLPI	Secretory leukocyte protease inhibitor
SOFA	Sepsis-related Organ Failure Assessment
STED	Stimulated emission depletion
TCEP	Tris(2-carboxyethyl)phosphine
TEAB	Triethylammonium bicarbonate
TLR-x	Toll-like receptor-x
TNF-x	Tumour necrosis factor-X
TOM1	Target of Myb protein 1
T_{reg}	Regulatory T cell
VATPase	Vacuolar H+ ATPase
VCAMxx	Vascular cellular adhesion molecule XX
ZFYVE16	Zinc finger FYVE domain-containing protein 16
βME	2-mercaptoethanol

Structure of thesis

This thesis is structured into seven chapters, and is navigable using hyperlinks for figures, tables and subheadings if reading in Word or Adobe Acrobat Reader. Bookmarks for ease of navigation are accessible by enabling the ‘Navigation pane’ in both Word and Adobe Acrobat Reader. The first chapter (literature review) outlines the relevant literature pertaining to this work and identifies key areas in need of further investigation. The second chapter (Methods) details the experimental and statistical techniques used to generate and analyse data presented throughout the rest of the thesis. The methods discussed in Chapter II: are supplemented by full-length protocols for key experiments provided in the Appendices.

Chapters III-VI are the experimental chapters. Each is structured identically, beginning with a brief recapitulation of relevant literature, before hypotheses and aims for the chapter are discussed. Notes on the methods used throughout the chapter are provided, before results are presented. Each chapter concludes with a detailed discussion of the results in the context of the thesis and the wider literature. The final chapter summarises key findings and outlines my approach to further questions which arose during the course of the thesis.

Chapter I: Literature review

This chapter is divided into three parts. It begins with a discussion of the many and varied functions of polymorphonuclear neutrophils (PMN), with a focus on microbicidal capabilities of relevance to this thesis. This is followed by an overview of critical illness, with a focus on the immune dysfunction known to occur in this context. The discussion then turns to the activated complement fragment C5a, the inflammatory molecule of central importance to this thesis. The generation, functions, receptors and role of this anaphylatoxin in immune and other organ dysfunction is discussed, before the chapter is summarised and further avenues for investigation are highlighted.

1. Neutrophils

The polymorphonuclear neutrophil is commonly described as the foot soldier or first responder of the immune system. These cells make up 70% of circulating human leucocytes (ref), can be rapidly mobilised from the bone marrow[1] and infiltrate inflamed tissues[2] where they carry out a diverse range of functions, from bacterial killing to modulation of adaptive immune responses.[3] Their importance for homeostasis is demonstrated by the high prevalence of severe bacterial and fungal infections seen in individuals with inherited or acquired neutrophil dysfunction.[1,4]

1.1. Mobilisation

Neutrophil development can be traced backwards to as early as week three of embryogenesis, after which an exquisitely complex and regulated process occurs, transitioning haematopoietic stem cells through common myeloid progenitors and eventually into mature neutrophils, capable of leaving the bone marrow.[5] In the adult, between $5x10^{10}$-$10x10^{10}$ neutrophils are produced in the bone marrow each day from common myelocyte progenitors under the control of multiple proliferation signals including granulocyte/macrophage colony stimulating factors (G-CSF, GM-CSF) and interleukins 3 and 6 (IL-3, IL-6).[1] In the context of systemic inflammation or infection, upregulation of these cytokines stimulates increased myeloid progenitor proliferation, known as emergency granulopoiesis[6] which can lead to the observation of band-type subsets of neutrophils in the circulation.[6,7]

Stromal cell-derived factor 1α/C-X-C receptor 4 (SDF-1α/CXCR4) interaction tends to retain neutrophils within the bone marrow.[1] It is the gradual loss of CXCR4 from the neutrophil cell surface with maturity, in combination with increased expression of CXCR2, that shifts the balance of signals from retention to release, allowing trans-endothelial migration into the circulation.[1,5,8] This balance is further shifted during infection and inflammation by interleukin 8, C5a, formylated peptides, tumour necrosis factor alpha and leukotriene B_4 (IL-8, TNF-α,

LTB_4) leading to the neutrophilia characteristic of systemic inflammation and sepsis.[9–11] More recently, the significance of the IL-8/CXCR2 interaction in this context has become clearer as phase 1 and 2 clinical trials demonstrated a reversible reduction in circulating neutrophil count after treatment with CXCR2 antagonists.[12,13]

1.2. Neutrophils in the circulation

Physiological concentrations of neutrophils in the blood range between 1.8 – 7.7 x 10^9 cells/L.[14] The half-life of neutrophils in the circulation has been the subject of some debate, with early estimates generated by re-injection of radiolabelled neutrophils into healthy humans ranging from six to seven hours.[15–17] More recent data from Pillay et al[18] estimated a half-life of nearly four days, though methodological concerns have been raised related to that study's high approximation of the blood:precursor neutrophil ratio erroneously increasing their estimate of half-life.[19] It would seem that the weight of published evidence would suggest a half-life closer to the original estimate.[1,8,15,19–21] Importantly, the vast majority of total blood neutrophils in health are in an unprimed state, where they are minimally responsive to activating stimuli,[22,23] and can be found distributed equally between the freely circulating and marginated pools (consisting of liver, spleen and bone marrow).[1] In disease states, this homeostatic unprimed state is disrupted, leading to neutrophil retention in a variety of vascular beds and associated tissue destruction,[1,23,24] which is discussed further in Section 1.5.

1.3. Transmigration and chemotaxis

A key determinant of appropriately targeted neutrophil function is migration toward and around sites of infection and inflammation. Many recent advances in this field have been facilitated by the use of genetically tractable and transparent zebrafish models and high-speed, high-resolution microscopy techniques alongside in-vitro and in-vivo models using primary human cells (reference in-vitro model, cell coculture transmigration and skin blister window work).[12,25] The first step is transmigration of neutrophils from the bloodstream across post-capillary venules and into tissues. In response to pathogen and damage associated molecular patterns (PAMPs and DAMPs respectively) as well as cytokines such as IL-1β and TNF-α secreted by macrophages and dendritic cells,[2] neutrophils participate in a leukocyte adhesion cascade.[26,27] This series of events begins with weak neutrophil-endothelium interactions, followed by rolling, firmer adhesion and extension of neutrophil processes through and between endothelial cells. The leukocyte adhesion cascade is mediated primarily by two families of molecules; integrins and selectins, key members of which include P- and E- selectin, vascular cell adhesion molecule 1 (VCAM-1) and intercellular adhesion molecules 1 and 2 (ICAM-1,2).[26,27] Neutrophil migration is not a one-way phenomenon; reverse transendothelial migration (rTEM)[28] mediated by ICAM-1 junctional adhesion

molecule C (JAM-C)[29] and redox-regulated Src family kinases[30] has now been confirmed *in vitro* and *in vivo* and shown to be of importance in mediating systemic inflammation.[31]

For many years the importance of nuclear deformation during leukocyte transmigration has been appreciated,[32–34] though the mechanisms regulating this process remain only partially understood. Human neutrophils (diameter 7-10 μM) regularly pass through spaces which are much smaller during their transit through capillary beds (5.5 μM)[34] cellular membranes and the interstitium.[35] This necessitates the application of deforming forces to the nucleus, both during migration through endothelial cell membranes[36] and during rapid, integrin-independent migration through three-dimensional spaces.[37] In an elegant study of mammalian dendritic cell migration, Rabb and colleagues[38] provided evidence for nuclear envelope disintegration and importantly, repair, carried out by endosomal sorting complexes (ESCRT) required for cell survival during migration through tight spaces. The relevance of these observations to other leucocyte functions involving deformation of the actin cytoskeleton (such as phagocytosis) have yet to be explored.

During and following transmigration, neutrophils both move randomly (Brownian random walk)[39] and respond to established gradients of inflammatory molecules which lead them to the site of injury or infection; a process known as chemotaxis. Neutrophil chemotaxis is regulated primarily by the ligation of G protein-coupled receptors (GPCRs) by chemokines such as CXCL1, N-formylmethionyl-leucyl-phenylalanine (fMLP), LTB_4 and CXCL8/IL-8.[2,12] In response to GPCR ligation, signalling molecules (phosphoinositide-3-kinases (PI3Ks), phospholipase C (PLC), Rho-family GTPases and their regulators such as P-Rex1) accumulate at the leading edge of the cell, leading to actin polymerisation and cell movement toward the increasing chemokine concentrations.[12,40,41]

Work by Sarris and colleagues[39] demonstrated an important role for extracellular heparan sulfate proteoglycans for the maintenance of chemokine gradients in tissues, and the ability of CXCL8/IL-8 to increase neutrophil speed and straightness only when moving toward maximal chemokine concentration. Another key phenomenon recently identified is neutrophil swarming, a process whereby neutrophils self-amplify their recruitment by secretion of LTB_4, facilitating isolation of damaged tissue from healthy.[42,43] These complex interactions between neutrophils and chemokines allow these cells to survey the tissue environment, and eventually get to where they need to be.

It should be noted at this point that the transmigrated or tissue neutrophil is distinct from its circulating counterpart.[44] Sorensen and colleagues observed that tissue neutrophils were more phagocytically active.[45] Data from the Nourshargh lab and others[28] has demonstrated that neutrophil expression of ICAM-1 is increased in cells that have undergone rTEM,[29] and that expression of this molecule has consequent effects on phagocytosis and ROS

production in mice.[46] Further, transmigrated neutrophils produce cytokines differently and display discrete transcriptional signatures, which may be related to wound healing.[44] Whether these phenotypic changes are due simply to priming or activation, which commonly accompany transmigration,[47] or are due to changes induced by the act of transmigration itself is presently unclear. Once neutrophils have reached the site of inflammation, their destructive potential is brought to bear, where host-pathogen interactions result in phagocytosis, phagosome maturation and the respiratory burst.

1.4. Phagosome formation

Phagocytosis (internalisation of particles > 0.5 μm)[48,49] is a complex and dynamic process involving multiple signalling pathways which differ according to phagocytic target.[48] Phagocytosis begins with engagement of phagocytic receptors on the surface of phagocytes often by endogenous opsonic ligands such as immunoglobulins or iC3b, a product of the complement system, but also by microbial PAMPs binding to a variety of receptors.[49,50] Once immunoglobulin or complement receptors (Fc receptors and CD11b/CD18 respectively) are engaged, particle binding is further enhanced by diffusion of more receptors through the phagocyte membrane and extensions of cellular processes around the pathogen.[49,51,52]

Following receptor clustering around prey, multiple signalling cascades are activated through SRC-family kinases (SFKs) and phospholipases.[53] The consequent tyrosine residue phosphorylation and phosphatidylinositol 3,4,5 trisphosphate (PtdIns(3,4,5)P_3) accumulation (following phosphoinositide-3-kinase action) drives Rho family GTPase activation and rearrangement of the actin cytoskeleton into a nascent phagosome, after which phagosomal maturation and pathogen killing occur.[49,53,54] It should be noted that complement-mediated and Fc-receptor mediated phagocytosis tend to engage different Rho family GTPases (RhoA and cell division control protein homolog 42/Rac respectively)[55] which explain important mechanistic differences between these pathways.[48,49] Further discussion of intracellular signalling pathways leading to phagocytic dysfunction in the context of C5a is provided in Section 3.5.

1.5. Phagosomal maturation and bacterial killing

Once a pathogen-containing phagosome is formed, a choreographed process of granule fusion, pH change, and degradative enzyme activation occurs, collectively known as phagosome maturation. Neutrophil phagocytosis begins seconds after prey encounter and is generally complete by 15-20 minutes for large particles such as complement-opsonised zymosan.[56,57] Important signalling proteins involved in these processes are the small GTPases of the Rab family, many of which are recruited to the phagosomal membrane by phosphatidylinositol-3-phosphate (PtdIns3P, note difference from PtdIns(3,4,5)P_3 above) produced predominantly by the class III PI3-kinase Vps34.[48,58] Many aspects of phagosome

maturation have been studied in macrophages and applied to neutrophils, though there are substantive differences between the two cell types. For instance, neutrophils are thought to have a less acidic phagosomal pH compared to macrophages, at least at early time-points.[59,60] Further, neutrophil phagosome maturation is characterised by PtdIns3P-dependent fusion with pre-formed, oxidase-containing granules present within the cytosol,[61,62] as opposed to the gradual endosomal maturation which occurs in macrophages.[48,49,63]

Four categories of neutrophil granule are recognised; azurophilic, specific, gelatinase and secretory vesicles.[64] Granules contain a multitude of microbicidal components; myeloperoxidase (MPO), cathepsin G, elastase and proteinase 3 as well as components of the nicotinamide adenine dinucleotide phosphate oxidase complex (NADPH-oxidase, NOX-2).[54,64,65] Release of granule contents into the phagosome is accompanied by the neutrophil respiratory burst; a NOX-2-mediated process responsible for electron transfer to oxygen, forming the superoxide anion (O_2^-) which dismutates to hydrogen peroxide (H_2O_2) both of which are toxic to microbes.[49,54,64] The production of these reactive oxygen species (ROS) can be greatly augmented or 'primed' by pre-exposure to PAMPs (fMLP, LPS) and endogenous proteins including platelet activating factor (PAF), GM-CSF or TNF-α.[23] Priming is thought to ensure the appropriate activation of neutrophil destructive mechanisms to control collateral tissue damage and augment microbicidal activity.[23,66] Recent data from our group provides evidence for neutrophil de-priming, which can occur secondary to repetitive mechanical distortion (such as induced by transit through the pulmonary vasculature) and is disturbed in ARDS.[24,67]

Phagosomal biochemical events following the respiratory burst are only partially understood, owing to the difficulty in interrogating molecular events in such conditions. The large charge shift and membrane depolarisation generated by NOX-2 is compensated by ion channels and active proton pumps, including cystic fibrosis transmembrane conductance regulator (CFTR) and vacuolar ATPases (V-ATPases). This charge compensation allows further oxidative species to be generated.[63,68] Using halogens such as chloride in combination with H_2O_2, MPO generates cytotoxic hypochlorous acid (HOCl) and other hypohalous acids.[54] Proteases are also released from granules, and are likely to function inside phagolysosomes, at least for certain phases of phagosomal maturation.[54] Whilst the biochemistry may not yet be fully understood, it is clear that these interdependent processes generate an environment which is highly toxic to microbes, resulting in their destruction.[54,63,64] The careful control of these destructive processes is necessary to prevent destruction of the neutrophils themselves and damage to healthy bystander tissue.[69] It should be noted, however, that pathogens also have an extensive armamentarium of evasive measures at their disposal, which have been reviewed elsewhere.[70,71]

Neutrophils serve a variety of other functions; cytokine production, modulation of the adaptive immune system,[15,20] neutrophil extracellular trap (NET) production[72–74] and resolution of inflammation through apoptosis and removal by macrophages.[3,20] These functions, whilst important, are not the focus of this thesis and as such will not be discussed in detail.

In summary, neutrophils are far from the simple foot soldiers of the immune system they were once thought to be. These motile first-responders are mobilised in large numbers during infection and inflammation. Neutrophils adhere to and exit the microvasculature and migrate along chemotactic gradients to sites of infection. There, they engulf microbes in an intricate and complex process involving a multitude of receptors and signalling pathways, eventually culminating in actin polymerisation and internalisation of pathogens. Once microbes are phagocytosed, toxic granules and the NADPH-oxidase complex fuse with the phagosome, thus creating a highly destructive milieu leading to pathogen neutralisation. Defects in the above functions predispose humans to infection and can be driven by endogenous molecules such as complement activation product C5a, a key mediator present at high concentrations during critical illness. Before we enter into a detailed discussion of the generation and effects of C5a, an understanding of critical illness biology is necessary. It is to this topic that we now turn.

2. Critical illness, immune perturbation and organ failure

2.1. Definitions, epidemiology

Critical illness is difficult to define but can be conceptualised pragmatically as any severe illness necessitating invasive monitoring and organ support, usually within an intensive care or therapy unit (ICU/ITU).[75] Common causes of critical illness are severe infections, trauma-haemorrhage, burns, pancreatitis and post cardiac-arrest reperfusion. Differences in definitions, treatment thresholds and surveillance make the burden of critical illness challenging to accurately quantify. Based on a systematic meta-analysis, Adhikari and colleagues estimated the absolute number of adult deaths due to critical illness syndromes worldwide to be over 58 million in 2004.[76] More recently, a worldwide prospective audit revealed crude mortality rates for critically ill patients of 13 % in high income countries, though mortality estimates vary depending on aetiology, from less than 3 % for routine post-operative care[77] to 26 % for severe sepsis[78] to over 40 % with acute respiratory distress syndrome[79] and septic shock.[76,80,81]

A key predictor of these widely variable mortality rates is the number of dysfunctional organs and the degree to which they are impaired.[82] Several mortality prediction tools such as Simplified Acute Physiology Score (SAPS)[83], Sepsis-related Organ Failure Assessment (SOFA)[84] and Acute Physiology and Chronic Health Evaluation II (APACHE II)[85] are

predicated on this fact, and their respective predictive validities have been validated in a wide variety of cohorts by multiple groups.[80,86–88] Indeed Sepsis-3,[89] the most recent consensus definition of this prototypical critical illness syndrome, relies on the presence of organ dysfunction for the diagnosis of sepsis. Impaired functioning of more than one organ system is known as multi-organ dysfunction syndrome (MODS), which is often a final common pathway for critically ill patients who die, regardless of the initial insult leading to their ICU admission.[90] Of importance to this thesis, and arguably to patients, is the ability to assess, predict and ameliorate organ dysfunction, regardless of initial insult or arbitrary critical illness syndrome. The following section provides an overview of the known pathophysiological mechanisms which lead to organ dysfunction in critically ill patients, before we consider the specific biology and role of the complement component C5a in these processes.

2.2. PAMPS, DAMPS and immune activation

Injury to host tissues may be caused by a number of insults such as microbial invasion, trauma, ischaemia, burns or chemical (including pancreatic enzyme) exposure. Following tissue destruction or microbial invasion, DAMPs and PAMPs are released.[91,92] These compounds, such as high mobility group box 1 (HMGB1)[93] and mitochondrial DNA[94] from damaged cells, LPS,[95] formylated peptides and flagellin from bacteria[96–98] signal via pattern recognition receptors (PRRs) including toll-like receptors (TLRs) on innate immune and endothelial cells, leading to neutrophil priming, pro-inflammatory gene transcription and cytokine release.[69,96,97,99] PAMPs are also potent activators of the complement and coagulation cascades, which further generate inflammatory and pro-coagulant compounds[92,97] and are discussed in Section 3.1.

Key to critical illness pathology is the concept of systemic overspill of PAMPs and DAMPs, with resultant systemic or non-specific immune activation. In the context of localised infection or injury, PAMPs and DAMPs act locally to drive a controlled immune response, leading to inflammation, control of damage or pathogens and eventual resolution. However, in critical illness this tight control is lost,[92,100] due to the magnitude of the insult or virulence of the pathogen along with a multitude of inherited and acquired host factors.[101] The result is a global, overactive immune response, often driven by multiple positive feedback loops and cross-amplification. An important component of this phenomenon is known as the cytokine storm, which is discussed in the next section.

2.3. Cytokine storm

Systemic stimulation of neutrophils, monocytes, macrophages and T-cells by DAMPs and PAMPs leads to direct functional responses, such as chemotaxis and reactive oxygen species (ROS) generation, as well as secretion of multiple cytokines.[102] Whilst the term ‘cytokine storm’ is not precisely defined, it can be thought of as a deleterious positive

feedback loop where activated cells secrete cytokines, which then further activate immune cells, generating a profoundly dysregulated inflammatory state.[97,102,103] The functions of cytokines in critical illness are protean and have been reviewed extensively elsewhere.[97,102–105] Two prototypical cytokines produced in critical illness (TNF-α and IL-1beta) are released within 30 minutes of LPS challenge or trauma and upregulate adhesion molecules, drive inflammasome formation,[106] nuclear factor kappa-light-chain-enhancer of activated B cells (NF-κB) signalling[107] and stimulate neutrophils to produce ROS and neutrophil extracellular traps (NETs).[97,103,105] Other cytokines share similar functions but differ in their plasma profile, cellular targets and signalling mechanisms. Whilst elevated levels of certain cytokines such as (IL-6) have been associated with mortality, trials of cytokine antagonists have failed to show an improvement in meaningful clinical outcomes.[108,109] The reasons for this apparently disparate finding have been the subject of much research and debate within the intensive care community in recent years, and likely relate to inadequate immunophenotyping of patients prior to randomisation.[108,110,111] This constellation of tissue destruction, pathogen invasion, systemic DAMP or PAMP release and the cytokine storm leads to the hallmark of critical illness, organ dysfunction, which is the focus of the next section.

2.4. Mechanisms of organ dysfunction

The exact mechanisms underlying organ dysfunction in critical illness remain poorly understood, though the factors identified below play a significant role. In this Section, general mechanisms that lead to organ dysfunction are discussed, to give the reader an overview of the existing literature. After C5a is introduced, the specific defects induced by this anaphylatoxin are reviewed in Section 3.4, and as such are not discussed in detail here.

2.4.1. Hyperinflammation and collateral damage

Perhaps the most obvious category is collateral damage to tissues secondary to immune cell activation and the cytokine storm. Such immune-mediated damage is most obvious in the acute respiratory distress syndrome (ARDS) where neutrophil protease release and ROS production directly damage alveolar epithelium and pulmonary vascular endothelium.[97,112,113] Neutrophil extracellular traps have also been shown to play an important role in causing collateral damage and driving inflammation during critical illness[73,114,115]and other disease such as cystic fibrosis.[73] Such cell-mediated toxicity is not limited to the lung or to one cell type; infiltration by macrophages and neutrophils, as well as neutrophil degranulation, have been demonstrated in the liver, kidney and gastrointestinal tract of multiple species in the context of sepsis and trauma.[97,116,117] These findings are consistent with the premise that immune cells can damage bystander organs, though organs are differentially affected and tissue destruction is not always obvious (Section 2.4.4).

2.4.2. The gastrointestinal tract

A further driver of organ dysfunction in critical illness is the gastrointestinal tract (GIT). Initially, microbial translocation through the epithelial barrier secondary to increased barrier permeability and GIT stasis was thought to occur.[118–121] However, data in support of this hypothesis in critically ill humans is lacking.[82,122] Current models list several other factors, including epithelial apoptosis, mucous disruption, alterations to the microbiome and the secretion of cytokines, PAMPs and DAMPs through the mesenteric lymphatic systems as key drivers of distant organ failure.[122–125]

2.4.3. Hypoperfusion and hypoxia

Another mechanism of organ dysfunction is compromised tissue perfusion. There are many ways in which this can occur, including distributive shock secondary to vasodilation[90] and myocardial depression caused by cytokines and complement activation products (particularly C5a and TNF-α).[103,105,126] Indiscriminate activation of the complement and coagulation cascades can precipitate disseminated intravascular coagulation (DIC) and leucocyte-platelet aggregates which lead to microvascular occlusion, endothelial damage and tissue hypoxia.[97,127–129] These perturbations often manifest clinically as hypotension, altered mental status, lactate accumulation, reduced urine output and microcirculatory abnormalities.[82] Whilst these phenomena have been well documented in critical illness and sepsis particularly, the dogma that hypoperfusion and lack of oxygen leads to widespread tissue necrosis has little supporting evidence.[130–133] The effects of these physiological phenomena on cellular metabolism and machinery are becoming clearer, and may provide a more accurate picture of what causes organs to fail.

2.4.4. Cellular energy processing

Mitochondrial synthesis of adenosine triphosphate (ATP) through oxidative phosphorylation is a process critical for normal cellular function. Critical illness induces defects in cellular respiration firstly through impairing oxygen delivery to cells as outlined above, as well as inducing defects in vital cellular machinery. For example, activated macrophages can induce an open configuration of the mitochondrial permeability transition pore (MPTP). When MPTP is constitutively open, the proton gradient necessary for electron transfer is lost, and the cell is deprived of an essential method of ATP production, leading to necrosis.[134] Similar mechanisms of impaired cellular respiration have been demonstrated in hepatocytes exposed to TNF-α[135] and in a rat myocardial ischaemia model.[136]

Another example of damage to vital cellular machinery in critical illness is widespread activation of poly ADP-ribose polymerase (PARP) by ROS, which are abundant in critical illness.[137] Under these conditions, PARP depletes the cell of ATP-forming substrates.[137,138] Inhibition of PARP in animal models of sepsis and multiple organ dysfunction is associated

with a survival benefit and (with appropriate targeting) offers an attractive option for pharmacotherapy in critical illness.[137,139] In addition to impairment of cellular energy supply, mitochondrial components are DAMPs which may further exacerbate critical illness-induced inflammation.[94] In a recent review, Singer[140] synthesised available evidence and suggested that together, mitochondrial dysfunction induced by initial hypoperfusion, nitric oxide species, ROS, failure to maintain mitochondrial numbers and uncoupling of mitochondrial action from ATP production are central components of organ dysfunction.

The roles of collateral tissue damage, hypoperfusion, the GIT and impaired cellular metabolism in organ dysfunction are becoming clearer, though several questions remain. Severe organ dysfunction (outside of ARDS) is generally not accompanied by histological evidence of widespread tissue destruction, as one might expect.[97,133,137] Why this is the case remains the subject of intense investigation; cellular 'hibernation' and apoptosis have been offered as potential explanations to date.[133,140–142] Intelligent therapeutic trial design also remains a challenge, given the failure of multiple biologically promising strategies to show benefit[133,143–145] Up to now, this thesis has focussed on the initial inflammatory response which occurs in critically ill patients. This response, however, is only part of the story. The coexistence of a profound immunological impairment with hyperinflammation in critical illness is well-documented, only partially understood and is the subject of the next section.

2.5. Immune dysfunction: vulnerability to nosocomial infection and worsening sepsis

It has been clear for decades that the function of the immune system, including neutrophil function, is impaired in critical illness, with coexisting profound systemic inflammation and immunoparesis.[146–148] Furthermore, immune cell impairment predicts nosocomial (hospital acquired) infection.[133,147,149,150] Nosocomial infections can affect as many as 37 % of ICU patients, are a major determinant of morbidity and mortality and claim $ 3.5 billion from the US healthcare budget per year.[133,151–154] Critical illness-related immune dysfunction can be divided broadly into phenomena driving cell loss or cellular functional impairment, which are discussed below. There is significant crossover between mechanisms involved in both aspects, and it is important to bear in mind that the immune impairment discussed below can occur concomitantly with, or after hyperinflammation. Finally, the following paragraphs give an overview of generalised immune cellular changes in the context of critical illness; specific effects of C5a on neutrophils are discussed in greater detail in Section 3.5.

2.5.1. Changes in immune cell populations

Impairment of immunity in critical illness is driven partly by a reduction in numbers of multiple cell types. Cell loss was first characterised through autopsy studies of bowel and spleens harvested peri-mortem in patients with sepsis[142,155,156] or acute trauma-haemorrhage.[157]

These seminal studies displayed depletion of epithelial cells, CD4 and CD8 T, B and dendritic cell populations, in the blood and the organ in question. Similar observations have now been made in thymus, lymph nodes and gut-associated lymphoid tissue.[133,158] A key mechanism responsible for this reduction in cell numbers is caspase-9-driven apoptotic cell death.[155] Apoptosis in critical illness affects different cell populations to different degrees; for example, regulatory T cells (T_{regs}) and myeloid-derived suppressor cells (MDSCs) have an immunosuppressive phenotype and tend to be resistant to apoptosis.[133,147,159–162]

Neutrophil numbers may be dramatically increased in critical illness states, particularly sepsis. This increase in neutrophil number is thought to be driven by release of neutrophils from marginated pools by the presence of pro-inflammatory mediators such as TNF-α, C5a, and IL-6.[1] Similar mediators including LPS and GM-CSF drive a decrease in apoptotic cell death, often culminating in a significant circulating neutrophilia,[1,23,149] though the supply is not inexhaustible and can be overwhelmed by high bacterial loads or concomitant stimuli.[163] Despite this neutrophilia, patients remain profoundly vulnerable to bacterial infections traditionally controlled by neutrophils such as *Staphylococcus aureus and Pseudomonas aeruginosa.*[69,147] An attractive explanation for this paradox is that neutrophils observed in critical illness or systemic inflammatory states are characterised by altered or reduced function, and is discussed below.

2.5.2. Decreased functional responses of immune cells

One of the best-characterised functional immune defects is known as endotoxin tolerance, which Cavaillon and Adib-Conquy[164] define as a "reduced responsiveness to LPS challenge following a first encounter with endotoxin." Endotoxin tolerance has been shown to occur in a variety of immune cell types with diverse responses,[165] though is perhaps best known to refer to reduced TNF-α secretion by monocyte-macrophages in response to prolonged or repeated LPS exposure.[164,166,167] Associated with this defect is the T-cell receptor ligand, D-related human leukocyte antigen (HLA-DR). Initially, persistently low monocyte HLA-DR levels[147,168] were shown to be associated with nosocomial infection in sepsis.[150,169] More recently, HLA-DR levels have been shown to predict mortality and nosocomial infection in critical illness generally.[133,147,170]

A more recently characterised cell-surface marker is programmed death ligand 1 (PD-L1). Expressed on the surface of neutrophils, PD-L1 expression is upregulated in sepsis and in response to LPS challenge, and suppresses T-cell proliferation through an interferon-γ-dependent mechanism.[69,133,171] Anti-PD-1 antibody treatment reverses immune dysfunction and improves survival in mouse models,[172] and has been shown to increase phagocytic capacity in neutrophils from septic humans.[173]

Neutrophil subsets also appear and behave differently during systemic inflammation and critical illness. Circulating neutrophils in this context have been demonstrated to have low expression of maturation markers CD10 and CD16, kill activated T-cells and were associated with progression of sepsis.[174] Pillay and colleagues have also provided evidence for a subset of neutrophils found after LPS challenge or trauma which suppress T-cell proliferation via the integrin dimer macrophage-1 antigen (Mac-1, complement receptor 3 or $\alpha_M\beta_2$ integrin).[7]

In addition to these defects, the direct antimicrobial functions of neutrophils have been shown to be significantly impaired in critical illness by multiple groups. In a comprehensive assessment of septic shock patients at days three-six and six-eight after onset of shock, Demaret and colleagues[149] demonstrated impaired chemotaxis toward multiple chemoattractants, defective phagocytosis and oxidative response to *E. coli,* and correlated these findings with mortality. Many other groups have found similar results with respect to chemotaxis,[175] phagocytosis[176–179] and ROS generation[179–181] in different critical illness states including burns, sepsis and trauma. Data on ROS generation by neutrophils can at times be difficult to interpret, with some groups showing an increase in ROS production in sepsis[182,183] and ARDS[184] whereas many others show decreased ROS production as outlined previously and summarised in authoritative reviews.[167,185] These contrasting findings illustrate the importance of context in interpreting neutrophil functional responses, and in most cases can be explained by differences in experimental time-points, stimuli and purification procedures.

It is clear that both the number, subsets and diverse functions of multiple immune cell types are profoundly altered in the context of critical illness, and that these alterations predict clinically significant outcomes. Further, a focus of current work is understanding how these changes persist over time, and the role of epigenetic and post-translational modifications in the persistence of these effects after critical illness.[167,186] Equipped with an understanding of the effects of critical illness on immune cells in general, it is now time to explore the central role of C5a in mediating these defects.

3. C5a as a central mediator of organ and immune dysfunction

3.1. Complement cascade

The term ‘complement’ was coined in 1899 by Paul Ehrlich after the heat-sensitive ability of serum to kill bacteria was noted in 1888 and 1891.[92,187] The name is derived from Ehrlich’s thought that the system ‘complemented’ the antimicrobial functions of antibodies. It is a cascade of over 30 plasma glycoproteins (designated C-xq, where x indicates a protein number and q the protein subunit) which are activated through proteolytic cleavage at sites of inflammation, in a similar way to the coagulation cascade.[187,188] The precursor proteins (zymogens) are predominantly synthesised by hepatocytes but tissue macrophages,

monocytes and epithelial cells are also capable of synthesis.[92,187] There are four key functions of the complement system, namely; opsonisation, propagation of the inflammatory response, pathogen destruction by the membrane attack complex (MAC) and enhancement of adaptive immunity.[187,189] There are multiple activation pathways; three are well-characterised and converge on the activation of the C3 convertase.[189] Others have more recently been identified such as the macrophage serine protease- and thrombin-triggered arms.[92,190,191] Figure I-1 summarises known complement activation pathways and demonstrates how C5a is produced.

3.2. C5a anaphylatoxin

Human C5a is a 74 amino acid protein, composed of four α-helices in anti-parallel with bridging disulphide bonds.[192–194] It is formed from cleavage of the amino terminal of C5 by the C5a convertase in the plasma.[192,195,196] Along with the less-potent C3a, C5a is a key inflammatory anaphylatoxin generated by multiple upstream pathways of the complement cascade (classical, lectin and alternative) as well as being generated directly or indirectly by activated neutrophils,[197] macrophages,[191] platelets[198] and coagulant cascade proteins.[199] Figure I-1 provides a summary of the pathways of relevance to C5a production.[50,200,201]

Several mechanisms determine the regulation of C5a function in the plasma. Firstly, C5a is cleared by receptor-mediated internalisation by immune cells in vascular organs such as the lung, spleen, liver and kidney.[202,203] Furthermore, removal of the C-terminal arginine residue (desargination) from the C5a molecule[204] by serum carboxypeptidases N, B or R yields $C5a_{des\text{-}arg}$, which exerts less potent inflammatory effects, as discussed below.[204–207] Under normal conditions, the plasma concentration of C5a is very low (in the range of 1-5 nM)[208] as the anaphylatoxin is cleared within 3-5 minutes through the mechanisms outlined above.[203,209] In critical illness, tight control of C5a production is lost, and plasma concentrations can exceed 100 nM.[92,208,210] However, given the rapidity of C5a clearance, it is hypothesised that the presence of detectable plasma C5a concentrations most likely indicate receptor saturation and hence the plasma concentration of C5a may give a relatively unreliable indication of the cellular exposure to this agent. Ligation of the C5a receptor by C5a leads to internalisation, and hence several authors have used neutrophil C5a receptor surface expression as a more accurate marker of C5a exposure. Whilst down-regulation of neutrophil surface C5a receptor expression may not be caused solely by C5a, at least in vitro,[211,212] it is a reliable marker of neutrophil phagocytic dysfunction[213] and has been associated with poor outcomes in several cohorts of critically ill patients.[110,147,214]

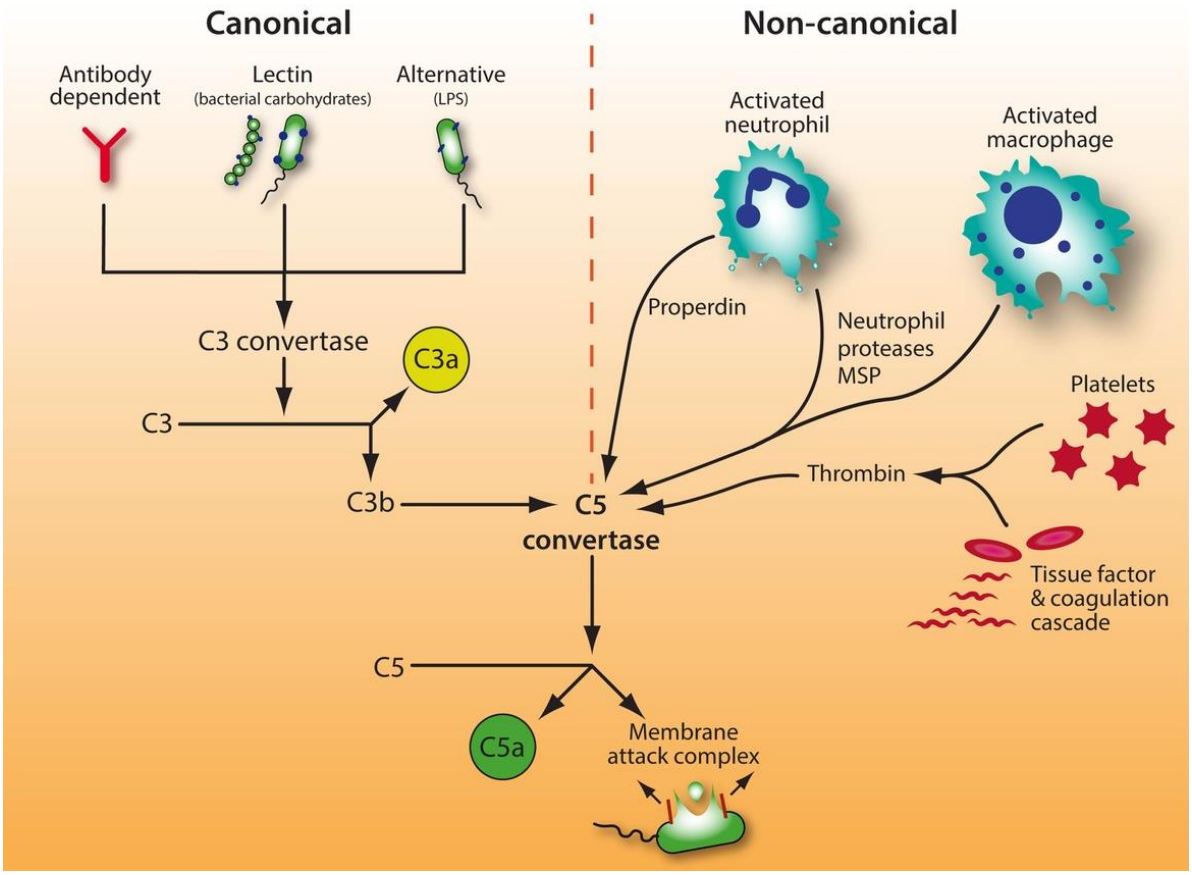

Figure I-1: Simplified overview of C5a generation

The classical complement pathway is activated by IgG and IgM-induced activation of C1 subunits. The lectin pathway is activated after exposure of mannose binding lectin (MBL) in serum to bacterial mannose monomers. This interaction generates active MBL-associated serine proteases 1 (MASPs) in the serum. The alternative pathway relies on the gram-negative bacterial pathogen associated molecular pattern (PAMP) lipopolysaccharide (LPS). Through intermediary complement proteins, the canonical pathways converge on the C3 convertase. Non-canonical pathways generally converge on the C5 convertase, and are initiated by proteases released by activated neutrophils and tissue macrophages[191], as well as thrombin[190] and properdin.[197]

3.3. C5a receptors

There are two known receptors for C5a; C5aR1 or cluster of differentiation molecule 88 (CD88) and C5L2, also known as G-protein coupled receptor 77 (GPR77).[193,215] For the purposes of this thesis, abbreviations C5aR1 and C5aR2 refer to CD88 and C5L2 respectively. C5aR1 is a G-protein coupled receptor with seven transmembrane domains and three extracellular loops.[92,193,216] In a series of seminal papers, Chenoweth and Hugli first identified the receptor on human neutrophils in 1978, and demonstrated distinct roles for the carboxyl terminal of the C5a molecule in terms of receptor binding and activation.[196,206,217] Since then, debate has ensued regarding the nature of C5a-C5aR1 interactions. Data generated using three distinct peptides able to impair C5a binding and functional responses suggested three interaction sites between recombinant C5a and C5aR1 on human

neutrophils.[193] More recently, Baranski's group have used 3D modelling and saturation mutagenesis in yeast to provide further evidence for a 'two-site' C5a:C5aR1 binding model advanced by Siciliano in 1994.[218–220] These authors propose multiple interactions between the N-terminals of C5a and C5aR1 as the first binding site, whereas the second site is formed by salt bridges and hydrogen bonds between the extracellular loops of the transmembrane domains of C5aR1 with the carboxyl terminus of C5a.[218,220,221] These findings differentiate C5aR1 from the C3a receptor at which the biological activity of the ligand is largely determined by the carboxyl terminus.[222,223] These nuances are of paramount importance for effective drug design, which is discussed in more detail below.

In 2000 Ohno and colleagues identified a second receptor (C5aR2) in immature dendritic cells and granulocytes which was subsequently found to bind C5a, and its desarginated form, with high affinity.[215,224] Since that time, the effects, ligand selectivity and physiological relevance of C5aR2 have been the subject of debate.[210,225,226] Like C5aR1, C5aR2 is a seven transmembrane domain receptor, encoded on chromosome 19.[227] C5aR2 shares 37% of its amino acid sequence identity with C5aR1[228] and binds C5a with high affinity.[215,227] Relative to C5aR1, C5aR2 binds the desarginated form of C5a with 10-50 times higher affinity as evidenced by competitive ligand-binding assays in transfected cell lines.[227,229]

A key difference between the receptors is the uncoupling of C5aR2 from G-protein signal transduction pathways; in cell lines transfected with C5aR2, minimal C5a-induced calcium flux,[230] degranulation,[215] C5aR2 phosphorylation or extracellular signal related kinase (ERK) phosphorylation[229] occurred. Bamberg and colleagues demonstrated that C5aR2 co-localised with β-arrestins after C5a stimulation of primary human neutrophils and downregulated ERK1/2 signalling,[231] a known mechanism of GPCR signal modulation.[232] Van Lith[233] and Cui[234] also demonstrated similar colocalization of C5aR2 with β-arrestins in transfected human osteosarcoma and embryonic kidney cells respectively. This work was extended by Croker et al, who showed that C5aR2-related inhibition of ERK activation may be related to C5aR1/2 heteromer formation in human monocyte-derived macrophages.[235] Collectively, these findings lent weight to the hypothesis that C5aR2 may act as a 'decoy' receptor or even dampen C5a responses.[227,229,236] From the conflicting data presented, it is difficult to make generalisations about the relative role of C5aR2, and indeed any effects are almost certainly context-dependent. Bearing this in mind, we now turn to the effects of C5a on key organ systems and neutrophils in the context of critical illness.

3.4. C5a in critical illness: effects on key organ systems

In critical illness states there is systemic overspill of cytokines, DAMPs and PAMPs (see Section 2).[102,185] A similar phenomenon occurs with C5a; rather than localised, controlled generation of the anaphylatoxin, C5a is generated in massive quantities throughout the

circulation, saturating its receptors on organ systems and driving the effects discussed below.[92,208]

3.4.1. Cardiovascular system and endothelium

C5a induces cardiac dysfunction in multiple rodent models, with defects being detectable by echocardiography in as little as 8 hours.[126,237,238] The roles of mitogen activated protein kinases, action potential disturbances and the inflammasome have only more recently been elucidated in subsequent studies by the same group.[238–240] With respect to the endothelium, C5a stimulates tissue factor and adhesion molecule expression with resulting disruption of the endothelial glycocalyx, leading to further DAMP release into the circulation.[127,185,241] Collectively, these data indicate C5a worsens cardiovascular dysfunction both through vascular leakage and pump failure, exacerbating refractory shock and tissue hypoperfusion.

3.4.2. Platelets and coagulation

There are multiple sites of interaction between the complement and coagulation cascades, two evolutionarily ancient but distinct systems, which aim to maintain homeostasis in the face of infection and haemorrhage respectively.[199,242] The importance of this interplay cannot be overstated in the setting of critical illness, where haemorrhage and pathogen invasion frequently co-exist and disseminated intravascular coagulopathy (DIC) is common.[185] C5a has been shown to play an important role in the interaction between these two systems; it may be generated by multiple enzymes present at the site of clot, including thrombin,[190] tissue plasminogen activator,[243] damaged endothelium, plasmin,[185] elastase and free DNA.[242] Furthermore, C5a and other complement products, once generated, go on to induce platelet activation, endothelial glycocalyx disruption,[185] leukocyte-platelet aggregation and further tissue factor activation.[244–248] Once this vicious cycle begins, microvascular occlusion, endothelial damage and tissue hypoxia follow, worsening organ damage and mortality.[97,127–129,249]

3.5. C5a in critical illness: effects on neutrophils

Data from the Ensembl database[250] indicate both C5a receptors are widely transcribed (reviewed by Lee et al[227]) and enriched amongst cells of the immune system, particularly in neutrophils and monocytes, suggesting a key role in the modulation of innate immunity. Transcriptional data almost certainly does not fully reflect the tissue-specific expression of C5a receptors, and it is likely that new data arising from systematic proteomic studies will shed new light on this important area in the near future. Below is a brief outline of the known effects of C5aR1 and C5aR2 ligation in human neutrophils, with substitution of animal data where human studies have not yet been conducted.

C5a has long been known to induce chemotaxis in neutrophils.[251,252] More recently, the signalling pathways driving chemotaxis and ROS production have been elucidated. After C5a

ligation of C5aR1, conformational changes activate the α- and βγ-subunits of the G-protein complex. The α-subunit activates the small guanosine triphosphatase (GTPase) Ras, whereas the βγ-subunits activate adenylyl cyclase, phospholipase C (PLC) and other downstream targets including PI3K.[92,227,253,254] Ras can also independently activate PLC. Specifically of relevance to chemotaxis is the spatial localisation of PtdIns(3,4,5)P_3 and its key phosphatase, phosphatase and tensin homolog (PTEN), to the leading edge and peripheries of the cell respectively,[255,256] allowing actin polymerisation and directional migration in the presence of multiple chemoattractants.[257,258]

Phosphorylated PLC strongly activates protein kinase C (PKC) which leads to downstream activation of the mitogen activated protein kinase (MAPK)/extracellular signal-related kinase (ERK) pathway and mobilisation of intracellular calcium stores.[92,227,253] Activation of the MAPK pathway results in translocation of the cytosolic subunits of the NADPH oxidase to cellular and phagosomal membranes and the generation of ROS.[179,259,260] Recent reports by Denk and colleagues demonstrated that C5a-C5aR1 interactions lead to sodium/hydrogen exchanger (NHE1) dependent changes in intracellular pH and fluid content, driving neutrophil degranulation, shape change and chemotaxis.[261,262] C5aR1 ligation also prolongs neutrophil survival through potentiation of the Akt/Bad pathway and decreasing activity of the pro-apoptotic caspase 9.[227,263,264] In neutrophils, the effects of C5a on ROS production and apoptosis have been demonstrated to be dependent on phosphoinositide signalling.[259,263–265]

Phagocytosis is also affected by C5a. Ingestion of *E. coli* by neutrophils and monocytes in a human whole-blood model was shown to be dependent on preserved C5a-C5aR1 interactions.[266] The authors postulated that the effect was mediated by upregulation of the complement receptor 3 complex (CR3) on leukocyte membranes, which increases phagocytosis by binding to its ligand iC3b deposited on pathogen surfaces during opsonisation.[200,266,267] A similar C5a-mediated CR3 upregulation and increased phagocytosis was demonstrated by Demaster and colleagues using streptococci.[268]

In the context of critical illness, the effects of C5a on neutrophils appear divergent from the effects identified above. As discussed above, C5a signals through pathways known to drive chemotaxis, form ROS and enhance phagocytosis. One would think these enhanced immune responses would be of benefit in critical illness states, where control of pathogens is necessary. However, a seminal study published in 1999 by Czermak and colleagues[269] demonstrated a survival benefit of C5a blockade in a CLP-induced sepsis model in rats. The authors showed that antibody blockade of C5a resulted in increased neutrophil ROS production and better control of bacterial outgrowth, evidenced by bacterial colony forming unit counts in liver and spleen, relative to control-treated animals.[269]

Since the late 1990s, advances have been made in understanding the mechanism of these effects. Huber-Lang and colleagues demonstrated in 2002 that pre-exposure of adherent, purified, rat neutrophils to C5a reduced phagocytosis of opsonised zymosan particles, as well as subsequent ROS production and chemotaxis in similar studies.[179,270,271] Further studies also showed a deleterious effect of C5a in sepsis induced by caecal ligation and puncture (CLP) in mice.[179,269,270] Work from our group has demonstrated pivotal roles for the small GTPase RhoA and PI3K-δ in mediating the C5a-induced reduction in phagocytosis.[213] This work showed that PI3K-δ inhibition prevented the C5a-dependent impairment of phagocytosis of serum-opsonised zymosan by adherent human neutrophils, and that this was accompanied by restored RhoA activity.[213] This inhibitory role for PI3K-δ is supported by work from Papakonstanti and colleagues[272] who suggested active PI3K-δ inhibits RhoA activation via p190 Rho-GTPase activating protein (GAP). Papakonstanti went on to demonstrate that in a mouse macrophage cell line with constitutively inactivated PI3K-δ, RhoA activity was increased, and that it returned to wild-type levels when RhoA's downstream effector Rho-associated, coiled-coil-containing protein kinase 1 (ROCK) was inhibited.[272] Beta-adrenoreceptor agonist induced defects in phagocytosis are also mediated by PI3K-delta and inhibition of RhoA,[273] although in contrast to the C5a-induced defect, adenylyl cyclase is a key upstream mediator in this setting.[177,213] These signalling effects of C5aR1 ligation in neutrophils are summarised in Figure I-2.

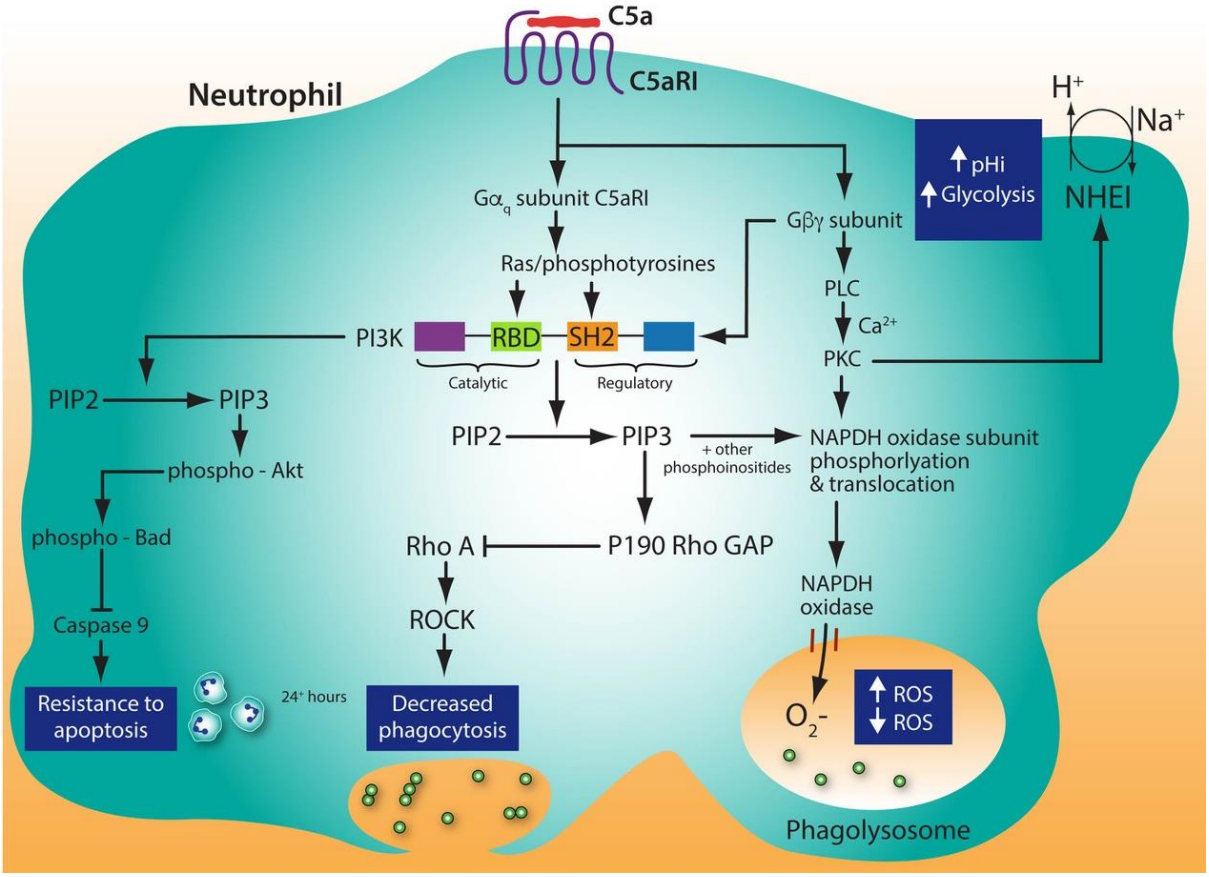

Figure I-2: C5a-induced signalling through C5aR1 affecting key neutrophil functions

Signalling in neutrophils after C5a-C5aR1 ligation leads to activation of cAMP (not shown), PLC and Ras. Phosphorylated PLC activates PKC which leads to MAPK/ERK signalling, release of calcium, phosphorylation of the NADPH oxidase and activation of NHE1.[179,261] These events lead to translocation of the oxidase to the phagosome, increased intracellular pH and glycolysis. The dual effect of C5a on ROS production appears to be dependent on whether C5a exposure is a primary stimulus (generates ROS) or occurs prior to another stimulus (dampens subsequent ROS production).[179,259] C5aR1 activation also leads to the inhibition of caspase 9 activity mediated by p-Akt, resulting in prolonged neutrophil survival.[263,264] The effect of C5a on phagocytosis appears to be mediated through PI3K signalling and inhibition of RhoA/ROCK activity, which is required for effective actin polymerisation and phagocytosis.[213,272] cAMP: cyclic adenosine monophosphate; MAPK: mitogen-activated protein kinase, also known as ERK: extracellular signal-regulated kinase; NADPH: nicotinamide adenine dinucleotide phosphate-oxidase; NHE1: sodium/hydrogen exchanger 1; p190RhoGAP: Rho GTPase activating protein 190; PI3K: phosphatidylinositol-3-kinase; PIP2: phosphatidylinositol 4,5-bisphosphate; PIP3: phosphatidylinositol 3,4,5-trisphosphate; PKC: protein kinase C; PLC: phospholipase C; RBD: Ras-binding domain; ROCK: Rho-associated, coiled-coil-containing protein kinase; ROS: reactive oxygen species; SH2: Src homology domain.

These *in vitro* findings have more recently been extended to human critical illness, where neutrophil phagocytosis and bactericidal capacity is defective, and decreased C5aR1 expression (indicating C5a exposure) is correlated with the development of nosocomial infection.[147,177,213] In addition to C5aR1 downregulation, C5aR2 is also involved; data from septic humans showed associations between C5aR2 downregulation, multi-organ failure and death.[226]

In addition to disruption of vital neutrophil functions, C5a exerts a number of effects on macrophages and their circulating precursors. C5aR1 and C5aR2 are highly transcribed in monocytes (similar to neutrophils) but less abundantly so in tissue macrophages.[92,210,250] C5a is able to potentiate LPS-induced production of TNF-α by alveolar macrophages in rats, and is required for efficient *E. coli*-induced ROS production in human circulating monocytes.[266,274] In addition to TNF-α production, C5a induces HMGB-1 production through C5aR2 in mouse peritoneal macrophages.[127,210] Paradoxically, macrophages seem to have enhanced functional responses following exposure to C5a, whereas neutrophil function is depressed. This may be due to reduced receptor expression in macrophages, or may reflect changes in monocyte/macrophage signalling mechanisms induced by endothelial transmigration and the differentiation from monocyte to macrophage.[275] A summary of C5a-induced effects on key organ systems in critical illness is provided in Figure I-3.

It has been hypothesised that the divergence of C5a-induced effects is due to the concentration of C5a present.[92,270,276] However, published dose-response curves do not support this biphasic response. To my knowledge, published data only demonstrate decreasing phagocytosis[177,270] and increasing ROS production[277,278] with increasing concentrations of exogenous C5a in the absence of other stimulants. However, regardless of potential concentration effects, preliminary data from our lab (discussed in Chapter V:) indicate that timing of C5a exposure with respect to pathogen encounter may be a critical factor that drives different responses. While C5a can facilitate neutrophil phagocytosis, ROS production, and bacterial killing when pathogens are encountered, exposure to C5a prior to such encounters may result in subsequent inhibition of these processes during pathogen encounter, potentially driving susceptibility to nosocomial infection and increased mortality.[147,177,213,269–271] Whilst some key signalling ‘nodes’ have been identified in previous studies, a comprehensive picture of C5a-induced signalling in neutrophils has yet to be compiled, and could yield important functional and therapeutic insights.

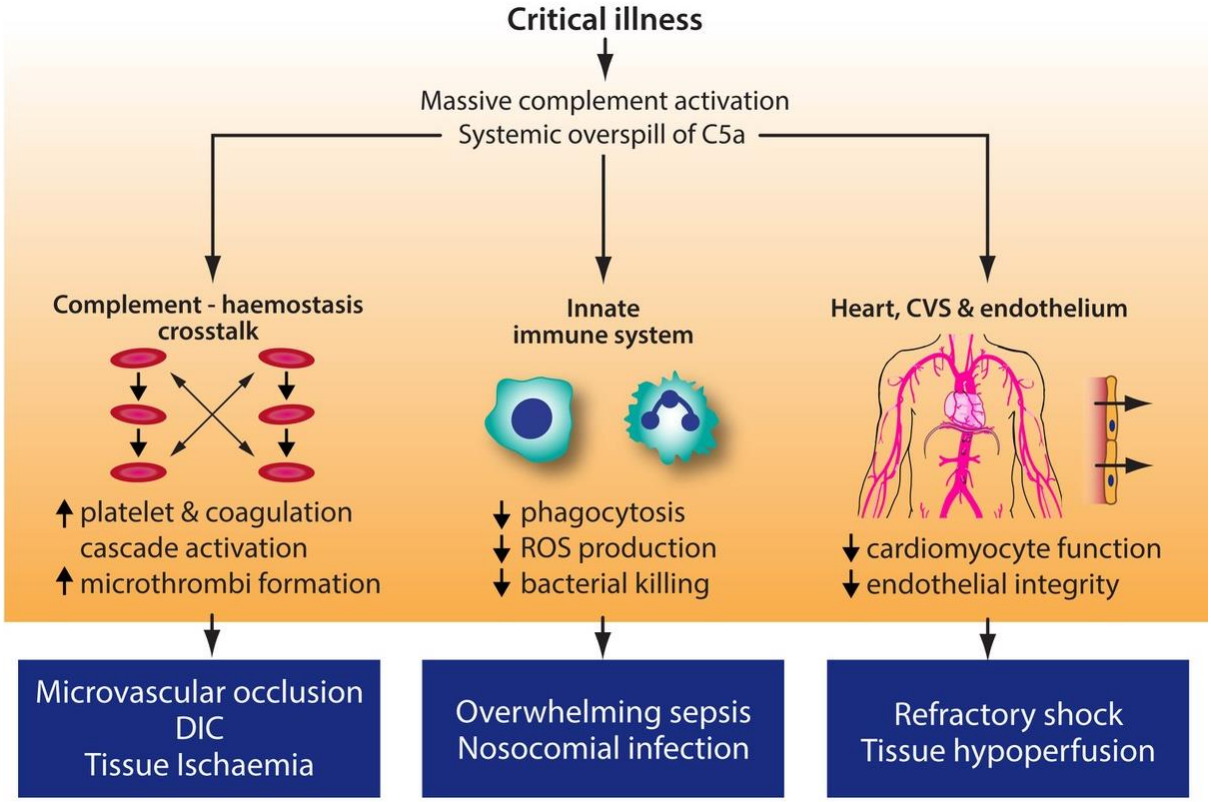

Figure I-3: C5a-induced organ dysfunction during critical illness

During critical illness, unbridled activation of the complement pathway occurs, leading to systemic overspill of complement proteins, particularly C5a. In this context, C5a leads to widespread platelet activation and thrombus formation, reduced cardiomyocte function and impaired antimicrobial activity of the innate immune system.[177,179,238]

3.6. Therapies targeting C5a

C5a signalling is an attractive therapeutic target in critical illness, given its multiple deleterious functions, the need for novel immunomodulatory therapies and increasing antimicrobial resistance in the intensive care unit.[111,185] Anti-C5a antibodies have been employed for many years and have shown significant mortality benefits in animal sepsis models.[179,269,279] Despite such promising findings, the only licenced therapy which manipulates the C5a axis directly is eculizumab. This monoclonal antibody targets C5, preventing the generation of both C5a and the terminal complement complex. Blockade of C5 in this way reduces complement-mediated intravascular haemolysis, which is the hallmark of paroxysmal nocturnal haemoglobinuria, the disease for which eculizumab is licenced.[280] However, the increased susceptibility of patients treated with eculizumab to *Neissieria spp* infection (likely due to impaired complement haemolytic activity) sounds a note of caution with respect to use of this agent in a critical illness context.[281]

Newer monoclonal antibodies which selectively target C5aR1 and/or 2 without inhibiting membrane attack complex formation are currently in various stages of development for

indications as diverse as macular degeneration and vasculitis.[282–285] Of key relevance to critical illness is IFX-1, a monoclonal antibody which has enjoyed success in phase II dose-escalation trials for early sepsis-induced organ dysfunction, though full trial results have not yet been reported.[286]

4. Chapter summary and areas for further research

Neutrophils are now known to be much more than the simple infantry of the immune system, with a diverse array of effects on multiple cell types and the ability to rapidly adapt to diverse environments. Amongst these functions, neutrophil phagocytosis, and the subsequent maturation of the phagosome are critical events for pathogen killing. In the context of critical illness, which often culminates in nosocomial infections, organ failure and death, neutrophil dysfunction is pronounced, and has been correlated with numerous patient-centred outcomes. The causes of neutrophil and the broader immune dysfunction observed in these patients are the subject of ongoing investigation, though it is clear a key mediator is the anaphylatoxin C5a.

Whilst our understanding of C5a and critical illness biology has increased substantially in the last two decades, fundamental questions remain. The *in vitro* effects of C5a exposure on neutrophil phagocytosis have not been assessed in the context of clinically relevant pathogens, or over periods of time greater than one hour. Further, whilst changes in C5aR1 expression have been documented in response to C5a, the fate of the receptor has yet to be interrogated in settings in which C5a clearly has an impact, such as phagocytosis. There remains a relative paucity of data on interactions between cells of the immune system after exposure to C5a in clinically relevant models such as human whole blood. Often, studies of critical illness-related immune dysfunction have measured cell surface marker expression or cytokine levels, rather than cellular function in response to a known stimulus. Quantifying important cellular functions is currently cumbersome and not scalable, hampering our understanding of important biology in clinical settings.

Finally, our understanding of C5a-induced intracellular signalling networks in immune cells was generated using inhibitors and pull-down assays in isolated cell populations.[179,213] The field will benefit from unbiased transcriptomic or proteomic approaches which more completely capture the complex networks involved, and may uncover previously unappreciated signalling processes. This thesis aims to address these issues and hypotheses pertaining to them are presented in each experimental chapter.

Chapter II: Methods

1. Consumables and reagents

Table 1: Consumables and reagents

Consumable/reagent	Supplier	Location
IPI-549 PI3K inhibitor	Active Biochem	Kowloon, Hong Kong
Methicillin sensitive *S. aureus* strain ASASM 6	Addenbrooke's microbiology laboratory	Cambridge, UK
CAL-101 PI3K inhibitor	ApexBio	Boston, USA
Pasteur pipettes, strippettes (10 ml, 25 ml)	Appleton Woods	Birmingham, UK
Sterile saline (0.9%)	Baxter Healthcare	Berkshire, UK
CellFIX stock solution, polypropylene Falcon tubes (15 ml, 50 ml), polystyrene round bottom tube (5 ml), syringes (50 ml)	BD Biosciences	Oxford, UK
Bio-Rad Quick start protein assay kit, lipoteichoic acid (LTA)	Bio-Rad	Watford, UK
Purified human C5a	Complement Technology Inc	Tyler, USA
5ml round bottom polystyrene FACS tube	Corning	New York, USA
PCR-clean 2 mL safe-lock microcentrifuge tubes	Eppendorf	Hamburg, Germany
Dextran 500, ECL prime western blotting detection reagent, high performance chemiluminescence film	GE Healthcare	Little Chalfont, UK
19-gauge Butterfly needle	Hospira	Lake Forest, UK
AF488 *S. aureus* (Wood strain) Bioparticles, phenol red-free Iscove's Modified Dulbecco's Medium (IMDM), pHrodo Bioparticles (*E. coli*, *S. aureus*), trypan blue, Abc total antibody compensation beads	Life Technologies	Paisley, UK
Sterile calcium chloride, sterile sodium citrate	Martindale/Ethyfarm	Wooburn Green, UK
24-well cover glass imaging plates	Miltenyi Biotech	Bergisch-Gladbach, Germany
Dried semi-skinned milk powder	Premier Foods	St Alban's, UK
Argatroban, secretory leukocyte protease inhibitor (SLPI), TNF-α	R&D Systems	Abingdon, UK
S-Monovette citrate, EDTA, heparin vacutainers, 24- and 96- well tissue culture plates	Sarstedt	Numbrecht, Germany
Cytocentrifuge white filter cards, Diff-Quick stain kit	Shandon Lipshaw	Pittsburgh, USA
Ammonium persulfate, calcium chloride, chloroform, diphenyleneiodonium chloride (DPI), Dulbecco's phosphate buffered saline, fMLP, glycine, hydrochloric acid, lipopolysaccharide derived from *E. coli*, Luria broth base, lyophilised bovine serum albumin (BSA), lyophilised zymosan particles, marimastat	Sigma-Aldrich	Dorset, UK

metalloprotease inhibitor, methyl methanethiosulfonate, Percoll Plus, polyvinylidene difluoride membrane, sodium dodecyl sufate (SDS), tris(2-carboxyethyl)phosphine (TCEP), Triethylammonium bicarbonate (TEAB), Triton X-100, Trizma base, Tween-20		
Pipette tips (graduated, filter tip)	Starlab	Milton Keynes, UK
12 % NuPage Bis-Tris gels, GM-CSF, HALT protease inhibitor cocktail, High-Select™ Fe-NTA Phosphopeptide enrichment Kit, PageRuler Plus prestained protein ladder, pHrodo dye conjugation kit, Pierce trypsin protease, RPMI 1640 media (phenol-free), TMT labelling kit	ThermoFisher Scientific	Massachusetts, USA
PAF	Tocris Bioscience	Abingdon, UK
DPX mountant, glycerol, methanol	VWR International	Lutterworth, UK

Table 2: Antibodies and stains for flow cytometry, fluorescence microscopy or western blotting

Antibody	Supplier	Location
BV421 mouse anti-human CD54 clone LB.2	BD Biosciences	Oxford, UK
BV711 mouse anti-human CD64 clone 10.1		
PerCP/Cy5.5 mouse anti-human C5aR1 clone S5/1	Biolegend	London, UK
PerCP/Cy5.5 mouse isotype control clone MOPC		
BV605 rat anti-mouse/human CD11b clone M1/70		
Pacific Blue mouse anti-human CD16 clone 3G8		
Purified mouse IgG2a, κ Isotype Ctrl clone MG2A-53		
Purified mouse anti-C5aR1 clone S5/1		
PerCP-Cy7 mouse anti-human CD32 clone FUN-2		
FITC mouse anti-human C5aR1 IgG2a antibody, clone S5/1	BioRad	Hertfordshire, UK
FITC mouse IgG2a isotype control		
DRAQ7 far-red fluorescent live/dead stain	Biostatus	Leicestershire, UK
Dihydrorhodamine (DHR) ROS probe	CalBiochem	Watford, UK
Rabbit anti-human Akt primary	Cell Signalling Technologies	Hitchin, UK
Rabbit anti-human p-Akt primary		
HRP polyclonal goat anti-rabbit IgG secondary	Dako Agilent Technologies	Stockport, UK
AF488-phalloidin	ThermoFisher Scientific	Massachusetts, USA
Hoechst 33342		
AF488 mouse anti-human TNFR1 clone H398		
AF488 mouse IgG1 isotype control		
AF568 polyclonal goat anti-mouse IgG secondary		

2. Preparation of human neutrophils

Ethical permission for taking peripheral blood from healthy volunteers was obtained from the Cambridge Local Research Ethics Committee (REC reference 06/Q0108/281). Neutrophils were isolated from citrated peripheral blood by using a modification of the technique initially described by Böyum in 1968,[287] routinely employed in the Chilvers'/Summers' laboratory. Briefly, red cells were removed by dextran sedimentation of whole blood, before the leukocyte-rich layer was aspirated and centrifuged over 42 and 51 % plasma-Percoll gradients. Granulocytes (including neutrophils) separate from peripheral blood mononuclear cells (PBMCs) according to density, with granulocytes located at the interface between the 51 and 42 % gradients. The granulocyte layer is then aspirated, washed, counted and checked for purity > 95 % by cytospin before resuspension in the required media for use in experiments. The complete neutrophil preparation protocol is provided in the Appendices.

3. Prepared neutrophil viability

Neutrophil purity and cell viability were assessed by visual examination of cytospins under light microscopy at a magnification of 400X. Numbers of neutrophils, red blood cells (RBCs), PBMCs and eosinophils were counted in three fields containing at least 100 cells for each preparation. Preparations yielding a neutrophil purity ≥ 95 % were used in subsequent experiments.

4. Phagocytosis of zymosan by adherent, purified neutrophils

Purified human neutrophils (suspended in phenol red-free IMDM with 1 % autologous serum (AS) at a concentration of 10^6/mL) were allowed to adhere to 24-well tissue culture plates for 20 minutes, before being exposed to 100 nM C5a or vehicle control for 30 minutes as previously reported.[177] Opsonised zymosan (five µg/mL) was then added for 30 minutes, before non-internalised zymosan particles were washed off with warm IMDM. Plates were incubated at all stages at 37 °C in 5 % CO_2. Plates were allowed to air dry before being fixed with methanol and stained with QuickDIFF staining kit. Phagocytosis was measured by manual counting of cells under light microscopy at 400 X. Neutrophils with ≥ 2 internalised zymosan particles were counted as a proportion of total neutrophils in two separate fields per well as previously described.[177] Each condition was run in triplicate.

5. Phagocytosis of pHrodo *S. aureus* and *E. coli* Bioparticles by purified neutrophils

pHrodo Bioparticles™ (referred to as Bioparticles throughout the remainder of this thesis) are microbe particle-dye conjugates used to assess phagocytosis. The complex consists of a proprietary pH-sensitive fluorophore (pHrodo 'green' or 'red') conjugated to either heat-killed

S. aureus, *E. coli* or zymosan derived from *S. cerevisiae*. The pH-sensitive nature of the dye means it increases fluorescence in acidic conditions,[288] such as inside the phagolysosome and therefore allows for the detection of phagocytosis without the need to quench extracellular fluorescence from non-phagocytosed, cell adherent particles. A detailed protocol for the use of Bioparticles to assess phagocytosis is included in the Appendices. In brief, purified human neutrophils (200 µL suspended in phenol red-free IMDM with 1 % AS at a concentration of 5 x 10^6/mL) were incubated in 2 mL round-bottom microcentrifuge tubes with C5a or controls for one hour. Meanwhile pHrodo-conjugated *S. aureus* or *E. coli* Bioparticles were serum opsonised, by incubation in 50 % AS. Opsonised Bioparticles were then added to the neutrophil suspension for 120 minutes, before the mixture was fixed (1:40 BD CellFIX) and analysed by flow cytometry (FACSCalibur and Accuri C6; BD Biosciences, Attune Nxt™; Life Technologies). Phagocytosis was quantified by the phagocytic index[53] (PI: percentage of Bioparticle-positive cells x the median fluorescence intensity (MFI) in the relevant channel).

6. Confirmation of flow cytometry phagocytosis signals

The purpose of these experiments was to provide visual evidence of pHrodo Bioparticle fluorescence inside human neutrophils, to support the work done by flow cytometry. These experiments are not intended for quantification purposes in their current form. Purified human neutrophils (200 µL suspended in phenol red-free IMDM with 1 % AS at a concentration of 5 x 10^6/mL) were incubated in 2 mL round-bottom micro-tubes with semi-log increasing ratios of Bioparticles:PMNs for 120 minutes. Cells were then fixed, stained with DAPI for 10 minutes and analysed on an ImageStream X Mark II cytometer (Millipore; Hertfordshire; UK) which allows cell-by-cell concurrent fluorescence microscopy and flow cytometry.

7. Confocal microscopy of purified human neutrophils

Confocal microscopy was used to confirm pHrodo particle ingestion and fluorescence as well as to localise C5aR1. Purified human neutrophils at a concentration of 10^6/mL in RPMI 1640, 10 mM HEPES and 1 % AS were adhered to AS-coated 24-well glass imaging plates for 30 minutes in the presence of Hoescht 22342. Neutrophils were fixed using 1:40 diluted BD CellFix, washed and permeabilised with 0.1 % Triton X-100 and blocked in 5 % BSA for 60 minutes. Primary antibodies were added, and cells stained for 60 minutes. Cells were washed, secondary antibodies or stains were added, and cells stained for 60 minutes protected from light. Neutrophils were washed, left in PBS and visualised by confocal microscopy at 630 X magnification using a Leica Sp5 confocal microscope (Leica Microsystems, Milton Keynes, UK). Antibodies used are specified in relevant figure legends and Table 1.

8. PtdIns(3,4,5)P_3 production assay

In order to independently confirm that C5a generates PtdIns(3,4,5)P_3 intracellularly in human neutrophils, a highly sensitive mass spectrometric method was employed as previously described.[289] Neutrophils were isolated according to our standard protocol and resuspended at a concentration of 3 x 10^7/mL in PBS containing Ca^{2+} and Mg^{2+}. Aliquots of cells (170 uL) in triplicate were primed with 100 ng/mL LPS or PBS control for 30 minutes. Cells were then stimulated with fMLP (100 nM), C5a (100 nM) or PBS control for 15 seconds, before reactions were quenched by addition of 750 uL ice-cold quench mix (65 % methanol, 32 % chloroform and 3 % 1M HCl) before storage at -80°C for transport to the Babraham Institute, Cambridge, UK. I observed the remainder of this process being carried out by Dr Karen Anderson working within Professor Len Stephen's laboratory at the Babraham Institute.

Lipids were extracted by centrifugation into lipid and protein phases and a non-organic PtdIns(3,4,5)P_3 internal standard was spiked into the mixture to allow quantification of neutrophil-derived PtdIns(3,4,5)P_3. Lipids were derivatised using trimethylsilyl diazomethane, which chemically protects the acidic phosphate groups on PtdIns(3,4,5)P_3 allowing for accurate identification by mass spectrometry. Complete details of this experimental protocol and mass spectrometer settings is available in the group's 2011 paper.[289] PtdIns(3,4,5)P_3 abundance was quantified as a ratio of the C38:4 species to the spike-in internal standard, thus accounting for differences in lipid extraction and derivatisation during this process.

9. Bacterial killing assay

Methicillin-sensitive *Staphylococcus aureus* (MSSA) bacteria were grown on a Columbia blood agar plate overnight at 37 ^oC in 5 % CO_2. A single colony-forming unit (CFU) from the plate was removed and cultured in 10 mLs of Luria broth (LB) overnight at 200 rpm, 37 ^oC. 50 μL of this liquid culture was placed into a fresh 10 mLs of LB and grown to early log-phase growth indicated by an optical density (OD) of 0.5 – 0.7, which took approximately 3 hours.

In the interim, neutrophils were prepared at a concentration of 5 million/mL in IMDM. 180 μL of the cell solution was transferred into 2 mL round-bottom Eppendorf tubes and treated with 100 nM C5a or PBS vehicle control for 60 minutes. 10 μL of the final MSSA culture was subsequently fed to the pre-treated neutrophils with an average multiplicity of infection (MOI) of 10:1, for one hour at 200 rpm, 37 ^oC. 50 μL of the cell solution was transferred to 450 μL of pH 11, distilled water for 3 minutes to lyse the neutrophils without adversely affecting MSSA viability. The solution was then vigorously vortexed for 15 seconds and 1 μL transferred to 999 μL of LB. 100 μL of this final dilution was plated and grown overnight at 37 ^oC at 5 % CO_2. CFUs were visually counted the following morning. These experiments were planned by myself but carried out by my colleague, Dr Arlette Vassallo. I am very grateful for her assistance.

10. No-wash, no-lyse whole blood assay of neutrophil phagocytosis and ROS production

The method discussed here is an adaptation of work initially described by Life Technologies[290] and a detailed protocol for this procedure is included in the Appendices. Blood was drawn from a peripheral vein into the anticoagulant of choice (Ethylenediaminetetraacetic acid (EDTA), trisodium citrate, heparin or argatroban where specified). The initial choice of anticoagulant was informed by work from Mollnes, Brekke and colleagues[266,267] which showed that direct thrombin inhibitors (lepirudin was used in their studies but is no longer available so argatroban was substituted) allowed complement activation and minimally affected leukocyte function. This was subsequently confirmed in my own experiments shown in Figure IV-2. Argatroban concentration was 150 µg/mL, which was the lowest concentration allowing for successful macroscopic anticoagulation at 37 °C for 7 hours. Concentrations of EDTA, citrate and heparin when used were 1.6 mg/mL, 27.34 µg/mL and 16 IU/mL as determined by their respective Sarstedt vacutainers listed in Table 1.

Blood was treated with inhibitors or priming agents as indicated in respective figure legends. After treatment, 50 µL of blood was aliquoted into 96 well plates in triplicate and a combined *S. aureus* pHrodo red/dihydrorhodamine-123 (DHR) probe was added at final concentrations of 15 µg/mL and 3 µM respectively. The function of pHrodo is to indicate phagocytosis as discussed in Section 5 of this chapter. Dihydrorhodamine-123 is a non-fluorescent compound that is readily oxidised by ROS to polarised rhodamine-123, which remains intracellular owing to its electrostatic charge, and can be detected by devices such as flow cytometers or confocal microcopes.[291] Volume was made up to 100 uL with RPMI 1640 and plates were incubated at 37 °C and 5 % CO_2 for 30 minutes to allow phagocytosis to occur. 5 uL from each well was transferred into ice-cold RPMI 1640 media in flow cytometry tubes and stained with anti-CD16 antibody on ice in the dark for 30 minutes. Volume was made up to 4 mL with ice-cold PBS before the cells were analysed on an Attune Nxt™ Acoustic Focusing Cytometer (LifeTechnologies, Paisely, UK). This cytometer uses a combination of hydrodynamic and ultrasound focusing to allow much higher flow rates (up to 1 mL/minute) and consequent processing of highly dilute samples. Dilution of RBCs in this way allows discrimination from leukocytes based on cell-surface markers or violet laser scatter properties, as shown in Figure IV-1. Neutrophils were gated on CD16 expression and light scatter properties, phagocytosis was quantified by phagocytic index (excitation 561 nM, emission 585/16 nM) as previously described and ROS production by MFI of the DHR signal (excitation 488 nM, emission 530/30 nM).

10.1. *S. aureus* pHrodo vs AlexaFluor 488 assessment

In a slight variation to this assay, a non pH-sensitive fluorophore (AlexaFluor 488: AF488) was used to confirm that the results with the pHrodo dyes were not simply due to an effect of C5a on intracellular pH. In these experiments, blood was drawn as usual and aliquoted into 96-well plates. The *S. aureus*-AF488 probe (without DHR) was added at a concentration of 15 µg/mL and plates were incubated at 37 °C and 5 % CO_2 for 30 minutes to allow phagocytosis. 5 uL from each well was transferred into ice-cold RPMI 1640 media in flow cytometry tubes and fluorescence of extracellular particles was quenched with 15 µL of trypan blue. Volume was made up to 4 mL with ice-cold PBS before the cells were analysed on an Attune Nxt™ as previous. Violet laser scatter properties were used to identify the neutrophil population as trypan blue prevents the use of extracellular antibody stains.

10.2. Dual phagocytic challenge

Another variation to the basic phagocytosis assay made use of two pHrodo *S. aureus* Bioparticles with different fluorescence excitation and emission properties; pHrodo green and pHrodo red. These two Bioparticles can be measured in separate channels by flow cytometry, allowing for assessment of phagocytosis of two different particles or 'meals' in the same sample. Blood was drawn and treated with inhibitors or priming agents as indicated in respective figure legends. After treatment, 50 µL of blood was aliquoted into 96 well plates in triplicate and the first Bioparticle *S. aureus* pHrodo red was added at a final concentration of 15 µg/mL and incubated for 30 minutes at 37 °C and 5 % CO_2 to allow phagocytosis to occur. The second Bioparticle *S. aureus* pHrodo green was then added and cells were allowed to phagocytose as before. 5 uL from each well was transferred into ice-cold RPMI 1640 media in flow cytometry tubes and stained with anti-CD16 antibody on ice in the dark for 30 minutes. Volume was made up to 4 mL with ice-cold PBS before the cells were analysed on an Attune Nxt™.

10.3. Phagosomal maturation assessments

Combinations of fluorophores were used to provide an assessment of phagosomal maturation. AlexaFluor 488-labelled *S. aureus* Bioparticles as above were conjugated to pHrodo dye according to the manufacturer's instructions, providing a particle that could measure internalisation in a non-pH dependent manner (AF488) as well as an estimate of phagosomal acidification (pHrodo).[292] In duplicate conditions, DHR was used in combination with pHrodo *S. aureus* red as previously described to provide a side-by-side assessment of phagosomal ROS production as the final component of phagosomal maturation.

10.4. Patient recruitment

Patients were recruited under existing local ethical approvals (12/WA/0148) from routine immunology outpatient clinic appointments at a tertiary referral centre. Written informed consent was obtained directly from patients. Inclusion criteria were: age 16 – 75 years and a diagnosed congenital immunodeficiency syndrome. Exclusion criteria were: cancer diagnosis, HIV infection, pregnancy or lack of informed consent.

11. Whole blood assay of neutrophil ROS production

Blood was drawn from a peripheral vein into 150 µg/mL argatroban and 50 uL of blood was aliquoted into 2 mL microcentrifuge tubes in triplicate. Cells were primed with 20 ng/mL TNF-α and the volume made up to 100 uL with RPMI 1640 media. Cells were incubated at 37° C and 300 rpm in a thermomixer for 30 minutes. Dihydrorhodamine-123 and fMLP were then added at concentrations of 30 µM and 1 µM respectively and cells were incubated for 20 minutes. Tubes were placed on ice and stained with anti-CD16 antibody for 30 minutes in the dark, before ice-cold PBS was added to make the volume up to 2 mL. Cells were analysed on an Attune Nxt™ Acoustic Focusing Cytometer, neutrophils were gated based on CD16 and light scatter properties and ROS was quantified by MFI of the DHR signal.

12. Whole blood phagocytic receptor profiling

Blood was drawn from a peripheral vein into 150 µg/mL argatroban and 50 uL of blood was aliquoted into 2 mL microcentrifuge tubes in triplicate. Blood was pre-treated as indicated in figure legends before 5 uL of blood was transferred into 95 µL ice-cold RPMI 1640 media in flow cytometry tubes containing antibody master-mix. The master-mix consisted of pre-titrated dilutions of the following antibodies: ICAM-1, 1:40; CD11b, 1:50; CD16, 1:200; CD88, 1:100; CD32 1:50. Manufacturer and clone details can be found in Table 1. Tubes were placed on ice and stained for 30 minutes in the dark, before ice-cold PBS was added to make the volume up to 2 mL. Cells were analysed on an Attune Nxt™.

13. Preparation of whole human neutrophil lysates

Neutrophils were isolated from whole blood as detailed in Section 2 and resuspended in RPMI 1640 media containing 10 mM HEPES with 1 % AS at a concentration of 10×10^6 cells/mL. Cells were treated as detailed in figure legends, centrifuged at 400 g for 5 minutes at 4 °C, supernatants were aspirated and cell pellets were snap frozen in liquid N_2 at relevant time points. Lysis buffers (detailed in Table 3) were added and cells were subjected to freeze thaw cycles or sonicated to achieve cell lysis. Lysates were centrifuged at 20 000 g at 4 °C for 10 minutes to remove insoluble fractions and stored at – 70 °C until use.

Table 3: Lysis buffers for neutrophil protein extraction

Lysis buffer	Base	Protease/phosphatase inhibitors	Procedure
4 % SDS	4 % sodium dodecyl sulfate (SDS) 250 mM Tris-HCl pH 6.8 20 % glycerol v/v	Pepstatin A 10 µg/mL Aprotinin 10 µg/mL Leupeptin 10 µg/mL ABSF 1mM	Add 200 µL to 10 x 10^6 cells. 2 x freeze-thaw cycles (dry ice – room temperature) followed by vigorous vortexing.
SDS/ TEAB	0.5 % SDS 0.1 M triethylammonium bicarbonate (TEAB)	1 X or 3 X HALT™ protease and phosphatase inhibitor cocktail as specified in figure legends.	Add 200 µL to 10 x 10^6 cells. 1 x freeze-thaw cycle and 2 x 20 s probe sonication.

14. SDS-polyacrylamide gel electrophoresis (SDS-PAGE)

Lysate protein concentration was determined by Bradford Protein Assay (Bio-Rad, Quick Start). Proteins were reduced by heating to 90 °C for 5 minutes in the presence of beta-mercaptoethanol (βME). Protein (25 µg) or a pre-stained protein ladder (PageRuler™ Plus) was loaded into each well of a 12 % pre-cast SDS NuPAGE™ Bis-Tris gel and run according to the manufacturer's instructions in an adaptation of the original method described by Laemmli.[293]

15. Silver staining of SDS-PAGE gels

SDS-PAGE gels were fixed in 30 % ethanol and 10 % acetic acid for 30 minutes at room temperature on a gel rocker. Gels were washed three times for 10 minutes in 30 % ethanol on a gel rocker ad sensitised for 1 minute in 370 µg/mL sodium thiosulfate-5-hydrate. Gels were then washed twice in deionised water (dH_2O) for 1 minute each before being stained in 2 mg/mL silver nitrate and 0.75 µL/mL of 38 % formaldehyde. Gels were washed in dH_2O and developed in 600 mg/mL sodium carbonate, 0.45 µL/mL, 38 % formaldehyde and 5 µg/mL sodium thiosulfate for 8 minutes or until bands were visible. Staining was terminated by addition of acetic acid, gels were washed once in dH_2O and photographed.

16. Western blotting

Proteins were transferred to a polyvinylidene difluoride (PVDF) membrane using a wet tris/glycine/methanol-based transfer method on ice. Membranes were washed, blocked in 5 % milk or 5 % bovine serum albumin (BSA) and stained with primary antibodies (1:5 000) overnight at 4 °C. Membranes were washed, stained with secondary antibody (1:10 000) for one hour at room temperature, washed again and developed with ECL prime detection reagent according to the manufacturer's instructions.

17. Proteomic and phosphoproteomic studies

17.1. Neutrophil preparation

Neutrophils were isolated from whole blood of n = 4 healthy human volunteers as detailed in Section 2 and resuspended in RPMI 1640 media containing 10 mM HEPES with 1 % AS at a concentration of 10^7 cells/mL. Cells were treated as outlined below.

17.2. Treatments and conditions

Technical triplicates of 10^7 neutrophils each were treated in 2 mL Eppendorf microcentrifuge tubes with control (PBS, 60 minutes), C5a (100 nM, 60 minutes), or PAF (1 µM, 5 minutes) at 37 °C in a thermomixer rotating at 300 rpm before pHrodo *S. aureus* Bioparticles were added at a concentration of 15 µg/mL. Cells were allowed to phagocytose for 15 minutes. At baseline, immediately before Bioparticles were added and after phagocytosis aliquots of 400 µL were withdrawn from each replicate and pooled to give 12 million cells per condition. Each pooled condition was centrifuged at 400 g for 5 minutes at 4 °C, supernatant was aspirated and the cell pellets were snap frozen in liquid N_2. The experimental design including relevant conditions is depicted in Figure II-1. Samples were stored at -70 before transfer to Cancer Research UK; Cambridge Institute (CRUK-CI) for the following processing steps.

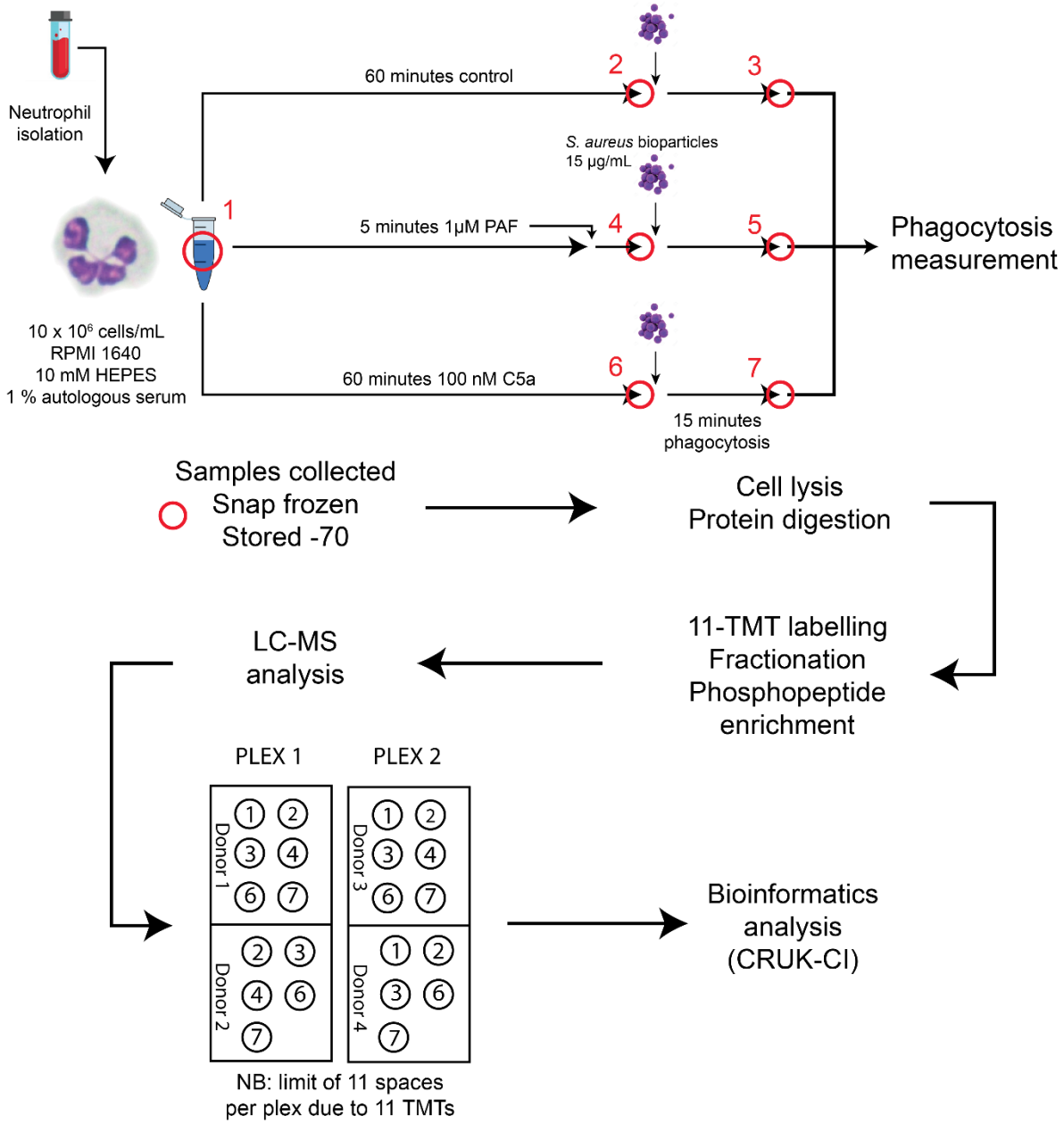

Figure II-1: Phosphoproteomics experimental design

Neutrophils were purified as described and suspended in RPMI 1640 media supplemented with 10 mM HEPES and one % AS. Red circles indicate instances where aliquots of cells were removed for analysis. An untreated aliquot was removed and snap frozen and cells were then treated with 100 nM C5a, 1 µM PAF or control for 60 minutes (5 minutes for PAF). Post-treatment, pre-phagocytosis aliquots were removed and snap frozen, and pHrodo *S. aureus* Bioparticles were added; cells were allowed to phagocytose for 15 minutes before the final aliquots were removed and snap frozen. Phagocytosis was measured at the end of the procedure by flow cytometry of remaining (non-frozen) sample. Samples were batched until all 22 conditions were ready for analysis. Samples were transported to CRUK-CI on dry ice, lysed and digested as specified. The phosphoproteomic workflow included TMT labelling, fractionation and enrichment of phosphopeptides prior to LC-MS analysis in two separate batches or plexes with the 22 samples from four donors distributed across them as shown. Bioinformatics analysis (extraction of protein data from measured peptides and normalisation of peptide intensities) was completed at CRUK-CI before the data was transferred to me for further analysis.

17.3. Cell lysis and trypsin digestion

Cells were lysed in freshly prepared ice-cold lysis buffer (0.5 % SDS, 0.1 M TEAB containing 1 X HALT protease and phosphatase inhibitors). Cell suspensions were incubated at 90 °C for 5 minutes and sonicated twice for 20 seconds (EpiShear™ Probe Sonicator, Active Motif). The insoluble fraction was removed by centrifugation at 20 000 g for 10 minutes at 4 °C. Lysate protein concentration was determined by Bradford Protein Assay (Bio-Rad, Quick Start).

100 µg of protein per sample was reduced in 5 mM Tris(2-carboxyethyl)phosphine (TCEP) for one hour at 60 °C, which was followed by alkylation of cysteines with 10 mM methyl methanethiosulfonate in the dark at room temperature. Lysates were then diluted 1:10 with 0.1 M TEAB before trypsin was added at a 1:30 trypsin:protein ratio by mass. Digestion was carried out overnight at room temperature.

17.4. Tandem mass tag labelling

Tandem mass tag (TMT) reagents (0.8 mg) were reconstituted in 40 µl anhydrous acetonitrile and peptide samples were labelled according to the manufacturer's protocol. Following incubation at room temperature for one hour, the reaction was quenched with hydroxylamine to a final concentration of 5% (v/v) for 15 min at room temperature. The TMT-labelled samples were pooled at 1: 1: 1: 1: 1: 1: 1: 1: 1: 1: 1 across the 11 samples. The pooled sample was vacuum centrifuged to dryness and subjected to basic pH reversed-phase (bRP) fractionation.

17.5. Off-line reverse phase fractionation at basic pH

The TMT mixture was fractionated on a Dionex Ultimate 3000 system (Thermo Fisher Scientific) at high pH. The labelled peptide mixture was reconstituted in 20 mM ammonium hydroxide in water (pH 10) and subjected to a 45 minute linear gradient from 4.5% to 45% acetonitrile in 20 mM ammonium hydroxide (pH 10) at a flow rate of 0.2 ml/min over an XBridge C18 column Reversed-Phase (3.5 µm particles, 2.1 mm ID, 150 mm in length; Waters). The peptide mixture was fractionated into a total of 48 fractions. 15% (v/v) of each fraction was separated into a new tube and was used for full proteome analysis. The remaining volume in each fraction will be subjected to phosphopeptide enrichment. All fractions were dried on a centrifugal vacuum concentrator.

17.6. Phosphopeptide enrichment

The initial 48 fractions were consolidated into 14 and submitted to phosphopeptide enrichment by using the High-Select™ Fe-NTA Phosphopeptide Enrichment Kit according to the manufacturer's protocol. Eluates containing the phosphopeptides were dried via vacuum

centrifugation and reconstituted in 10 µl of 0.1 % formic acid for liquid chromatography and tandem mass spectrometry (LC-MS/MS) processing.

17.7. LC-MS/MS analysis of full proteome fractions

The initial 48 fractions were pooled into a final number of 32 fractions. Each fraction was reconstituted in 10 µl of 0.1% formic acid and 5 µl were analysed on a Dionex Ultimate 3000 UHPLC system coupled with an Orbitrap Fusion Lumos mass spectrometer (Thermo Fisher Scientific, San Jose, CA). Samples were loaded on an Acclaim PepMap 100, 100 µm × 2 cm C18, 5 µm, 100 Å trapping column with the ulPickUp injection method at a loading flow rate of 5 µL/min for 10 min. For peptide separation, an EASY-Spray analytical column 75 µm × 25 cm, C18, 2 µm, 100 Å column was used for multi-step gradient elution at a flow rate of 300 nL/min. Mobile phase (A) was composed of 2 % acetonitrile, 0.1 % formic acid; mobile phase (B) was composed of 80 % acetonitrile, 0.1 % formic acid. Peptides were eluted using a gradient as follows: 0 - 10 min, 5 % mobile phase B; 10 – 95 min, 5 – 45% mobile phase B; 95 -100 min, 45% - 95% B; 100 - 108 min, 95% B; 108 – 110min, 95% - 5% B; 110 – 120 min, 5% B.

Data-dependent acquisition began with an MS survey scan in the Orbitrap (380 – 1500 m/z, resolution 120,000 full width half maximum (FWHM), automatic gain control (AGC) target 3E5, maximum injection time 100 ms). The top ten precursors were then selected for MS2/MS3 analysis. MS2 analysis consisted of: collision-induced dissociation (CID), quadrupole ion trap analysis, AGC target 1E4, normalized collision energy (NCE) 35, q-value 0.25, maximum injection time 35 ms, an isolation window at 0.7, and a dynamic exclusion duration of 45 seconds. Following acquisition of MS2 spectrum, MS3 precursors were fragmented by high energy collision-induced dissociation (HCD) using 10 frequency notches and analysed in the Orbitrap (resolution 50,000 FWHM, AGC target 5E4, NCE 55, maximum injection time 86 ms, and isolation window at 0.7.

17.8. LC-MS/MS analysis of phosphopeptide-enriched fractions

All the fractions (10 µl) were analysed on a Dionex Ultimate 3000 UHPLC system coupled to a Q-Exactive HF mass spectrometer (Thermo Fisher Scientific, San Jose, CA). Samples were loaded on an Acclaim PepMap 100, 100 µm × 2 cm C18, 5 µm, 100 Å trapping column with the ulPickUp injection method at a loading flow rate of 5 µL/min for 10 min. For peptide separation, an EASY-Spray analytical column 75 µm × 25 cm, C18, 2 µm, 100 Å column was used for multi-step gradient elution at a flow rate of 300 nL/min. Mobile phase (A) was composed of 2 % acetonitrile, 0.1 % formic acid, 5 % dimethyl sulfoxide (DMSO); mobile phase (B) was composed of 80 % acetonitrile, 0.1 % formic acid, 5 % DMSO. Peptides were eluted using a gradient as follows: 0 - 10 min, 5 % mobile phase B; 10 – 95 min, 5 – 45 %

mobile phase B; 95 -100 min, 45 % - 95% B; 100 - 108 min, 95 % B; 108 – 110min, 95 % - 5 % B; 110 – 120 min, 5 % B.

Data-dependent acquisition began with an MS survey scan in the Orbitrap (400 – 1600 m/z, resolution 60,000 FWHM, AGC target 3E6, maximum injection time 100 ms). The top 10 precursors were then isolated and fragmented with CID. MS2 analysis consisted of: resolution 30,000 FWHM, AGC target 2E4, NCE 33, maximum injection time 100 ms, MS2 isolation window 2.0 m/z.

17.9. Phosphoproteomics data analysis

Spectral .raw files from data dependent acquisition were processed with the SequestHT search engine on Thermo Scientific Proteome Discoverer™ 2.1 software. Data was searched against both human and *Staphylococcus aereus* UniProt reviewed databases at a 1 % spectrum level false discover rate (FDR) criteria using Percolator (University of Washington). MS1 mass tolerance was constrained to 20 ppm and the fragment ion mass tolerance was set to 0.5 Da. TMT tags on lysine residues and peptide N termini (+229.163 Da) and methylthio (+45.988) of cysteine residues (+57.021 Da) were set as static modifications, while oxidation of methionine residues (+15.995 Da) and deamidation (+0.984) of asparagine and glutamine residues were set as variable modifications. For TMT-based reporter ion quantitation, we extracted the signal-to-noise (S:N) ratio for each TMT channel. Moreover, parsimony principle was applied for protein grouping.

18. Statistical analysis

18.1. Wet-laboratory data

Data are presented as individual data points with summary statistics (median and interquartile range; IQR or mean and standard deviation (SD) specified in the figure legend according to whether data are normally distributed. Parametric or non-parametric statistical tests were applied as appropriate after data was tested for normality using the D'Agostino-Pearson or Shapiro-Wilk tests as appropriate. Differences between two groups were assessed by paired or unpaired t-tests or Wilcoxon’s test. Differences between three or more groups were assessed by one-way ANOVA or Friedman’s test with Dunn’s multiple comparisons correction as appropriate. Differences between grouped data were assessed with two-way ANOVA with Sidak’s or Dunnett’s multiple comparisons test as appropriate. Differences where $p < 0.05$ were considered statistically significant, and non-significant differences have not been indicated in figures for clarity. Statistical analysis was performed with GraphPad Prism v8.0 (GraphPad Software; San Diego; California).

18.2. Phosphoproteomics data

Peptide and phosphopeptide intensities were normalised across conditions using median scaling and then summed to generate protein and phosphoprotein intensities. Log base 2 fold-changes (Log2FC) were calculated between conditions of interest, compared across n = 4 donors and tested for statistical significance by limma-based linear models with Bonferroni's correction for multiple testing. Hierarchical clustering using Euclidean distance was performed on the entire dataset and heatmaps generated and volcano plots generated as shown in Results. Statistical analysis was performed in RStudio[294] using the qPLEXanalyzer[295] package and plots were produced using the ggplot2[296] package.

Chapter III: C5a rapidly induces a prolonged impairment of neutrophil phagocytosis

1. Chapter summary

C5a has been shown to reduce neutrophil phagocytosis *in vitro* in rats[179] and humans.[177,213] in addition to mediating organ failure and death in various *in-vivo* studies discussed in Section 3.5 of Chapter I:. This *in vitro* work[177,179,213] made use of an experimental system that appears to be quite abstracted from the cellular environment *in vivo*; neutrophils were purified from whole blood, allowed to adhere to tissue culture plastic and exposed to zymosan particles (a derivative of *Saccharomyces cerevisiae* or Baker's yeast). Furthermore, quantification of phagocytosis relied on manual counting following visual inspection of microscope fields. Work from our group has shown that, in this experimental system, the phagocytic defect induced by C5a is dependent on signalling via the δ isoform of PI3K.[177]

Phosphatidylinositol-3-kinases are intracellular enzymes which selectively phosphorylate the 3-hydroxyl group of the inositol ring of phosphatidylinositol lipids.[297] They are widely expressed throughout mammalian cells and mediate a plethora of cellular functions. Neutrophils are rich in the gamma and delta isoforms of this enzyme[254] and PI3K signalling is crucially involved in phagocytosis.[58,63,298]

Given the context-sensitivity of intracellular signalling, it seems that interrogating neutrophils in a context significantly different from the situation *in vivo* could lead to difficulties extrapolating mechanistic understanding to critically ill patients. This chapter establishes and validates an assay of phagocytosis of clinically relevant pathogens, confirms PI3K involvement and demonstrates C5a impairs phagocytosis rapidly, and that the impairment is much longer-lasting than previously appreciated. Finally, it demonstrates that impairment of phagocytosis translates to impaired microbicidal activity of the common nosocomial pathogen, *S. aureus.*

2. Hypotheses and aims

C5a induces a prolonged defect in neutrophil phagocytosis of clinically relevant pathogens, and this leads to impaired bacterial killing.

- To replicate previous work demonstrating a defect in phagocytosis of zymosan particles by purified adherent neutrophils.
- To establish and validate an assay of neutrophil phagocytosis by cells in suspension using clinically relevant bacterial targets.
- To confirm that C5a exposure is accompanied by a spike in PtdIns(3,4,5)P_3 production.
- To demonstrate that C5a impairs phagocytosis by neutrophils in this new experimental system and confirm that this impairment is preventable by pre-treatment with PI3K inhibitors.
- To confirm that C5a-induced phagocytic impairment translates to impaired bacterial killing.
- To assess the time course of C5a-induced neutrophil phagocytic impairment.

3. Notes on methods

Methods used in this chapter were developed in an iterative process as described. Assays used to generate data shown in figures are presented in Chapter II: Methods and full protocols are included in Appendices. Data for *E. coli* red Bioparticles and *S. aureus* killing presented in Figure III-4 and Figure III-6 respectively were kindly generated by Dr Arlette Vassallo, a fellow PhD student in the Department of Medicine, University of Cambridge.

4. Results

4.1. C5a pre-treatment reduces phagocytosis of zymosan by purified, adherent human neutrophils

I first attempted to replicate results demonstrated by Conway-Morris[213] and show that C5a applied to adherent human neutrophils reduces phagocytosis of zymosan particles. Figure III-1A and B are representative images of control- and C5a-treated adherent neutrophils, with positive and negative cells indicated. Figure III-1C provides quantification of phagocytosis, showing a reduction in the median proportion of neutrophils with ≥ 2 zymosan particles from 71.4 to 57.1 % ($p = 0.031$) with C5a treatment relative to PBS control.

4.2. pHrodo fluorescence indicates ingestion of particles

Prior to my project, pHrodo Bioparticles had not been used extensively in our group for flow cytometric assessment of phagocytosis, and thus characterisation of their performance in-assay was required. In order to verify the manufacturer's claims of pH-related Bioparticle fluorescence (i.e. Bioparticles only fluoresce when intracellular due to low phagosomal pH) confocal microscopy (Leica Sp5) was undertaken. Figure III-2 demonstrates increasing intracellular fluorescence with increasing concentrations of *S. aureus* Bioparticles by confocal microscopy (A, B) though at higher concentrations some extracellular fluorescence is also noted. Similarly, increasing intracellular fluorescence was noted by concurrent fluorescence microscopy and flow cytometry using an ImageStream X Mark II cytometer (BD Biosciences), which also demonstrated that positive cells by flow cytometry correspond to cells with intracellular, fluorescent particles, and their negative counterparts have no intracellular fluorescence. Taken together, these results suggest pHrodo Bioparticles reliably indicate successful phagocytosis, with minimal confounding by extracellular fluorescence, especially when the neutrophil population is gated by forward and side scatter.

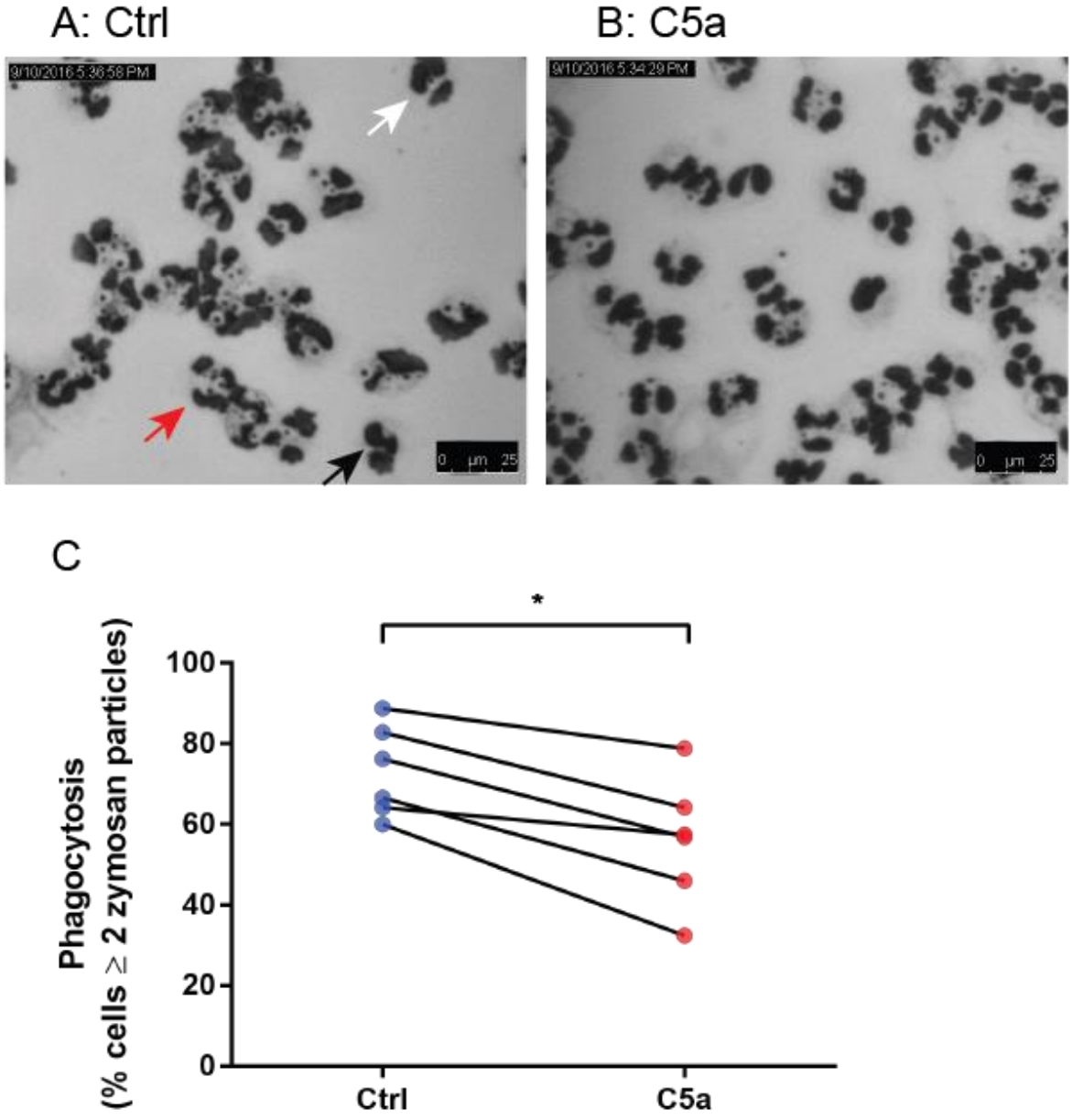

Figure III-1: C5a pre-treatment reduces phagocytosis of zymosan by purified, adherent human neutrophils

Purified human neutrophils were allowed to adhere to 24-well tissue culture plates for 30 minutes before being treated with PBS control (A) or C5a (B) for 30 minutes. Serum-opsonised zymosan was then added for 30 minutes, before phagocytosis was quantified. An example positive cell (≥ 2 internalised zymosan particles) is indicated by the red arrow in A. White and black arrows in A indicate negative cells (with 1 and 0 internalised zymosan particles respectively) viewed at 400 X magnification. C: Quantification of 6 separate experiments, showing a reduction in the median percentage of cells with ≥ 2 internalised zymosan particles from 71.4 to 57.1 % ($p = 0.031$, Wilcoxon) with C5a treatment relative to control.

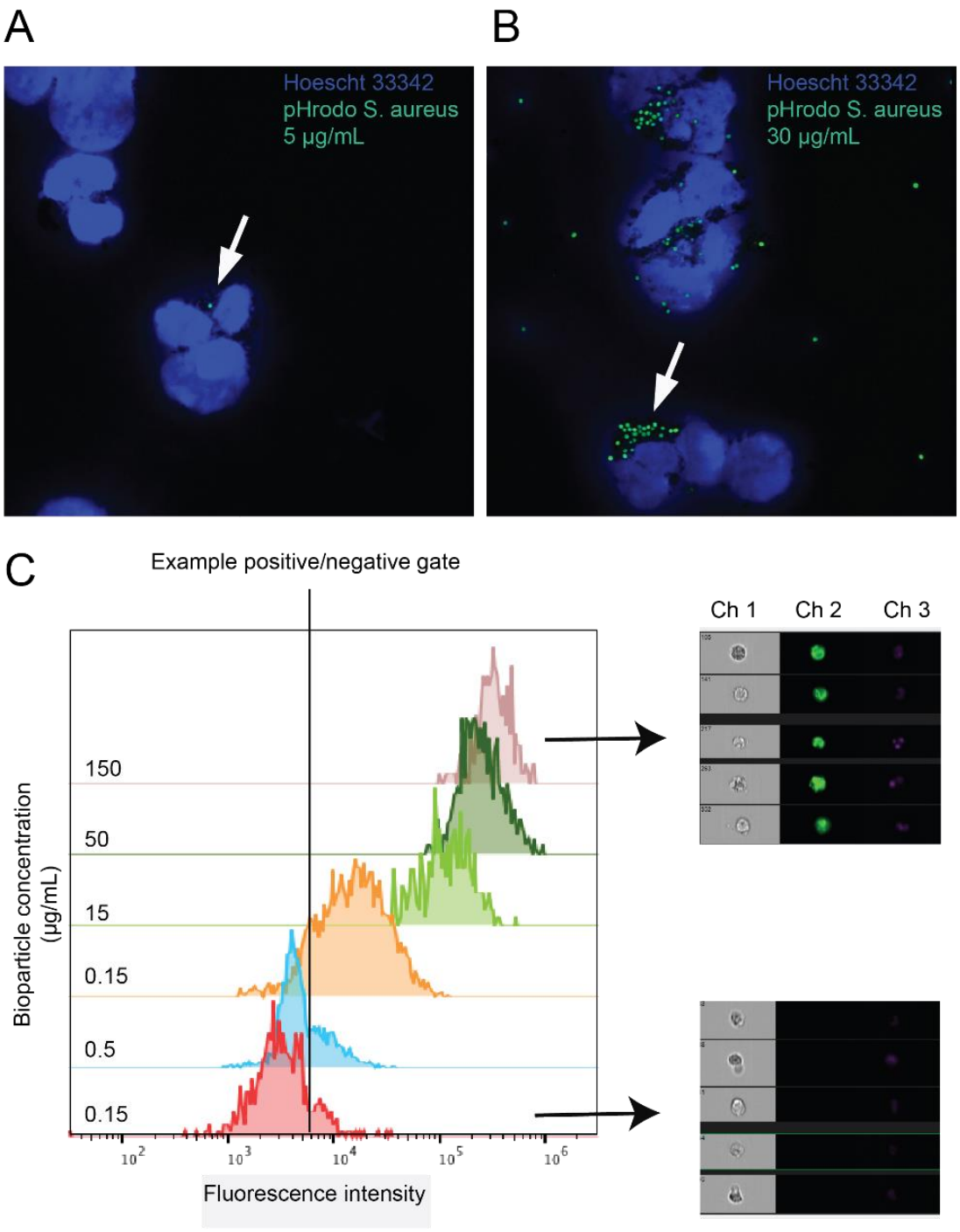

Figure III-2: pHrodo fluorescence indicates ingestion of particles

Neutrophils were incubated in 24-well glass imaging plates with *S. aureus* green Bioparticles for 30 minutes at concentrations of 5 (A) and 30 µg/mL (B) as shown. Neutrophils were fixed, nuclei stained with Hoechst 33342 and visualised by confocal microscopy at 630 X magnification. White arrows indicate intracellular *S. aureus* Bioparticles (green). C: Increasing concentrations of *S. aureus* green Bioparticles were incubated with PMNs for 2 hours, fixed and analysed. A single cell is photographed/excited by lasers and is shown in three channels: channel 1 shows bright-field images; channel 2 shows fluorescence of pHrodo green *S. aureus* Bioparticles; channel 3 shows fluorescence of DAPI nuclear staining. Images correspond to histograms of channel 2 Bioparticle fluorescence, showing that fluorescence as measured by flow cytometry indicates intracellular Bioparticles.

4.3. pHrodo bioparticles quantify phagocytosis

Figure III-3 shows the gating strategy to identify neutrophils, and subsequently pHrodo-positive phagocytosis events for 4 (no phagocytosis) and 37˚C (efficient phagocytosis) in orange and blue respectively. Dose-response experiments were conducted to ascertain the optimal Bioparticle concentration to reliably demonstrate phagocytosis. Figure III-4A and B show the resulting dose-response curves assessed by % phagocytosing cells (Bioparticle positive) and phagocytic index with accompanying EC_{50} values for each Bioparticle type. A Bioparticle concentration close to the established EC_{50} concentration was used in subsequent experiments.

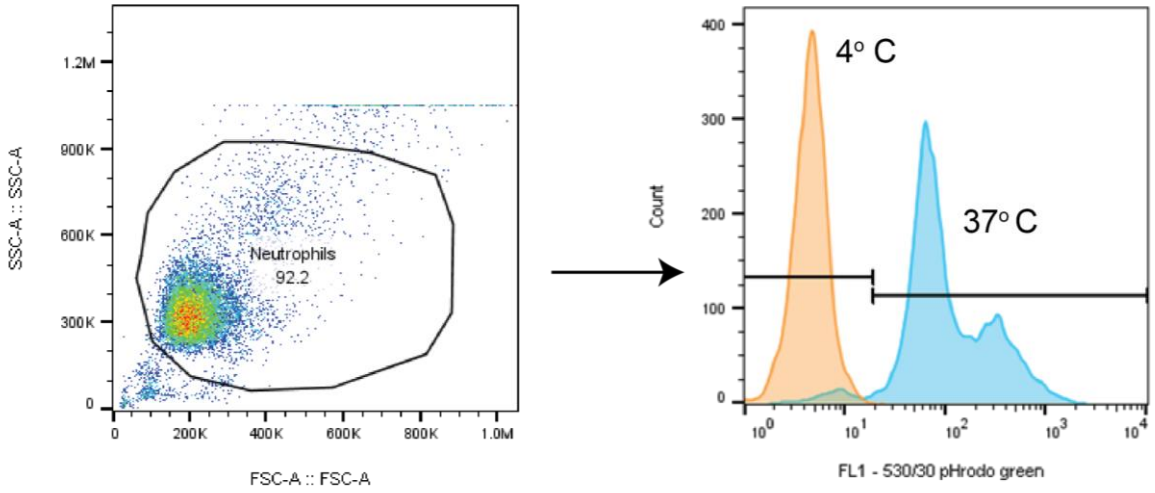

Figure III-3: Gating strategy for assessing neutrophil phagocytosis

PMNs were incubated at 4˚C (no phagocytosis) and 37˚C to determine the fluorescence which constitutes a positive cell in terms of pHrodo Bioparticle ingestion. Positive cells are those lying to the right of the gate, negative to the left.

The optimal time point for measurement of phagocytosis was then assessed through time-course experiments using the EC_{50} Bioparticle concentration. Phagocytosis was again quantified by the proportion of Bioparticle-positive cells (C) and phagocytic index (median fluorescence intensity x % positive cells: D) at intervals over five hours to determine the kinetics of Bioparticle phagocytosis. Figure Figure III-4C demonstrates that phagocytosis is an extremely rapid process, beginning within minutes. Taken together, these results suggest pHrodo Bioparticles reliably indicate successful phagocytosis, with minimal confounding by extracellular fluorescence, especially when neutrophils are gated by forward and side scatter.

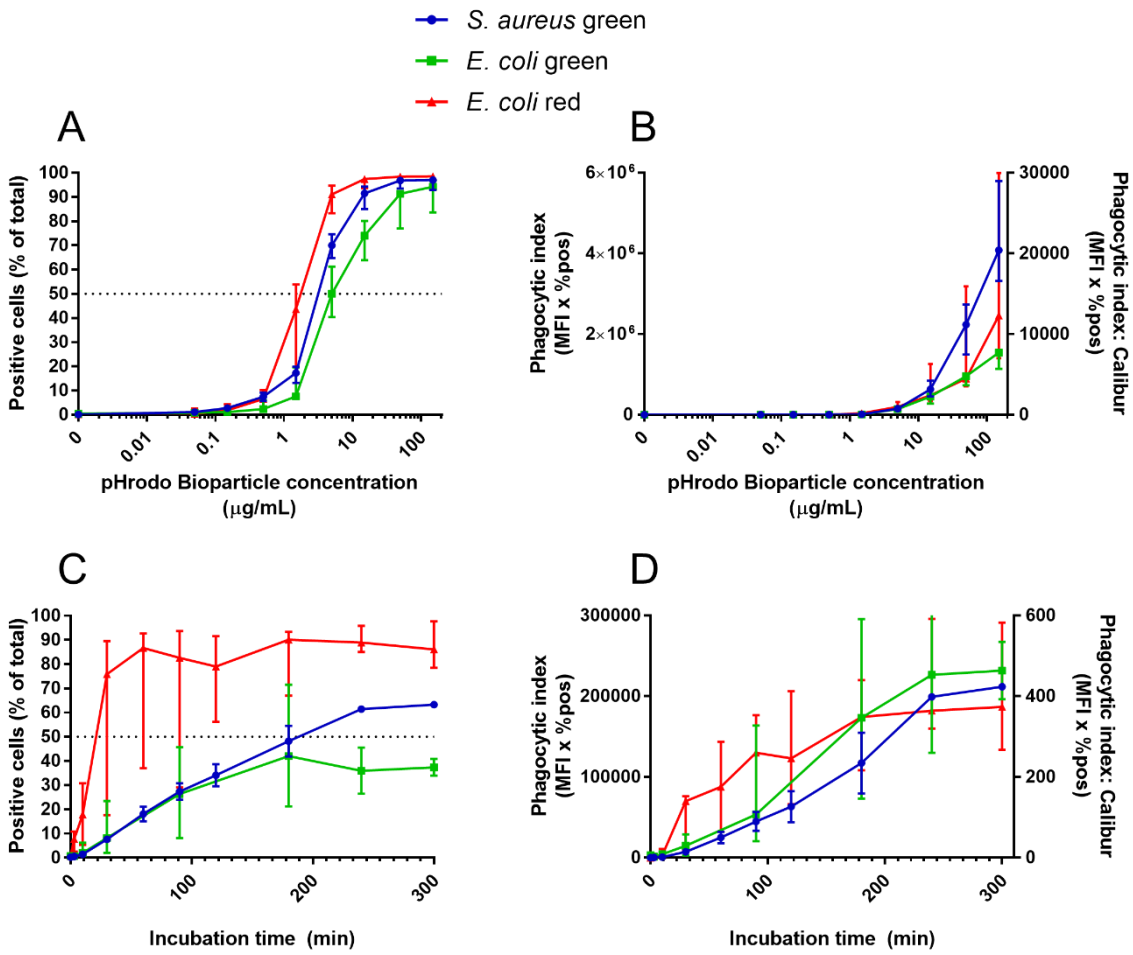

Figure III-4: pHrodo bioparticles can quantify phagocytosis

PMNs were incubated with increasing concentrations of pHrodo *S. aureus* green, *E. coli* green and *E. coli* red Bioparticles and the percentage of positive cells (A) or phagocytic index (B) were measured by flow cytometry. The Bioparticle concentration required for 50 % cell positivity (EC50 (95 % CI)) was calculated for each bacteria/dye combination: *S. aureus* green 3.26 µg/mL (3.014 – 3.027); *E. coli* green 4.692 µg/mL (3.713 – 5.928); *E. coli* red 1.85 µg/mL (1.644 – 2.081). PMNs were then incubated with the EC50 of each bacteria/dye combination for up to 5 hours. Cells were fixed at the indicated time points and the percentage of positive cells (C) and phagocytic index (D) were measured by flow cytometry. Results are presented as median and IQR of n = 4 - 6 (A and B) and 2 (*S. aureus* green) 4 (*E. coli* green) and 9 (*E. coli* red; C and D) independent experiments. Data for *E. coli* red kindly collected by Dr Arlette Vassallo as part of her own experiments.

4.4. C5a pre-treatment induces a phagocytic defect of *S. aureus* and *E. coli* Bioparticles that is PI3K-dependent

Having observed the previously demonstrated effect of C5a on adherent neutrophils, the effect of C5a on neutrophil phagocytosis in suspension with physiologically relevant bacterial targets was evaluated. Figure III-5A and B show a relative reduction in phagocytic index of 29.66 % for *S. aureus* and 29.25 % with *E. coli* respectively for cells treated with C5a relative to control. Previous data from our group has shown that C5a-mediated impairment of neutrophil phagocytosis was PI3K-dependent.[177,213] I first confirmed that C5a induced a rapid spike in PtdIns(3,4,5)P_3 production at 15 s similar to fMLP, with minimal effect of LPS at 30 minutes, shown in Figure III-5C. Finally, the role of PI3K enzymes in mediating C5a-induced neutrophil phagocytic dysfunction was assessed in the newly characterised assay of phagocytosis. Figure III-5D shows that pre-treatment with PI3K inhibitors selective for either the delta (idelalisib 100 nM) or gamma isoform (IPI-549 100 nM) prevented C5a-induced impairment of phagocytosis.

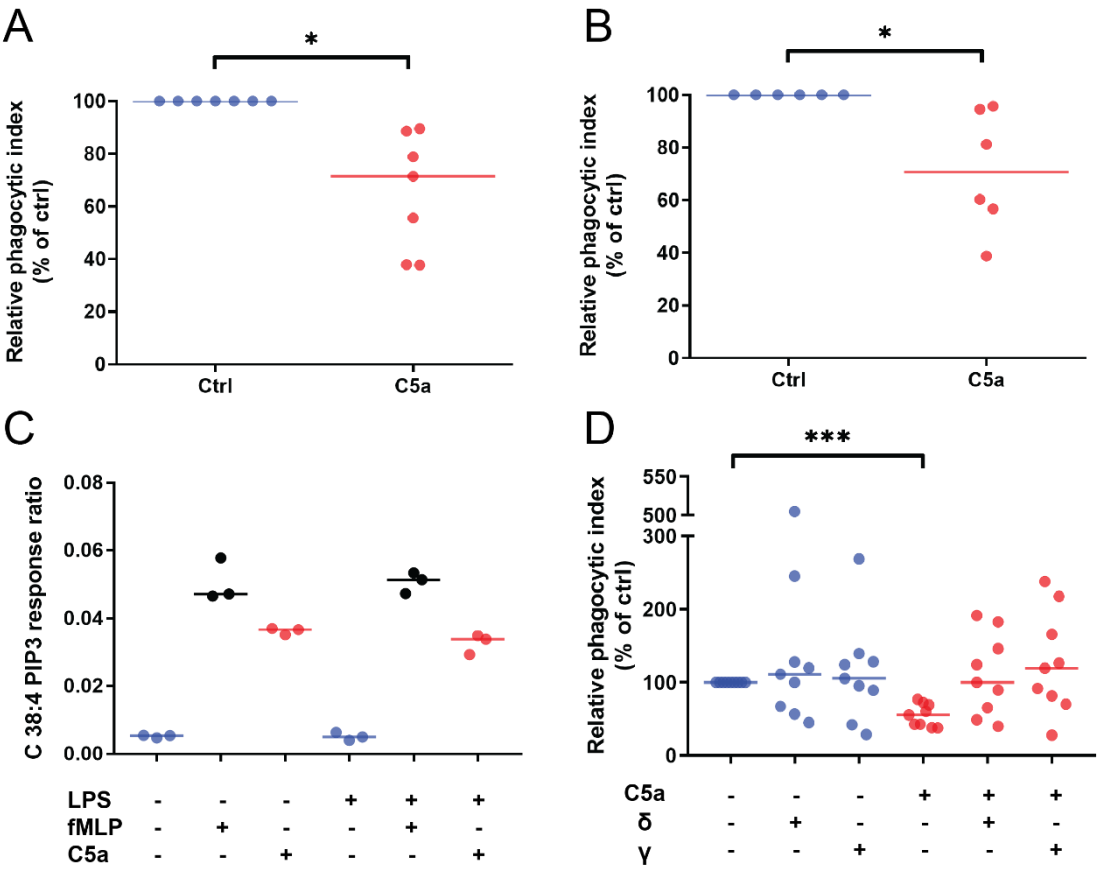

Figure III-5: C5a induces phagocytic defect of *S. aureus* and *E. coli* bioparticles that is PI3K-dependent

Neutrophils were pre-treated with 100 nM C5a or vehicle control for 60 minutes before incubation with *S. aureus* green (A) or *E. coli* green (B) Bioparticles at their respective EC_{50} concentrations before being fixed and analysed by flow cytometry. Data are presented as the median phagocytic index of C5a-treated cells relative to their paired PBS control for 7 (A) or 6 (B) independent experiments, *p-value < 0.05 by Wilcoxon's matched-pairs signed rank test. C: PtdIns(3,4,5)P_3 production was quantified as a ratio of the C38:4 PtdIns(3,4,5)P_3 to internal standard after 30 minutes of priming and 15 s of stimulation with the agents identified. Data shown are triplicates from one independent experiment, thus no statistical tests were performed. D: Neutrophils were pre-treated with 100 nM idelalisib (δ isoform inhibitor) or 100 nM IPI-549 (γ isoform inhibitor) for 30 minutes prior to C5a treatment (60 minutes) before phagocytosis was quantified as above. p = 0.03 by two-way repeated measures ANOVA, ***p < 0.001 by Sidak's test for multiple comparisons.

4.5. C5a pre-treatment impairs neutrophil bactericidal activity

Killing of bacteria is a key neutrophil function dependent on a variety of processes (including phagocytosis) as discussed in Chapter 1. To confirm the relevance of C5a-mediated phagocytic impairment to bacterial killing, the ability of neutrophils to kill the common nosocomial pathogen *S. aureus* was assessed in vitro. Pre-incubation of neutrophils with 100 nM C5a for 60 minutes prior to the bacterial killing assay resulted in an increase in CFU counts of 25.94 % relative to control, demonstrating that C5a induces a defect in bacterial killing.

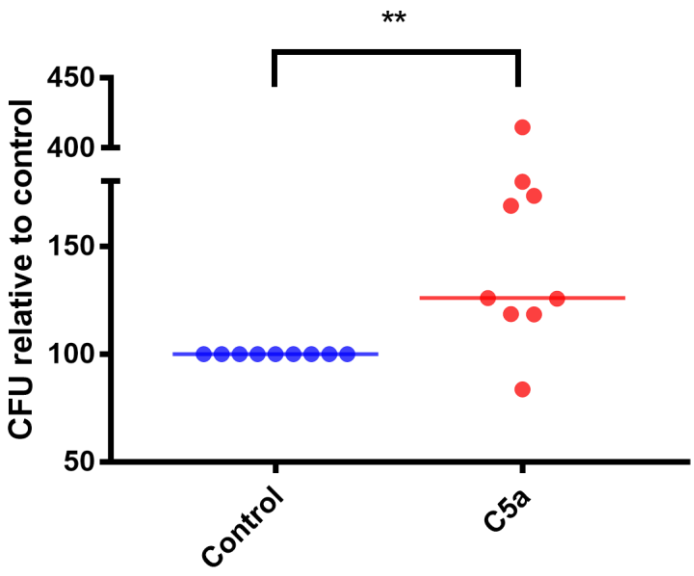

Figure III-6: C5a pre-treatment reduces killing of *S. aureus* by human neutrophils

Live MSSA (strain ASASM6) were fed to human neutrophils for 60 minutes at an MOI of 10:1 bacteria per neutrophil. Neutrophils were lysed, bacteria plated and grown overnight and CFUs quantified by visual inspection. ** $p < 0.01$ by Wilcoxon.

4.6. Transient C5a pre-treatment induces prolonged impairment of neutrophil phagocytosis

The effect of duration and timing of exposure to C5a was assessed in a time-course experiment using the basic phagocytosis assay established above. Purified neutrophils were exposed to C5a or control for the durations indicated, C5a was removed by washing, and cells were then exposed to Bioparticles for up to 7 hours, the results of which are shown in Figure III-7. C5a induces a defect in phagocytosis, and this defect is induced after short periods of exposure (as little as 5 minutes in some cases). Further, this experiment shows that the defect induced by C5a is persistent and affects phagocytosis for at least 7 hours even after removal of C5a. Importantly, these results are not due to experimental treatments reducing cell viability, as shown in B.

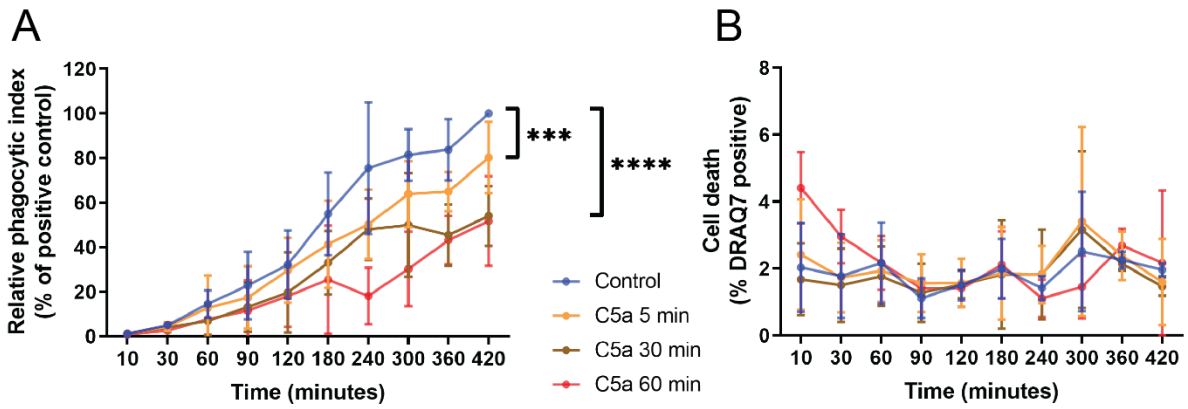

Figure III-7: C5a rapidly induces long-lasting impairment of human neutrophil phagocytosis without inducing cell death

Neutrophils were pre-treated with 100 nM C5a or PBS control for 60 minutes, which was removed by large volume washes. *S. aureus* Bioparticles were then added and cells were incubated for the indicated time points. A: data are presented as the mean and SD of the phagocytic index of C5a-treated cells relative to their paired PBS control for 5 independent experiments. $p < 0.0001$ for time and $p = 0.0186$ for treatment by two-way ANOVA. ***$p = 0.0001$ ****$p < 0.0001$ by Dunnett's multiple comparisons. B: data are presented as the mean and SD of the percentage of DRAQ7 positive, dead cells for $n = 5$ independent experiments. $p = 0.378$ for time and $p = 0.349$ for treatment by two-way ANOVA, non-significant ANOVA so multiple comparisons not computed.

5. Discussion

This chapter discussed initial work which lays the foundation for the rest of this thesis and characterises the tools with which I will proceed to interrogate neutrophil phagocytosis. Using the same phagocytic target and adherent neutrophils as Conway-Morris[177] and Huber-Lang[179] I have replicated the finding that neutrophils from healthy volunteers exposed to C5a exhibit reduced phagocytosis (Figure III-1), confirming the basis on which this thesis rests. Neutrophil behaviour is extremely context-dependent, with well-demonstrated changes in function secondary to chemoattractant exposure[23] and even simple adhesion.[299] Further, the size of the phagocytic particle has a profound effect on Rho-family GTPase signalling and the involvement of PI3Ks, which have been shown to be important for phagocytosis of large particles (e.g. fungi, zymosan, apoptotic cells) but not small particles (e.g. bacteria) during IgG-mediated phagocytosis by RAW 264.7 cells.[300] Therefore, for any interrogation of intracellular signalling networks related to phagocytosis and C5a exposure to be relevant to critically ill patients, a more physiological assay was needed.

pHrodo Bioparticles™ offer an attractive option for assessing phagocytosis, as the fluorescence intensity of the proprietary pH-sensitive dye increases in acidic conditions,[301] and can therefore indicate completed phagocytosis, distinguishing particles that are 'inside' the cell from those that are simply 'on' the cell.[302] The Bioparticles were tested in initial experiments and confirmed to indicate completed phagocytosis and phagosomal acidification by both confocal microscopy and flow cytometry (Figure III-2 and Figure III-3). The kinetics of phagocytosis and maturation in this system was assessed (Figure III-4) and found to be consistent with previously published kinetic data on phagocytosis.[56,57]

Our group has previously shown that selective inhibition of the PI3K-δ isoform prevented C5a-mediated neutrophil phagocytic impairment in the adherent neutrophil and zymosan system previously described.[177] I therefore aimed to test this hypothesis in my newly characterised experimental system. Figure III-5A and B show that C5a impaired phagocytosis of *S. aureus* and *E. coli* Bioparticles in the new assay, which extended the relevance of previous findings to clinical pathogens and indicated that the effect of C5a on phagocytosis is likely pathogen and size-independent.

I then sought to demonstrate that C5a induced production of PtdIns(3,4,5)P_3 and therefore that the use of PI3K-inhibitors to modulate cellular signalling was appropriate in this context. The PtdIns(3,4,5)P_3 production induced by C5a at 15 s is similar to that induced by fMLP (Figure III-5C) and consistent with that expected from stimulation of neutrophil GPCRs and previous work on C5a.[66,289] Interestingly, priming did not seem to increase the magnitude of the PtdIns(3,4,5)P_3 spike, as may be expected from the effect of priming on ROS production (see Chapter I: Section 1.5). However, previous work from our laboratory showed that

priming with TNF-α did not increase the magnitude of the PtdIns(3,4,5)P_3 response at 15 s but tended to maintain the magnitude of the response over time,[303] consistent with data shown above.

Pre-treatment of neutrophils with selective inhibitors of the gamma and delta isoforms of PI3K demonstrated that signalling through both enzymes is required to mediate the effect of C5a on phagocytosis (Figure III-5D) in contrast to previous data showing that only PI3K-δ was required.[177] There are a number of potential explanations for these divergent observations. Firstly, the use of isoform-selective inhibitors is always fraught with uncertainty, which I strove to minimise by choosing next-generation PI3K inhibitors with IC_{50}s orders of magnitude lower for the preferred isoform which had been validated in similar cell types.[304–306] However, there remains a possibility that off-target effects of the PI3K-γ inhibitor are responsible for this observation. I believe a more plausible explanation is that differences in mechanism exist between the two experimental systems, and that this may well be mediated by the cells in my assay being non-adherent and therefore unprimed prior to C5a exposure, with consequent differences in outcome.

The primary function of neutrophils in the context of infection is bacterial killing, and therefore it was important to demonstrate that C5a-induced impairment in phagocytosis resulted in impaired bacterial killing. C5a-treatment has been previously shown to impair the killing of *P. aeruginosa in vitro*[177] though the effect of C5a on the killing of other bacteria was previously unknown. With kind assistance from my colleague Dr Vassallo who performed the killing assays alongside her own work, C5a has now been shown to impair the killing of *S. aureus* by neutrophils in suspension (Figure III-6) providing important functional relevance for the phagocytic defect induced by C5a.

The experimental work of this chapter concluded with an assessment of the effects of C5a on phagocytosis over time. Previous studies of C5a on neutrophil phagocytosis have focussed on early time-points of up to one hour after C5a exposure.[177,179,213] Given the time-courses of GPCR- and PI3K-mediated signal transduction (seconds to minutes)[254,307] a recovery of phagocytic function or phagosome maturation was expected. The data in Figure III-7 show this is not the case, with even short exposures to C5a inducing prolonged defects in phagocytosis lasting for up to seven hours. It would appear that a rapid initial signalling phenomenon results in a fundamental change in cellular behaviour, or that ongoing signalling is occurring, as has recently been described for endosomal GPCRs-beta-arrestin complexes.[308] Whilst the pHrodo signal was used here primarily as an indicator of internalised particles, the signal is actually a composite of internalisation and phagosomal pH, as fluorescence increases with decreasing pH.[301] The data described here were the basis for the time points selected for phosphoproteomic studies discussed in Chapter VI:. A

further discussion of persistent signalling changes and phagosomal pH in the context of C5a and phagocytosis is reserved until then.

Chapter IV: Development and application of a rapid, scalable whole blood assay of neutrophil function

1. Chapter summary

As discussed previously, numerous studies have demonstrated associations between immune cell phenotypes and outcomes such as nosocomial infection and mortality.[110,147,149] However, as a community of clinicians and researchers we have failed to translate our understanding of immune dysfunction to efficacious therapies.[108,109] There is now a consensus in the field that a key driver of this failure has been an inability to target therapies to patients manifesting the immune dysfunction of interest, in a context that bears some relation to the situation *in vivo*.[111,185,309] Therefore a key challenge for the field is to develop tools which allow accurate interrogation of immune cellular function that can be applied in clinical contexts. I argue that these tools need to directly interrogate cellular function rather than proxies of function such as cell surface marker expression[310,311] or gene transcripts[312] and that if large clinical studies are to be possible, such methods need to be readily scalable, and ideally avoid cell preparation steps used in previous targeted trials.[313] This chapter discusses the development of a protocol for rapidly assessing neutrophil function in small samples of whole blood, and applies this method to questions of C5a biology.

2. Hypotheses and aims

Neutrophil function can be rapidly interrogated in small samples of whole blood, providing insights into mechanisms of C5a-induced neutrophil dysfunction.

- To establish methods for measurement of neutrophil phagocytosis and ROS production in small samples of minimally manipulated whole blood.
- To determine the optimal anticoagulant to preserve important neutrophil functions and mimic the situation *in vivo.*
- To confirm C5a induces a prolonged defect in neutrophil phagocytosis in whole blood, whereas other common neutrophil priming agents do not.
- To demonstrate that C5a decreases both phagocytosis and phagosomal maturation.
- To assess the role of PI3K enzymes in mediating C5a-induced neutrophil dysfunction in whole blood.
- To assess whether C5a exposure reduces the expression of common phagocytic receptors on neutrophils.
- To apply this novel assay of neutrophil function in a clinical context.

3. Notes on methods

This chapter presents results generated using methods detailed in Chapter II: Section 10; namely, the assessment of neutrophil phagocytosis, ROS production and receptor expression in whole blood analysed without RBC lysis or wash steps. These experimental techniques make use of an Attune Nxt™ Acoustic Focusing Cytometer from Life Technologies (Paisely, UK), which allows large, dilute samples to be run very rapidly, thus eliminating the need for RBC lysis and wash steps. Quantitative data presented in Figure IV-7C were generated by experiments designed and carried out in conjunction with Carmelo Zinnato, a talented summer student from the University of Pavia to whom I provided direct supervision directed by Dr Andrew Conway Morris. The ethical approval number for the patient studies presented in this chapter is: 12/WA/0148.

4. Results

4.1. Use of Attune Nxt™ to interrogate multiple neutrophil functions in whole blood

The novel whole-blood assay of neutrophil function presented in this chapter makes use of a recently developed flow cytometer from Life Technologies, without which the assay is not possible in its no-wash, no-lyse form. Figure IV-1 shows the basic workflow of the assay which can be completed in under 60 minutes and provide an estimate of two key neutrophil functions, phagocytosis and the respiratory burst. Two mL of blood allows quantification of up to 13 experimental conditions in triplicate. Example dot plots and histograms in Figure IV-1 show the distinction of neutrophils from other leukocytes and RBCs by CD16 expression and scatter characteristics, as well as the phagocytosis and ROS signals elicited from healthy control neutrophils.

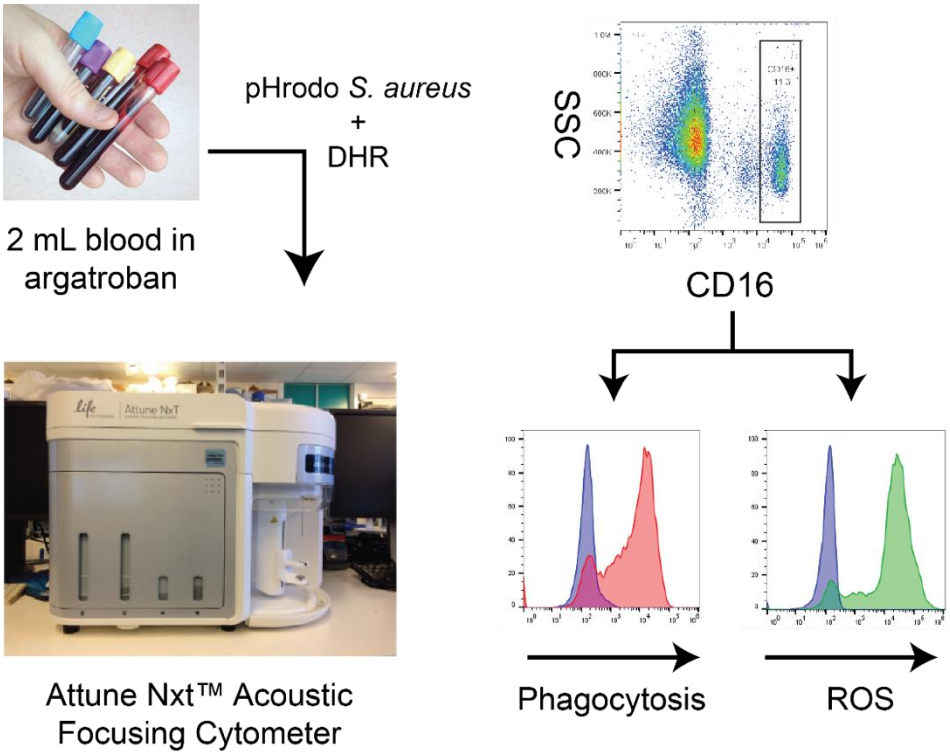

Figure IV-1: Schematic of interrogation of neutrophil function in whole blood without lysis of RBCs or wash steps

Whole blood was collected into the anticoagulant of choice. Blood was aliquoted into 96-well plates and a combined pHrodo/DHR probe was added at concentrations of 15 µg/mL and 3 µM respectively for 30 minutes at 37 °C and five % CO_2 to allow phagocytosis and ROS production. Five µL of reaction mix was aliquoted into ice-cold PBS with anti-CD16 for 30 minutes on ice in the dark. Volume was made up to 4 mL with ice-cold PBS and cells were analysed on an Attune Nxt™ cytometer. Neutrophils were identified by CD16 positivity as shown, and phagocytosis and ROS were quantified by phagocytic index and MFI respectively. The procedure takes less than 60 minutes from blood draw to data analysis and involves no RBC lysis or cell fixation steps.

4.2. Assessment of anticoagulant effects on neutrophil functions and selection of argatroban

The presence of anticoagulant during measurement of neutrophil functions in whole blood assays necessitates careful selection of anticoagulants that minimally alter neutrophil function. To this end, argatroban, a direct thrombin inhibitor, was selected based on previously published studies[266,267] and compared to 3 commonly available anticoagulants; trisodium citrate, heparin sodium and EDTA. The effect of all 4 anticoagulants on the important neutrophil functions of priming, phagocytosis and ROS production were assessed using the assay described above. Figure IV-2A shows the PI of pHrodo Bioparticles in the presence of argatroban, citrate, heparin and EDTA respectively at both 37 °C and 4 °C, indicating that argatroban allows the most phagocytosis of all 4 anticoagulants, and that EDTA virtually abolishes it. Cold conditions were included as negative controls, as phagocytosis is greatly inhibited at these temperatures.[53] Figure IV-2B illustrates two functions; priming and ROS production. Argatroban allows the greatest degree of priming in response to 30 minutes of TNF-α treatment as well as the greatest absolute ROS production when stimulated with Bioparticles.

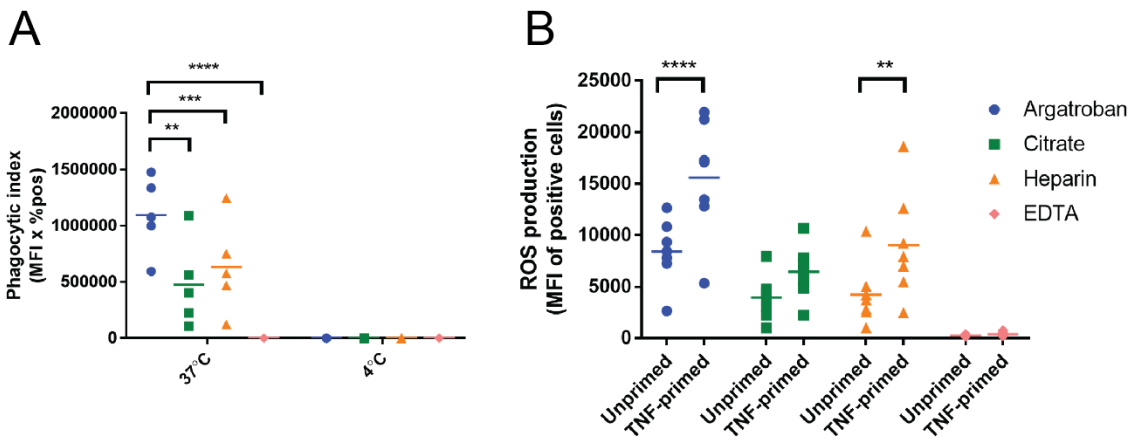

Figure IV-2: Effect of anticoagulants on neutrophil phagocytosis and priming

Whole blood was collected into argatroban (150 µg/mL) citrate (27.34 µg/mL) heparin (16 IU/mL) and EDTA (1.6 mg/mL). Cells were treated with 20 ng/mL TNF-α or control (PBS) for 30 minutes, before the combined pHrodo/DHR probe was added for 30 minutes at 37 °C or 4 °C as indicated. Cells were stained for CD16 to identify the neutrophil population and analysed on an Attune Nxt™. Phagocytosis by unprimed cells after 30 minutes at either 37 °C or 4 °C is shown in A. Priming and ROS production are shown in B. There was no statistically significant effect of priming in the citrate-anticoagulated conditions, and EDTA virtually abolished ROS production. $p < 0.0001$ by two-way ANOVA for A and B, ****$p < 0.0001$, ***$p < 0.001$,**$p < 0.01$ by Sidak's test of multiple comparisons.

4.3. C5a-induces a marked defect in phagocytosis and ROS production while other priming agents do not

Having selected an anticoagulant and developed the basic mechanics of the whole blood assay, I set out to apply it to questions of C5a biology. First, I assessed whether C5a decreased phagocytosis in this new whole blood assay and to establish the concentration of C5a necessary for this effect. Figure IV-4A demonstrates the results of these experiments, with a progressive reduction in phagocytosis relative to control, from 10-1000nM. I elected to proceed with a concentration of 300 nM for further experiments, as this concentration reliably induced a significant defect, was likely to overcome plasma carboxypeptidases[203,204,314] and lowered costs relative to higher doses.

Figure IV-3B and C demonstrate that the finding of reduced neutrophil phagocytosis is not dependent upon the pH-sensitivity of the probe used to measure phagocytosis, and that 300 nM C5a treatment is sufficient to induce a phagocytic defect. In B, the conventional pHrodo *S. aureus* Bioparticles were used, whereas in C, a non-pH-sensitive AF488-conjugated *S. aureus* indicator was used with trypan blue to quench extracellular fluorescence. Both assays showed a reduction in phagocytosis, which is important given C5a has been shown to alter neutrophil cytoplasmic pH[261] which could have confounded results acquired using pHrodo alone.

Given that C5a had been shown to markedly reduce phagocytosis in a whole blood model, I chose to assess whether this was a characteristic unique to C5a, or whether it occurred in response to other conventional neutrophil priming agents. Figure IV-3D and E show that C5a pre-treatment markedly reduced phagocytosis and phagosomal ROS production by neutrophils in whole blood, whereas other priming agents either had no effect or enhanced these neutrophil functions. For pre-treatment durations and priming agent concentrations please see the figure legend, these were determined by optimal priming protocols used within the Chilvers laboratory. Taken together, these results indicate that C5a, uniquely amongst the priming agents investigated, induces a phagocytic and phagosomal ROS production defect in neutrophils in a variety of experimental settings.

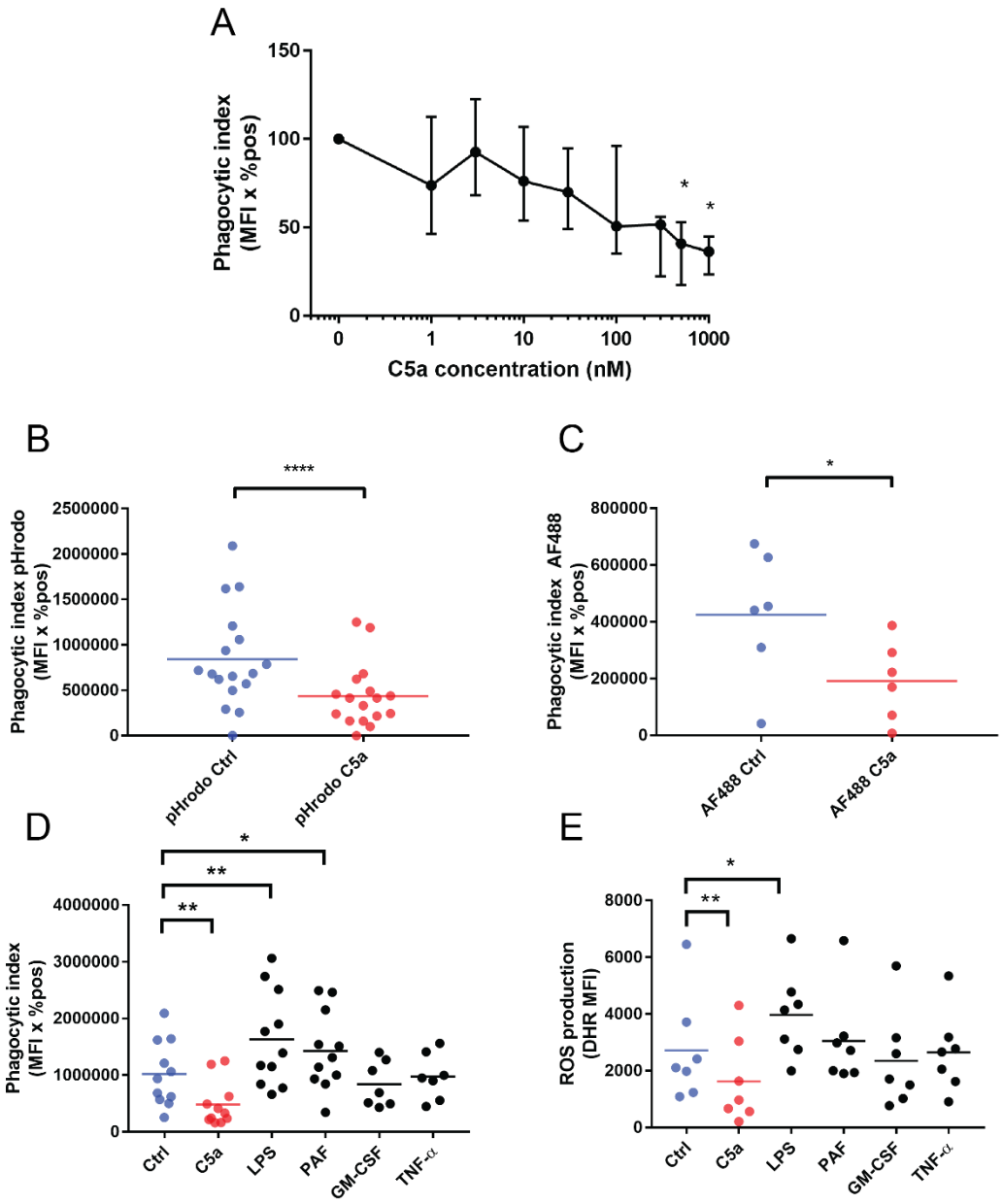

Figure IV-3: C5a impairs neutrophil phagocytosis and ROS production in whole blood while other priming agents do not

A: Whole blood was pre-treated with semi-log increasing concentrations of C5a from 1 nM to 1000 nM for 60 minutes prior to phagocytosis of pHrodo Bioparticles. Data are shown as the median and IQR of 4 independent experiments relative to control-treated blood. Friedman p-value = 0.0024, *p < 0.05 by Dunn's multiple comparisons. B and C: Whole blood was pre-treated with 300 nM C5a or control and phagocytosis was measured by pHrodo *S. aureus* Bioparticles (B: p < 0.0001 by Wilcoxon) or AF488 *S. aureus* Bioparticles (C: p = 0.03 by Wilcoxon). Phagocytosis (D) and ROS production (E) after pre-treatment with various agonists were assessed. Concentrations and pre-treatment durations were as follows: Ctrl (PBS) 60 minutes; C5a 300 nM, 60 minutes; LPS 100 ng/mL, 60 minutes; PAF 1 uM, 5 minutes; GM-CSF 10 ng/mL, 30 minutes; TNF-α 20 ng/mL, 30 minutes. C5a reduced phagocytosis whereas LPS and PAF increased phagocytosis. C5a reduced ROS production and LPS increased ROS production. ANOVA p-value < 0.0001 for both D and E, *p < 0.05, **p < 0.01 for Dunnett's multiple comparisons.

4.4. C5a induces a prolonged impairment in phagocytosis in whole blood

A novel finding of this thesis is the demonstration of marked C5a-induced phagocytic impairment that is long-lasting (Figure III-7). In order to further develop this finding, I established whether a similar long-lasting impairment develops in my newly characterised whole blood assay. In a slightly different approach from the previous work in purified cells, whole blood was exposed to C5a for up to 7 hours, before aliquots were removed for the assessment of phagocytosis for 30 minutes as previously described. In this way, phagocytosis was measured after each hour of C5a incubation, rather than continually from the beginning of the assay as in Figure III-7. Figure IV-4 shows that phagocytosis is markedly impaired by C5a, and that this phagocytic defect increases with duration of C5a exposure in whole blood.

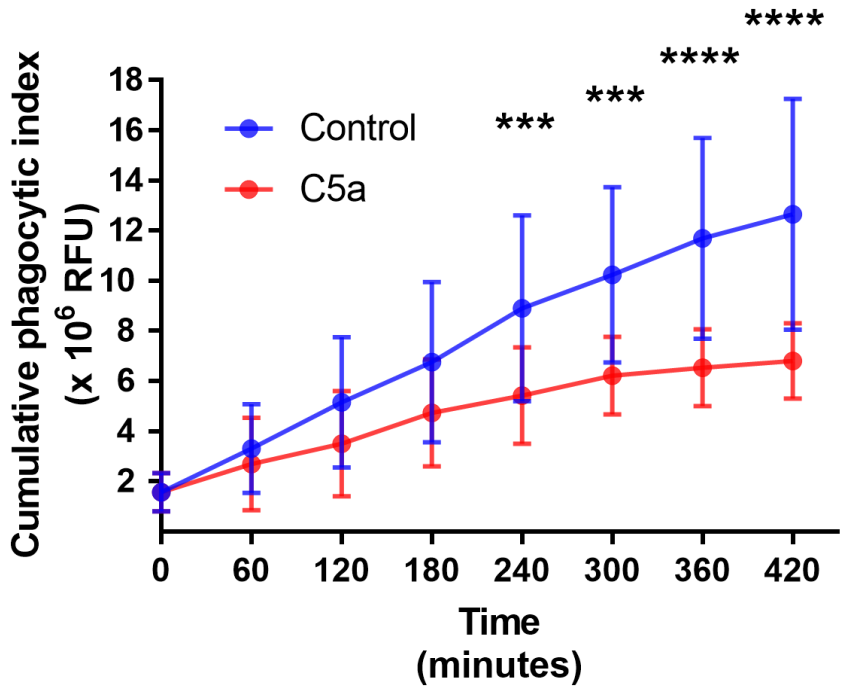

Figure IV-4: C5a induces a prolonged phagocytic defect in whole blood

Whole blood was pre-treated with 300 nM C5a or control for the indicated duration before phagocytosis was measured as previously indicated. Data are presented as the mean and SD of the cumulative phagocytic index for 4 independent experiments. $p < 0.0001$ by two-way ANOVA, ****$p < 0.0001$, ***$p < 0.001$ by Sidak's multiple comparisons test.

4.5. C5a-induced neutrophil dysfunction is not preventable by PI3K inhibition in whole blood

To further interrogate mechanisms driving the C5a-induced defect in phagocytosis, the role of PI3K inhibition in whole blood was determined. In order to establish the concentration of PI3K inhibitors to use in whole blood, dose-response curves based on ROS production (also known to be PI3K-dependent[66]) were used to establish functionally active concentrations of each inhibitor. The curves shown in Figure IV-5A and B demonstrate the IC_{50} for both the γ and δ isoform-selective inhibitors are 54.6 and 197 nM respectively, indicating a significantly higher functional potency than older PI3K inhibitors with which our group is familiar.[66] Concentrations of 50 and 200 nM were used for subsequent studies on phagocytosis. Figure IV-5C shows that C5a-induced phagocytic impairment in whole blood is not PI3K-dependent, in contrast to data obtained in purified cells with the same inhibitors (Figure III-5). To further interrogate this discrepancy, both inhibitors were used at a wide range of concentrations to determine if the C5a defect could be prevented. As Figure IV-5 D and E show, no concentration of the inhibitors prevented the C5a-induced phagocytic defect in whole blood, though given the small number of experimental repeats, statistical tests were not applied.

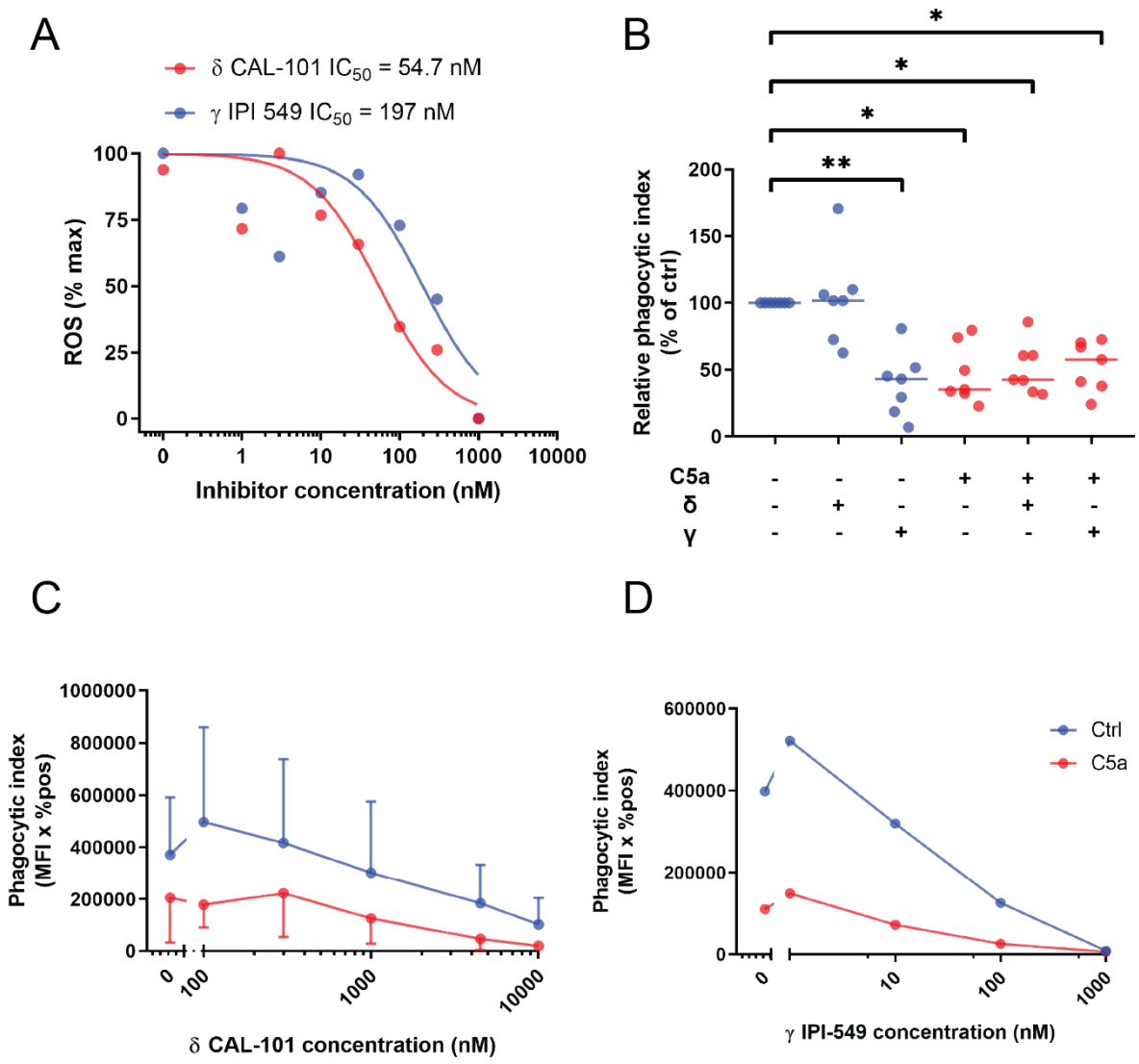

Figure IV-5: C5a-induced phagocytic defect is not PI3K-dependent in whole blood

A: Intracellular ROS production was assessed as detailed in Methods. Whole blood was primed with 20 ng/mL TNF-α for 30 minutes and stimulated with 1 µM fMLP for 20 minutes and the neutrophil DHR fluorescence was measured by flow cytometry. Data are shown as normalised mean values of 5 independent experiments with a non-linear curve fitted. IC_{50} (95 % CI) values were 54.7 nM (18.9-156.3) and 197 nM (57.8-651.7) for the δ-isoform inhibitor CAL-101/idelalisib and γ-isoform inhibitor IPI-549 respectively. B Whole blood was pre-treated with 60 nM idelalisib (δ isoform inhibitor) or 200 nM IPI-549 (γ isoform inhibitor) for 30 minutes prior to C5a treatment (60 minutes) before phagocytosis was quantified as previously. P = 0.0033 by two-way repeated measures ANOVA, **p < 0.01, *p < 0.05 by Sidak's test for multiple comparisons. C and D: whole blood was pre-treated for 30 minutes with increasing concentrations of δ-isoform inhibitor CAL-101/idelalisib (C) or γ-isoform inhibitor IPI-549 (D) prior to C5a exposure for 60 minutes. Phagocytosis was quantified as previously. No statistical tests were performed on these data as they represent the median and IQR of only 3 (C) or 1 (D) independent experiment.

4.6. C5a does not appear to reduce cell-surface phagocytic receptor expression

To assess whether C5a induced defects in phagocytosis by mechanisms other than intracellular signalling involving PI3Ks, the effect of C5a on common phagocytic receptors was assessed by flow cytometry. Figure IV-6 shows that over a wide range of concentrations known to induce a phagocytic defect, C5a did not decrease surface expression of common phagocytic receptors. In fact, C5a exposure led to increased expression of complement receptor 3 subunit CD11b. As expected, C5a exposure decreased the expression of C5aR1 (CD88). Taken together, these data suggest the phagocytic defect induced by C5a is not mediated by downregulation of the assessed phagocytic receptors.

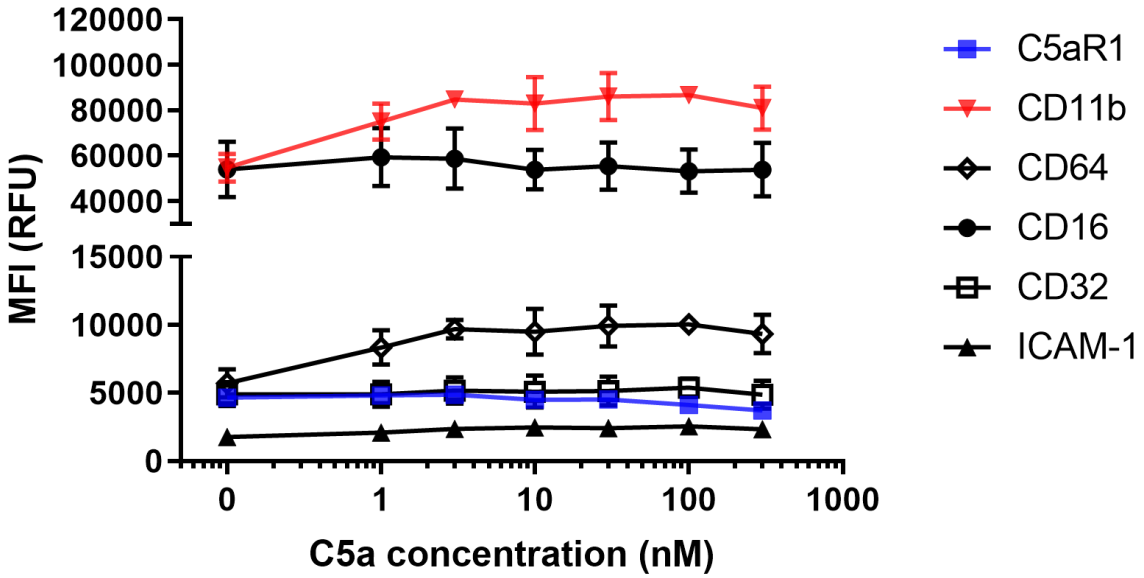

Figure IV-6: C5a does not appear to decrease surface expression of common phagocytic receptors

Whole blood was incubated with semi-log increasing concentrations of C5a for 60 minutes as outlined in Chapter II:12. Blood was then stained for the above cell surface receptors and expression was quantified using an Attune Nxt™ cytometer. Data area shown as the median and range of 2 independent experiments. Statistical tests were not performed owing to the low number of repeats.

4.7. Dual phagocytic challenges reveal subsets of phagocytically avid and non-avid cells in healthy human blood

Throughout the experiments presented to date, both in whole blood and in purified neutrophils, I have observed distinct populations of cells; those that phagocytose large numbers of particles, and those that phagocytose few or none. In order to interrogate this observation in more detail, a double feeding model was used, whereby whole blood was sequentially challenged with 2 phagocytic targets detectable in different channels on the cytometer as detailed in Chapter II:10.2. Figure IV-7A shows an example of how the phagocytic intake of both challenges can be visualised and indicates that pre-treatment with C5a decreases the intake during both challenges. Important to note is the presence of cells that remain negative for both particles (bottom left quadrant) and cells that become positive for both (top right). Interestingly, very few cells that were negative for the first challenge become positive on the second challenge (top left quadrant). These effects were quantified over a range of concentrations of the first phagocytic stimulus (pHrodo red); results are shown in Figure IV-7B. These data indicate cells that do not phagocytose the first challenge are also unlikely to phagocytose the second challenge, and that this difference in phagocytic avidity becomes more pronounced as the intensity (pHrodo red concentration) of the first challenge increases.

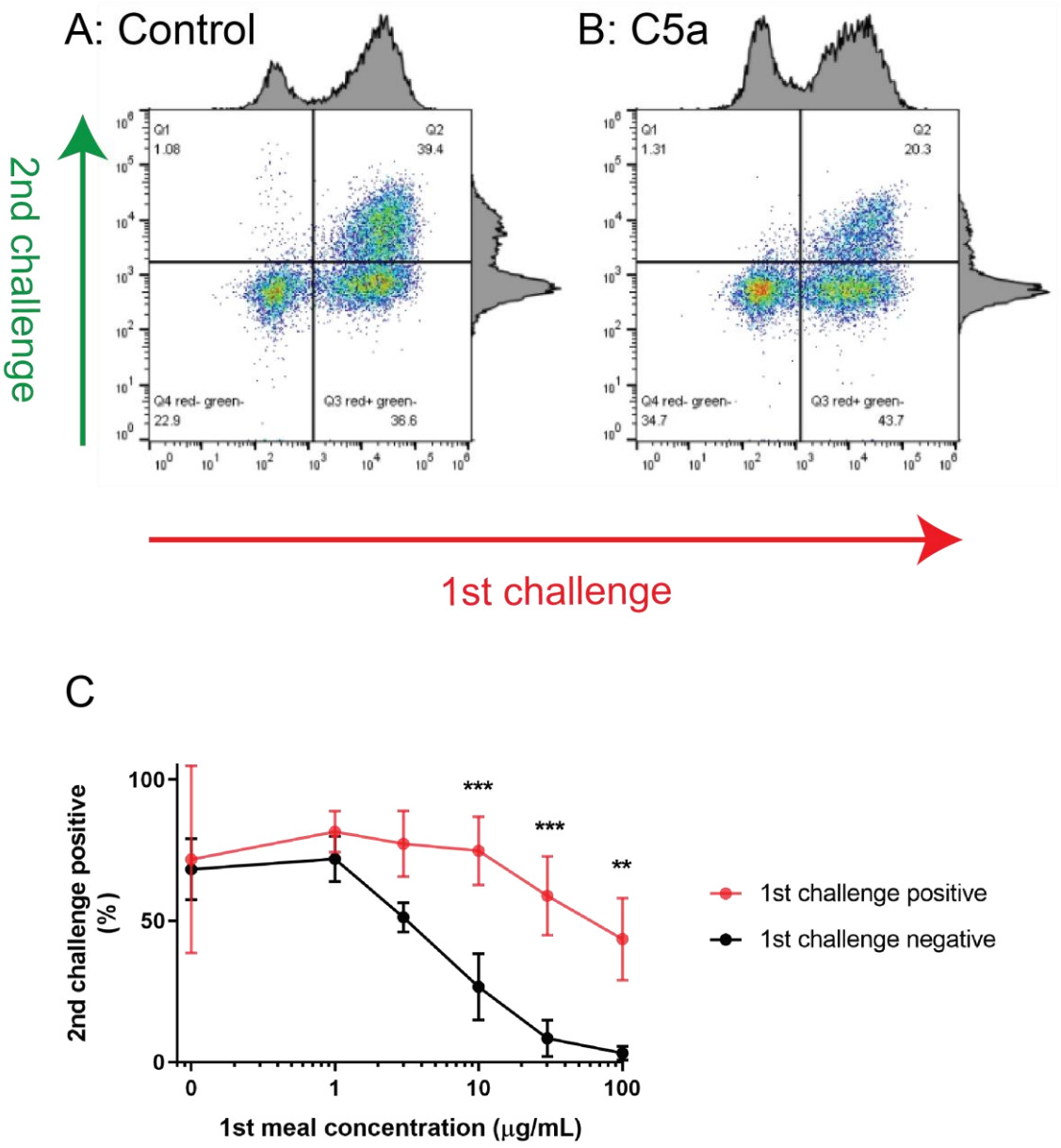

Figure IV-7: Distinct phagocytic subsets of neutrophils exist in healthy human blood

Dual phagocytic challenges were administered as detailed in Chapter II::10.2. A (Ctrl) and B (C5a) are example flow cytometry dot plots of whole blood neutrophils that have been sequentially challenged with pHrodo *S. aureus* red Bioparticles (15 µg/mL, 30 minutes) then pHrodo *S. aureus* green Bioparticles (15 µg/mL, 30 minutes) before being stained for CD16 and analysed. Four distinct populations of cells are evident: non-phagocytic, bottom left quadrants; 1st challenge-only positive, bottom right; double challenge positive, top right; 2nd challenge-only positive, top left. B shows the effect of pre-treatment with 300 nM C5a is to decrease phagocytosis of both challenges, shifting cells downward and leftward. The data shown in C quantify results shown in A and B, whereby the percentage of cells phagocytosing during the second challenge is shown based on whether the cells phagocytosed during the first challenge (1st challenge positive, red) or not (1st challenge negative, black). Data is presented as the mean and SD of 5 independent experiments. $p < 0.0001$ by two-way repeated measures ANOVA, ***$p < 0.001$, **$p < 0.01$ by Sidak's multiple comparisons test. Data presented in C kindly generated by Carmelo Zinnato.

4.8. Novel whole blood assay can be applied in clinical settings

Having developed a novel assay of neutrophil function in small, minimally manipulated samples of human whole blood, I aimed to demonstrate its utility in an outpatient clinical setting. Five individuals with diagnosed immunodeficiency syndromes were recruited from the immunodeficiency clinic of a tertiary hospital in the UK. Patient details are listed in Table 4, and there was no clinical evidence of infection at the time of blood draw. Patient blood samples were drawn after standard clinical blood samples during routine outpatient appointments. The standard whole-blood assay was performed on patient samples within one hour of blood draw, and unmatched controls were drawn from the routine blood donors of the Chilvers'/Summers' group on separate days. Table 4 shows patients were a wide variety of ages and were affected by different causes of immune deficiency. Figure IV-8 shows that all 5 patients recruited had their neutrophil phagocytosis and ROS production in response to *S. aureus* Bioparticles successfully measured by a single operator, and that there appears to be a similar reduction in phagocytosis in response to C5a pre-treatment amongst immunodeficient patients. Further, the data show that neutrophils from NFKB deficient patients may phagocytose less and produce less ROS in response to an *S. aureus* stimulus relative to controls. The 1 APDS patient assessed appeared to have a higher baseline level of phagocytosis and ROS production, and their neutrophil phagocytosis was not augmented by LPS pre-treatment, in contrast to controls. These results demonstrate successful application of this assay in a clinical setting,and raise intriguing questions with respect to neutrophil function in patients with immunodeficiency syndromes.

Table 4: Immunodeficient patient characteristics

Diagnosis	Abbreviation	Sex	Mutation	Phenotype
NFκB deficiency[315]	NFKB	F	NFκB subunit 1 loss of function	Hypogammaglobulinaemia (IgG 3) and recurrent respiratory infections.
NFκB deficiency	NFKB	M	As above	As above
NFκB deficiency	NFKB	M	As above	As above
Activated PI3 kinase delta syndrome[316]	APDS	F	E1021K conferring hyperactivity of PI3Kδ.	Recurrent respiratory infections, lymphopaenia.
Severe combined immunodeficiency not otherwise specified	SCID NOS	M	Unknown	Combined T- and B-cell immunodeficiency, recurrent mycobacterial infections.

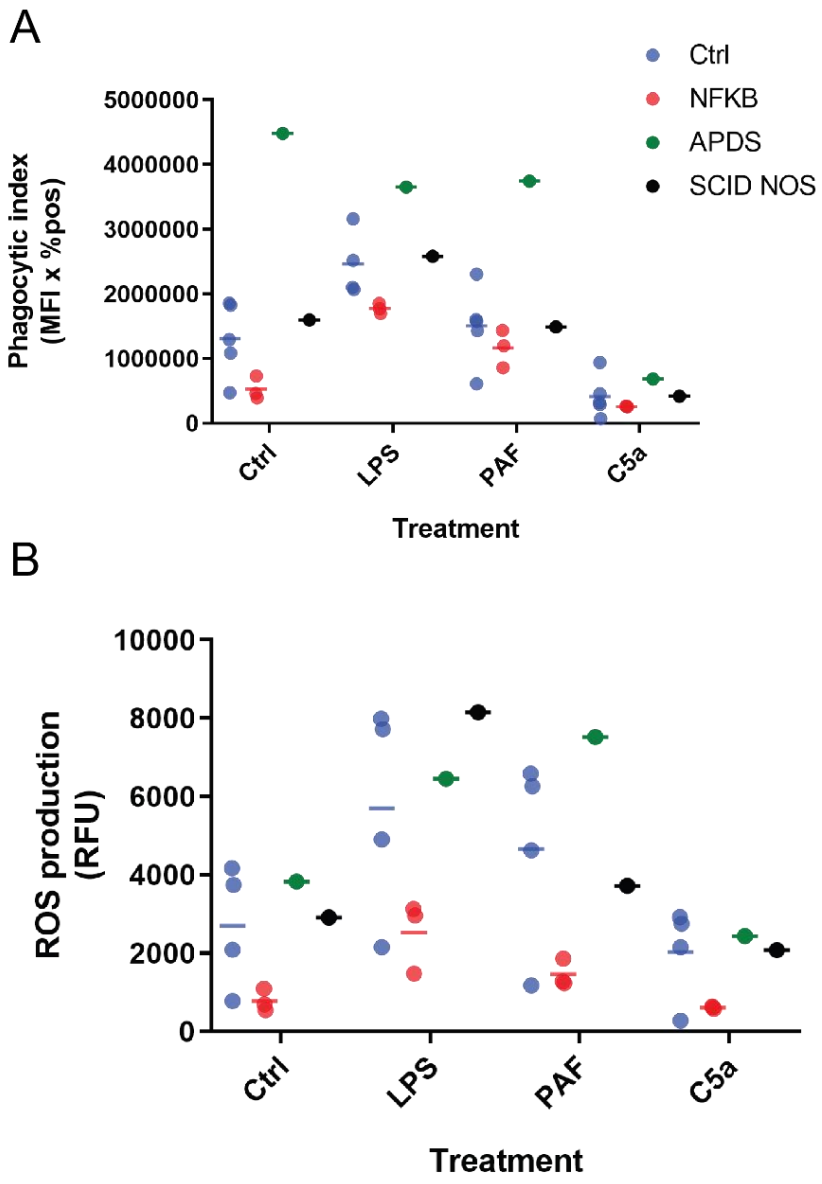

Figure IV-8: The whole blood assay can be applied in clinical settings

2 mL blood was drawn from 5 patients with immunodeficiency syndromes during routine outpatient appointments, and neutrophil phagocytosis and ROS production in response to *S. aureus* Bioparticles were measured within one hour of blood draw by the standard whole-blood assay as previously described. Patient characteristics are described in Chapter II:10.4. Control samples were drawn on separate occasions. Blood was pre-treated with the following agonists and durations: Ctrl (PBS) 60 minutes; LPS 100 ng/mL 60 minutes; PAF 1 µM 5 minutes; C5a 300 nM 60 minutes. Studies were completed by 1 operator and data was available for analysis within 120 minutes of blood draw. No statistical tests were applied as these data are exploratory and intended to demonstrate feasibility only.

5. Discussion

A key challenge facing investigators of immunotherapies for critically ill patients is the appropriate targeting of therapies.[108,167,317] Investigators should consider immunophenotyping patients before stratification into intervention arms to ensure the relevant cellular dysfunction is actually present before treating it. The adoption of such targeted therapies holds promise; a recent retrospective subgroup analysis of the multicentre phase III Sepsis Syndrome Study[318] of recombinant human IL-1 receptor antagonist in sepsis showed a mortality benefit of the drug in patients who had higher baseline plasma IL-1 receptor antagonist levels.[319] The authors suggest another, targeted trial of the same therapy is indicated. Neutrophil dysfunction is known to be a key driver of poor outcomes in critically ill patients,[147,149,177,213] though trials targeting therapies such as GM-CSF to patients with neutrophil dysfunction measured by conventional strategies were laborious and unfortunately did not achieve statistical significance of the primary outcome.[313]

Therefore, there is a need for rapid, scalable assessments of neutrophil dysfunction if investigators are to reliably target novel immunotherapies in clinical trials. This chapter discusses the initial development of such an assay, its use to interrogate C5a-induced neutrophil dysfunction and demonstrates feasibility in a clinical setting. Figure IV-1 shows the simple workflow for interrogating neutrophil function without RBC lysis or fixation steps, made possible by the novel Attune Nxt™ Acoustic Focusing Cytometer from Life Technologies. Couple this cytometer with the pH-sensitive pHrodo Bioparticles used throughout this thesis and the well-established indicator of ROS production, DHR,[291] and two key neutrophil functions can be readily measured in small samples of whole blood.

In this setting, anticoagulants are not removed by washing steps, and chelated divalent metal cations are not replaced as they are in conventional neutrophil preparations (see protocol in Appendices). The effect of anticoagulants on cell function therefore become much more important when working with whole blood. Previous work by Mollnes and others demonstrated brisk complement activation by citrate and heparin,[320] whereas the direct thrombin inhibitor lepirudin did not interfere with complement activation.[266] These data informed my choices of anticoagulants for assessment of neutrophil functions. Argatroban is an FDA-approved synthetic direct thrombin inhibitor[321] analogous to lepirudin, and was used as lepirudin is no longer available. The concentration of argatroban was adopted from previous *ex vivo* studies[322] and titrated down to the minimal concentration that maintained blood in a macroscopically anticoagulated state at 7 hours, which was 150 µg/mL. As Figure IV-2 shows, argatroban at a concentration of 150 µg/mL allows the greatest degree of neutrophil priming and highest rates of phagocytosis and ROS production relative to EDTA, citrate and heparin at respective concentrations recommended by the manufacturer.[323] Given these data, argatroban was adopted as the anticoagulant used in future studies.

Having established this novel assay, I then assessed the effect of C5a and other priming agents in this system. The titration of C5a shown in Figure IV-3A shows a dose-response effect of C5a on neutrophil phagocytosis in this model, with peak effects reached at excessively high concentrations of C5a. A concentration of 300 nM was chosen as it balanced the necessity of achieving a robust response with excessive use of costly purified human C5a. The higher concentration of C5a used in the whole blood studies may have been driven by the presence of plasma carboxypeptidases, known to cleave and inactivate C5a which were not present in purified cell systems.[204,207] Regardless, concentrations as high as 1000 nM have been measured in critical illness,[92] and as discussed in Chapter I:, receptor saturation rather than concentration of agonist is likely to be a more important determinant of functional consequences of C5a.

Figure IV-3B and C demonstrate the sizeable defect in phagocytosis induced by C5a in this model and show that these effects are not simply an artefact of using a pH-sensitive dye. Work by Huber-Lang's group published in 2017 demonstrated that C5a exposure transiently increased neutrophil intracellular pH.[261] Given the pH-sensitivity of pHrodo fluorescence, it therefore became important to demonstrate that the decreased pHrodo fluorescence I had observed was genuinely the result of decreased phagocytosis, as opposed simply to a reduction in cellular acidification. The use of a non-pH sensitive dye (AF488) conjugated to *S. aureus* Bioparticles confirmed the defect was indeed due to phagocytic failure and justified ongoing use of pHrodo Bioparticles.

Figure IV-3D and E address the question of whether phagocytosis and ROS production were uniquely inhibited by C5a, or whether these effects were shared with other typical neutrophil priming agents in my hands. A variety of GPCR (PAF) and non-GPCR (LPS, TNF-α, GM-CSF) ligands were selected to provide a broad cross-section of priming agents acting through different pathways[324] and pre-treatment durations were chosen based on known maximal adhesion molecule upregulation demonstrated by members of our group.[325] The data presented show C5a reduced phagocytosis and phagosomal ROS production, whereas LPS and PAF increased phagocytosis, and LPS alone increased ROS production. GM-CSF and TNF-α had no effect in this system. These results are consistent with those of Rosales[326] and Hayashi[327] who showed PAF and LPS increased rates of IgG-mediated phagocytosis by purified neutrophils respectively, but contrast with data from Mookerjee and colleagues[328], which showed a reduction in phagocytosis by neutrophils from cirrhotic patients after LPS exposure. Previous data from our group showed GM-CSF increased phagocytosis of zymosan by adherent, purified neutrophils,[177,213] thus the lack of effect of GM-CSF in this system was surprising. However, given the exquisitely context-sensitive characteristics of neutrophil phagocytosis, it is likely that these discrepant results can be explained by differences in phagocytic target and the presence of a multitude of factors in whole blood not

assessed in previous assays of phagocytic function. The key finding of a significant functional impairment induced by C5a in multiple experimental systems remains and appears to be unique to this agent in whole blood. Further experiments are necessary before these findings can be generalised and interpreted in the context of conflicting data from other experimental systems.

In keeping with my work in purified cells, C5a induces a marked and prolonged defect in neutrophil phagocytosis in whole blood, as shown in Figure IV-4. This defect is persistent for up to 7 hours after C5a was added, in keeping with data from purified cells shown in Figure III-7. In the whole blood system, phagocytosis was measured after each hour of C5a incubation, rather than continually from the beginning of the assay as in Figure III-7. This slight difference in methodology ensured that the same phagocytic challenge was applied after each hour of C5a exposure and demonstrated that neutrophil phagocytosis was decreased by C5a at each successive time point. To my knowledge, this is the first time such a prolonged phagocytic defect induced by C5a has been demonstrated in either whole blood or purified neutrophils *in vitro*. This finding has implications for the immunosuppression evident in critically ill patients which can persist for days[147] and even weeks after an initial insult.[167,329] Reversal or amelioration of this prolonged deficit are attractive therapeutic targets, though total C5a-C5aR blockade, whilst promising in initial animal studies, has not yet enjoyed success in human clinical trials and is likely to have a plethora of unwanted off-target effects.[330,331] Therefore, it remains important to identify the signalling events in neutrophils precipitated by C5a which mediate this phagocytic defect, so that they may be selectively targeted. To this end, the role of PI3K enzymes in the whole blood model was assessed.

Given the role of PI3Ks in mediating C5a-induced phagocytic defects demonstrated earlier in this thesis and their previously established role in C5a-mediated impairment of phagocytosis of zymosan[177,213]I set out to assess their role in whole blood, given the important contextual difference that this new experimental system represents. The concentration at which to use these compounds in whole blood was unclear, as IC_{50} values drawn from biochemical and cellular assays differed markedly depending on function measured and cells used, and wide concentrations have been reported in the literature.[305,306] Without being able to assess directly PI3K activation in whole blood, a surrogate process which is known to PI3K-dependent was used, namely production of ROS in response to a soluble fMLP stimulus.[66] Data presented in Figure IV-5A shows the resultant dose-response curves and the IC_{50} values for CAL-101/idelalisib and IPI-549. Interestingly, in this system the ROS response appears to be more sensitive to inhibition of the delta isoform, which may be due to the delta isoform selectively being responsible for the prolonged phase of ROS production in human cells.[66] The IC_{50} values generated here are significantly higher than published cell-free

biochemical IC_{50}'s for the relevant isoform of PI3K, which were 16 nM for IP-549[306] and 2.5 nM for CAL-101.[332] However, this observation is not surprising given the requirement of these compounds for cell penetration and the complex physiological milieu in which they are operating in whole blood. These compounds were then used at their IC_{50} values to generate the data in Figure IV-5B, which demonstrates that PI3K inhibition at these concentrations had no effect on C5a-mediated phagocytic impairment induced in whole blood, in stark contrast to the finding in Figure III-5. It would also appear from the same data that the gamma-selective inhibitor IPI-549 has a potent effect on phagocytosis, as even at its IC_{50} concentration for ROS production, it induced a significant reduction in baseline phagocytosis.

To confirm these results were not simply due to inadequate concentrations of each drug in this system, or inactivation by components of RBCs or plasma, a wide range of concentrations were assessed in Figure IV-5C and D. No concentration of these compounds ameliorated C5a-induced phagocytic defects, though as expected at high concentrations both drugs inhibited phagocytosis in general. The data presented sound a note of caution with respect to the use of systemically administered PI3K inhibitors to treat neutrophil dysfunction, in that they may not be as effective as when the drugs are applied directly to neutrophils in tissue compartments. This is of particular relevance given idelalisib is already licenced for the treatment of relapsed lymphomas[333], and that Phase II trials of inhaled PI3K-δ inhibitors are underway in chronic obstructive pulmonary disease[334] and APDS.[335]

Given the above data on showing PI3K inhibition did not prevent C5a-induced phagocytic impairment in whole blood, I assessed whether C5a reduced cell surface expression of common phagocytic receptors, as a further attempt to understand the mechanism of our previous observations. Over a wide array of concentrations, C5a did not appear to reduce cell surface expression of common IgG and complement receptors, and in fact appeared to increase the expression of the CR3 component CD11b, consistent with previous data on neutrophil priming,[325] and as has previously been demonstrated in a whole blood model of complement activation.[266] C5aR1 expression was downregulated with increasing C5a concentrations as expected.[336,337] Changes of the C5aR and their relation to phagocytosis are the subject of Chapter V: and as such are not discussed in detail here. These data indicate simple changes in cell surface phagocytic receptor expression do not explain C5a-induced phagocytic defects in this system, thus other mechanisms must be sought. We chose to adopt an unbiased assessment of the neutrophil phosphoproteome, and these experiments are detailed in Chapter VI:.

The presence of circulating neutrophil subsets in health and disease has long been studied and debated within the literature.[7,338,339] The novel whole blood assay developed in this chapter offers an exciting way to add to this discussion as differences in function are now easily measurable in unmanipulated, circulating cells. I used this method to further address

an observation long noted by myself and colleagues in the lab; that of apparently phagocytically avid and non-avid cells present in most individuals. Figure IV-7A shows the stark difference in phagocytosis between cells circulating at the same time in the same individual, and that C5a tends to make all cell types phagocytose less (B). Quantification of these populations in Figure IV-7C demonstrates that the difference between these cells is preserved on the second challenge and becomes more pronounced as the initial stimulus intensity is increased. These data are consistent with data from Koenderman's group who have also shown distinct phagocytic functional subsets of purified neutrophils using a cell-sorting approach.[340] Taken together, the data indicate the difference in phagocytic uptake between neutrophils observed in experiments to date is not simply due to stochastic encounters between cells and target. Rather, there is an intrinsic difference in the phagocytic avidity of circulating human neutrophils in healthy individuals, which may be susceptible to manipulation, by C5a for instance.

A key aim of this chapter was to demonstrate the whole blood assay may be suitable for eventual clinical use. Having refined an approach made possible by the Attune Nxt™ and applied it to questions of C5a biology, I set out to ascertain whether the assay may be usable in a clinical setting. To this end we recruited patients with known immunodeficiency syndromes covered by existing research ethics committee approvals who were having blood drawn for routine clinical tests. Table 4 shows these patients were diagnosed with one of three immunodeficiency syndromes, and none of these conditions are associated with neutrophil dysfunction based on disease phenotypes identified in the literature.[316,341] Figure IV-8 illustrates the neutrophil phagocytosis and phagosomal ROS production of five patients and four unmatched controls, and demonstrates that data was easily acquired during routine clinic appointments from multiple patients by one operator. Further, the data raise the possibility of defective phagocytosis by neutrophils from individuals with the NFκB1 mutation, a previously undescribed characteristic of these patients.[315,341]

The work in this chapter is a further stepwise improvement from a non-physiological system with unlikely phagocytic target (adherent neutrophils with zymosan) to a more physiological system with relevant pathogens (neutrophils in suspension with *S. aureus* or *E. coli*) finally to a rapid assay of neutrophil function in whole blood that is applicable in a clinical setting. A key finding of this thesis (prolonged impairment of neutrophil phagocytosis by C5a) has been replicated in whole blood, and important mechanistic details (PI3K signalling and cell surface receptor changes) have been interrogated and found insufficient to wholly explain C5a-induced dysfunction in this system. Therefore, alternate approaches were used, and are discussed in the following chapters.

Chapter V: Phagocytosis decreases surface C5aR1 expression and confers resistance to C5a

1. Chapter summary

The work in this chapter arose from the observation that exposing neutrophils to C5a at the same time as bacteria (as opposed to pre-treatment models used elsewhere in this thesis) did not lead to impairment of phagocytosis. Further, I had often noted a decrease in C5aR1 expression measured on the surface of neutrophils after phagocytosis (without C5a present) and wondered whether this receptor was directly involved in phagocytosis, and if this reduced receptor expression mediated the subsequent resistance to C5a-induced phagocytic impairment. To my knowledge, a report by Doroshenko and colleagues[211] is the only published study to make note of C5aR1 downregulation during phagocytosis, though it was not the focus of the report and the data were not shown or discussed. An intriguing possibility was also raised by Bamberg and colleagues[231] who demonstrated co-localisation of C5aR1, 2 and β-arrestin in endosomes, and posited an ongoing signalling function of this complex. I therefore wanted to establish whether pre-incubation with bacteria prevents C5a-induced phagocytic defects, and then to interrogate the fate of C5aR1 in the context of phagocytosis.

2. Hypotheses and aims

C5aR1 is internalised during phagocytosis, localises to phagosomes and plays a role in subsequent signalling and phagosomal maturation.

- To demonstrate that cells allowed to phagocytose pathogens prior to C5a exposure are protected from C5a-induced phagocytic defects.
- To assess whether C5aR1 surface expression is reduced by phagocytosis of pathogens.
- To assess whether the reduction in surface C5aR1 expression is due to protease-dependent receptor shedding.
- To visualise the fate of C5aR1 during phagocytosis using confocal microscopy.

3. Notes on methods

Methods used within this chapter are not dissimilar to assays discussed extensively in previous chapters and in the Methods section. Two protease inhibitors were used to generate data presented in Figure V-3: recombinant human secretory leukocyte protease inhibitor (SLPI, R&D Systems) a broad-spectrum endogenous protease inhibitor with high potency against common neutrophil proteases including neutrophil elastase and cathepsin G[342] and marimastat (Sigma) a broad spectrum metalloprotease inhibitor.[51] These inhibitors were chosen as they were found to have no inhibitory effect on phagocytosis, unlike other protease inhibitors such as (1,10)phenanthroline (data not shown). Protease inhibitors were chosen and the data in Figure V-3 were produced by Carmelo Zinnato, who was introduced in the previous chapter. All other modifications of standard assays are detailed in figure legends.

4. Results

4.1. C5a-induced impairment of phagocytosis is prevented by exposure to phagocytic target

The data presented here arose from experiments initially designed in parallel with those shown in Figure 4.6, with the aim of understanding the duration of C5a exposure required to impair phagocytosis. As these were purified cells (as opposed to whole blood) neutrophils were exposed to 100 nM C5a at various time points (either 60 minutes before, at the same time, or 60 minutes after addition of *S. aureus*). C5a was not removed by washing, and the cells were allowed to phagocytose for the time points indicated. Figure V-1A shows that exposure of cells to C5a at the same time or after pathogen exposure fails to induce the customary phagocytic defect, and that this phenomenon persists over the 7 hours of assessment. Data from an experiment testing the same hypothesis in whole blood is shown in Figure V-1B, which indicate 60 of C5a pre-treatment induces a phagocytic defect as expected, but co-administration of C5a with the *S. aureus* challenge fails to induce the same defect.

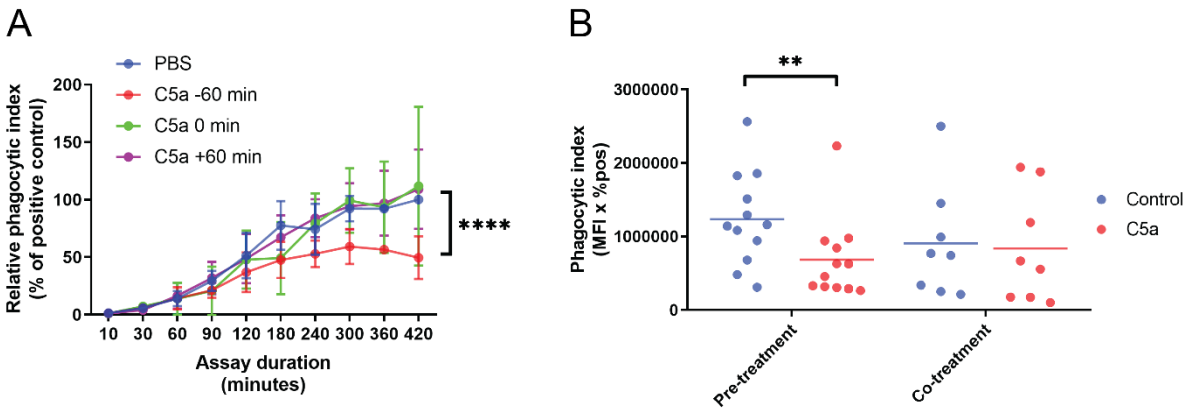

Figure V-1: C5a-induced impairment of phagocytosis is prevented by pre-exposure to *S. aureus*

A: *S. aureus* Bioparticles (3 µg/mL) were incubated with isolated PMNs in the presence of 100 nM C5a or PBS, which was added at the indicated time points, with time 0 representing the time at which *S. aureus* Bioparticles were added. Cells were allowed to phagocytose for the indicated time points and phagocytic index was quantified by flow cytometry as previous. Data are presented as the mean and SD of the phagocytic index of C5a-treated cells relative to their paired PBS control for 5 independent experiments. $p < 0.0001$ for time and $p = 0.0186$ for treatment by two-way ANOVA. ****$p < 0.0001$ by Dunnett's multiple comparisons test. B: Whole blood was incubated with 300 nM C5a, added 60 minutes prior to (pre-treatment) or at the same time (co-treatment) as addition of *S. aureus* Bioparticles. Cells were allowed to phagocytose for 30 minutes and phagocytic index was quantified by flow cytometry as previous. $p = 0.0173$ for pre-treatment vs co-treatment by two-way ANOVA. ** $p = 0.0035$ by Sidak's test of multiple comparisons.

4.2. C5aR1 expression is reduced by multiple stimuli but only prior phagocytosis protects from C5a-induced dysfunction

To interrogate the role of C5aR1 in mediating the protective effects of phagocytosis, C5aR1 expression was assessed on neutrophils in whole blood incubated with a variety of neutrophil priming agents and inflammatory stimuli. Data shown in Figure V-2A indicate that multiple, different stimuli appear to reduce surface expression of C5aR1, though only C5a reached a statistically significant reduction on post-hoc testing for multiple comparisons. In light of these findings, experiments assessing the ability of these other agents to protect against C5a-induced phagocytic impairment were performed. The data shown in Figure V-2B demonstrate that these stimuli, despite their ability to downregulate C5aR1 surface expression, had no ability to protect from C5a-induced phagocytic dysfunction, with the exception of *S. aureus* as already demonstrated. Shown in Figure V-2C are C5aR1 expression measurements from the dual phagocytic challenge experiments originally shown in Figure IV-7. These data illustrate that the downregulation of C5aR1 after phagocytosis is dose-responsive to the amount of phagocytosis that has occurred, with cells positive for both phagocytic challenges having lower levels of C5aR1 surface expression relative to single positive and negative cells in the same milieu.

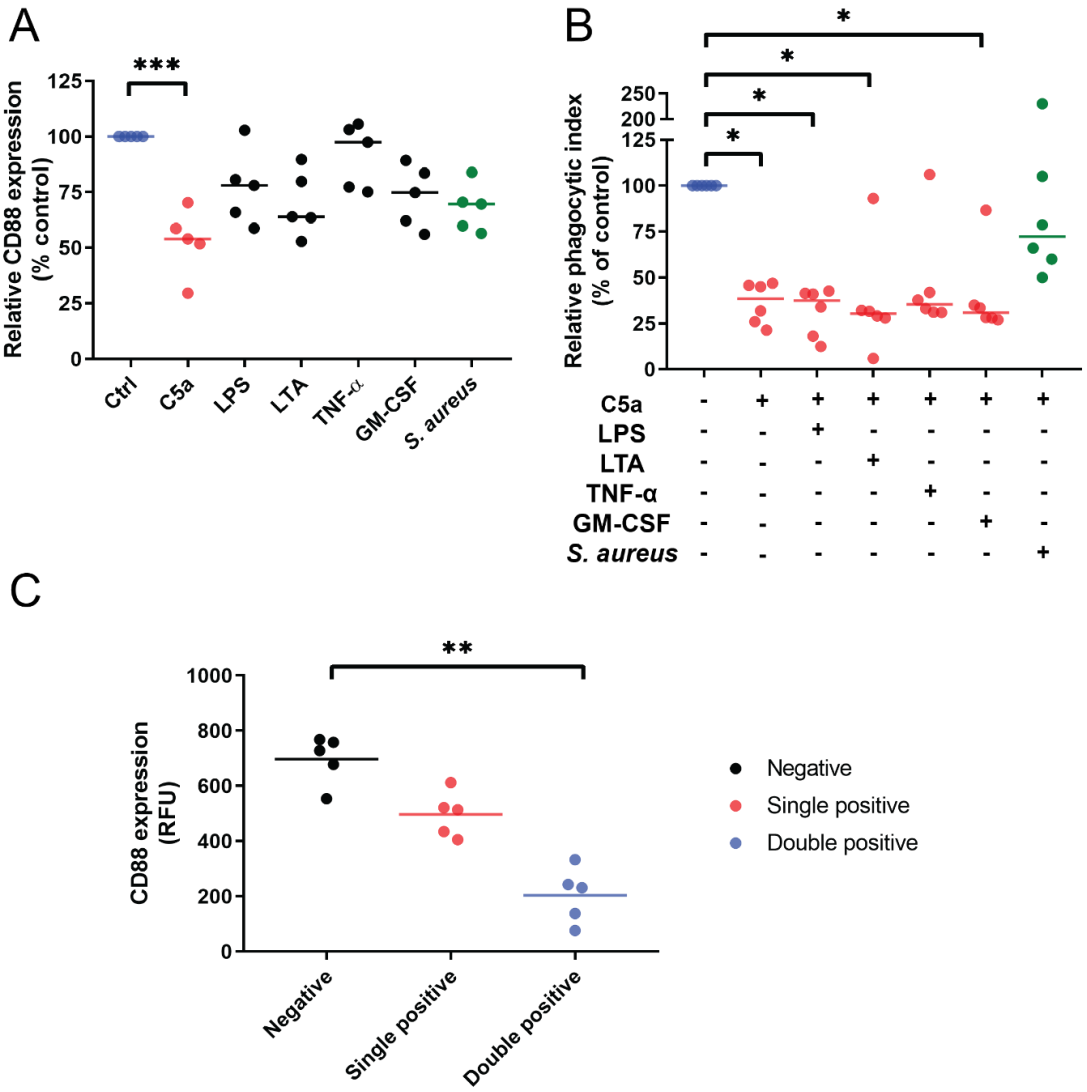

Figure V-2: C5aR1 surface expression is reduced by multiple inflammatory stimuli, only phagocytosis confers protection from C5a

A: Whole blood was incubated with the following inflammatory stimuli for 60 minutes prior to measurement of neutrophil C5aR1 expression by flow cytometry: 300 nM C5a; 100 ng/mL LPS; 10 µg/mL LTA; 20 ng/L TNF-α; 10 ng/mL GM-CSF; *S. aureus* green 10 µg/mL. Individual data points and their median values from n = 5 independent experiments are shown. Friedman's test with p-value = 0.0003, ***p < 0.001 by Dunn's multiple comparisons test. B: whole blood was pre-incubated with control or inflammatory stimuli as in (A) and then with 300 nM C5a for 60 minutes. Cells were then allowed to phagocytose 10 µg/mL *S. aureus* red Bioparticles for 60 minutes before phagocytosis was assessed by flow cytometry as previously described. Individual data points and their median values from n = 6 independent experiments are shown. Friedman's test with p-value = 0.0038, *p < 0.05 by Dunn's multiple comparisons test. C: whole blood was subjected to dual phagocytic challenges (15 µg/mL *S. aureus* red, 30 minutes then 15 µg/mL *S. aureus* green, 30 minutes) as previously described and C5aR1 expression was measured by flow cytometry. Individual data points and their median values from n = 5 independent experiments are shown. Friedman's test p-value 0.0008 **p < 0.01 by Dunn's multiple comparison's test.

4.3. Decreased C5aR1 expression is not due to protease action

A potential explanation for the data above is that plasma or liberated cellular proteases cleave C5aR1 from the neutrophil surface. We therefore assessed expression of the cell surface receptors C5aR1, TNFR1 and CD16 (FcγRIII) after stimulation with *S. aureus* or fMLP in the context of protease inhibition. The protease inhibitors were SLPI and marimastat which inhibit serine/threonine proteases and metalloproteases respectively, as previously discussed. Figure V-3 demonstrates that the reduction in surface C5aR1 mediated by *S. aureus* phagocytosis or fMLP is not dependent on either subset of protease. This contrasts with TNFR1 shedding, which could be prevented by metalloprotease inhibition but not serine/threonine protease inhibition, as shown in B. Finally, the data presented in Figure V-3C show that surface expression of CD16 does not appear to be significantly altered in this setting, indicating that the downregulation of TNFR1 and C5aR1 during *S. aureus* exposure are not simply due to internalisation of large portions of cell membrane during phagocytosis.

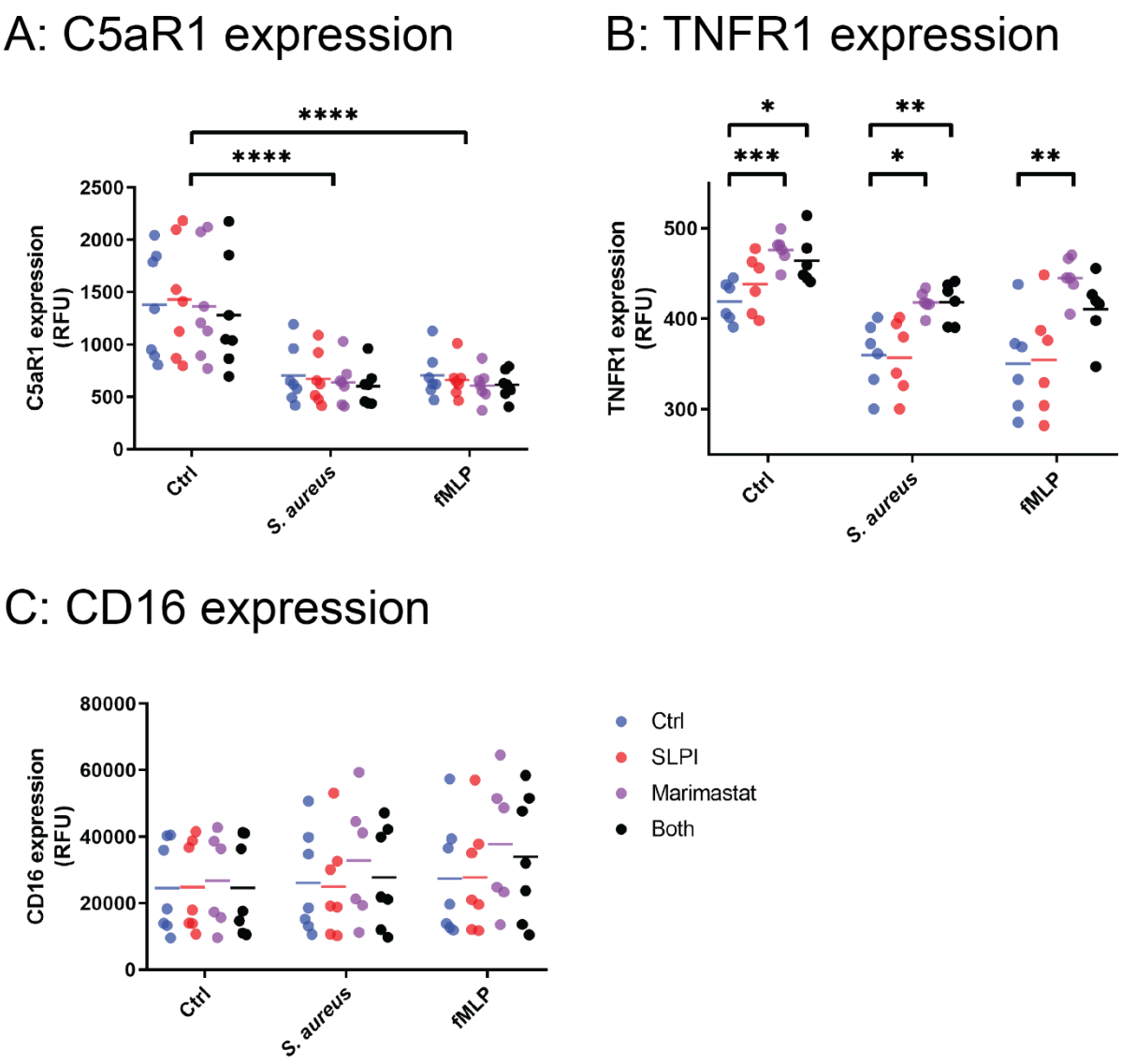

Figure V-3: C5aR1 is not shed by proteases as opposed to TNFR1. Reduction of C5aR1 is not simply due to gross membrane internalisation with phagocytosis

Whole blood was treated with vehicle control, 10 µg/mL SLPI, 100 nM marimastat or both for 30 minutes. Blood was then stimulated with vehicle control, 10 µg/mL *S. aureus* or 1 µM fMLP for 60 minutes. Cells were stained for C5aR1 (A), TNFR1 (B) and CD16 (C) on ice in the dark before being analysed by flow cytometry as previously described. Individual data points with respective mean values are shown for n = 7 independent experiments. A: Two-way ANOVA p = 0.154 for drug and p = 0.0021 for stimuli, p = ****p < 0.0001 by Dunnett's test of multiple comparisons. B: Two-way ANOVA p = 0.0063 for drug and p < 0.0001 for stimuli *p < 0.05 **p < 0.01 ***p < 0.001 by Dunnett's test of multiple comparisons. C: Mixed-effects model (due to missing data for marimastat treatment for one experiment) p = 0.62 for drug and p = 0.058 for stimuli, not significant so no post-hoc testing performed.

4.4. Investigating the fate of C5aR1 after phagocytosis

Given the data presented above, I hypothesised that C5aR1 is internalised (rather than shed into the extracellular milieu) during phagocytosis and exposure to other pro-inflammatory stimuli. I attempted to identify and localise C5aR1 in unstimulated cells as it should be mostly present on the cell surface. Using the protocol outlined in Methods, I was able to visualise f-actin and cell nuclei but failed to achieve convincing staining of C5aR1. Figure V-4 demonstrates that the isotype control antibody stains similar structures within the cell to a similar degree (if not brighter) than the anti-C5aR1 antibody.

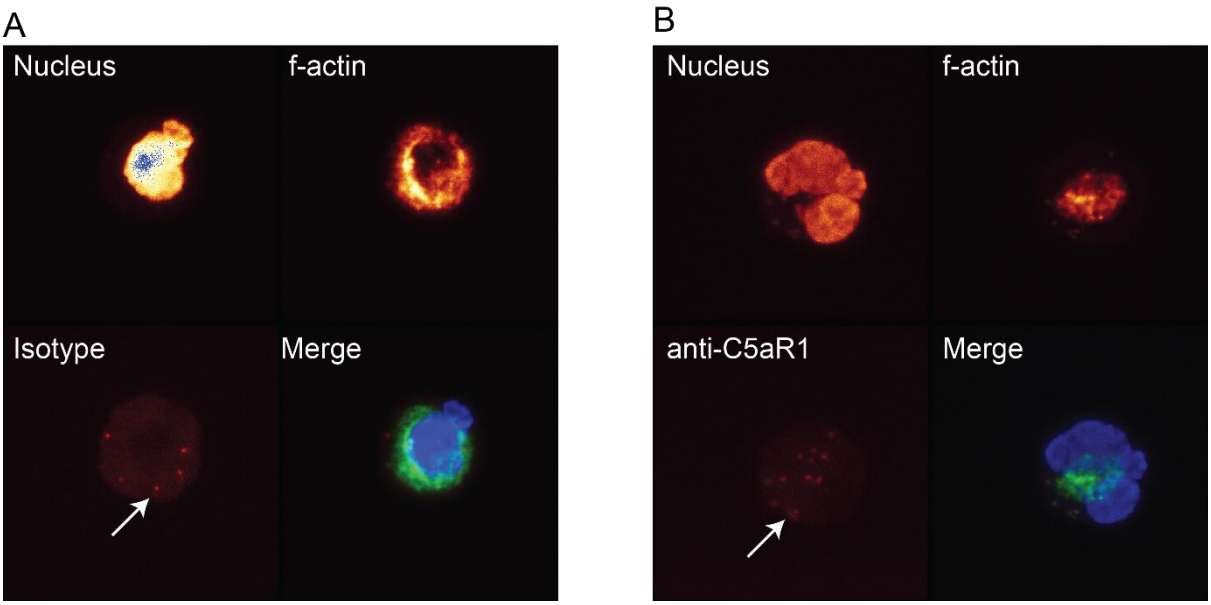

Figure V-4: Confocal staining of purified neutrophil cell-surface C5aR1 was unsuccessful

Purified human neutrophils were adhered to AS-coated 24-well glass imaging plates for 30 minutes in the presence of Hoescht 22342. Neutrophils were fixed, washed and permeabilised and blocked as in Methods. Primary antibody (A: mouse monoclonal anti-human C5aR1 clone S5/1, 1:200) or isotype control (B: mouse monoclonal IgG2a κ clone MG2A-53, 1:200) were added and cells stained for 60 minutes. Cells were washed and secondary antibody (AF568-goat polyclonal anti-mouse IgG heavy and light chain, 1:500) and AF488-phalloidin (1:200) were added and cells stained for 60 minutes protected from light. Neutrophils were washed, left in PBS and visualised by confocal microscopy at 630 X magnification. White arrows indicate areas of non-specific staining observed with antibody and isotype control.

5. Discussion

The work presented in this chapter details my attempts to understand changes that occur with C5aR1 during phagocytosis, and if these changes mediate resistance to the effects of C5a observed in Figure V-1 and Figure V-2B. There are numerous reports of C5aR1 expression in a variety of contexts by our group[147,213] and others.[225] However, to my knowledge, only one study mentions any association between decreased C5aR1 expression and phagocytosis specifically,[211] though others have identified the ability of *S. aureus* supernatants to downregulate C5aR1 expression.[343] Given that a known mechanism modulating responsiveness to inflammatory molecules is homologous or heterologous downregulation of surface receptors,[344–346] I wondered whether phagocytosis-induced downregulation of cell surface C5aR1 was a mechanism by which cells controlled responsiveness to subsequent C5a exposure, perhaps allowing them to remain in-situ and destroy internalised bacteria. Another explanation advanced by Veldkamp and colleagues[343] is that C5aR1 downregulation is in response to an *S. aureus* virulence factor which impairs neutrophil function, though this is a less likely explanation for my data as the bacteria used in the pHrodo Bioparticles are heat-killed and inert.

The data shown in Figure V-2A demonstrate that multiple inflammatory molecules cause a reduction in cell surface C5aR1 expression, though none to the same degree as C5a itself. However, the data in part B demonstrate that despite all of the same molecules causing a decrease in C5aR1 surface expression, only exposure to and phagocytosis of an initial *S. aureus* stimulus demonstrated any ability to protect phagocytosis from subsequent C5a exposure. The data shown in Figure V-2C provide further evidence that the reduction in C5aR1 with phagocytosis is indeed related to the process of phagocytosis itself (as opposed to unidentified paracrine factors in the experimental milieu) as there is a dose-response relationship between C5aR1 downregulation and the number of particles ingested. Dandekar and colleagues have suggested that actin dynamics modulate subsequent signal responses to chemoattractants such as fMLP and C5a,[347] though they did not report on phagocytic stimuli specifically. Further, the necessity of using an inhibitor cocktail (previously characterised by that group[348]) to arrest actin dynamics limits extrapolation of these results to the situation *in vivo*. In context of these reports and the data presented in this chapter, there is a suggestion that significant actin dynamics (rather than simply receptor downregulation) modulates responsiveness to subsequent C5a exposure.

The final two figures presented in this chapter attempt to address the fate of C5aR1 after it has disappeared from the cell surface. Figure V-3A shows that C5aR1 does not appear to be shed in a serine/threonine protease or metalloprotease-dependent manner during phagocytosis or treatment with fMLP, in contrast to TNFR1 (B), which is protected from shedding by inhibition of metalloproteases. These data are consistent with those from van

den Berg[212] who also showed a reduction in C5aR1 expression after fMLP treatment. There was a slight increase in TNFR1 surface expression when control cells were exposed to marimastat, which likely reflects background metalloprotease activity being slightly enhanced in blood anticoagulated with a direct thrombin inhibitor such as the argatroban used in these assays.[349]

Given the indirect evidence above for C5aR1 being internalised rather than shed in the context of phagocytosis or soluble inflammatory mediator exposure, I elected to attempt to directly visualise the fate of C5aR1 using confocal microscopy. In 2010 Bamberg and colleagues[231] published a seminal report on the localisation of both C5aR1 and C5aR2 in primary human neutrophils after stimulation with C5a. I attempted to replicate these methods in my studies given their previous success. Unfortunately, I was not able to source the specific clone (3C5) used for immunofluorescence by those authors, and thus used a well-established clone (S5/1) with which most of my other studies had been conducted without issue. After initial failures to demonstrate appropriate specific signal with this antibody combination, I suspected the issue was related to the permeabilisation technique stripping epitope off the cell surface, and tried different solutions Triton X-100, methanol and no permeabilisation step without improvement. I also used a variety of blocking solutions (none, human and mouse serum), overnight antibody staining and staining of non-adherent cells prior to spinning onto glass microscopy slides without success (results not shown). Further potential steps to troubleshoot these experimental issues are detailed in Chapter VII:. At this stage, results from my phosphoproteomics screen became available and the focus shifted to analysis of those data.

Chapter VI: unbiased phosphoproteomic profiling reveals novel biology of C5a-induced neutrophil dysfunction

1. Chapter summary

A priority for this thesis has been the identification of signalling pathways within neutrophils that mediate C5a-induced phagocytic dysfunction. If pathway(s) relevant to this dysfunction can be identified, consideration can be given to pharmacological manipulation to rescue this functional defect. Should such efforts meet with success, they would present an attractive option for further drug development in a treatment space currently devoid of effective immunotherapies.

Significant progress has been made toward understanding C5a-induced signalling changes in purified neutrophils by our group and others, including reduced phosphorylation of NOX-2 subunits,[179] activation of NHE1,[261] and a class I PI3K-mediated reduction in RhoA activity[213] and phagocytosis (see Figure III-5). This work has revealed important signalling 'nodes' affected by C5a, however a challenge has been to integrate these isolated changes into wider signalling networks and different cellular contexts, as discussed in Chapters III and IV. To address this challenge, I have adopted an unbiased phosphoproteomic approach to assess global changes in neutrophil signalling networks after C5a exposure and phagocytosis. Given the rapidity of C5a-induced phagocytic impairment demonstrated in Chapter III: 4.6, and the signalling kinetics of PI3Ks[66,303] and GPCRs[350] an examination of post-translational modification by phosphorylation (i.e. a phosphoproteomic approach) was considered most likely to reveal signalling mechanisms of interest.

Proteomic and phosphoproteomic studies have been attempted previously in this cell type, though they are traditionally hampered by the low expression of kinase proteins, low stoichiometry and short time-courses of phosphorylation, in addition to the highly destructive nature of neutrophil lysates, rich in phosphatases and proteases.[351] Recent proteomic studies of whole, human neutrophil lysates have yielded a depth of < 2200 proteins[352] and < 960 phosphoproteins,[353] which provide a benchmark by which contemporaneous proteomic studies can be measured. This chapter discusses the workup involved in developing an appropriate neutrophil lysis buffer, technical validation of our results and finally, key novel signalling pathways identified from these studies.

2. Hypotheses and aims

The phosphoproteome of whole neutrophil lysates after C5a exposure and phagocytosis of S. aureus Bioparticles will reveal novel pathways driving complement-induced neutrophil dysfunction.

- To optimise a cell lysis buffer that balances competing requirements of protease and phosphatase inhibition with downstream proteomics workflows.
- To demonstrate that C5a-induced phagocytic impairment has occurred in the samples analysed (functional positive control).
- To assess the technical validity of the resultant neutrophil proteome and phosphoproteome.
- To compare phosphoprotein changes between conditions of interest: control vs C5a; control + *S. aureus* vs C5a + *S. aureus*) and map them to known signalling pathways.
- To interrogate the functional significance of these pathways through pharmacological manipulation in a relevant *in vitro* system such as whole blood.

3. Notes on methods

The techniques discussed in this chapter have been detailed in the Methods Chapter II:13-17, summarised in Figure II-1 and chiefly relate to the extraction of minimally degraded protein from human neutrophils. First, an appropriate lysis buffer was developed which preserved protein integrity despite the abundant proteases and phosphatases in neutrophil lysates. This aim had to be balanced with downstream phosphoproteomics workflow requirements; namely trypsin activity for protein digestion and low levels of detergents and metal chelators for phosphopeptide enrichment.[354,355] The suitability of lysis buffers was determined by silver staining of SDS-PAGE gels and Western blotting for the phosphoprotein p-Akt (protein kinase B: PKB) to indicate protein and phosphoprotein integrity in the lysates, using GM-CSF stimulation previously described by our group.[356] Once the lysis buffer was optimised, the proteomics workflow could commence, the results of these key elements are detailed below.

4. Results

4.1. Optimisation of proteomics lysis buffer

Protein abundance and integrity was assessed in neutrophil lysates prepared with a variety of buffers by silver staining of SDS-PAGE gels. The initial lysis buffer suggested by the CRUK-CI proteomics core was SDS 0.1 % and TEAB 0.1 %. As demonstrated in Figure VI-1A, SDS concentrations of 0.1 % were insufficient to prevent almost total protein degradation in neutrophil lysates. The addition of protease inhibitors markedly reduced degradation (2nd lane from left) however the absolute protein abundance was still lower than the control 4 % SDS buffer previously used in our laboratory. Titration of SDS concentrations down to 0.5 % preserved proteins almost as well as the 4 % SDS buffer. Assessment of phosphoprotein integrity was performed using Western blotting for p-Akt, shown in B. All samples (except control second from right) were treated with GM-CSF to stimulate p-Akt production and lysed in different buffers as indicated. Again, the inability of 0.1 % SDS to prevent protein degradation in neutrophil lysates was demonstrated, with virtually no staining in those lanes, even when the concentration of protease/phosphatase inhibitor was trebled. The samples lysed in 0.5 % SDS had good preservation of p-Akt staining, and the addition of extra HALT protease/phosphatase inhibitor did not appear to improve this. Therefore, the 0.5 % SDS/0.1 M TEAB + HALT buffer was chosen as an appropriate compromise between phosphoproteomics requirements and preservation of protein integrity in neutrophil lysates.

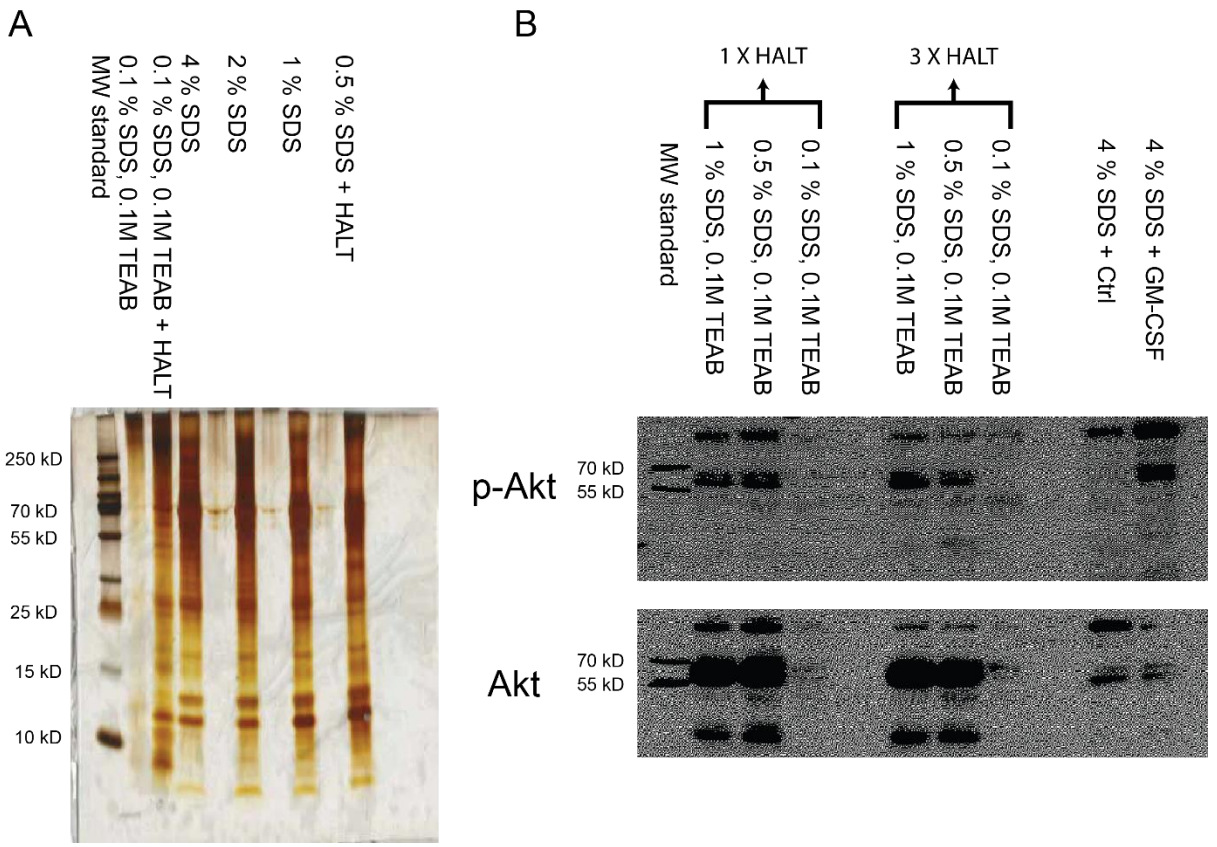

Figure VI-1: Optimisation of proteomics lysis buffer

A: Neutrophils were purified, left untreated and then lysed in different lysis buffers as indicated. Lysates were run in 12 % SDS-PAGE gels and then stained using the silver stain protocol detailed in Chapter II:14. B: Neutrophils were purified and treated with 10 ng/mL GM-CSF for 10 minutes (to stimulate Akt phosphorylation) in all lanes except control second from right. Cells were lysed in different lysis buffers as indicated and run in 12 % SDS-PAGE gels. Proteins were transferred to PVDF membranes using a wet transfer method, membranes were blocked (5 % BSA) and stained for p-Akt (1:5000, rabbit anti-human) and Akt (1:5000, rabbit anti-human) overnight at 4 °C. Secondary HRP-conjugated goat anti-rabbit antibodies (1:10 000) were added for 60 minutes at room temperature, before membranes were washed and developed.

4.2. Technical validation of phosphoproteomics experiment

To ensure the validity of the phosphoproteomics results, it is important to demonstrate the phenotype of interest (C5a-induced neutrophil phagocytic dysfunction) was present in the samples sent for phosphoproteomic analysis. For this reason, phagocytosis was assessed in aliquots of the same neutrophils sent for phosphoproteomics analysis using a variation of the assay described in Chapter II:0. Figure VI-2 shows a significant reduction in phagocytosis occurred with 60 minutes of C5a pre-treatment in the samples that were sent for phosphoproteomics analysis.

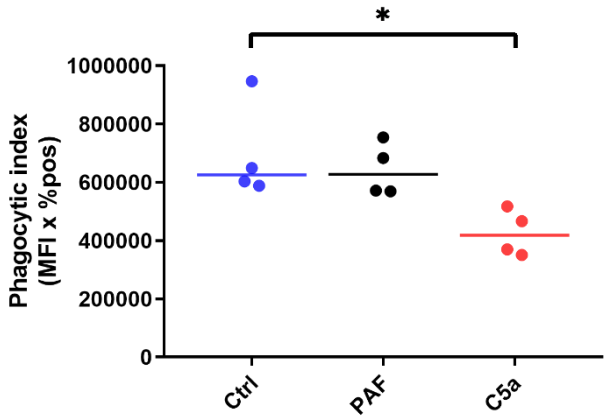

Figure VI-2: Phagocytosis analysis confirms defect in C5a-treated samples sent for phosphoproteomics

Neutrophils were purified and treated with 100 nM C5a for 60 minutes or 1 µM PAF for 5 minutes prior to phagocytosis of 15 µg/mL of *S. aureus* Bioparticles for 15 minutes. C5a pre-treatment led to a reduction in median phagocytosis of 33.2 % relative to control. Data points are shown with medians. Friedman p-value 0.042, *p < 0.05 by Dunn's multiple comparisons test.

Further evidence of technical validity can be gained from interpretation of the proteomics data. Table 5 demonstrates the unprecedented depth of sequencing from this study; 4859 proteins and 2712 phosphoproteins were quantified by peptide intensity. Of note, each protein and phosphoprotein was independently identified and quantified in all four donors; species identified in fewer than four donors were not included in subsequent analyses. This table also shows the number and percentage of proteins and phosphoproteins that were significantly altered between the conditions indicated. These data indicate protein expression was relatively stable across conditions, indicated by the low percentage of total protein changes, as expected for the time points and stimuli involved. Phosphoprotein expression, however, varied markedly between conditions as expected. Figure VI-3 demonstrates that the measured phosphoprotein intensities are highly consistent between conditions on each plex, indicating technically reproducible phosphoprotein measurements prior to normalisation of data. Finally, Figure VI-4 shows a selection of two key phosphoproteins (C5aR1 and PI3K subunit alpha) which, based on the literature discussed in Sections 3.3, demonstrated increased phosphorylation after C5a treatment as expected.[336,337,357]

Table 5: Marked phosphoproteome changes with treatment

This table shows statistically significant numbers of protein/phosphoprotein alterations in the total proteome and total phosphoproteome between the conditions indicated. These alterations are shown as both the absolute number and as a percentage of the respective proteome/phosphoproteome.

	Total proteome (4859 proteins quantified)		**Total phosphoproteome (2712 phosphoproteins quantified)**	
Conditions compared	Number of proteins significantly altered	Percentage of total proteome significantly altered	Number of phosphoproteins significantly altered	Percentage of total phosphoproteome significantly altered
Ctrl-untreated	0	0.0%	16	0.6%
C5a-ctrl	7	0.1%	111	4.1%
S. aureus-ctrl	95	2.0%	858	31.6%

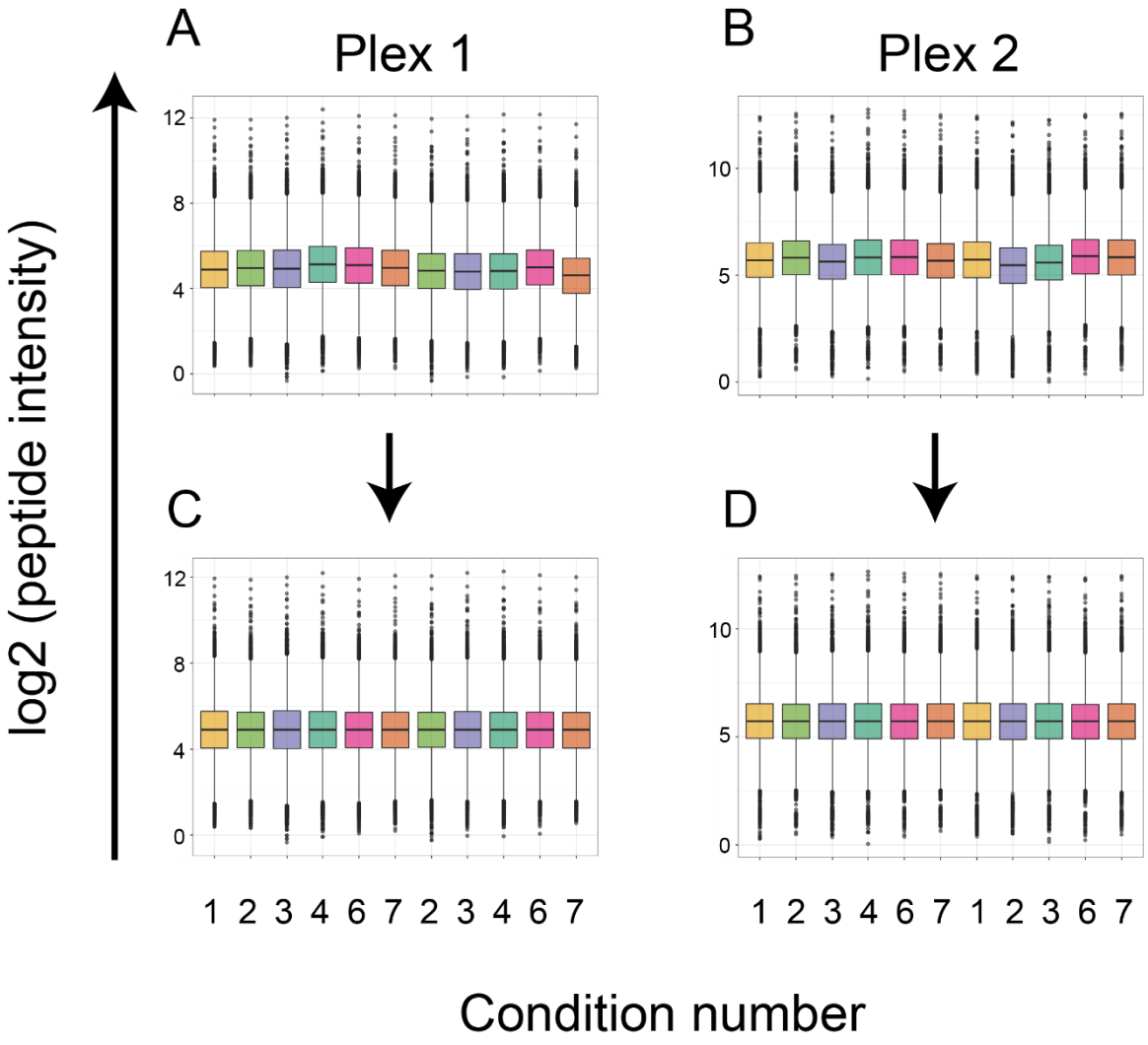

Figure VI-3: Peptide intensities are highly consistent between conditions

Median, IQR and outliers of the measured peptide intensity for the 2712 quantified phosphoproteins are shown for each experimental condition on each plex. Intensities are shown before (A, B) and after (C, D) median scaling normalisation of data.

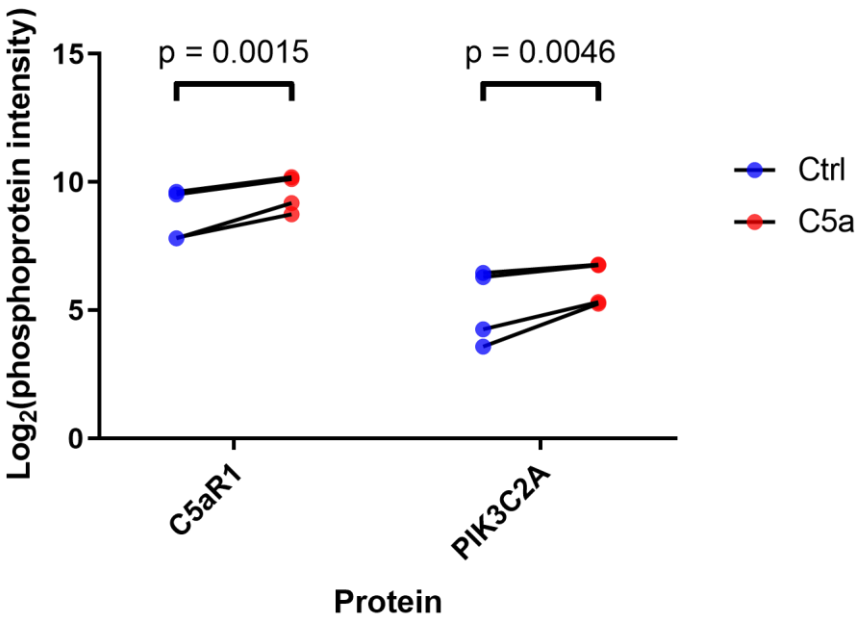

Figure VI-4: Phosphorylation of key proteins expected in C5a condition

Log_2-transformed normalised phosphoprotein intensities are shown for C5aR1 and phosphatidylinositol 4-phosphate 3-kinase C2 domain-containing subunit alpha (PIK3C2α), both of which have undergone the phosphorylation expected after C5a treatment. p-values were computed by limma-based linear models with Bonferroni's correction for multiple testing.

4.3. Global assessment of proteome and phosphoproteome

Following validation of technical success of the experiment, attention can be turned to analysis of phosphoproteomic data. Given the small changes evident in the total proteome over the time points of this experiment, the majority of analysis is focussed on the phosphoproteome. Raw data used to generate the figures and tables in this section has yet to be published but can viewed using the following Dropbox link for the purposes of this thesis: https://www.dropbox.com/sh/lsveytwgscznd9o/AABe5RB5XHNdtftXX5kbaQe8a?dl=0

Figure VI-5 is a heatmap diagram of the entire 2712 quantified phosphoproteins and their fold change over each experimental condition or time point relative to the untreated control condition (not shown). Hierarchical clustering shows the *S. aureus* conditions cluster closely together, followed by PAF-treated cells, whereas control and C5a tend to cluster separately. There are clear differences in relative expression between subsets of phosphoproteins across conditions; notably there are subsets which are phosphorylated in the Control + *S. aureus* condition which are less phosphorylated in the C5a + *S. aureus* condition. These phosphoproteins are discussed in further detail below.

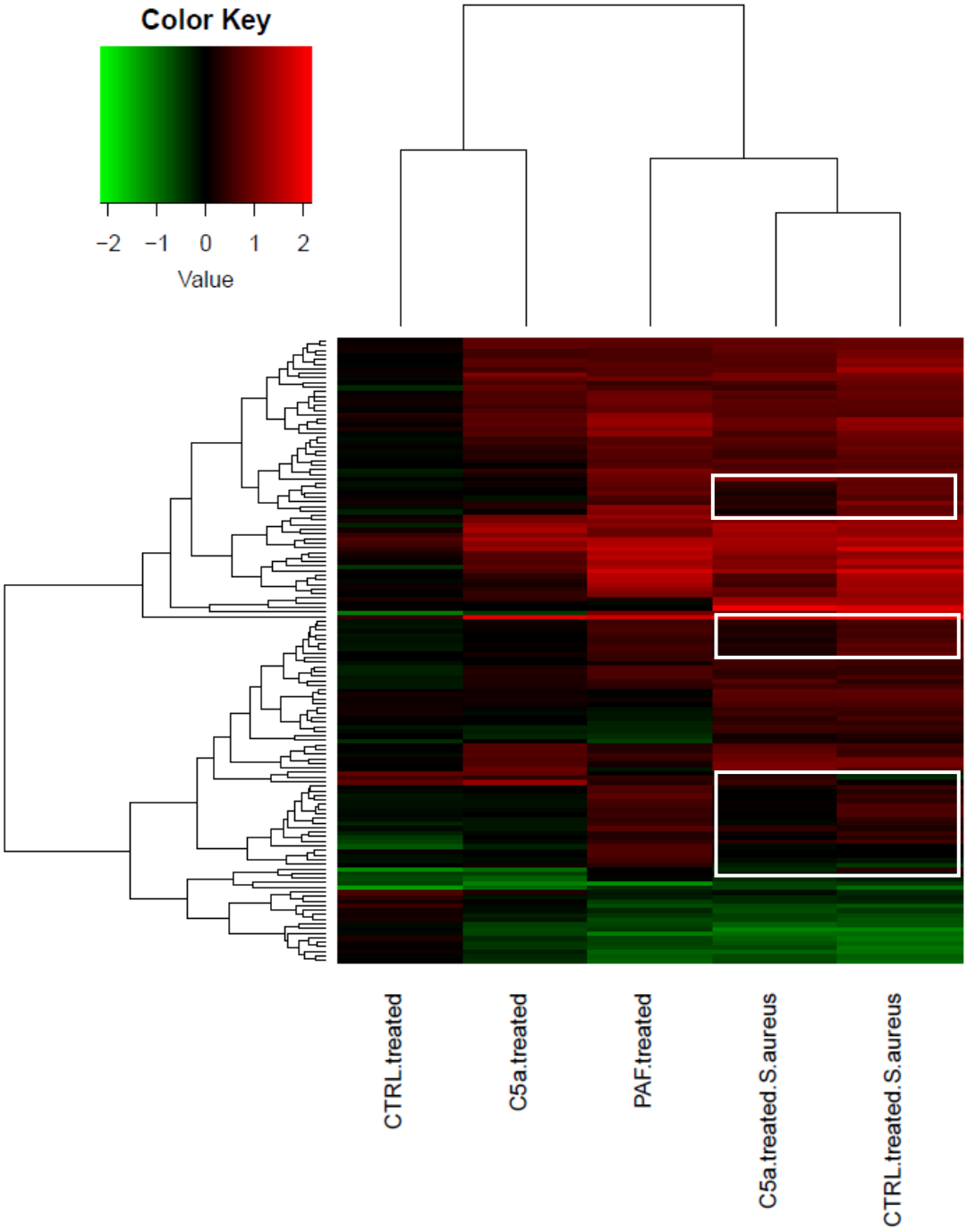

Figure VI-5: Global phosphoprotein expression changes

Phosphoprotein expression intensity was quantified by mass spectrometry and normalised using median scaling as in discussed in Methods. Log2FC was calculated for each phosphoprotein relative to untreated baseline condition (not shown) for each experimental condition. Increased phosphoprotein expression is indicated in red, decreased in green. White boxes draw attention to phosphoproteins with grossly different expression between the *S. aureus*-treated conditions pre-treated with either control or C5a.

4.4. Effect of C5a on the human neutrophil phosphoproteome

C5a treatment for 60 minutes induced a marked change in phosphoprotein expression of human neutrophils, with 119 phosphoproteins expressed differentially relative to control-treated cells. Of these 119 hits, 87 were phosphorylated and 32 were de-phosphorylated relative to control, as the volcano plot in Figure VI-6 shows. Subsequent pathway analysis of the phosphorylated and de-phosphorylated proteins using the Reactome Pathway Knowledgebase[358] identified 60 pathways significantly phosphorylated and 31 dephosphorylated by C5a exposure. The pathways with the 10 lowest Benjamini-Hochberg corrected p-values from each analysis are shown in Table 6. Multiple pathways related to downstream signal transduction are phosphorylated in the C5a pre-treated condition including MAP-kinases and small GTPases as expected. There also appears to be involvement of endosomal sorting pathways such as SUMOylation and membrane trafficking in both groups of proteins, indicating a role for these pathways in C5a-mediated effects, as discussed below.

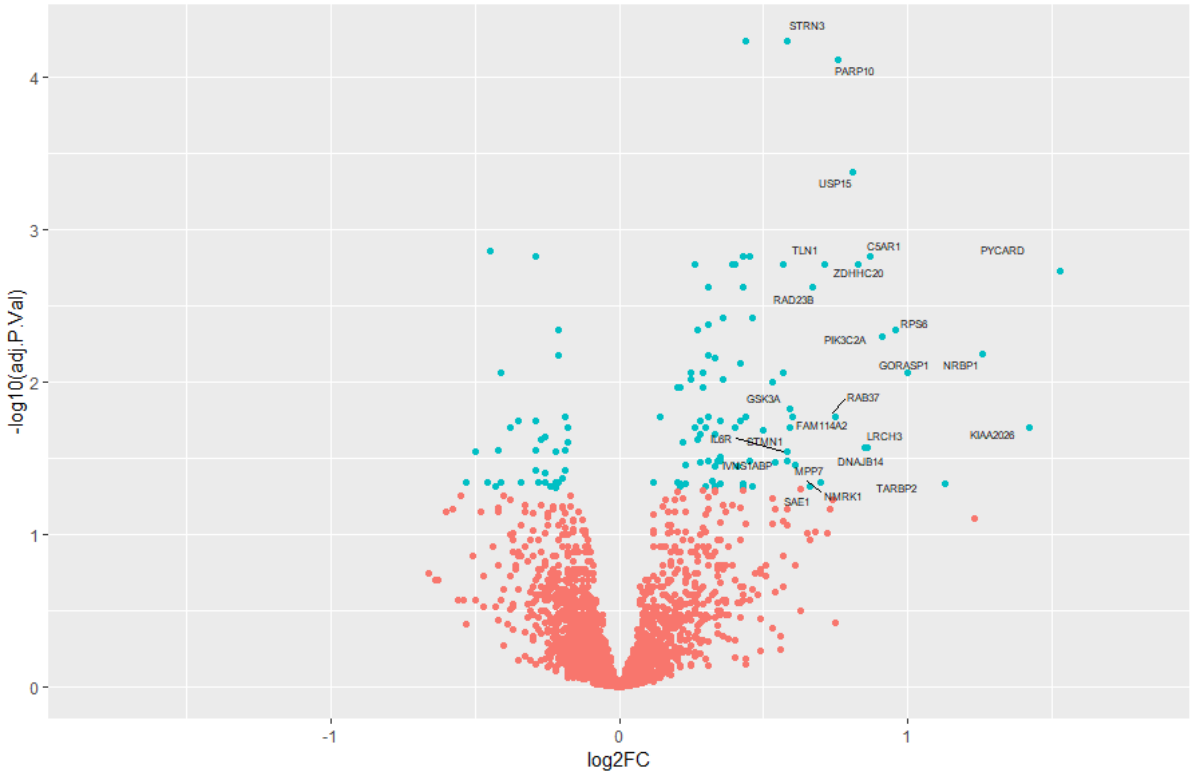

Figure VI-6: Volcano plot of C5a-induced protein phosphorylation

2712 proteins are shown, with increasing phosphorylation shown on the right and decreased on the left. Proteins with adjusted p-values < 0.05 are shown in blue, and the 25 proteins with the highest absolute log2FC are labelled. p-values were computed by limma-based linear models with Bonferroni's correction for multiple testing.

Table 6: Top 10 signalling pathways significantly enriched by C5a exposure

Significantly (adjusted p < 0.05 in the C5a vs control comparison) phosphorylated or de-phosphorylated proteins were identified from the phosphoproteomic screen and input into the Reactome database, which maps the input proteins to known signalling pathways and determines whether pathways are enriched in the data submitted. Key pathways of mechanistic interest are shown in bold. Entities found: the number of curated molecules that are common between the submitted data set and the pathway named in column; Entities total: known proteins involved in the signalling pathway; p-values: Benjamini-Hochberg corrected p-values for significant pathway enrichment.

Pathway name	Entities found	Entities total	p-value
PHOSPHORYLATED			
Processing and activation of SUMO	3	10	8.66E-05
Activation of RAC1	3	13	1.87E-04
Smooth Muscle Contraction	4	35	2.22E-04
Gastrin-CREB signalling pathway via PKC and MAPK	3	18	4.82E-04
SUMO is proteolytically processed	2	6	1.19E-03
RSK activation	2	6	1.19E-03
CREB phosphorylation	2	7	1.61E-03
MAPK1 (ERK2) activation	2	10	3.22E-03
Innate Immune System	19	1180	3.45E-03
SLBP Dependent Processing of Replication-Dependent Histone Pre-mRNAs	2	11	3.88E-03
DE-PHOSPHORYLATED			
Glycogen storage disease type II (GAA)	1	2	6.29E-03
Glycogen storage disease type XV (GYG1)	1	2	6.29E-03
Glycogen storage disease type 0 (muscle GYS1)	1	2	6.29E-03
Ovarian tumor domain proteases	2	38	6.48E-03
TRAF3 deficiency - HSE	1	3	9.42E-03
Membrane Trafficking	6	631	1.32E-02
E3 ubiquitin ligases ubiquitinate target proteins	2	60	1.55E-02
Neutrophil degranulation	5	480	1.67E-02
HuR (ELAVL1) binds and stabilizes mRNA	1	8	2.49E-02
Role of ABL in ROBO-SLIT signalling	1	8	2.49E-02

4.5. C5a pre-treatment reduces phosphorylation of signalling pathways involved in transcription and nuclear structural change

A key goal of this experiment was to assess the C5a-induced changes in signalling in the context of phagocytosis of *S. aureus* to allow identification of phosphorylation changes of relevance to this complex biological process. Figure VI-7 shows the phosphoproteins differentially expressed in neutrophils after pre-treatment with control or C5a followed by 15 minutes of phagocytosis. Of note, only 20 proteins are differentially phosphorylated between the two conditions when the effect of *S. aureus* phagocytosis is controlled experimentally. All 20 of these differentially phosphorylated proteins are more phosphorylated in cells pre-treated with control relative to C5a, an observation that is further explored in Section 4.6

below. When the 20 differentially expressed phosphoproteins are entered into the Reactome pathway database, a preponderance of pathways involving changes in nuclear morphology, apoptosis and transcriptional regulation are enriched, as shown in Table 7.

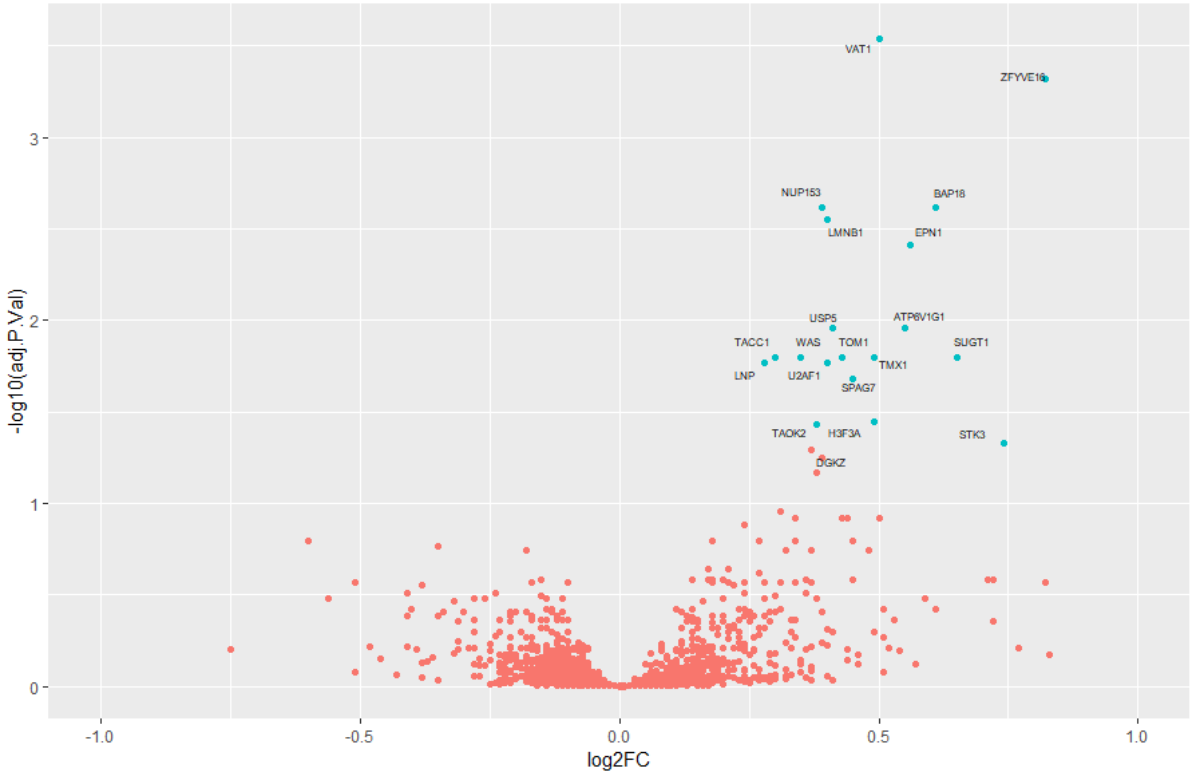

Figure VI-7: Volcano plot of phagocytosing cells pre-treated with control relative to C5a

2712 phosphoproteins are shown, with increased phosphorylation in the Ctrl + *S. aureus* vs C5a + *S. aureus* shown on the right. Proteins with adjusted p-values < 0.05 are shown in blue and labelled. p-values were computed by limma-based linear models with Bonferroni's correction for multiple testing.

Table 7: Signalling pathways differentially phosphorylated between phagocytosing cells pre-treated with control relative to C5a

Significantly (adjusted p < 0.05 in the Ctrl + *S. aureus* vs C5a + *S. aureus* comparison) phosphorylated proteins were identified from the phosphoproteomic screen and input into the Reactome database, which maps the input proteins to known signalling pathways and determines whether pathways are enriched in the data submitted. Key pathways of mechanistic interest are shown in bold. Entities found: the number of curated molecules that are common between the submitted data set and the pathway named in column; Entities total: known proteins involved in the signalling pathway; p-values: Benjamini-Hochberg corrected p-values for significant pathway enrichment.

Pathway name	Entities found	Entities total	Entities p-value
Mitotic Prophase	3	133	1.00E-03
Apoptotic cleavage of cellular proteins	2	38	2.00E-03
Apoptotic execution phase	2	54	4.00E-03
Nuclear Envelope Breakdown	2	63	5.00E-03
Breakdown of the nuclear lamina	1	3	5.00E-03
Gene and protein expression by JAK-STAT signalling after Interleukin-12 stimulation	2	74	7.00E-03
Transcriptional regulation by small RNAs	2	79	7.00E-03
Transport of Mature mRNA derived from an Intron-Containing Transcript	2	81	8.00E-03
Interleukin-12 signalling	2	85	9.00E-03
Transport of Mature Transcript to Cytoplasm	2	90	1.00E-02

4.6. C5a induces a profound ‘phosphorylation failure’ during phagocytosis

One of the most striking features of the phosphoproteome screen is the marked difference in the magnitude of the phosphorylation response to *S. aureus* depending on whether cells were pre-treated with C5a or control. This is most evident in Figure VI-8; *S. aureus* after control pre-treatment significantly changed the phosphorylation status of 31 % of the phosphoproteome, which illustrates the enormous stimulation encountering this pathogen represents for the cell. In contrast, cells that were pre-treated with C5a and then allowed to phagocytose *S. aureus* demonstrated a statistically significant change in phosphorylation status of 0.63 % of the phosphoproteome. When proteins significantly phosphorylated by phagocytosis of *S. aureus* in cells pre-treated with control are mapped to known pathways using the Reactome database and compared to their counterparts in C5a pre-treated cells, a pattern of defective or absent phosphorylation emerges, as shown in Table 8. Pathways involved in PIK3C2α, Rho-GTPase and phosphoinositide signalling are prominently phosphorylated in control but not C5a pre-treatment. Further, the previously unappreciated pathways related to endosomal sorting, membrane trafficking and nuclear morphology changes again appear, and are deficient in cells pre-treated with C5a.

A: *S. aureus*-induced phosphorylation

B: *S. aureus*-induced phosphorylation after C5a

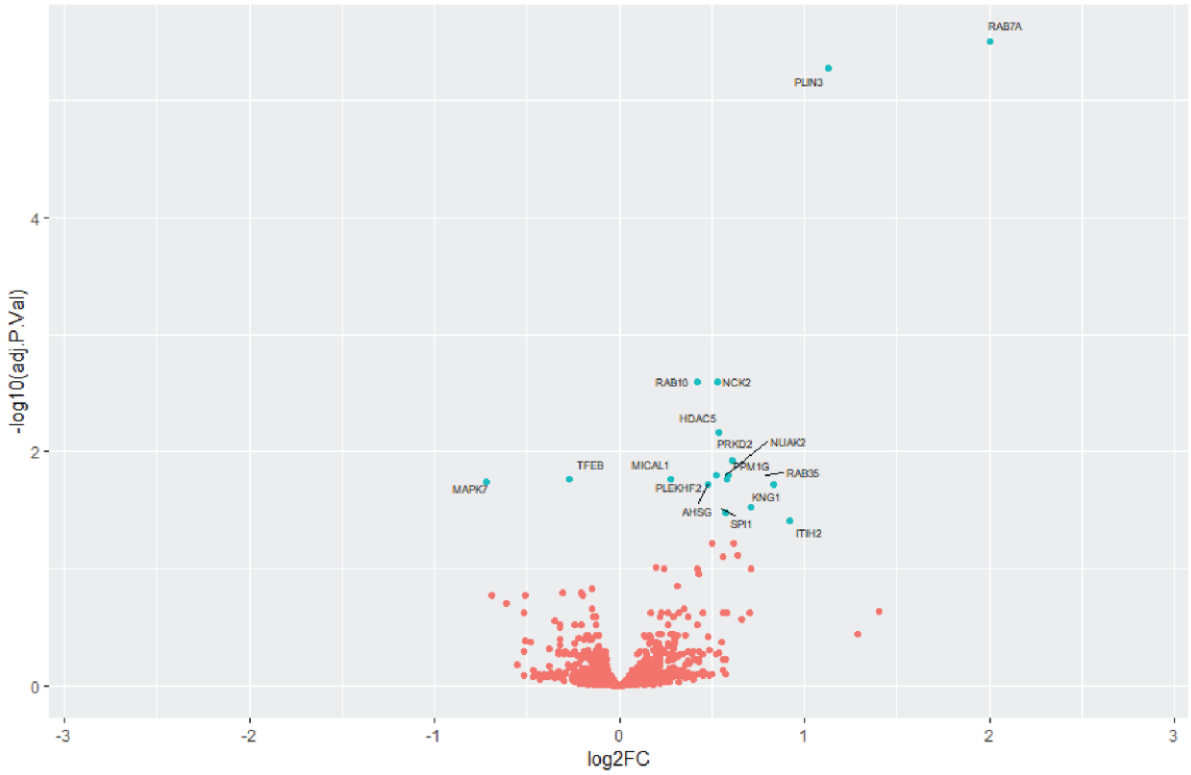

Figure VI-8: C5a-induced phosphorylation failure in response to *S. aureus*

2712 phosphoproteins are shown, with increased phosphorylation after *S. aureus* shown on the right of each plot. A: Protein phosphorylation in the control + *S. aureus* condition relative to control alone condition. *S. aureus* treatment after control increased phosphorylation of 391 proteins and decreased phosphorylation of 472 proteins, the sum of which (863) corresponds to 31 % of the phosphoproteome. B: Protein phosphorylation in the C5a + *S. aureus* condition relative to C5a alone condition. *S. aureus* treatment after C5a increased phosphorylation of 15 proteins and decreased phosphorylation of 2 proteins, the sum of which (17) corresponds to 0.63 % of the phosphoproteome. Proteins with adjusted p-values < 0.05 are shown in blue and the 25 (A) or 17 (B) proteins with the highest absolute log2FC are labelled. p-values were computed by limma-based linear models with Bonferroni's correction for multiple testing.

Table 8: Key C5a-driven phosphorylation failures

Significantly (adjusted p < 0.05 in the control + *S. aureus* condition vs control alone condition) phosphorylated proteins were identified from the phosphoproteomic screen and input into the Reactome database, which maps the input proteins to known signalling pathways and determines whether pathways are enriched in the data submitted. Key pathways of mechanistic interest are shown in **bold**. Blue columns indicate phosphoproteins and enrichment p-values from the control + *S. aureus* vs control alone comparison; red columns from the C5a + *S. aureus* vs C5a alone comparison. Entities found: the number of curated molecules that are common between the submitted data set and the pathway named in column; Entities total: known proteins involved in the signalling pathway; p-values: Benjamini-Hochberg corrected p-values for significant pathway enrichment.

Pathway name	Entities Ctrl + *S. aureus*	Entities C5a + *S. aureus*	Total entities	p-value Ctrl + *S. aureus*	p-value C5a + *S. aureus*
Cytokine Signalling in Immune system	60	0	1055	8.51E-06	N/A
Innate Immune System	65	3	1302	1.73E-04	1.82E-01
Membrane Trafficking	**45**	**4**	**661**	**1.60E-06**	**5.75E-03**
Neutrophil degranulation	**35**	**3**	**480**	**5.84E-06**	**1.62E-02**
Nuclear Envelope Breakdown	**11**	**0**	**63**	**7.34E-06**	**N/A**
Nuclear Pore Complex (NPC) Disassembly	**9**	**0**	**40**	**6.91E-06**	**N/A**
PtdIns(3,4,5)P_3 activates AKT signalling	**18**	**0**	**312**	**1.17E-02**	**N/A**
PTEN Regulation	**12**	**1**	**171**	**9.26E-03**	**1.79E-01**
Signalling by Receptor Tyrosine Kinases	29	1	518	2.50E-03	4.53E-01
Signalling by Rho GTPases	**32**	**0**	**447**	**2.10E-05**	**N/A**
SUMOylation	17	0	187	1.29E-04	N/A
Toll Like Receptor 2 (TLR2) Cascade	10	0	113	3.65E-03	N/A
Vesicle-mediated transport	**46**	**4**	**820**	**1.42E-04**	**1.22E-02**

4.7. Phosphorylation failure of PI3K and membrane trafficking pathways impairs phagosomal maturation

As noted in Table 8, key signalling pathways which fail to be phosphorylated after *S. aureus* in the context of C5a pre-treatment are related to endosomal transport or trafficking, PI3K function and notably, the V-type ATPase subunit G1 which is critical to phagosomal acidification. I therefore went on to examine whether C5a induced a specific defect in phagosomal acidification, distinct from its inhibition of phagocytosis. Using the maturation probe discussed in Chapter II: Section 10.3 (which allows simultaneous assessment of ROS, phagosomal pH and particle ingestion in the existing whole blood assay) I have shown that C5a does indeed impair phagosomal acidification in addition to phagocytosis itself (Figure VI-9). As discussed in Section 1.5 of Chapter I:, these endosomal maturation processes are key for the effective maturation of a nascent phagosome into a bactericidal phagolysosome, and rely heavily on PI3P which is predominantly produced by the class III PI3K, Vps34.[62,254] The phosphoproteomic screen identified several proteins likely to be involved in these processes: Zinc finger FYVE domain-containing protein 16 (ZFYVE16), target of Myb protein 1 (TOM1) and Ras-related protein 7a (RAB7A). All were significantly phosphorylated in the control + *S. aureus* condition (log2FCs 1.19, 0.77, 1.81 respectively) with ZFYVE16 and TOM1 not significantly phosphorylated in the C5a + *S. aureus* condition. These proteins are known to be dependent on PI3P for effective recruitment to the phagolysosome.[359] Thus, pharmacological inhibition of Vps34 may reproduce C5a-induced defects in phagocytosis, and particularly, phagosomal maturation. I then made use of a recently-developed selective inhibitor of Vps34 (VPS34-IN1) and showed that inhibition of Vps34 recapitulates the phagosomal acidification defect, with no statistically significant effect on phagocytosis or ROS production measured in the same assay (Figure VI-10). These data functionally validate the phosphoproteomic studies conducted and shed new light on the mechanisms by which C5a impairs not only phagocytosis but phagosomal maturation in a physiologically relevant context.

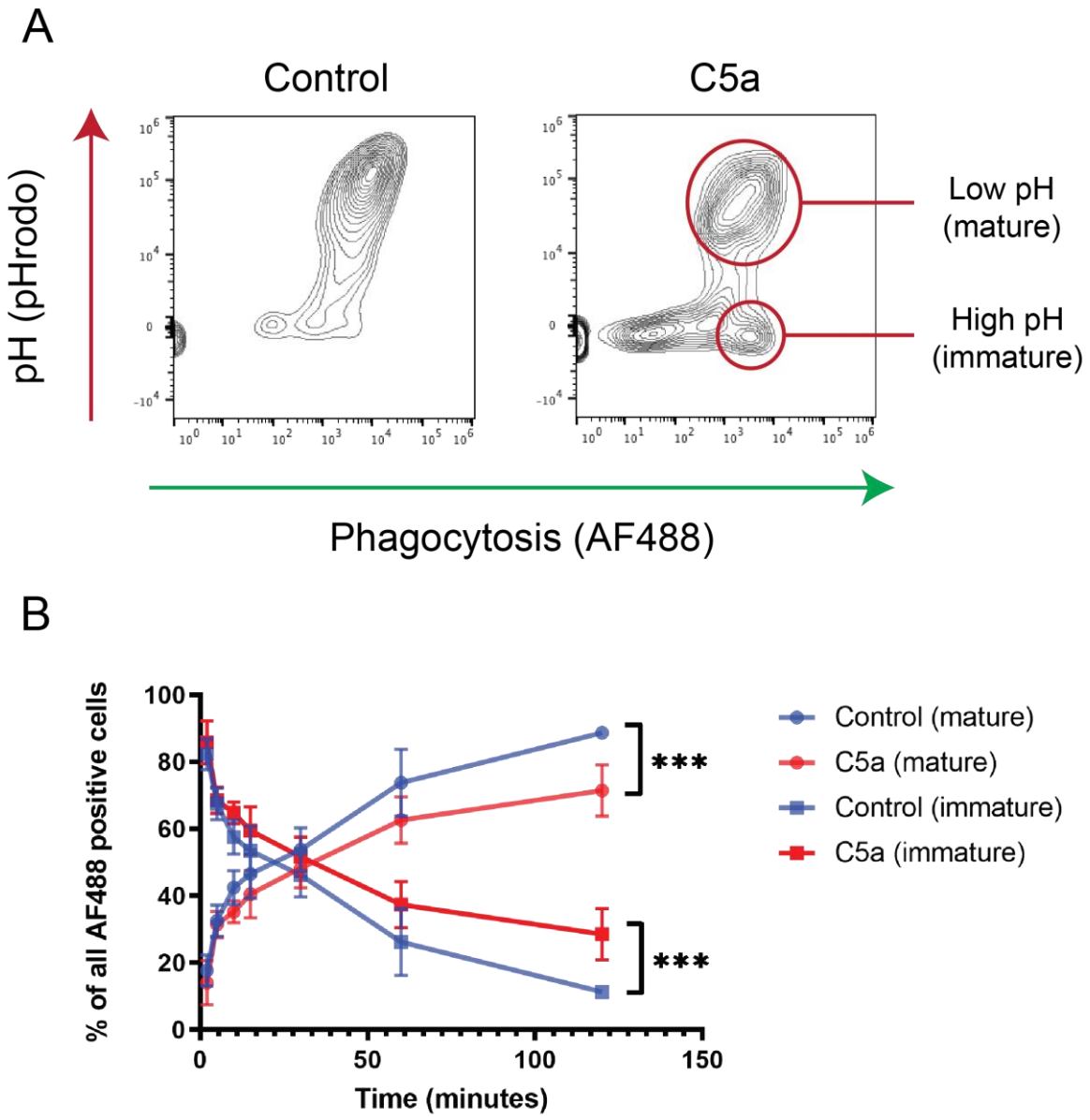

Figure VI-9: C5a induces a failure in phagosomal maturation

Whole blood was pre-treated with 300 nM C5a for 60 minutes prior to addition of 5 µg/mL phagosomal maturation probe. A: Contour flow plots after 60 minutes 300 nM C5a or control and then 120 minutes phagocytosis showing how both phagocytosis (x-axis) and phagosomal pH (y-axis) can be measured simultaneously in the same population of cells. pHrodo fluorescence increases with decreasing pH, indicating phagosomal maturity as shown. B: Cells were allowed to phagocytose for the time points indicated and the percentage of particle positive (AF488 positive) cells with low pH (mature) and high pH (immature) phagolysosomes is shown for control and C5a-treated conditions. Data are shown as mean and SD of n = 5 independent experiments. ***p < 0.0001 by repeated-measures two-way ANOVA with Tukey's multiple comparisons test. NB: these experiments were carried out using my whole blood assay by Dr Andrew Conway Morris and have been included here with his permission.

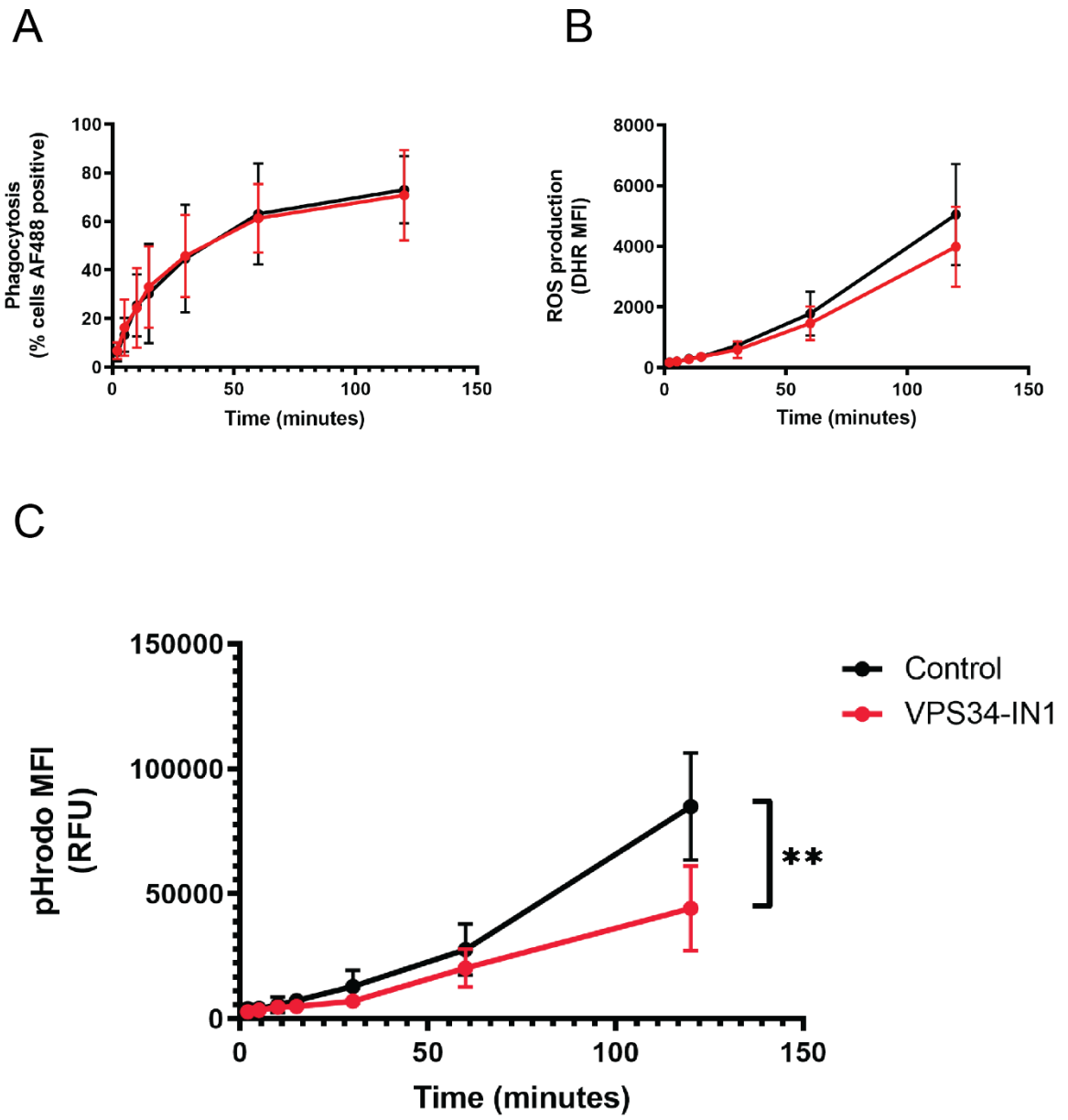

Figure VI-10: VPS34-IN1 impairs neutrophil phagosomal maturation but not phagocytosis or ROS production in whole blood

Whole blood was pre-treated with 1 µM VPS34-IN1 nM for 60 minutes prior to addition of the phagosomal maturation probe. Cells were allowed to phagocytose for the time points indicated. As previously described, phagocytosis (A) ROS production (B) and phagosomal pH (C) were quantified by flow cytometry. There were no significant differences according to drug treatment in phagocytosis or ROS. There was a reduction in phagosomal acidification as shown. Data are shown as mean and SD of n = 5 independent experiments. **p = 0.0058 for drug by repeated measures two-way ANOVA with Bonferroni's multiple comparisons test. NB: these experiments were carried out using my whole blood assay by Dr Andrew Conway Morris and have been included here with his permission.

5. Discussion

The data presented in this chapter constitute, to my knowledge, the deepest sequencing of the human neutrophil proteome and phosphoproteome published, and certainly the first such assessment of the neutrophil response to C5a.[353,360,361] Further, these data provide the first phosphoproteomic assessment of the host neutrophil response to *S. aureus* (as opposed to changes in the proteome of the pathogen) once again in the context of C5a, a key driver of innate immune dysfunction.[362] Unlike previous studies using transcriptomic or microarray data[363–365] proteomics provides a direct assessment of mediators and may be more likely to have functional implications, especially in short-lived cells such as neutrophils.[351,366] Therefore, these data provide an opportunity to uncover mechanisms driving important bactericidal processes and their impairment in primary human neutrophils. This discussion begins by contextualising and validating the phosphoproteomic screen. It then divides into two parts: the first deals with hits from the phosphoproteome which may indicate a role for nuclear morphological change in allowing efficient phagocytosis. The second discusses the expanded role (identified and validated during this work) of membrane trafficking signals in driving phagosomal maturation.

My first aim was to isolate protein of a high quality from primary human neutrophils which would be suitable for downstream phosphoproteomic analysis. The CRUK-CI proteomics core makes use of an SDS/TEAB-based buffer system for trypsin digestion and downstream LC-MS/MS which requires an SDS concentration of ≤ 0.1 % and at least 100 µg of protein per sample. To assess protein integrity in neutrophil lysates, I used a combination of silver staining and Western blotting of SDS-PAGE gels. As shown in Figure VI-1, an SDS concentration of 0.1 % was inadequate to prevent significant protein degradation, even when high concentrations of protease and phosphatase inhibitors were used, in keeping with the high concentrations of proteases in neutrophil lysates.[361] I therefore elected to use large numbers of cells (12 x 10^6/condition) and an SDS concentration of 0.5 % which would allow dilution of the resultant lysate down to 0.1 % SDS whilst maintaining amounts of protein sufficient for phosphoproteomic analysis. This buffer was designed to represent a compromise between the maintenance of protein integrity and providing an appropriate lysate for downstream analysis. Of note, protein degradation was not completely abolished (note lower MW bands in the p-Akt Western Figure VI-1) which may represent an area for improvement in subsequent experiments.

Once the phosphoproteome screen was conducted, the first task was technical validation of the results. I approached this issue in three ways: first I ensured that only samples with a demonstrable C5a-induced phagocytic defect were sent for phosphoproteomic analysis (Figure VI-2) to avoid sequencing samples without the phenotype of interest. At this short time-point with a high inoculum of *S. aureus* Bioparticles (15 minutes and 15 µg/mL

respectively) there was no augmentation of phagocytosis with PAF as previously observed in whole blood (Chapter IV:5) though these differences are most probably due to differences in experimental setup. Second, the raw phosphopeptide intensities were inspected for uniformity between conditions (Figure VI-3) which confirmed there were no sizeable differences between experimental conditions which could confound interpretation of results. Finally, the depth of sequencing was found to be much higher than previous reports of proteins obtained from primary human neutrophils,[352,353] with a total of 4859 proteins and 2712 phosphoproteins of which expression was not only detected but quantified. Whilst this depth of sequencing is substantially less than the 20 397 curated human proteins listed in the Uniprot[367] database and less than recent proteomics of human fetal fibroblast cells,[368] it compares extremely favourably to other primary human neutrophil datasets as previously discussed.[352,353] These observations are most probably due to the multitude of proteases and phosphatases in neutrophil lysates as well as substantial variations in genome translation between tissues. The reasons for the success of this experiment relative to comparable cell types include: careful testing of lysis buffers in this specific context, fractionation of lysates prior to phosphopeptide enrichment and recent advances in LC-MS/MS technology employed at CRUK-CI (personal communication: Dr Clive D'Santos, Proteomics Core, CRUK-CI). Receptor phosphorylation has been shown to mediate signalling driven by C5a-C5aR[92] along with other GPCRs[350] and PI3K signalling.[177,213,331] In this dataset, such proteins were indeed phosphorylated after C5a exposure, providing more evidence which validates this screen as shown in Figure VI-4.

An overall impression of the phosphoproteomic dataset is given in Figure VI-5. This figure shows Log2FC values relative to the untreated control condition (not shown), as well as hierarchical clustering of phosphoproteins (left dendrogram) and experimental conditions (top dendrogram). These data show, as expected, the enormous stimulus pathogen exposure constitutes for the cell, as these conditions cluster together irrespective of pre-treatment. There are at least three groups of proteins that are differentially phosphorylated between phagocytosing cells pre-treated with C5a or control; these are highlighted by white boxes and discussed below. These proteins are generally more phosphorylated in the control + *S. aureus* condition relative to the C5a + *S. aureus* condition, an observation further delineated in subsequent pathway analyses.

Figure VI-6 shows phosphorylation changes induced by 60 minutes of C5a exposure, which map to pathways identified in Table 6. It is interesting to note the persistence of a phosphorylation signal in multiple proteins 60 minutes after chemoattractant exposure, a process traditionally thought to induce responses over seconds to minutes and indicates that prolonged signalling may be responsible for the prolonged defects noted in Chapter III:4.6.[324,350,369] Rather unsurprisingly, pathways involving promiscuous neutrophil signalling

molecules are phosphorylated, including MAPK/ERK signalling and membrane trafficking proteins. Interestingly, proteins related to neutrophil degranulation and other membrane trafficking functions are de-phosphorylated, which may reflect time-dependent changes in the metabolism of these proteins, or indicate the development of an 'exhaustion phenotype' occurring after stimulation by an agonist known to induce degranulation.[261]

We now turn to the novel and unanticipated results shown in Figure VI-7, which indicate pre-treatment with C5a of cells phagocytosing *S. aureus* significantly reduced phosphorylation of just 20 proteins relative to phagocytosing cells pre-treated with control. Pathway analysis shown in Table 7 demonstrates enrichment of several pathways related to modulation of nuclear morphology, transcription and apoptosis. The concept of phagocytosis-induced cell death (PICD) as a transcriptionally-regulated host response to phagocytosis of pathogenic bacteria was advanced by Kobayashi and colleagues in 2002,[365] and extended in 2003.[370] These authors assessed apoptosis of neutrophils in response to live bacteria at late time points (the earliest was 90 minutes) after phagocytosis.[365,370] Whilst the enrichment of pathways involved in apoptosis and nuclear envelope breakdown observed in our dataset may simply represent an earlier, phosphoproteomic response driving PICD or indeed NETosis,[371] this explanation would not account for the demonstrated phagocytic defect noted in the C5a-treated cells. Further, previous work has demonstrated minimal apoptosis in response to heat-killed bacteria,[372] as used in this thesis. It is tempting to speculate that the nucleus is an active player in phagocytosis, as it is in other processes involving significant changes to the cytoskeleton such as transmigration,[36,38] and that C5a impairs nuclear morphological change, thus leading to rapid defects in phagocytic function.

Key players within these pathways include Lamin B1 (LMNB1), which has known dose-responsive associations with nuclear morphology,[373,374] and NUP153, a component of the nuclear pore complex,[375] both of which were less phosphorylated in phagocytosing cells pre-treated with C5a. The combination of mechanistic plausability (significantly altered proteins in our screen correspond to known modulators of nuclear morphology) and the precedent set by evidence of nuclear deformation occurring during transmigration[36,38,376] make this an attractive target for further research, as discussed in Chapter VII:.

The second key set of findings from this phosphoproteomic screen relate to the profound phosphorylation failure induced by C5a pre-treatment in response to phagocytosis of *S. aureus*, illustrated in Figure VI-8. These data indicate that cells pre-treated with C5a are unable to respond to a pathogen challenge in the same way that control-treated cells are. These data also provide a potential explanation for the inability of C5a to inhibit phagocytosis if phagocytosis has already commenced (Figure V-1) whereby the overwhelming phosphoproteomic response of cells to *S. aureus* has already been initiated and is thus resistant to fatigue by C5a. There are, however, some important points to consider here.

Firstly, it should be noted that the amount of phagocytosis occurring in the C5a pre-treated cells was less than in their control pre-treated counterparts (Figure VI-2) and indeed this was a key component of experimental design. I would suggest that whilst the amount of phagocytosis may have been less in the C5a pre-treated cells, the total stimulus (amount of *S. aureus*) administered to the cells was the same between the conditions. Therefore whilst a component of the reduced signal in the C5a pre-treated cells may have been due to les phagocytosis, the cells can indeed be considered significantly less responsive to the same pathogenic stimulus. Further, the relative reduction in phagocytosis shown is modest (33.2 %) relative to the profound alteration in the phosphoproteome.

There is a possibility that the lack of phosphoproteomic signal we see after C5a pre-treatment simply represents cellular exhaustion[377] or reduced signalling secondary to heterologous receptor desensitisation.[378] I would argue that this is not the case for several reasons: firstly, heterologous desensitisation has only been demonstrated with chemoattractant receptors and only shown to persist for a few minutes,[378] whereas we observe persistent C5a-induced dysfunction hours after exposure. Secondly, other chemoattractants and priming agents do not induce a phagocytic defect like C5a, as shown in Figure IV-3, which argues against receptor desensitisation or exhaustion being the cause. Finally, the selective nature of the diminished response (affecting signalling pathways with a common theme) and its functional effects argue against a whole-cell exhaustion phenotype. On a related note, whether this phosphorylation failure is a cause of the diminished phagocytic response or a consequence of it can only be answered by subsequent experiments examining specific pathways and by a more granular temporal profile of the phosphoproteome. This is often case with many findings from ‘omics’ datasets and these data should therefore be interpreted in light of these considerations.

When the proteins phosphorylated by *S. aureus* phagocytosis in control cells are subjected to pathway analysis, several pathways of interest are highly enriched, and are markedly less so in the C5a pre-treated condition (Table 8). Of interest, pathways related to phosphoinositide signalling, Rho GTPase function and membrane trafficking feature prominently. These data provide further evidence for the role of PI3Ks and Rho GTPases in C5a-mediated phagocytic dysfunction previously described by our group, and importantly demonstrate that these are not restricted to the context in which they were originally identified.[177,213] In addition, the preponderance of membrane trafficking and endosomal sorting signals raised an intriguing possibility that C5a not only influences the action of class I PI3Ks involved in phagocytosis, but also the class III PI3K driving maturation of the phagosome, and that impairment of both pathways combined drives the killing defect demonstrated in Figure III-6.

Using a maturation probe prepared in-house by Dr Conway Morris, I show in Figure VI-9 that cells pre-treated with C5a demonstrated not only a defect in baseline phagocytosis but a defect in phagosomal acidification, designated maturation in the figure for simplicity. I then sought to functionally validate hits from our phosphoproteomic screen using a recently characterised, highly selective inhibitor of the class III PI3K, Vps34, appropriately designated VPS34-IN1.[379,380] The selected concentration of 1 µM for 60 minutes was based on data established in osteosarcoma cell lines showing inhibition of PI(3)P co-localisation with endosomes,[379] as well as this being the concentration used in the laboratory of our collaborator and PI3K biologist, Professor Klaus Okkenhaug. Using the same maturation probe and DHR in duplicate conditions (as DHR and AF488 cannot be analysed in the same cells due to overlapping emission spectra) I demonstrated that VPS34-IN1 selectively impaired phagosomal maturation, without impairing phagocytosis, with a trend to reduction in phagosomal ROS Figure VI-10. These data are broadly consistent with those of Anderson and colleagues, who showed Vps34 did not play an appreciable role in phagocytosis.[381] Our data showed a trend to decreased ROS production with Vps34 inhibition, though this was not as marked as that shown by the authors above[381] and others.[62,382] The reasons for this difference are likely due to different cellular contexts, measures of phagosomal ROS, and the use of a highly selective VPS34 inhibitor in this current work.

To summarise, the data presented in this chapter provide an unprecedented insight into the phosphoproteomic response of primary human neutrophils to a common pathogenic stimulus, and the perturbation of this response by C5a. These data indicate that C5a exerts pleiotropic effects on neutrophils and induces a profound phosphorylation failure in response to subsequent pathogen encounter. This failure is characterised by defects in multiple signalling pathways, including phosphoinositide signalling. In follow-up experiments, the phosphoproteomic data has been validated in a physiologically-relevant *in vitro* system, where we have shown that Vps34 inhibition selectively recapitulates the phagosomal maturation defect induced by C5a. The screen has also raised the intriguing and exciting prospect of direct nuclear involvement in phagocytosis, and the impairment of nuclear membrane disassembly by C5a as another mechanism by which C5a may drive neutrophil dysfunction. As usual, such experiments generate a host of new avenues for investigation, some of which are discussed in the next, and final, chapter.

Chapter VII: Future directions and conclusion

1. Summary of key findings

Throughout the course of this body of work, several novel findings were made, which together have implications for our understanding of innate immune dysfunction in critical illness. This section summarises these findings and relates them both to each other and to our understanding of critical illness-induced immune dysfunction.

First, and of critical importance to the remainder of work presented here, is the demonstration and extension of the C5a-induced defect in neutrophil phagocytosis. Whilst C5a-induced defects in phagocytosis have been noted for some time by our group[177,213] and others[179,269,270] these studies were performed in isolated cells with a large phagocytic target, zymosan. Here, I have extended these findings in several ways. The first was demonstration of C5a-induced phagocytic defects of the physically smaller, physiologically relevant pathogens *E. coli* and *S. aureus* by purified cells in suspension (Figure III-5), and then in whole blood, showing an accompanying reduction in phagosomal ROS production (Figure IV-3). Further, the relevance of these findings to bacterial killing of *S. aureus* has now been demonstrated (Figure III-6). Importantly, in both experimental systems the rapid onset and persistence of the effects of C5a have been shown (Figure III-7 and Figure IV-4), findings of particular interest given the prolonged and often fatal immunosuppression observed in diverse groups of critically ill patients.[97,158,167]

I made use of my time in Cambridge to work with new technologies; the Attune Nxt™ flow cytometer made possible the whole blood assay I refined, without RBC lysis or wash steps. This cytometer, when combined with fluorescent probes and an appropriate anticoagulant (argatroban), allows rapid assessment of neutrophil functions in small samples of blood (Figure IV-1). This technique is readily applicable in clinical settings (Figure IV-8). Further, the assay has been used by my supervisor, Dr Andrew Conway Morris, to interrogate neutrophil function in murine blood samples with success (not shown). The ready availability of this assay facilitated further work on the biology of C5a: this work demonstrated important differences in the involvement of PI3K signalling between whole blood and purified cells (Figure III-5 and Figure IV-5). The reasons for this difference are not clear at present, though likely candidates include other cell types such as monocytes, which have previously been shown to modulate neutrophil responses to LPS.[383] Further, the plethora of complement and coagulation factors present in whole blood, once stimulated by the addition of C5a,[190,200] may generate a response so intense it is not preventable by inhibition of any one signalling pathway, necessitating multi-pronged pathway blockade similar to that recently employed by Skjeflo and colleagues in a porcine model of sepsis.[384]

An unanticipated finding of my work was the resistance to C5a-induced phagocytic impairment by previous *S. aureus* phagocytosis (Figure V-1). Initially I believed this was due to phagocytosis reducing C5aR1 expression, thereby rendering the cell unresponsive to subsequent C5a exposure. However, other priming agents and stimuli (including the soluble, *S. aureus*-derived TLR2 agonist LTA) also reduce C5aR1 expression but do not protect from subsequent C5a-induced impairment (Figure V-2), refuting that hypothesis. Given the known interplay between actin remodelling, endocytosis and signalling,[347,359] a more likely explanation may be that large-scale actin changes induced by phagocytosis[49] affect the signalling functions of C5aR1. Further, given what we now know about the massive phosphoproteomic response to *S. aureus*, a simple 'drowning out' of any subsequent C5a signal should also be considered a potential explanation for the above observations.

A key consideration arising from the data presented throughout this thesis is the possibility that the inhibitory effect of C5a pre-treatment on phagocytosis is due to homologous desensitisation of C5aR1. This line of reasoning posits that C5aR1 allows efficient phagocytosis of pathogens under homeostatic conditions as demonstrated in both mice[385] and humans[266] and discussed in Chapter I: Section 3. Therefore, pre-exposure to C5a results in homologous desensitisation, reducing cell-surface C5aR1 and hence the efficiency of subsequent phagocytosis. I do not believe that this homologous desensitisation hypothesis wholly explains the C5a-induced phagocytic defect observed throughout my thesis for a number of reasons outlined below.

Firstly, data from the two studies cited above indeed demonstrate that intact C5a-C5aR1 signaling is required for efficient phagocytosis when neutrophils encounter *E. coli*[266] or *Cryptococcus neoformans.*[385] However, a key difference between the above studies and my own work is the rapidity of C5a exposure. In the above publications, C5a was generated endogenously in whole blood or serum after bacteria were added, as occurs in localised tissue infection or low-volume bacteraemia.[92] In my system, C5a was spiked into the experimental milieu in high concentrations, as observed in critical illness,[92] which resulted in an immediate, pre-phagocytic flood of C5a rather than a gradual increase of C5a concentrations alongside phagocytosis. The mechanism by which C5a-C5aR1 signaling was shown to enhance phagocytosis was upregulation of CD11b on the cell surface.[266,385] Importantly, I have also shown that CD11b is upregulated by pre-treatment with high-concentrations of C5a (Figure IV-6) yet under the same conditions, these cells exhibit defective phagocytosis (Figure IV-3). In short, the two experimental systems differ in their physiology and C5a exerts different effects in different contexts. I therefore believe it is more likely that my data indicate a specific effect of C5a pre-treatment on phagocytosis, rather than dampening of an effect shown in a significantly different system.

Further, data presented in Figure IV-7 from the 'double phagocytic challenge' experiment show that the overwhelming majority of cells positive for the second phagocytic challenge were positive on the first challenge, and Figure V-2C shows that C5aR1 expression decreases with phagocytosis of each challenge. Therefore, my data indicate that cells which have phagocytosed on the first challenge (and hence have lower C5aR1) are actually more likely to phagocytose when challenged again, relative to their non-phagocytic, C5aR1 high counterparts. I have also shown in Figure V-2 that GM-CSF, LPS and LTA induce a trend toward reduced C5aR1 expression whilst driving an increase in phagocytosis. Figure III-7 demonstrates that phagocytic defects increase with time after C5a exposure (minimal at 10 minutes but marked at 60 minutes) despite the receptor being near-maximally internalised by 5-10 minutes.[386,387] Taken together, these data indicate that homologous desensitisation of C5aR1 by C5a pre-treatment is unlikely to fully explain the phagocytic defect induced by C5a.

This question could be addressed experimentally through pre-treatment of neutrophils with the small molecule C5aR1 inhibitor PMX-53[388] or monoclonal antibodies against C5aR1 signaling such as MEDI7814[284] and IFX-1 prior to C5a exposure.[389] Indeed, Conway Morris and colleagues have shown that pre-treatment with a monoclonal antibody against C5aR1 had a negligible effect on phagocytosis in control cells, and partially prevented C5a-induced phagocytic defects.[177] However, from the above experiment (and any that employ the strategy of C5aR1 blockade) it is impossible to dissect whether the observed results are due to a prevention of homologous desensitisation or inhibition of direct C5a-induced signaling which impairs phagocytosis. Another option would be to selectively inhibit receptor endocytosis as reviewed by Dutta and Donaldson,[390] though it is likely that inhibition of endocytosis would have off-target effects on the closely related phenomenon of phagocytosis. Given these considerations, I believed a global assessment of C5a-induced signalling followed by experimental interrogation of key pathways was more likely to yield insights into the mechanism of C5a-induced phagocytic defects, as discussed below.

The carefully planned phosphoproteomic screen has provided a wealth of data and constitutes the deepest profile of the human neutrophil phosphoproteome to date. It is the first phosphoproteomic assessment of this cell type in response to *S. aureus*, and certainly the first to interrogate the effect of C5a in this context. Despite the importance of this particular host-pathogen interaction for human disease,[391] there is a paucity of systematic proteomic data interrogating this relationship: a search of the comprehensive ProteomeXchange database[392,393] using the keyword 'neutrophil' yields four studies on human neutrophils, two of which have yet to be published and hence data are unavailable, one with which I have compared my own dataset already,[352] and the last relates to proteomic profiling of granule subsets of limited relevance for global cell signalling networks.[364] None of

these datasets relate to neutrophils in the context of phagocytosis or *S. aureus* infection. Further, the above search, coupled with interrogation of the PubMed database using the subject headings 'neutrophil' '*S. aureus'* and 'proteome' revealed no publications addressing the host neutrophil phosphoproteomic (or indeed proteomic) response to *S. aureus* infection. Given the lack of other datasets addressing *S. aureus*-host interactions, comparisons must be made with other cell types encountering this pathogen.

Richter and colleagues infected human bronchial epithelial (16HBE14o) cells with live *S. aureus* (strain HG001) and measured the 'host' cell phosphoproteome at 15, 120 and 240 minutes, with concomitant assessments of phagocytosis and bacterial replication.[394] Peak phosphoproteomic responses were observed at 120 and 240 minutes in this cell type,[394] likely owing to the much slower rate of phagocytosis of non-professional phagocytes relative to neutrophils.[49,53,63] Given these caveats, it is reassuring to note enrichment of pathways similar to those found in my dataset associated with phagocytosis, including cytoskeletal reorganisation, Rho-family GTPase signalling, and vesicle trafficking.[394] There is a notable lack of protein phosphorylation related to nuclear membrane dissolution,[394] which currently appears to be unique to my dataset. Of note, there is a significant literature on viral infection of other cell-types,[368,395,396] and on *S. aureus* proteomes in the context of infection, as recently reviewed by Hecker and colleagues.[362] However, the absence of active phagocytosis and assessment of the host response in the above studies, respectively, limits meaningful comparisons with my dataset.

Analysis of the differential expression of the 2712 phosphoproteins quantified in Chapter VI: demonstrated three key findings. First, C5a pre-treatment induced a profound phosphorylation failure in response to *S. aureus* (Figure VI-8). This paralysis of subsequent responses is evident in the phosphoprotein signature for at least one hour after C5a stimulation, and indeed our phagocytosis data suggests that it persists for several hours. This finding led to the second and third important insights: pathway analysis revealed signalling failures disproportionately affecting nuclear envelope breakdown and class III PI3K-mediated phagosomal maturation.

The finding of class III PI3K involvement in phagosomal maturation and appropriate targeting of endosomes is not new,[62,381,397] which provides further validation of the phosphoproteomic screen. However, C5a-induced impairment of PtdIns3P signals in response to *S. aureus* have not been shown before and constitutes yet another way in which C5a impairs neutrophil microbicidal function. Further, the data presented in Figure VI-9 and Figure VI-10 provide initial functional validation of observed phosphoproteomic signals in the whole blood model, the importance of which cannot be understated if these signalling findings are to be translated to therapies for patients.

Finally, the phosphorylation of proteins involved in nuclear membrane disassembly, to my knowledge, had not been demonstrated in the context of phagocytosis. The concept of nuclear envelope breakdown and reorganisation has precedent in the transmigration literature, where nuclei are inserted into the leading edges of cells[36] and undergo rupture and repair cycles.[38] Further, nuclear deformations during transmigration have recently been shown to involve lamins,[398] components of the fibrous nuclear lamina, which also modulate nuclear hypersegmentation.[35,374] A prominent 'hit' from the phosphoproteomic screen was lamin B1 (LMNB1, Figure VI-7) which further strengthens my suspicion that nuclear envelope changes may well be involved in phagocytosis, and impaired by C5a pre-treatment. The relevance of these findings, if functionally validated, could extend from neutrophils in the context of C5a exposure to phagocytes and phagocytosis in general. However, demonstrating nuclear involvement in functional assays of phagocytosis will be challenging, and is discussed in the next section.

2. Avenues for further investigation

2.1. Reconcile contrasting data on the effect of C5a and other agonists in different circumstances

The question of why C5a, the prototypical anaphylatoxin, which induces inflammation and tissue infiltration of immune cells, simultaneously seems to impair other functions of the very cells it recruits, remains unanswered. Many groups have demonstrated C5a-induced defects in phagocytosis[177,179,213,270] (and we can now extend this to ROS production and phagosomal acidification in whole blood) whilst others have shown that signalling through C5a is, at the same time, important for efficient phagocytosis.[266] The idea that these differential effects are simply concentration-dependent, as advanced by Ward and colleagues,[92,210] whilst likely a contributor, does not withstand the weight of published evidence and is not supported by data I have collected. Could the subset of immune cell involved, timing of exposure, presence of a concentration gradient or differential receptor ligation explain these apparent paradoxes? Whilst many reported differences may be due to context, I think an important component of future work will be to address these conflicting findings in contexts relevant to the situation *in vivo*. We now have workable, scalable assays with which to address these questions.

Investigation could commence with a paired comparison of whole blood, purified neutrophils in plasma or serum and ultrapure neutrophils treated with a range of concentrations of C5a with subsequent measurement of phagocytosis, phagosomal ROS and maturation. C5a exposure before and after transmigration (either through transwells, or endothelial cells) could also be assessed for differential effects. There is some precedent for susceptibility to C5a being driven by cellular maturation or transmigration: Seow and colleagues have shown C5a is known to exert different effects on monocytes compared to macrophages,[275] and it

would be interesting to explore this hypothesis in terminally differentiated neutrophils. Finally, the concept of biased agonism of GPCRs (different cellular effects from ligation of the same receptor, recently reviewed by Lefkowitz and others[399,400]) may drive the contrasting effects of C5a observed in different experiments, and this problem could be interrogated by a proteomic approach as we have previously employed.

2.2. Interrogate C5aR1 localisation after phagocytosis

In Chapter V:4.4 I attempted to localise C5aR1 by confocal microscopy, but these attempts were unsuccessful, most likely due to non-specific staining of the antibody. I believe this is an important component of work, as the direct involvement of C5aR1 in phagocytosis has not previously been explored. To troubleshoot the issues I had during these experiments I would first change the primary antibody and test a variety of concentrations. If that failed, I'd consider permeabilising cells with saponin (as employed by Bamberg and colleagues[231] to localise the receptor) rather than Triton X-100 or methanol, as these harsher agents may degrade antibody-binding epitopes of the receptor.[401] Once reliable antibody staining has been achieved, time courses of phagocytosis of *S. aureus* could be carried out and C5aR1/2 localisation assessed.

2.3. Follow-up on class III PI3K impairment after C5a

Preliminary data acquired in whole blood validates significant hits from the phosphoproteomic dataset with respect to the importance of PtdIns3P in phagosomal maturation, and its impairment by C5a. In order to follow-up on these findings, further experiments should assess the effect of VPS34-IN1 treatment on whole blood staphylococcal killing. For completeness, an increase in PtdIns3P levels in the context of *S. aureus* phagocytosis and their reduction by C5a and VPS34-IN1 treatment should also be demonstrated. Assays similar to the one I used to quantify PtdIns(3,4,5)P_3 (Chapter II::8) are now employed by our collaborators at the Babraham Institute, Professors Phillip Hawkins and Len Stephens, to measure other phosphoinositide species and are thus readily available.[402]

2.4. Validate whole blood assay as a scalable, clinically useful tool

I demonstrated the whole blood assay is feasible in a clinical setting, though it has not yet been validated or correlated with known measures of neutrophil function or patient-important outcomes. Before these aims can be achieved, I believe the assay would benefit from a concerted effort to minimise experimental variation, and assessment of whether this variation represents true biological variation or 'noise' within the system. I suspect a significant source of variation is pipetting error or incomplete homogenisation of the pHrodo *S. aureus* Bioparticles, despite aliquots being taken from the same batch and stored at -20°C. These

issues could be addressed initially by measuring neutrophil function in samples of blood drawn from the same donors on the same day and on subsequent days to determine whether function remains stable over time. Should reproducibility be shown, the next step would be to apply the assay to clinical populations. This process could begin to correlate neutrophil function with established measures of immunosuppression, such as monocyte HLA-DR and C5aR1 expression and T_{reg} numbers.[110,147] Eventually patient-important outcomes such as nosocomial infection and mortality could be interrogated, and receiver operator characteristic (ROC) curves, predictive values, sensitivity and specificity could be generated.[403] The use of whole blood samples in this assay easily lends itself to the assessment of multiple cell types identified by cell surface markers, allowing a global snapshot of immune function to be generated. Whilst these processes are certain to require new ethical approvals as well as significant time and financial investment, a sensitive, scalable test which will allow clinicians and researchers to accurately immunophenotype patients is of pivotal importance for the development of novel therapies in the critical illness space.[111,317,404]

2.5. Map neutrophil phosphoproteomic response to *S. aureus* in critical illness

My work has identified discrete C5a-induced phosphorylation failures in purified neutrophils from healthy donors. For this work to have translational relevance, I believe it is important to establish whether similar phosphorylation failures are evident in patient neutrophils exposed to the same stimulus. Therefore, experiments are underway to assess the phosphoproteomic signature of critically ill patient neutrophils. Importantly, I am interested in a specific, immunophenotypically defined group of patients with impaired phagocytosis; therefore, only those with phagocytic impairment and evidence of C5a exposure will be assayed. These parameters will be assessed in whole blood and purified cells prior to sending samples for phosphoproteomic analysis.

Another key aspect of this experiment is the application of a known stimulus (*S. aureus*) and measurement of a phosphoproteomic response, rather than simply assessing the ‘baseline’ phosphoproteome of critically ill patient neutrophils. This is important as the heterogeneity of this population will undoubtedly lead to substantial baseline variation in signalling networks, which is less relevant to this question, and indeed has already been assessed in much larger studies using a transcriptomic approach.[312,405,406] Clinical variables will be collected but in this sample size (n = 5 patients) these are unlikely to be informative. Should similar patterns of phosphorylation failure in response to *S. aureus* challenge be demonstrated in patient neutrophils, the translational relevance of my findings will be significantly increased.

2.6. Interrogate the role of nuclear reformation in phagocytosis

Further exploration of the role of nuclear membrane dissociation in phagocytosis poses a significant challenge and will most likely necessitate a shift in methodology. Initial work should start with simply observing the nucleus during phagocytosis, which should be achievable using live cell confocal microscopy in combination with non-toxic nuclear stains such as Hoescht 22342. Such techniques are currently employed in our laboratory. However, it is likely that more advanced, higher-resolution microscopy techniques (such as stimulated emission depletion; STED microscopy) combined with selective nuclear membrane staining will be required to progress this project further. Such work has been performed transmigrating murine dendritic cells expressing green-fluorescent protein-tagged nuclei[38] and I anticipate a similar approach will be possible with the promyelocytic HL-60 cell line.[407]

Once techniques above have been established and validated, pathways of interest can be perturbed in primary human neutrophils using commercially-available small molecule inhibitors of cyclin-dependent kinases, aurora kinase B and MAPK3, which have been identified as kinases mediating observed phosphoprotein signals in our dataset. Further, in HL-60 cells, siRNA-induced gene silencing or clustered regularly interspaced short palindromic repeats (CRISPR) editing can be attempted to mitigate issues of drug selectivity and off-target effects likely to be encountered in primary human cells. It is anticipated that this work will again involve significant time and financial investments.

3. Conclusion

Neutrophils are key components of the innate immune response. They are produced in enormous numbers and migrate rapidly through complex environments to phagocytose and destroy pathogens. Defects in these processes drive disease and comprise a significant component of the morbidity associated with critical illness. Factors driving neutrophil dysfunction are only partially understood, though we know somewhat paradoxically, a key role is played by the anaphylatoxin C5a, released in saturating concentrations during critical illness.

This project sought to understand the mechanisms of C5a-induced neutrophil dysfunction. Key findings from this research include the unanticipated persistence of C5a-induced neutrophil dysfunction, mirroring the immunosuppressive phase we observe in patients. I have taken steps towards developing an assay that may one day facilitate rapid, reliable and functional immunophenotyping of patient blood samples. I have shown that C5a is unique amongst other priming agents in inducing phagocytic dysfunction and performed the first ever phosphoproteomic study of the neutrophil response to *S. aureus* in the context of C5a. These data have demonstrated a profound phosphorylation failure evident in cells pre-treated with C5a, with downstream effects on phosphoinositide metabolism and nuclear

reorganisation. Over the course of this work, some questions were answered, though many more possibilities and uncertainties have arisen. I am reassured, however, that collaborative efforts and translation of detailed biological understanding to clinical practice will ultimately drive better outcomes for our sickest patients.

Chapter VIII: Bibliography

1 Summers C, Rankin SM, Condliffe AM, Singh N, Peters a. M, Chilvers ER. Neutrophil kinetics in health and disease. *Trends Immunol* 2010; **31**: 318–324.

2 Kolaczkowska E, Kubes P. Neutrophil recruitment and function in health and inflammation. *Nat Rev Immunol* 2013; **13**: 159–75.

3 Nauseef WM. Neutrophils, from cradle to grave and beyond. *Immunol Rev* 2016; **273**: 5–10.

4 Goldblatt D. Recent advances in chronic granulomatous disease. *J Infect* 2014; **69**: S32–S35.

5 Lawrence SM, Corriden R, Nizet V. The Ontogeny of a Neutrophil: Mechanisms of Granulopoiesis and Homeostasis. *Microbiol Mol Biol Rev* 2018; **82**: 1–22.

6 Manz MG, Boettcher S. Emergency granulopoiesis. *Nat Rev Immunol* 2014; **14**. doi:10.1038/nri3660.

7 Pillay J, Kamp VM, Hoffen E Van, Visser T, Tak T, Lammers J *et al.* A subset of neutrophils in human systemic inflammation inhibits T cell responses through Mac-1. *J Clin Invest* 2012; **122**: 327–336.

8 Furze RC, Rankin SM. Neutrophil mobilization and clearance in the bone marrow. *Immunology* 2008; **125**: 281–288.

9 Jagels MA, Hugli TE. Neutrophil chemotactic factors promote leukocytosis. A common mechanism for cellular recruitment from bone marrow. *J Immunol* 1992; **148**: 1119–1128.

10 Jagels BMA, Chambers JD, Arfors K, Hugli TE. C5a- and Tumor Necrosis Factor-a-Induced Leukocytosis Occurs Independently of. *Blood* 1995; **85**: 2900–2909.

11 Terashima T, English D, Hogg JC, Eeden SF van. Release of polymorphonuclear leukocytes from the bone marrow by interleukin-8.pdf. *Blood* 1998; **92**: 1062–1069.

12 de Oliveira S, Rosowski EE, Huttenlocher A. Neutrophil migration in infection and wound repair: going forward in reverse. *Nat Publ Gr* 2016; **16**. doi:10.1038/nri.2016.49.

13 Jurcevic S, Humfrey C, Uddin M, Warrington S, Larsson B, Keen C. The effect of a selective CXCR2 antagonist (AZD5069) on human blood neutrophil count and innate immune functions. *Br J Clin Pharmacol* 2015; **80**: 1324–1336.

14 Kratz A, Ferraro M, Sluss PM, Lewandrowski KB. Normal Reference Laboratory Values. *N Engl J Med* 2004; **351**: 1548–1563.

15 Malech HL, DeLeo FR, Quinn MT. *Neutrophil methods and protocols*. 2nd ed. Hamana Press: New York, USA, 2014 doi:10.1007/978-1-62703-845-4.

16 Saverymuttu SH, Peters AM, Keshavarzian A, Reavy HJ, Lavender JP. The kinetics of 111indium distribution following injection of 111indium labelled autologous granulocytes in man. *Br J Haematol* 1985; **61**: 675–85.

17 Cartwright GE, Wintrobe MM. Leukokinetic studies. IV. The total blood, circulating and marginal granulocyte pools and the granulocyte turnover rate in normal subjects. *J Clin Invest* 1961; **40**: 989–995.

18 Pillay J, Braber I Den, Vrisekoop N, Kwast LM, Boer RJ De, Borghans a M *et al.* In vivo labeling with 2H2O reveals a human neutrophil lifespan of 5.4 days. *Blood* 2010; **116**: 625–627.

19 Lahoz-Beneytez J, Elemans M, Zhang Y, Ahmed R, Salam A, Block M *et al.* Human neutrophil kinetics: modeling of stable isotope labeling data supports short blood neutrophil half-lives. *Blood* 2016; **127**: 3431–3439.

20 Mantovani A, Cassatella M a., Costantini C, Jaillon S. Neutrophils in the activation and regulation of innate and adaptive immunity. *Nat Rev Immunol* 2011; **11**: 519–531.

21 Farahi N, Singh NR, Heard S, Loutsios C, Summers C, Solanki CK *et al.* Brief report Use of 111-Indium – labeled autologous eosinophils to establish the in vivo kinetics of human eosinophils in healthy subjects. *Blood* 2012; **120**: 4068–4071.

22 Miralda I, Uriarte SM, McLeish KR. Multiple Phenotypic Changes Define Neutrophil Priming. *Front Cell Infect Microbiol* 2017; **7**: 1–13.

23 Condliffe a M, Kitchen E, Chilvers ER. Neutrophil priming: pathophysiological consequences and underlying mechanisms. *Clin Sci (Lond)* 1998; **94**: 461–71.

24 Summers C, Singh NR, White JF, Mackenzie IM, Johnston A, Solanki C *et al.* Pulmonary retention of primed neutrophils: a novel protective host response, which is impaired in the acute respiratory distress syndrome. *Thorax* 2014; **69**: 623–9.

25 Sarris M, Sixt M. Navigating in tissue mazes: Chemoattractant interpretation in complex environments. *Curr Opin Cell Biol* 2015; **36**: 93–102.

26 Ley K, Laudanna C, Cybulsky MI, Nourshargh S. Getting to the site of inflammation: the leukocyte adhesion cascade updated. *Nat Rev Immunol* 2007; **7**: 678–89.

27 Nourshargh S, Alon R. Leukocyte Migration into Inflamed Tissues. *Immunity* 2014; **41**: 694–707.

28 Buckley CD, Ross EA, McGettrick HM, Osborne CE, Haworth O, Schmutz C *et al.* Identification of a phenotypically and functionally distinct population of long-lived neutrophils in a model of reverse endothelial migration. *J Leukoc Biol* 2006; **79**: 303–311.

29 Woodfin A, Voisin MB, Beyrau M, Colom B, Caille D, Diapouli FM *et al.* The junctional adhesion molecule JAM-C regulates polarized transendothelial migration of neutrophils in vivo. *Nat Immunol* 2011; **12**: 761–769.

30 Tauzin S, Starnes TW, Becker FB, Lam P ying, Huttenlocher A. Redox and Src family kinase signaling control leukocyte wound attraction and neutrophil reverse migration. *J Cell Biol* 2014; **207**: 589–598.

31 Colom B, Bodkin J V., Beyrau M, Woodfin A, Ody C, Rourke C *et al.* Leukotriene B4-Neutrophil Elastase Axis Drives Neutrophil Reverse Transendothelial Cell Migration InVivo. *Immunity* 2015; **42**: 1075–1086.

32 Worthen GS, Schwab B, Elson EL, Downey GP. Mechanics of stimulated neutrophils: Cell stiffening induces retention in capillaries. *Science (80-)* 1989; **245**: 183–186.

33 Downey GP, Worthen GS, Henson PM, Hyde DM. Neutrophil sequestration and migration in localized pulmonary inflammation. Capillary localization and migration across the interalveolar septum. *Am Rev Respir Dis* 1993; **147**: 168–176.

34 Doerschuk CM, Beyers N, Coxson HO, Wiggs B, Hogg JC. Comparison of neutrophil and capillary diameters and their relation to neutrophil sequestration in the lung. *J Appl Physiol* 1993; **74**: 3040–3045.

35 Rowat AC, Jaalouk DE, Zwerger M, Ung WL, Eydelnant IA, Olins DE *et al.* Nuclear envelope composition determines the ability of neutrophil-type cells to passage through micron-scale constrictions. *J Biol Chem* 2013; **288**: 8610–8618.

36 Barzilai S, Yadav SK, Morrell S, Roncato F, Klein E, Stoler-Barak L *et al.* Leukocytes

Breach Endothelial Barriers by Insertion of Nuclear Lobes and Disassembly of Endothelial Actin Filaments. *Cell Rep* 2017; **18**: 685–699.

37 Lämmermann T, Bader BL, Monkley SJ, Worbs T, Wedlich-Söldner R, Hirsch K *et al.* Rapid leukocyte migration by integrin-independent flowing and squeezing. *Nature* 2008; **453**: 51–55.

38 Raab M, Gentili M, Belly H De, Thiam H, Vargas P, Jimenez AJ *et al.* ESCRT III repairs nuclear envelope ruptures during cell migration to limit DNA damage and cell death. *Science (80-)* 2016; **352**: 359–363.

39 Sarris M, Masson JB, Maurin D, Van Der Aa LM, Boudinot P, Lortat-Jacob H *et al.* Inflammatory Chemokines Direct and Restrict Leukocyte Migration within Live Tissues as Glycan-Bound Gradients. *Curr Biol* 2012; **22**: 2375–2382.

40 Welch HCE, Coadwell WJ, Ellson CD, Ferguson GJ, Andrews SR, Erdjument-Bromage H *et al.* P-Rex1, a PtdIns(3,4,5)P3- and Gbetagamma-regulated guanine-nucleotide exchange factor for Rac. *Cell* 2002; **108**: 809–821.

41 Afonso P V, Parent C a. PI3K and chemotaxis: a priming issue? *Sci Signal* 2011; **4**: 1–3.

42 Lämmermann T, Afonso P V, Angermann BR, Wang JM, Kastenmüller W, Parent CA *et al.* Neutrophil swarms require LTB4 and integrins at sites of cell death in vivo. *Nature* 2013; **498**: 371–5.

43 Lammermann T. In the eye of the neutrophil swarm-navigation signals that bring neutrophils together in inflamed and infected tissues. *J Leukoc Biol* 2015; **100**. doi:10.1189/jlb.1MR0915-403.

44 Borregaard N. Neutrophils, from Marrow to Microbes. *Immunity* 2010; **33**: 657–670.

45 Sørensen OE, Follin P, Johnsen AH, Calafat J, Sandra Tjabringa G, Hiemstra PS *et al.* Human cathelicidin, hCAP-18, is processed to the antimicrobial peptide LL-37 by extracellular cleavage with proteinase 3. *Blood* 2001; **97**: 3951–3959.

46 Woodfin A, Beyrau M, Voisin MB, Ma B, Whiteford JR, Hordijk PL *et al.* ICAM-1-expressing neutrophils exhibit enhanced effector functions in murine models of endotoxemia. *Blood* 2016; **127**: 898–907.

47 Silvestre-Roig C, Hidalgo A, Soehnlein O. Neutrophil heterogeneity: Implications for homeostasis and pathogenesis. *Blood* 2016; **127**: 2173–2181.

48 Levin R, Grinstein S, Canton J. The life cycle of phagosomes: formation, maturation, and resolution. *Immunol Rev* 2016; **273**: 156–179.

49 Flannagan RS, Jaumouillé V, Grinstein S. The cell biology of phagocytosis. *Annu Rev Pathol* 2012; **7**: 61–98.

50 Hajishengallis G, Reis ES, Mastellos DC, Ricklin D, Lambris JD. Novel mechanisms and functions of complement. *Nat Immunol* 2017; **18**: 1288–1298.

51 Freeman SA, Goyette J, Furuya W, Woods EC, Bertozzi CR, Bergmeier W *et al.* Integrins Form an Expanding Diffusional Barrier that Coordinates Phagocytosis [including supplement]. *Cell* 2016; **164**: 128–140.

52 Jaumouille V, Grinstein S. Receptor mobility, the cytoskeleton, and particle binding during phagocytosis. *Curr Opin Cell Biol* 2011; **23**: 22–29.

53 Chow C-W, Downey GP, Grinstein S. Measurements of phagocytosis and phagosomal maturation. In: Juan S. Bonifacino (Bethesda, Maryland); Joe B. Harford (Bethesda, Maryland); Jennifer Lippincott-Schwartz (Bethesda, Maryland); and Kenneth M. Yamada (Bethesda, Maryland); Past Editors: Mary Dasso (Bethesda M (ed). *Current*

Protocols in Cell Biology. 2004, p Unit 15.7.

54 Nauseef WM. William M. Nauseef How human neutrophils kill and degrade microbes: an integrated view. *Immunol Rev* 2007; **219**: 88–102.

55 Caron E, Hall A. Identification of two distinct mechanisms of phagocytosis controlled by different Rho GTPases. *Science (80-)* 1998; **282**: 1717–1721.

56 Segal AW, Dorling J, Coade S. Kinetics of fusion of the cytoplasmic granules with phagocytic vacuoles in human polymorphonuclear leukocytes: Biochemical and morphological studies. *J Cell Biol* 1980; **85**: 42–59.

57 Allen LA, DeLeo FR, Gallois A, Toyoshima S, Suzuki K, Nauseef WM. Transient association of the nicotinamide adenine dinucleotide phosphate oxidase subunits p47phox and p67phox with phagosomes in neutrophils from patients with X-linked chronic granulomatous disease. *Blood* 1999; **93**: 3521–3530.

58 Botelho RJ, Teruel M, Dierckman R, Anderson R, Wells A, York JD *et al.* Localized biphasic changes in phosphatidylinositol-4,5-bisphosphate at sites of phagocytosis. *J Cell Biol* 2000; **151**: 1353–68.

59 Segal AW, Geisow M, Garcia R, Harper A, Miller R. The respiratory burst of phagocytic cells is associated with a rise in vacuolar pH. *Nature* 1981; **290**: 406–409.

60 Jankowski A, Scott CC, Grinstein S. Determinants of the phagosomal pH in neutrophils. *J Biol Chem* 2002; **277**: 6059–6066.

61 Tapper H, Grinstein S. Fc receptor-triggered insertion of secretory Fc Receptor-Triggered Insertion of Secretory Granules into the Plasma Membrane of Human Neutrophils Selective Retrieval During Phagocytosis'. *J Immunol* 1997; **159**: 409–418.

62 Ellson C, Davidson K, Anderson K, Stephens LR, Hawkins PT. PtdIns3P binding to the PX domain of p40phox is a physiological signal in NADPH oxidase activation. *EMBO J* 2006; **25**: 4468–4478.

63 Nordenfelt P, Tapper H. Phagosome dynamics during phagocytosis by neutrophils. *J Leukoc Biol* 2011; **90**: 271–284.

64 Segal AW. How Neutrophils Kill Microbes. *Annu Rev Immunol* 2005; **23**: 197–223.

65 Nauseef WM. Myeloperoxidase in human neutrophil host defence. *Cell Microbiol* 2014; **16**: 1146–1155.

66 Condliffe AM, Davidson K, Anderson KE, Ellson CD, Crabbe T, Okkenhaug K *et al.* Sequential activation of class IB and class IA PI3K is important for the primed respiratory burst of human but not murine neutrophils. *Blood* 2005; **106**: 1432–1441.

67 Ekpenyong AE, Toepfner N, Fiddler C, Herbig M, Li W, Cojoc G *et al.* Mechanical deformation induces depolarization of neutrophils. *Sci Adv* 2017; **3**: 1–11.

68 Painter RG, Marrero L, Lombard GA, Valentine VG, Nauseef WM, Wang G. CFTR-mediated halide transport in phagosomes of human neutrophils. *J Leukoc Biol* 2010; **87**: 933–942.

69 Leliefeld PHC, Wessels CM, Leenen LPH, Koenderman L, Pillay J. The role of neutrophils in immune dysfunction during severe inflammation. *Crit Care* 2016; **20**: 73.

70 Nauseef WM, Borregaard N. Neutrophils at work. *Nat Immunol* 2014; **15**: 602–11.

71 Flannagan RS, Cosío G, Grinstein S. Antimicrobial mechanisms of phagocytes and bacterial evasion strategies. *Nat Rev Microbiol* 2009; **7**: 355–366.

72 Brinkmann V, Reichard U, Goosmann C, Fauler B, Uhlemann Y, Weiss DS *et al.* Neutrophil extracellular traps kill bacteria. *Science (80-)* 2004; **303**: 1532–1535.

73 Gray RD, Hardisty G, Regan KH, Smith M, Robb CT, Duffin R *et al.* Delayed neutrophil apoptosis enhances NET formation in cystic fibrosis. *Thorax* 2018; **73**: 134–144.

74 Law SM, Gray RD. Neutrophil extracellular traps and the dysfunctional innate immune response of cystic fibrosis lung disease: a review. *J Inflamm* 2017; **14**: 29.

75 Vincent J, Creteur J. The Critically Ill Patient. In: Ronco C, Bellomo R, Kellum JA, Ricci ZBT (eds). *Critical Care Nephrology*. Elsevier: Philadelphia, USA, 2019, pp 1–4.

76 Adhikari NK, Fowler RA, Bhagwanjee S, Rubenfeld GD. Critical care and the global burden of critical illness in adults. *Lancet* 2010; **376**: 1339–1346.

77 Pearse RM, Clavien PA, Demartines N, Fleisher LA, Grocott M, Haddow J *et al.* Global patient outcomes after elective surgery: Prospective cohort study in 27 low-, middle- and high-income countries. *Br J Anaesth* 2016; **117**: 601–609.

78 Fleischmann C, Scherag A, Adhikari NKJ, Hartog CS, Tsaganos T, Schlattmann P *et al.* Assessment of global incidence and mortality of hospital-treated sepsis current estimates and limitations. *Am J Respir Crit Care Med* 2016; **193**: 259–272.

79 Phua J, Badia JR, Adhikari NKJ, Friedrich JO, Fowler RA, Singh JM *et al.* Has Mortality from Acute Respiratory Distress Syndrome Decreased over Time? *Am J Respir Crit Care Med* 2009; **179**: 220–227.

80 Shankar-Hari M, Harrison DA, Rubenfeld GD, Rowan K. Epidemiology of sepsis and septic shock in critical care units: Comparison between sepsis-2 and sepsis-3 populations using a national critical care database. *Br J Anaesth* 2017; **119**: 626–636.

81 Annane D, Aegerter P, Jars-Guincestre MC, Guidet B. Current epidemiology of septic shock: The CUB-Réa network. *Am J Respir Crit Care Med* 2003; **168**: 165–172.

82 Lelubre C, Vincent J. Mechanisms and treatment of organ failure in sepsis. *Nat Rev Nephrol* 2018; **14**: 417–427.

83 Le Gall J, Lemeshow S, Saulnier F. A new simplified acute physiology score (SAPS II) based on a European/North American multicenter study. *JAMA* 1993; **270**: 2957–2963.

84 Vincent JL, Moreno R, Takala J, Willatts S, De Mendonca A, Bruining H *et al.* The SOFA (Sepsis-related Organ Failure Assessment) score to describe organ dysfunction/failure. On behalf of the Working Group on Sepsis-Related Problems of the European Society of Intensive Care Medicine. *Intensive Care Med* 1996; **22**: 707–710.

85 Knaus W, Draper E, Wagner D, Zimmerman J. APACHE II: A severity of disease classification system. *Crit Care Med* 1985; **13**.

86 Jones AE, Trzeciak S, Kline JA. The Sequential Organ Failure Assessment score for predicting outcome in patients with severe sepsis and evidence of hypoperfusion at the time of emergency department presentation. *Crit Care Med* 2009; **37**: 1649–1654.

87 Valpondi V, Sgarbi A, Bortolazzi S, Pavoni V, Gilli G, Candini G *et al.* Validation of severity scoring systems SAPS II and APACHE II in a single-center population. 2000; : 1779–1785.

88 Ranzani OT, Prina E, Menéndez R, Ceccato A, Cilloniz C, Méndez R *et al.* New Sepsis Definition (Sepsis-3) and Community-acquired Pneumonia Mortality: A Validation and Clinical Decision-making Study. *Am J Respir Crit Care Med* 2017; : rccm.201611-2262OC.

89 Singer M, Deutschman C, Seymour C, Shankar-Hari M, Annane D, Bauer M *et al.* The Third International Consensus Definitions for Sepsis and Septic Shock (Sepsis-3). *J*

Am Med Assoc 2016; **315**: 801–810.

90 Arulkumaran A, Singer M. Multiple Organ Dysfunction. In: Ronco C, Bellomo R, Kellum JA, Ricci ZBT (eds). *Critical Care Nephrology*. Elsevier: Philadelphia, USA, 2019.

91 Timmermans K, Kox M, Scheffer GJ, Pickkers P. Danger in the intensive care unit: Damps in critically ill patients. *Shock* 2016; **45**: 108–116.

92 Ward PA. The dark side of C5a in sepsis. *Nat Rev Immunol* 2004; **4**: 133–142.

93 Andersson U, Wang H, Palmblad K, Aveberger A-C, Bloom O, Erlandsson-Harris H *et al.* High Mobility Group 1 Protein (Hmg-1) Stimulates Proinflammatory Cytokine Synthesis in Human Monocytes. *J Exp Med* 2000; **192**: 565–570.

94 Zhang Q, Raoof M, Chen Y, Sumi Y, Sursal T, Junger W *et al.* Circulating mitochondrial DAMPs cause inflammatory responses to injury. *Nature* 2010; **464**: 104–7.

95 Beutler B, Rietschel ET. Innate immune sensing and its roots: the story of endotoxin. *Nat Rev Immunol* 2003; **3**: 169–176.

96 Bianchi ME. DAMPs, PAMPs and alarmins: all we need to know about danger. *J Leukoc Biol* 2007; **81**: 1–5.

97 Lord JM, Midwinter MJ, Chen YF, Belli A, Brohi K, Kovacs EJ *et al.* The systemic immune response to trauma: An overview of pathophysiology and treatment. *Lancet* 2014; **384**: 1455–1465.

98 Conway-Morris A, Wilson J, Shankar-Hari M. Immune Activation in Sepsis. *Crit Care Clin* 2018; **34**: 29–42.

99 O'Neill LAJ, Golenbock D, Bowie AG. The history of Toll-like receptors — redefining innate immunity. *Nat Rev Immunol* 2013; **13**: 453–460.

100 Delano MJ, Ward PA. The immune system's role in sepsis progression, resolution, and long-term outcome. *Immunol Rev* 2016; **274**: 330–353.

101 Davenport EE, Burnham KL, Radhakrishnan J, Humburg P, Hutton P, Mills TC *et al.* Genomic landscape of the individual host response and outcomes in sepsis: A prospective cohort study. *Lancet Respir Med* 2016; **4**: 259–271.

102 Matsuda N, Hattori Y. Systemic inflammatory response syndrome (SIRS): molecular pathophysiology and gene therapy. *J Pharmacol Sci* 2006; **101**: 189–98.

103 Ulloa L, Tracey KJ. The 'cytokine profile': A code for sepsis. *Trends Mol Med* 2005; **11**: 56–63.

104 Osuchowski MF, Welch K, Siddiqui J, Remick DG. Circulating cytokine/inhibitor profiles reshape the understanding of the SIRS/CARS continuum in sepsis and predict mortality. *J Immunol* 2006; **177**: 1967–1974.

105 Cohen J. The immunopathogenesis of sepsis. *Nature* 2002; **420**: 885–891.

106 Guo H, Callaway JB, Ting JPY. Inflammasomes: Mechanism of action, role in disease, and therapeutics. *Nat Med* 2015; **21**: 677–687.

107 Beutler BA. TLRs and innate immunity Review article TLRs and innate immunity. *Blood* 2009; **113**: 1399–1407.

108 Marshall JC. Why have clinical trials in sepsis failed? *Trends Mol Med* 2014; **20**: 195–203.

109 Berger D, Schefold JC. Life ain't no SOFA-Considerations after yet another failed

clinical sepsis trial. *J Thorac Dis* 2017; **9**: 438–440.

110 Conway Morris A, Datta D, Hari MS, Stephen J, Weir CJ, Rennie J *et al.* Cell-surface signatures of immune dysfunction risk-stratify critically ill patients: INFECT study. *Intensive Care Med* 2018; **44**: 627–635.

111 Perner A, Gordon AC, Angus DC, Lamontagne F, Machado F, Russell JA *et al.* The intensive care medicine research agenda on septic shock. *Intensive Care Med* 2017; **43**: 1294–1305.

112 Millar FR, Summers C, Griffiths MJ, Toshner MR, Proudfoot AG. The pulmonary endothelium in acute respiratory distress syndrome: insights and therapeutic opportunities. *Thorax* 2016; **71**: 462–73.

113 Segel GB, Halterman MW, Lichtman MA. The paradox of the neutrophil's role in tissue injury: a review. *J Leukoc Biol* 2010; **89**: 1–14.

114 Biron BM, Chung C-S, Chen Y, Wilson Z, Fallon EA, Reichner JS *et al.* PAD4 Deficiency Leads to Decreased Organ Dysfunction and Improved Survival in a Dual Insult Model of Hemorrhagic Shock and Sepsis. *J Immunol* 2018; : ji1700639.

115 Liu F-C, Chuang Y-H, Tsai Y-F, Yu H-P. Role of Neutrophil Extracellular Traps Following Injury. *Shock* 2014; **41**: 491–498.

116 Kabay B, Kocaefe C, Baykal A, ??zden H, Baycu C, Oner Z *et al.* Interleukin-10 gene transfer: Prevention of multiple organ injury in a murine cecal ligation and puncture model of sepsis. *World J Surg* 2007; **31**: 105–115.

117 Botha AJ, Moore FA, Moore EE, Sauaia A, Banerjee A, Peterson VM. Early neutrophil sequestration after injury: a pathogenic mechanism for multiple organ failure. *J Trauma* 1995; **39**: 411–417.

118 Leaphart CL, Tepas JJ. The gut is a motor of organ system dysfunction. *Surgery* 2007; **141**: 563–569.

119 Gatt M, Reddy BS, MacFie J. Review article: Bacterial translocation in the critically ill - Evidence and methods of prevention. *Aliment Pharmacol Ther* 2007; **25**: 741–757.

120 Dickson RP, Singer BH, Newstead MW, Falkowski NR, Erb-Downward JR, Standiford TJ *et al.* Enrichment of the lung microbiome with gut bacteria in sepsis and the acute respiratory distress syndrome. *Nat Microbiol* 2016; **113**: 1–9.

121 Berg RD, Garlington AW. Translocation of certain indigenous bacteria from the gastrointestinal tract to the mesenteric lymph nodes and other organs in a gnotobiotic mouse model. *Infect Immun* 1979; **23**: 403–411.

122 Klingensmith NJ, Coopersmith CM. The Gut as the Motor of Multiple Organ Dysfunction in Critical Illness. *Crit Care Clin* 2016; **32**: 203–212.

123 Mittal R, Coopersmith CM. Redefining the gut as the motor of critical illness. *Trends Mol Med* 2014; **20**: 214–223.

124 Deitch EA. Bacterial translocation or lymphatic drainage of toxic products from the gut: What is important in human beings? *Surgery* 2002; **131**: 241–244.

125 Dickson RP. The microbiome and critical illness. *Lancet Respir Med* 2016; **4**: 59–72.

126 Niederbichler AD, Hoesel LM, Westfall M V, Gao H, Ipaktchi KR, Sun L *et al.* An essential role for complement C5a in the pathogenesis of septic cardiac dysfunction. *J Exp Med* 2006; **203**: 53–61.

127 Rittirsch D, Flierl MA, Ward PA. Harmful molecular mechanisms in sepsis. *Nat Rev Immunol* 2008; **8**: 776–87.

128 van Gils JM, Zwaginga JJ, Hordijk PL. Molecular and functional interactions among monocytes, platelets, and endothelial cells and their relevance for cardiovascular diseases. *J Leukoc Biol* 2009; **85**: 195–204.

129 Brown KA, Brain SD, Pearson JD, Edgeworth JD, Lewis SM, Treacher DF. Neutrophils in development of multiple organ failure in sepsis. *Lancet* 2006; **368**: 157–169.

130 Takasu O, Gaut JP, Watanabe E, To K, Fagley RE, Sato B *et al.* Mechanisms of cardiac and renal dysfunction in patients dying of sepsis. *Am J Respir Crit Care Med* 2013; **187**: 509–517.

131 Lipcsey M, Bellomo R. Septic acute kidney injury: Hemodynamic syndrome, inflammatory disorder, or both? *Crit Care* 2011; **15**. doi:10.1186/cc10525.

132 Lerolle N, Nochy D, Guérot E, Bruneval P, Fagon JY, Diehl JL *et al.* Histopathology of septic shock induced acute kidney injury: Apoptosis and leukocytic infiltration. *Intensive Care Med* 2010; **36**: 471–478.

133 Hotchkiss RS, Monneret G, Payen D. Immunosuppression in sepsis: A novel understanding of the disorder and a new therapeutic approach. *Lancet Infect Dis* 2013; **13**: 260–268.

134 Granger DL, Taintor RR, Cook JL, Hibbs JB. Injury of neoplastic cells by murine macrophages leads to inhibition of mitochondrial respiration. *J Clin Invest* 1980; **65**: 357–370.

135 Pastorino JG, Simbula G, Yamamoto K, Glascott PA, Rothman RJ, Farber JL. The cytotoxicity of tumor necrosis factor depends on induction of the mitochondrial permeability transition. *J Biol Chem* 1996; **271**: 29792–29798.

136 Halestrap AP, Connern CP, Griffiths EJ, Kerr PM. Cyclosporin A binding to mitochondrial cyclophilin inhibits the permeability transition pore and protects hearts from ischaemia/reperfusion injury. *Mol Cell Biochem* 1997; **174**: 167–172.

137 Fink MP, Evans TW. Mechanisms of organ dysfunction in critical illness: Report from a Round table Conference held in Brussels. *Intensive Care Med* 2002; **28**: 369–375.

138 Andrabi SA, Umanah GKE, Chang C, Stevens DA, Karuppagounder SS, Gagné J-P *et al.* Poly(ADP-ribose) polymerase-dependent energy depletion occurs through inhibition of glycolysis. *Proc Natl Acad Sci U S A* 2014; **111**: 10209–14.

139 Cuzzocrea S, Zingarelli B, Costantino G, Sottile A, Teti D, Caputi AP. Protective effect of poly(ADP-ribose) synthetase inhibition on multiple organ failure after zymosan-induced peritonitis in the rat. *Crit Care Med* 1999; **27**: 1517–1523.

140 Singer M. Critical illness and flat batteries. *Crit Care* 2017; **21**. doi:10.1186/s13054-017-1913-9.

141 Hotchkiss RS, Nicholson DW. Apoptosis and caspases regulate death and inflammation in sepsis. *Nat Rev Immunol* 2006; **6**: 813–822.

142 Hotchkiss RS, Swanson PE, Freeman BD, Tinsley KW, Cobb JP, Matuschak GM *et al.* Apoptotic cell death in patients with sepsis, shock, and multiple organ dysfunction. *Crit Care Med* 1999; **27**: 1230–1251.

143 Cohen J, Opal S, Calandra T. Sepsis studies need new direction. *Lancet Infect Dis* 2012; **12**: 503–505.

144 Dolgin E. Trial failure prompts soul-searching for critical-care specialists. *Nat Med* 2012; **18**: 1000.

145 Williams SCP. After Xigris, researchers look to new targets to combat sepsis. *Nat Med* 2012; **18**: 1001–1001.

146 Meakins JL, Pietsch JB, Bubenick O, Kelly R, Rode H, Gordon J *et al.* Delayed hypersensitivity: indicator of acquired failure of host defenses in sepsis and trauma. *Ann Surg* 1977; **186**: 241–250.

147 Conway Morris A, Anderson N, Brittan M, Wilkinson TS, Mcauley DF, Antonelli J *et al.* Combined dysfunctions of immune cells predict nosocomial infection in critically ill patients. *Br J Anaesth* 2013; **111**: 778–787.

148 Bone RC. Sir Isaac Newton, sepsis, SIRS, and CARS. *Crit Care Med* 1996; **24**: 1125–1128.

149 Demaret J, Venet F, Friggeri a., Cazalis M -a., Plassais J, Jallades L *et al.* Marked alterations of neutrophil functions during sepsis-induced immunosuppression. *J Leukoc Biol* 2015; **98**: 1–10.

150 Landelle C, Lepape A, Voirin N, Tognet E, Venet F, Bohe J *et al.* Low monocyte human leukocyte antigen-DR is independently associated with nosocomial infections after septic shock. *Intensive Care Med* 2010; **36**: 1859–1866.

151 Vincent JL. Nosocomial infections in adult intensive-care units. *Lancet* 2003; **361**: 2068–2077.

152 Majumdar SS, Padiglione AA. Nosocomial infections in the intensive care unit. *Anaesth Intensive Care Med* 2012; **13**: 204–208.

153 Shankar-Hari M, Phillips GS, Levy ML, Seymour CW, Liu VX, Deutschman CS *et al.* Developing a New Definition and Assessing New Clinical Criteria for Septic Shock. *JAMA* 2016; **315**: 775.

154 Vincent J-L, Sakr Y, Sprung CL, Ranieri VM, Reinhart K, Gerlach H *et al.* Sepsis in European intensive care units: results of the SOAP study. *Crit Care Med* 2006; **34**: 344–353.

155 Hotchkiss RS, Tinsley KW, Swanson PE, Schmieg RE, Hui JJ, Chang KC *et al.* Sepsis-induced apoptosis causes progressive profound depletion of B and CD4+ T lymphocytes in humans. *J Immunol* 2001; **166**: 6952–63.

156 Hotchkiss RS, Tinsley KW, Swanson PE, Grayson MH, Osborne DF, Wagner TH *et al.* Depletion of dendritic cells, but not macrophages, in patients with sepsis. *J Immunol* 2002; **168**: 2493–2500.

157 Hotchkiss RS, Schmieg RE, Swanson PE, Freeman BD, Tinsley KW, Cobb JP *et al.* Rapid onset of intestinal epithelial and lymphocyte apoptotic cell death in patients with trauma and shock. *Crit Care Med* 2000; **28**: 3207–17.

158 Hotchkiss RS, Monneret G, Payen D. Sepsis-induced immunosuppression: from cellular dysfunctions to immunotherapy. *Nat Rev Immunol* 2013; **13**: 862–74.

159 Gabrilovich DI, Nagaraj S. Myeloid-derived suppressor cells as regulators of the immune system. *Nat Rev Immunol* 2009; **9**: 162–74.

160 Venet F, Chung CS, Kherouf H, Geeraert A, Malcus C, Poitevin F *et al.* Increased circulating regulatory T cells (CD4+CD25 +CD127-) contribute to lymphocyte anergy in septic shock patients. *Intensive Care Med* 2009; **35**: 678–686.

161 Venet F, Chung C-S, Monneret G, Huang X, Horner B, Garber M *et al.* Regulatory T cell populations in sepsis and trauma. *J Leukoc Biol* 2008; **83**: 523–535.

162 Cuenca A, Delano M. A Paradoxical Role for Myeloid-Derived Suppressor Cells in Sepsis and Trauma. *Mol Med* 2011; **17**: 1.

163 Navarini AA, Lang KS, Verschoor A, Recher M, Zinkernagel AS, Nizet V *et al.* Innate immune-induced depletion of bone marrow neutrophils aggravates systemic bacterial

infections. *Proc Natl Acad Sci* 2009; **106**: 7107–7112.

164 Cavaillon JM, Adib-Conquy M. Bench-to-bedside review: Endotoxin tolerance as a model of leukocyte reprogramming in sepsis. *Crit Care* 2006; **10**: 1–8.

165 Boomer J, To K, Chang K, et al. Immunosuppression in patients who die of sepsis and multiple organ failure. *Jama* 2011; **306**: 2594–605.

166 Mathison JC, Virca GD, Wolfson E, Tobias PS, Glaser K, Ulevitch RJ. Adaptation to Bacterial Lipopolysaccharide Controls Lipopolysaccharide- induced Tumor Necrosis Factor Production in Rabbit Macrophages. *J Clin Invest* 1990; **85**: 1108–1118.

167 Venet F, Monneret G. Advances in the understanding and treatment of sepsis-induced immunosuppression. *Nat Rev Nephrol* 2018; **14**: 121–137.

168 Meisel C, Schefold JC, Pschowski R, Baumann T, Hetzger K, Gregor J *et al.* Granulocyte-macrophage colony-stimulating factor to reverse sepsis-associated immunosuppression: A double-blind, randomized, placebo-controlled multicenter trial. *Am J Respir Crit Care Med* 2009; **180**: 640–648.

169 Monneret G, Lepape A, Voirin N, Boh?? J, Venet F, Debard AL *et al.* Persisting low monocyte human leukocyte antigen-DR expression predicts mortality in septic shock. *Intensive Care Med* 2006; **32**: 1175–1183.

170 Asadullah K, Woiciechowsky C, Docke WD, Liebenthal C, Wauer H, Kox W *et al.* Immunodepression following neurosurgical procedures. *Crit Care Med* 1995; **23**: 1976–1983.

171 de Kleijn S, Langereis JD, Leentjens J, Kox M, Netea MG, Koenderman L *et al.* IFN-γ-Stimulated Neutrophils Suppress Lymphocyte Proliferation through Expression of PD-L1. *PLoS One* 2013; **8**. doi:10.1371/journal.pone.0072249.

172 Brahmamdam P, Inoue S, Unsinger J, Chang KC, McDunn JE, Hotchkiss RS. Delayed administration of anti-PD-1 antibody reverses immune dysfunction and improves survival during sepsis. *J Leukoc Biol* 2010; **88**: 233–240.

173 Patera AC, Drewry AM, Chang K, Beiter ER, Osborne D, Hotchkiss RS. Frontline Science: Defects in immune function in patients with sepsis are associated with PD-1 or PD-L1 expression and can be restored by antibodies targeting PD-1 or PD-L1. *J Leukoc Biol* 2016; **100**: 1239–1254.

174 Guérin E, Orabona M, Raquil M-A, Giraudeau B, Bellier R, Gibot S *et al.* Circulating Immature Granulocytes With T-Cell Killing Functions Predict Sepsis Deterioration*. *Crit Care Med* 2014; **42**: 2007–2018.

175 Butler KL, Ambravaneswaran V, Agrawal N, Bilodeau M, Toner M, Tompkins RG *et al.* Burn injury reduces neutrophil directional migration speed in microfluidic devices. *PLoS One* 2010; **5**. doi:10.1371/journal.pone.0011921.

176 Danikas DD, Karakantza M, Theodorou GL, Sakellaropoulos GC, Gogos CA. Prognostic value of phagocytic activity of neutrophils and monocytes in sepsis. Correlation to CD64 and CD14 antigen expression. *Clin Exp Immunol* 2008; **154**: 87–97.

177 Conway Morris A, Kefala K, Wilkinson TS, Dhaliwal K, Farrell L, Walsh T *et al.* C5a mediates peripheral blood neutrophil dysfunction in critically ill patients. *Am J Respir Crit Care Med* 2009; **180**: 19–28.

178 Taneja R, Sharma AP, Hallett MB, Findlay GP, Morris MR. Immature Circulating Neutrophils in Sepsis Have Impaired Phagocytosis and Calcium Signaling. *Shock* 2008; **30**: 618–622.

179 Huber-Lang MS, Younkin EM, Sarma J V., McGuire SR, Lu KT, Guo RF *et al.*

Complement-Induced Impairment of Innate Immunity During Sepsis. *J Immunol* 2002; **169**: 3223–3231.

180 Gregoire M, Tadie J-M, Uhel F, Gacouin A, Piau C, Bone N *et al.* HMGB1 induces neutrophil dysfunction in experimental sepsis and in patients who survive septic shock. *J Leukoc Biol* 2016; **101**: 1281–1287.

181 Hampson P, Dinsdale RJ, Wearn CM, Bamford AL, Bishop JRB, Hazeldine J *et al.* Neutrophil dysfunction, immature granulocytes, and cell-free DNA are early biomarkers of sepsis in burn-injured patients: A prospective observational cohort study. *Ann Surg* 2017; **265**: 1241–1249.

182 Martins PS, Brunialti MKC, Martos LSW, Machado FR, Assunçao MS, Blecher S *et al.* Expression of cell surface receptors and oxidative metabolism modulation in the clinical continuum of sepsis. *Crit Care* 2008; **12**. doi:10.1186/cc6801.

183 Santos SS, Brunialti MKC, Rigato O, MacHado FR, Silva E, Salomao R. Generation of nitric oxide and reactive oxygen species by neutrophils and monocytes from septic patients and association with outcomes. *Shock* 2012; **38**: 18–23.

184 Simms HH, D'Amico R. Increased PMN CD11b/CD18 expression following post-traumatic ARDS. *J Surg Res* 1991; **50**: 362–367.

185 Van Der Poll T, Van De Veerdonk FL, Scicluna BP, Netea MG. The immunopathology of sepsis and potential therapeutic targets. *Nat Rev Immunol* 2017; **17**: 407–420.

186 Rol ML, Venet F, Rimmele T, Moucadel V, Cortez P, Quemeneur L *et al.* The REAnimation Low Immune Status Markers (REALISM) project: A protocol for broad characterisation and follow-up of injury-induced immunosuppression in intensive care unit (ICU) critically ill patients. *BMJ Open* 2017; **7**: 1–9.

187 Janeway CAJ, Travers P, Walport M, Shlomchik MJ. The complement system and innate immunity. In: *The Immune System in Health and Disease*. New York, USA, 2001.

188 Dunkelberger JR, Song W. Complement and its role in innate and adaptive immune responses. *Cell Res* 2010; **20**: 34–50.

189 Carroll MC. The complement system in regulation of adaptive immunity. *Nat Immunol* 2004; **5**: 981–986.

190 Huber-Lang M, Sarma JV, Zetoune FS, Rittirsch D, Neff TA, McGuire SR *et al.* Generation of C5a in the absence of C3: a new complement activation pathway. *Nat Med* 2006; **12**: 682–687.

191 Huber-Lang M, Younkin EM, Sarma JV, Riedemann N, McGuire SR, Lu KT *et al.* Generation of C5a by phagocytic cells. *Am J Pathol* 2002; **161**: 1849–59.

192 Hugli TE, Fernandez HN. Primary structural analysis of the polypeptide portion of human C5a anaphylatoxin. *J Biol Chem* 1978; **253**: 6955–6964.

193 Huber-Lang MS, Sarma JV, McGuire SR, Lu KT, Padgaonkar VA, Younkin EM *et al.* Structure-function relationships of human C5a and C5aR. *J Immunol* 2003; **170**: 6115–6124.

194 Zuiderweg ER, Nettesheim DG, Mollison KW, Carter GW. Tertiary structure of human complement component C5a in solution from nuclear magnetic resonance data. *Biochemistry* 1989; **28**: 172–185.

195 Cochrane CG, Muller-Eberhard HJ. The derivation of two distinct anaphylatoxin activities from the third and fifth components of human complement. *J Exp Med* 1968; **127**: 371–386.

196 Chenoweth DE, Hugli TE. Initial characterization of the human polymorphonuclear leukocyte (PMN) C5a receptor [abstract]. *J Immunol* 1978; **120**: 1768.

197 Camous L, Roumenina L, Bigot S, Brachemi S, Fremeaux-Bacchi V, Lesavre P *et al.* Complement alternative pathway acts as a positive feedback amplification of neutrophil activation. *Blood* 2011; **117**: 1340–1349.

198 del Conde I, Crúz MA, Zhang H, López JA, Afshar-Kharghan V. Platelet activation leads to activation and propagation of the complement system. *J Exp Med* 2005; **201**: 871–879.

199 Amara U, Rittirsch D, Flierl M, Bruckner U, Klos A, Gebhard F *et al.* Interaction between the coagulation and complement system. *Adv Exp Med Biol* 2008; **632**: 71–79.

200 Ricklin D, Reis ES, Lambris JD. Complement in disease: a defence system turning offensive. *Nat Rev Nephrol* 2016; **12**: 383–401.

201 Lachmann PJ. Looking back on the alternative complement pathway. *Immunobiology* 2018; **223**: 519–523.

202 Chenoweth DE, Hugli TE. Demonstration of specific C5a receptor on intact human polymorphonuclear leukocytes. *Proc Natl Acad Sci* 1978; **75**: 3943–3947.

203 Webster RO, Larsen GL, Henson PM. In vivo clearance and tissue distribution of C5a and C5a des arginine complement fragments in rabbits. *J Clin Invest* 1982; **70**: 1177–1183.

204 Bokisch VA, Müller-Eberhard HJ. Anaphylatoxin inactivator of human plasma: its isolation and characterization as a carboxypeptidase. *J Clin Invest* 1970; **49**: 2427–2436.

205 Campbell WD, Lazoura E, Okada N, Okada H. Inactivation of C3a and C5a octapeptides by carboxypeptidase R and carboxypeptidase N. *Microbiol Immunol* 2002; **46**: 131–134.

206 Chenoweth DE, Hugli TE. Human C5a and C5a analogs as probes of the neutrophil C5a receptor. *Mol Immunol* 1980; **17**: 151–161.

207 Webster RO, Hong SR, Johnston RB, Henson PM. Biological Effects of the Human Complement Fragments C5a and C5a-des-arg on Neutrophil Fuction. *Immunopharmacology* 1980; **2**: 201–219.

208 Solomkin JS, Jenkins MK, Nelson RD, Chenoweth D, Simmons RL. Neutrophil dysfunction in sepsis II: evidence for the role of complement activation products in cellular deactivation. *Surgery* 1981; **90**: 319–327.

209 Oppermann M, Götze O. Plasma clearance of the human C5a anaphylatoxin by binding to leucocyte C5a receptors. *Immunology* 1994; **82**: 516–521.

210 Ward PA. The harmful Role of C5a on innate immunity in sepsis. *J Innate Immun* 2010; **2**: 439–445.

211 Doroshenko T, Chaly Y, Savitskiy V, Maslakova O, Portyanko A, Gorudko I *et al.* Phagocytosing neutrophils down-regulate the expression of chemokine receptors CXCR1 and CXCR2. *Blood* 2002; **100**: 2668–2671.

212 van den Berg CW, Tambourgi D V, Clark HW, Hoong SJ, Spiller OB, McGreal EP. Mechanism of neutrophil dysfunction: neutrophil serine proteases cleave and inactivate the C5a receptor. *J Immunol* 2014; **192**: 1787–95.

213 Morris AC, Brittan M, Wilkinson TS, McAuley DF, Antonelli J, McCulloch C *et al.* C5a-mediated neutrophil dysfunction is RhoA-dependent and predicts infection in critically

ill patients. *Blood* 2011; **117**: 5178–5188.

214 Unnewehr H, Rittirsch D, Sarma JV, Flierl MA, Perl M, Denk S *et al.* Changes and Regulation of the C5a Receptor on Neutrophils during Septic Shock in Humans. *J Immunol* 2013; **190**: 1–11.

215 Cain SA, Monk PN. The orphan receptor C5L2 has high affinity binding sites for complement fragments C5a and C5a des-Arg74. *J Biol Chem* 2002; **277**: 7165–7169.

216 Gerard NP, Gerard C. The chemotactic receptor for human C5a anaphylatoxin. *Nature* 1991; **349**: 614–7.

217 Chenoweth DE, Erickson BW, Hugli TE. Human C5a-related synthetic peptides as neutrophil chemotactic factors. *Biochem Biophys Res Commun* 1979; **86**: 227–234.

218 Nikiforovich G V., Marshall GR, Baranski TJ. Modeling molecular mechanisms of binding of the anaphylatoxin C5a to the C5a receptor. *Biochemistry* 2008; **47**: 3117–3130.

219 Siciliano SJ, Rollins TE, DeMartino J, Konteatis Z, Malkowitz L, Van Riper G *et al.* Two-site binding of C5a by its receptor: an alternative binding paradigm for G protein-coupled receptors. *Proc Natl Acad Sci* 1994; **91**: 1214–1218.

220 Hagemann IS, Narzinski KD, Floyd DH, Baranski TJ. Random mutagenesis of the complement factor 5a (C5a) receptor N terminus provides a structural constraint for C5a docking. *J Biol Chem* 2006; **281**: 36783–36792.

221 Hagemann IS, Miller DL, Klco JM, Nikiforovich G V., Baranski TJ. Structure of the complement factor 5a receptor-ligand complex studied by disulfide trapping and molecular modeling. *J Biol Chem* 2008; **283**: 7763–7775.

222 Sahoo AR, Mishra R, Rana S. The model structures of the complement component 5a receptor (C5aR) bound to the native and engineered hC5a. *Sci Rep* 2018; **8**: 1–13.

223 Hoeprich PD, Hugli TE. Helical Conformation at the Carboxy-Terminal Portion of Human C3a Is Required for Full Activity. *Biochemistry* 1986; **25**: 1945–1950.

224 Ohno M, Hirata T, Enomoto M, Araki T, Ishimaru H, Takahashi TA. A putative chemoattractant receptor, C5L2, is expressed in granulocyte and immature dendritic cells, but not in mature dendritic cells. *Mol Immunol* 2000; **37**: 407–412.

225 Rittirsch D, Flierl MA, Nadeau B a, Day DE, Huber-Lang M, Mackay CR *et al.* Functional roles for C5a receptors in sepsis. *Nat Med* 2008; **14**: 551–557.

226 Huber-Lang M, Sarma J V., Rittirsch D, Schreiber H, Weiss M, Flierl M *et al.* Changes in the Novel Orphan, C5a Receptor (C5L2), during Experimental Sepsis and Sepsis in Humans. *J Immunol* 2005; **174**: 1104–1110.

227 Lee H, Whitfeld PL, Mackay CR. Receptors for complement C5a. The importance of C5aR and the enigmatic role of C5L2. *Immunol Cell Biol* 2008; **86**: 153–160.

228 Altschul SF, Madden TL, Schäffer AA, Zhang J, Zhang Z, Miller W *et al.* Gapped BLAST and PSI-BLAST: a new generation of protein database search programs. *Nucleic Acids Res* 1997; **25**: 3389–3402.

229 Okinaga S, Slattery D, Humbles A, Zsengeller Z, Morteau O, Kinrade MB *et al.* C5L2, a nonsignaling C5A binding protein. *Biochemistry* 2003; **42**: 9406–9415.

230 Johswich K, Martin M, Thalmann J, Rheinheimer C, Monk PN, Klos A. Ligand specificity of the anaphylatoxin C5L2 receptor and its regulation on myeloid and epithelial cell lines. *J Biol Chem* 2006; **281**: 39088–39095.

231 Bamberg CE, Mackay CR, Lee H, Zahra D, Jackson J, Lim YS *et al.* The C5a receptor

(C5aR) C5L2 is a modulator of C5aR-mediated signal transduction. *J Biol Chem* 2010; **285**: 7633–7644.

232 Lohse MJ, Benovic JL, Codina J, Caron MG, Lefkowitz RJ. Beta-Arrestin: a protein that regulates beta-adrenergic receptor function. *Science (80-)* 1990; **248**: 1547–1550.

233 Van Lith LH, Oosterom J, Van Elsas A, Zaman GJ. C5a-Stimulated Recruitment of ß-Arrestin2 to the Nonsignaling 7-Transmembrane Decoy Receptor C5L2. *J Biomol Screen* 2009; **14**: 1067–1075.

234 Cui W, Simaan M, Laporte S, Lodge R, Cianflone K. C5a- and ASP-mediated C5L2 activation, endocytosis and recycling are lost in S323I-C5L2 mutation. *Mol Immunol* 2009; **46**: 3086–3098.

235 Croker DE, Halai R, Kaeslin G, Wende E, Fehlhaber B, Klos A *et al.* C5a2 can modulate ERK1/2 signaling in macrophages via heteromer formation with C5a1 and β-arrestin recruitment. *Immunol Cell Biol* 2014; **92**: 631–639.

236 Gerard NP, Lu B, Liu P, Craig S, Fujiwara Y, Okinaga S *et al.* An anti-inflammatory function for the complement anaphylatoxin C5a-binding protein, C5L2. *J Biol Chem* 2005; **280**: 39677–39680.

237 del Balzo U, Sakuma I, Levi R. Cardiac Dysfunction Caused by Recombinant Human C5A Anaphylatoxin : Mediation by Histamine , Adenosine and Cyclooxygenase Arachidonate. *J Pharmacol Exp Ther* 1990; **253**: 171–179.

238 Fattahi F, Kalbitz M, Malan EA, Abe E, Jajou L, Huber-Lang MS *et al.* Complement-induced activation of MAPKs and Akt during sepsis: role in cardiac dysfunction. *FASEB J* 2017; **31**: 4129–4139.

239 Kalbitz M, Fattahi F, Grailer JJ, Jajou L, Malan EA, Zetoune FS *et al.* Complement-induced activation of the cardiac NLRP3 inflammasome in sepsis. *FASEB J* 2016; **30**: 3997–4006.

240 Fattahi F, Ward PA. Complement and sepsis-induced heart dysfunction. *Mol Immunol* 2017; **84**: 57–64.

241 Ikeda K, Nagasawa K, Horiuchi T, Tsuru T, Nishizaka H, Niho Y. C5a induces tissue factor activity on endothelial cells. *Thromb Haemostasis*; **77**: 394–398.

242 Foley JH. Examining coagulation-complement crosstalk: complement activation and thrombosis. *Thromb Res* 2016; **141**: S50–S54.

243 Foley JH, Walton BL, Aleman MM, O'Byrne AM, Lei V, Harrasser M *et al.* Complement Activation in Arterial and Venous Thrombosis is Mediated by Plasmin. *EBioMedicine* 2016; **5**: 175–182.

244 Landsem A, Fure H, Christiansen D, Nielsen EW, Østerud B, Mollnes TE *et al.* The key roles of complement and tissue factor in Escherichia coli-induced coagulation in human whole blood. *Clin Exp Immunol* 2015; **182**: 81–89.

245 Øvstebø R, Hellum M, Aass HCD, Trøseid AM, Brandtzaeg P, Mollnes TE *et al.* Microparticle-associated tissue factor activity is reduced by inhibition of the complement protein 5 in Neisseria meningitidis-exposed whole blood. *Innate Immun* 2014; **20**: 552–560.

246 Rinder CS, Rinder HM, Smith BR, Fitch JCK, Smith MJ, Tracey JB *et al.* Blockade of C5a and C5b-9 generation inhibits leukocyte and platelet activation during extracorporeal circulation. *J Clin Invest* 1995; **96**: 1564–1572.

247 Subramaniam S, Jurk K, Hobohm L, Jäckel S, Saffarzadeh M, Schwierczek K *et al.* Distinct contributions of complement factors to platelet activation and fibrin formation

in venous thrombus development. *Blood* 2017; **129**: blood-2016-11-749879.

248 Skjeflo EW, Christiansen D, Fure H, Ludviksen JK, Woodruff TM, Espevik T *et al.* Staphylococcus aureus-induced complement activation promotes tissue factor-mediated coagulation. *J Thromb Haemost* 2018; **16**: 905–918.

249 Yuan Y, Alwis I, Wu MCL, Kaplan Z, Ashworth K, Bark D *et al.* Neutrophil macroaggregates promote widespread pulmonary thrombosis after gut ischemia. *Sci Transl Med* 2017; **9**: 1–14.

250 Zerbino DR, Achuthan P, Akanni W, Amode MR, Barrell D, Bhai J *et al.* Ensembl 2018. *Nucleic Acids Res* 2017; **46**: 754–761.

251 Ward PA, Newman LJ. A Neutrophil Chemotactic Factor from Human C ′ 5. *J Immunol* 1969; **102**: 93–99.

252 Ehrengruber M, Geiser T, Deranleau D. Activation of human neutrophils by C3a and C5A Comparison of the effects on shape changes, chemotaxis, secretion, and respiratory burst. *FEBS Lett* 1994; **346**: 181–184.

253 Buhl AM, Avdi N, Worthen GS, Johnson GL. Mapping of the C5a receptor signal transduction network in human neutrophils. *Proc Natl Acad Sci* 1994; **91**: 9190–4.

254 Vanhaesebroeck B, Guillermet-Guibert J, Graupera M, Bilanges B. The emerging mechanisms of isoform-specific PI3K signalling. *Nat Rev Mol Cell Biol* 2010; **11**: 329–341.

255 Funamoto S, Meili R, Lee S, Parry L, Firtel RA. Spatial and Temporal Regulation of 3-Phosphoinositides by PI 3-Kinase and PTEN Mediates Chemotaxis. *Cell* 2002; **109**: 611–623.

256 Heit B, Robbins SM, Downey CM, Guan Z, Colarusso P, Miller JB *et al.* PTEN functions to 'prioritize' chemotactic cues and prevent 'distraction' in migrating neutrophils. *Nat Immunol* 2008; **9**: 743–752.

257 Foxman EF, Campbell JJ, Butcher EC. Multistep navigation and the combinatorial control of leukocyte chemotaxis. *J Cell Biol* 1997; **139**: 1349–1360.

258 Stephens L, Milne L, Hawkins P. Moving towards a Better Understanding of Chemotaxis. *Curr Biol* 2008; **18**: 485–494.

259 Suire S, Condliffe AM, Ferguson GJ, Ellson CD, Guillou H, Davidson K *et al.* Gbetagammas and the Ras binding domain of p110gamma are both important regulators of PI(3)Kgamma signalling in neutrophils. *Nat Cell Biol* 2006; **8**: 1303–9.

260 Mazaki Y, Hashimoto S, Tsujimura T, Morishige M, Hashimoto A, Aritake K *et al.* Neutrophil direction sensing and superoxide production linked by the GTPase-activating protein GIT2. *Nat Immunol* 2006; **7**: 724–31.

261 Denk S, Neher MD, Messerer DAC, Wiegner R, Nilsson B, Rittirsch D *et al.* Complement C5a Functions as a Master Switch for the pH Balance in Neutrophils Exerting Fundamental Immunometabolic Effects. *J Immunol* 2017. doi:10.4049/jimmunol.1700393.

262 Denk S, Taylor RP, Wiegner R, Cook EM, Lindorfer MA, Pfeiffer K *et al.* Complement C5a-Induced Changes in Neutrophil Morphology During Inflammation. *Scand J Immunol* 2017; **86**: 143–155.

263 Perianayagam MC, Balakrishnan VS, King AJ, Pereira BJG, Jaber BL. C5a delays apoptosis of human neutrophils by a phosphatidylinositol 3-kinase-signaling pathway. *Kidney Int* 2002; **61**: 456–463.

264 Perianayagam MC, Balakrishnan VS, Pereira BJG, Jaber BL. C5a delays apoptosis of

human neutrophils via an extracellular signal-regulated kinase and Bad-mediated signalling pathway. *Eur J Clin Invest* 2004; **34**: 50–56.

265 Dobos GJ, Andre M, Bohler J, Norgauer J, Lubrich-Birkner I, Steinhauer HB *et al.* Inhibition of C5a-induced actin polymerization, chemotaxis, and phagocytosis of human polymorphonuclear neutrophils incubated in a glucose-based dialysis solution. *Adv Perit Dial* 1993; **9**: 307–311.

266 Mollnes TE, Brekke O, Fung M, Fure H, Christiansen D, Bergseth G *et al.* Essential role of the C5a receptor in E coli − induced oxidative burst and phagocytosis revealed by a novel lepirudin-based human whole blood model of inflammation. *Blood* 2002; **100**: 1869–1877.

267 Brekke O-L, Christiansen D, Fure H, Fung M, Mollnes TE. The role of complement C3 opsonization, C5a receptor, and CD14 in E. coli-induced up-regulation of granulocyte and monocyte CD11b/CD18 (CR3), phagocytosis, and oxidative burst in human whole blood. *J Leukoc Biol* 2007; **81**: 1404–1413.

268 Demaster E, Schnitzler N, Cheng Q, Cleary P. M+ group A streptococci are phagocytized and killed in whole blood by C5a-activated polymorphonuclear leukocytes. *Infect Immun* 2002; **70**: 350–359.

269 Czermak BJ, Sarma V, Pierson CL, Warner RL, Huber-Lang M, Bless NM *et al.* Protective effects of C5a blockade in sepsis. *Nat Med* 1999; **5**: 788–92.

270 Huber-Lang MS, Riedeman NC, Sarma JV, Younkin EM, McGuire SR, Laudes IJ *et al.* Protection of innate immunity by C5aR antagonist in septic mice. *FASEB J* 2002; **16**: 1567–1574.

271 Huber-Lang M, Sarma VJ, Lu KT, McGuire SR, Padgaonkar V a, Guo RF *et al.* Role of C5a in multiorgan failure during sepsis. *J Immunol* 2001; **166**: 1193–1199.

272 Papakonstanti E a, Ridley AJ, Vanhaesebroeck B. The p110delta isoform of PI3-kinase negatively controls RhoA and PTEN. *EMBO J* 2007; **26**: 3050–3061.

273 Scott J, Harris GJ, Pinder EM, Macfarlane JG, Hellyer TP, Rostron AJ *et al.* Exchange protein directly activated by cyclic AMP (EPAC) activation reverses neutrophil dysfunction induced by β2-agonists, corticosteroids, and critical illness. *J Allergy Clin Immunol* 2015; : 1–10.

274 Riedemann NC, Guo RF, Bernacki KD, Reuben JS, Laudes IJ, Neff TA *et al.* Regulation by C5a of neutrophil activation during sepsis. *Immunity* 2003; **19**: 193–202.

275 Seow V, Lim J, Iyer A, Suen JY, Ariffin JK, Hohenhaus DM *et al.* Inflammatory Responses Induced by Lipopolysaccharide Are Amplified in Primary Human Monocytes but Suppressed in Macrophages by Complement Protein C5a. *J Immunol* 2013; **191**: 4308–4316.

276 Gerard C. Complement C5a in the Sepsis Syndrome — Too Much of a Good Thing? *N Engl J Med* 2003; **348**: 167–169.

277 Suire S, Lécureuil C, Anderson KE, Damoulakis G, Niewczas I, Davidson K *et al.* GPCR activation of Ras and PI3Kγ in neutrophils depends on PLCβ2/β3 and the RasGEF RasGRP4. *EMBO J* 2012; **31**: 3118–3129.

278 Goldstein IM, Roos D, Kaplan HB, Weissmann G. Complement and immunoglobulins stimulate superoxide production by human leukocytes independently of phagocytosis. *J Clin Invest* 1975; **56**: 1155–1163.

279 Riedemann N, Guo R, Ward P. Novel strategies for the treatment of sepsis. *Nat Med* 2003; **9**: 517–524.

280 Hillmen P, Young NS, Schubert J, Brodsky RA, Socié G, Muus P *et al.* The

Complement Inhibitor Eculizumab in Paroxysmal Nocturnal Hemoglobinuria. *N Engl J Med* 2006; **355**: 1233–1243.

281 Benamu E, Montoya JG. Infections associated with the use of eculizumab: recommendations for prevention and prophylaxis. *Curr Opin Infect Dis* 2016; **29**.

282 Hoehlig K, Maasch C, Shushakova N, Buchner K, Huber-Lang M, Purschke WG *et al.* A novel C5a-neutralizing mirror-image (l-)aptamer prevents organ failure and improves survival in experimental sepsis. *Mol Ther* 2013; **21**: 2236–2246.

283 Jain U, Woodruff TM, Stadnyk A. The C5a receptor antagonist PMX205 ameliorates experimentally induced colitis associated with increased IL-4 and IL-10. *Br J Pharmacol* 2013; **168**: 488–501.

284 Colley CS, Popovic B, Sridharan S, Debreczeni JE, Hargeaves D, Fung M *et al.* Structure and characterization of a high affinity C5a monoclonal antibody that blocks binding to C5aR1 and C5aR2 receptors. *MAbs* 2017; **0862**: 1–14.

285 Jayne DRW, Bruchfeld AN, Harper L, Schaier M, Venning MC, Hamilton P *et al.* Randomized Trial of C5a Receptor Inhibitor Avacopan in ANCA-Associated Vasculitis. *J Am Soc Nephrol* 2017; **28**: 2756–2767.

286 Clinical Trials.gov. NCT02246595 Studying Complement Inhibition in Early, Newly Developing Septic Organ Dysfunction (SCIENS). 2016.

287 Boyum A. Isolation of mononuclear cells and granulocytes from human blood. Isolation of monuclear cells by one centrifugation, and of granulocytes by combining centrifugation and sedimentation at 1 g. *Scand J Clin Lab Invest Suppl* 1968; **97**: 77–89.

288 Life Technologies. pHrodo Bioparticles datasheet. 2015; : 1–7.

289 Clark J, Anderson KE, Juvin V, Smith TS, Karpe F, Wakelam MJO *et al.* Quantification of PtdInsP3 molecular species in cells and tissues by mass spectrometry. *Nat Methods* 2011; **8**: 267–272.

290 Life Technologies. No-Wash, No-Lyse Detection of Leukocytes In Human Whole Blood on the Attune NxT Flow Cytometer. https://www.thermofisher.com/uk/en/home/life-science/cell-analysis/flow-cytometry/flow-cytometry-learning-center/flow-cytometry-resource-library/flow-cytometry-application-notes/no-wash-no-lyse-detection-leukocytes-human-whole-blood-attune-nxt-flow-cytome (accessed 15 Oct2018).

291 Bylund J, Björnsdottir H, Sundqvist M, Karlsson A, Dahlgren C. Measurement of Respiratory Burst Products, Released or Retained, During Activation of Professional Phagocytes. In: Quinn M, DeLeo F (eds). *Neutrophil methods and protocols*. Hamana Press: New York, USA, 2014, pp 321–338.

292 Chiswick EL, Mella JR, Bernardo J, Remick DG. Acute-Phase Deaths from Murine Polymicrobial Sepsis Are Characterized by Innate Immune Suppression Rather Than Exhaustion. *J Immunol* 2015; **195**: 3793–3802.

293 Laemmli U. Cleavage of structural proteins during the assembly of the head of bacteriophage T4. *Nature* 1970; **227**: 680–685.

294 (2018) RCT. R: A language and environment for statistical computing. 2018.

295 Papachristou EK, Kishore K, Holding AN, Harvey K, Roumeliotis TI, Chilamakuri CSR *et al.* A quantitative mass spectrometry-based approach to monitor the dynamics of endogenous chromatin-associated protein complexes. *Nat Commun* 2018; **9**: 2311.

296 Wickham M. ggplot2: Elegant Graphics for Data Analysis. 2016.

297 Whitman M, Downes P, Keeler M, Keller T, Cantley L. Type I phosphatidylinositol kinase makes a novel inositol phospholipid phosphatidylinositol-3-phosphate. *Nature* 1988; **332**: 644–646.

298 Levin R, Hammond GR V., Balla T, De Camilli P, Fairn GD, Grinstein S. Multiphasic dynamics of phosphatidylinositol 4-phosphate during phagocytosis. *Mol Biol Cell* 2017; **28**: 128–140.

299 Liles WC, Ledbetter JA, Waltersdorph AW, Klebanoff SJ. Cross-linking of CD18 primes human neutrophils for activation of the respiratory burst in response to specific stimuli: Implications for adhesion-dependent physiological responses in neutrophils. *J Leukoc Biol* 1995; **58**: 690–697.

300 Schlam D, Bagshaw RD, Freeman SA, Collins RF, Pawson T, Fairn GD *et al.* Phosphoinositide 3-kinase enables phagocytosis of large particles by terminating actin assembly through Rac/Cdc42 GTPase-activating proteins. *Nat Commun* 2015; **6**: 8623.

301 Life Technologies. pHrodo indicators for pH determination. Life Technol. Website. https://www.thermofisher.com/uk/en/home/brands/molecular-probes/key-molecular-probes-products/phrodo-indicators.html (accessed 10 Oct2018).

302 Allen L-AH. Immunofluorescence and confocal microscopy of neutrophils. In: Malech HL, DeLeo FR, Quinn MT (eds). *Neurophil Methods and Protocols*. Hamana Press: New York, USA, 2014.

303 Condliffe AM, Hawkins PT, Stephens LR, Haslett C, Chilvers ER. Priming of human neutrophil superoxide generation by tumour necrosis factor-α is signalled by enhanced phosphatidylinositol 3,4,5-trisphosphate but not inositol 1,4,5-trisphosphate accumulation. *FEBS Lett* 1998; **439**: 147–151.

304 Sapey E, Greenwood H, Walton G, Mann E, Love A, Aaronson N *et al.* Phosphoinositide 3-kinase inhibition restores neutrophil accuracy in the elderly: Toward targeted treatments for immunosenescence. *Blood* 2014; **123**: 239–248.

305 Kaneda MM, Messer KS, Ralainirina N, Li H, Leem CJ, Gorjestani S *et al.* PI3Kγ is a molecular switch that controls immune suppression. *Nature* 2016; **542**: 124–124.

306 Evans CA, Liu T, Lescarbeau A, Nair SJ, Grenier L, Pradeilles JA *et al.* Discovery of a Selective Phosphoinositide-3-Kinase (PI3K)-gamma Inhibitor (IPI-549) as an Immuno-Oncology Clinical Candidate. *ACS Med Chem Lett* 2016; **7**: 862–867.

307 Hilger D, Masureel M, Kobilka BK. Structure and dynamics of GPCR signaling complexes. *Nat Struct Mol Biol* 2018; **25**: 4–12.

308 Thomsen ARB, Plouffe B, Cahill TJ, Shukla AK, Tarrasch JT, Dosey AM *et al.* GPCR-G Protein-beta-Arrestin Super-Complex Mediates Sustained G Protein Signaling. *Cell* 2016; **166**: 907–919.

309 Conway Morris A, Datta D, Shankar-Hari M, Weir CJ, Rennie J, Antonelli J *et al.* Predictive value of cell-surface markers in infections in critically ill patients: Protocol for an observational study (ImmuNe FailurE in Critical Therapy (INFECT) Study). *BMJ Open* 2016; **6**. doi:10.1136/bmjopen-2016-011326.

310 Sprung C, Morales R, Kasdan H, Reiter A, Keren S, Meissonnier J. Comparison of Cd64 Levels Performed By the Facs and Accellix Systems. *Intensive Care Med Exp* 2015; **3**: A1012.

311 Zouiouich M, Gossez M, Venet F, Rimmelé T, Monneret G. Automated bedside flow cytometer for mHLA-DR expression measurement: a comparison study with reference protocol. *Intensive Care Med Exp* 2017; **5**: 39.

312 Dunning J, Blankley S, Hoang LT, Cox M, Graham CM, James PL *et al.* Progression of whole-blood transcriptional signatures from interferon-induced to neutrophil-associated patterns in severe influenza. *Nat Immunol* 2018; **19**: 625–635.

313 Pinder EM, Rostron AJ, Hellyer TP, Ruchaud-Sparagano M-H, Scott J, Macfarlane JG *et al.* Randomised controlled trial of GM-CSF in critically ill patients with impaired neutrophil phagocytosis. *Thorax* 2018; : thoraxjnl-2017-211323.

314 Matthews KW, Mueller-Ortiz SL, Wetsel RA. Carboxypeptidase N: A pleiotropic regulator of inflammation. *Mol Immunol* 2004; **40**: 785–793.

315 Tuijnenburg P, Lango Allen H, Burns SO, Greene D, Jansen MH, Staples E *et al.* Loss-of-function nuclear factor κB subunit 1 (NFKB1) variants are the most common monogenic cause of common variable immunodeficiency in Europeans. *J Allergy Clin Immunol* 2018; **1**: 1–12.

316 Angulo I, Vadas O, Garcon F, Banham-Hall E, Plagnol V, Leahy TR *et al.* Phosphoinositide 3-Kinase Gene Mutation Predisposes to Respiratory Infection and Airway Damage. *Science (80-)* 2013; **342**: 866–871.

317 Opal SM, Dellinger RP, Vincent J-L, Masur H, Angus DC. The Next Generation of Sepsis Clinical Trial Designs. *Crit Care Med* 2014; **42**: 1714–1721.

318 Fisher CJ, Dhainaut JFA, Opal SM, Pribble JP, Labrecque JF, Catalano MA *et al.* Recombinant Human Interleukin 1 Receptor Antagonist in the Treatment of Patients With Sepsis Syndrome: Results From a Randomized, Double-blind, Placebo-Controlled Trial. *JAMA* 1994; **271**: 1836–1843.

319 Meyer NJ, Reilly JP, Anderson BJ, Palakshappa JA, Jones TK, Dunn TG *et al.* Mortality Benefit of Recombinant Human Interleukin-1 Receptor Antagonist for Sepsis Varies by Initial Interleukin-1 Receptor Antagonist Plasma Concentration. *Crit Care Med* 2018; **46**: 21–28.

320 Mollnes TE, Garred P, Bergseth G. Effect of time, temperature and anticoagulants on in vitro complement activation: consequences for collection and preservation of samples to be examined for complement activation. *Clin Exp Immunol* 1988; **73**: 484–488.

321 GlaxoSmithKline. Argatroban product information sheet. 2009.

322 Beiderlinden M, Brau C, di Grazia S, Wehmeier M, Treschan TA. Argatroban for anticoagulation of a blood salvage system - an ex-vivo study. *BMC Anesthesiol* 2015; **16**: 37.

323 Sarstedt AG & Co. KG. S-Monovette vacutainer collection tubes. Prod. datasheets. 2018.https://www.sarstedt.com/en/products/diagnostic/venous-blood/s-monovetter/ (accessed 4 Nov2018).

324 Santana Silva J, Hajishengallis G, Serezani H, Mcleish KR, Miralda I, Uriarte SM. Multiple Phenotypic Changes Define Neutrophil Priming. *Front Cell Infect Microbiol* 2017; **7**. doi:10.3389/fcimb.2017.00217.

325 Condliffe A, Chilvers E, Haslett C, Dransfield I. Priming differentially regulates neutrophil adhesion molecule expression/function. *Immunology* 1996; **89**: 105–111.

326 Rosales C, Brown EJ. Two mechanisms for IgG Fc-receptor-mediated phagocytosis by human neutrophils. *J Immunol* 1991; **146**: 3937–3944.

327 Hayashi F, Means TK, Luster AD. Toll-like receptors stimulate human neutrophil function. *Blood* 2003; **102**: 2660–2669.

328 Mookerjee RP, Stadlbauer V, Lidder S, Wright GAK, Hodges SJ, Davies NA *et al.* Neutrophil dysfunction in alcoholic hepatitis superimposed on cirrhosis is reversible

and predicts the outcome. *Hepatology* 2007; **46**: 831–840.

329 Jensen IJ, Sjaastad F V, Griffith TS, Badovinac VP. Sepsis-Induced T Cell Immunoparalysis: The Ins and Outs of Impaired T Cell Immunity. *J Immunol* 2018; **200**: 1543–1553.

330 Woodruff TM, Nandakumar KS, Tedesco F. Inhibiting the C5-C5a receptor axis. *Mol Immunol* 2011; **48**: 1631–1642.

331 Wood AJT, Vassallo A, Summers C, Chilvers ER, Conway-Morris A. C5a anaphylatoxin and its role in critical illness-induced organ dysfunction. *Eur J Clin Invest* 2018; **48**: 1–11.

332 Lannutti BJ, Meadows SA, Herman SEM, Kashishian A, Steiner B, Johnson AJ *et al.* CAL-101, a p110δ selective phosphatidylinositol-3-kinase inhibitor for the treatment of B-cell malignancies, inhibits PI3K signaling and cellular viability. *Blood* 2011; **117**: 591–594.

333 Miller BW, Przepiorka D, De Claro RA, Lee K, Nie L, Simpson N *et al.* FDA approval: Idelalisib monotherapy for the treatment of patients with follicular lymphoma and small lymphocytic lymphoma. *Clin Cancer Res* 2015; **21**: 1525–1529.

334 Clinical Trials.gov. NCT03345407: Dose Finding Study of Nemiralisib (GSK2269557) in Subjects With an Acute Moderate or Severe Exacerbation of Chronic Obstructive Pulmonary Disease (COPD). 2017.

335 Clinical Trials.gov. NCT02593539: Safety, Pharmacokinetic (PK) and Pharmacodynamic (PD) Study of Repeat Doses of Inhaled GSK2269557 in Patients With APDS/PASLI. 2015.

336 Naik N, Giannini E, Brouchon L, Boulay F. Internalization and recycling of the C5a anaphylatoxin receptor: evidence that the agonist-mediated internalization is modulated by phosphorylation of the C-terminal domain. *J Cell Sci* 1997; **110**: 2381–2390.

337 Gilbert TL, Bennett TA, Maestas DC, Cimino DF, Prossnitz ER. Internalization of the human N-formyl peptide and C5a chemoattractant receptors occurs via clathrin-independent mechanisms. *Biochemistry* 2001; **40**: 3467–3475.

338 Deniset JF, Kubes P. Neutrophil heterogeneity: Bona fide subsets or polarization states? *J Leukoc Biol* 2018; : 1–10.

339 Sagiv JY, Michaeli J, Assi S, Mishalian I, Kisos H, Levy L *et al.* Phenotypic diversity and plasticity in circulating neutrophil subpopulations in cancer. *Cell Rep* 2015; **10**: 562–574.

340 Hellebrekers P, Hietbrink F, Vrisekoop N, Leenen LPH, Koenderman L. Neutrophil Functional Heterogeneity: Identification of Competitive Phagocytosis. *Front Immunol* 2017; **8**: 1–9.

341 Fliegauf M, Grimbacher B. Nuclear factor κB mutations in human subjects: The devil is in the details. *J Allergy Clin Immunol* 2018; **142**: 1062–1065.

342 Stapels DAC, Ramyar KX, Bischoff M, von Kockritz-Blickwede M, Milder FJ, Ruyken M *et al.* Staphylococcus aureus secretes a unique class of neutrophil serine protease inhibitors. *Proc Natl Acad Sci* 2014; **111**: 13187–13192.

343 Veldkamp KE, Heezius HCJM, Verhoef J, Van Strijp JAG, Van Kessel KPM. Modulation of neutrophil chemokine receptors by Staphylococcus aureus supernate. *Infect Immun* 2000; **68**: 5908–5913.

344 Sabroe I, Williams TJ, Hébert CA, Collins PD. Chemoattractant cross-desensitization of the human neutrophil IL-8 receptor involves receptor internalization and differential

receptor subtype regulation. *J Immunol* 1997; **158**: 1361–1369.

345 Sabroe I, Jones EC, Whyte MKB, Dower SK. Regulation of human neutrophil chemokine receptor expression and function by activation of Toll-like 2 and 4. *Immunology* 2005; **115**: 90–98.

346 Müllberg J, Durie FH, Otten-Evans C, Alderson MR, Rose-John S, Cosman D *et al.* A metalloprotease inhibitor blocks shedding of the IL-6 receptor and the p60 TNF receptor. *J Immunol* 1995; **155**: 5198–5205.

347 Dandekar SN, Park JS, Peng GE, Onuffer JJ, Lim W a, Weiner OD. Actin dynamics rapidly reset chemoattractant receptor sensitivity following adaptation in neutrophils. *Philos Trans R Soc Lond B Biol Sci* 2013; **368**: 20130008.

348 Peng GE, Wilson SR, Weiner OD. A pharmacological cocktail for arresting actin dynamics in living cells. *Mol Biol Cell* 2011; **22**: 3986–3994.

349 Koo BH, Park MY, Jeon OH, Kim DS. Regulatory mechanism of matrix metalloprotease-2 enzymatic activity by factor Xa and thrombin. *J Biol Chem* 2009; **284**: 23375–23385.

350 Lohse MJ, Hein P, Hoffmann C, Nikolaev VO, Vilardaga JP, Bunemann M. Kinetics of G-protein-coupled receptor signals in intact cells. *Br J Pharmacol* 2008; **153**: 125–132.

351 Luerman G, Uriarte S, Rane M, McLeish K. Application of proteomics to neutrophil biology. *J Proteomics* 2010; **73**: 552–561.

352 Tak T, Wijten P, Heeres M, Pickkers P, Scholten A, Heck AJR *et al.* Human CD62L(dim) Neutrophils Identified as a Separate Subset by Proteome Profiling and In Vivo Pulse-Chase Labelling. *Blood* 2017; **129**: blood-2016-07-727669.

353 Muschter S, Berthold T, Bhardwaj G, Hammer E, Dhople VM, Wesche J *et al.* Mass spectrometric phosphoproteome analysis of small-sized samples of human neutrophils. *Clin Chim Acta* 2015; **451**: 199–207.

354 Thermo Fisher Scientific. High-Select Fe-NTA Phosphopeptide Enrichment Kit Product Information Sheet. 2016.

355 Dunn J, Reid G, Bruening M. Techniques for phosphopeptide enrichment prior to analysis by mass spectrometry. *Mass Spectrom Rev* 2010; **29**: 29–54.

356 Hoenderdos K, Lodge KM, Hirst RA, Chen C, Palazzo SGC, Emerenciana A *et al.* Hypoxia upregulates neutrophil degranulation and potential for tissue injury. 2016; : 1030–1038.

357 Bertolotto M, Contini P, Ottonello L, Pende A, Dallegri F, Montecucco F. Neutrophil migration towards C5a and CXCL8 is prevented by non-steroidal anti-inflammatory drugs via inhibition of different pathways. *Br J Pharmacol* 2014; **171**: 3376–3393.

358 Fabregat A, Jupe S, Matthews L, Sidiropoulos K, Gillespie M, Garapati P *et al.* The Reactome Pathway Knowledgebase. *Nucleic Acids Res* 2018; **46**: D649–D655.

359 Sorkin A, Von Zastrow M. Endocytosis and signalling: Intertwining molecular networks. *Nat Rev Mol Cell Biol* 2009; **10**: 609–622.

360 Tak T, Rygiel TP, Karnam G, Bastian OW, Boon L, Viveen M *et al.* Neutrophil mediated suppression of influenza-induced pathology requires CD11b/CD18 (MAC-1). *Am J Respir Cell Mol Biol* 2017; **58**: 492–499.

361 McLeish KR, Merchant ML, Klein JB, Ward RA. Technical note: proteomic approaches to fundamental questions about neutrophil biology. *J Leukoc Biol* 2013; **94**: 683–692.

362 Hecker M, Mäder U, Völker U. From the genome sequence via the proteome to cell

physiology – Pathoproteomics and pathophysiology of Staphylococcus aureus. *Int J Med Microbiol* 2018; **308**: 545–557.

363 Juss JK, House D, Amour A, Begg M, Herre J, Storisteanu DML *et al.* Acute respiratory distress syndrome neutrophils have a distinct phenotype and are resistant to phosphoinositide 3-kinase inhibition. *Am J Respir Crit Care Med* 2016; **194**: 961–973.

364 Rorvig S, Ostergaard O, Heegaard NHH, Borregaard N. Proteome profiling of human neutrophil granule subsets, secretory vesicles, and cell membrane: correlation with transcriptome profiling of neutrophil precursors. *J Leukoc Biol* 2013; **94**: 711–721.

365 Kobayashi SD, Voyich JM, Buhl CL, Stahl RM, DeLeo FR. Global changes in gene expression by human polymorphonuclear leukocytes during receptor-mediated phagocytosis: cell fate is regulated at the level of gene expression. *Proc Natl Acad Sci* 2002; **99**: 6901–6906.

366 Fessler MB, Malcolm KC, Duncan MW, Scott Worthen G. A genomic and proteomic analysis of activation of the human neutrophil by lipopolysaccharide and its mediation by p38 mitogen-activated protein kinase. *J Biol Chem* 2002; **277**: 31291–31302.

367 Bateman A, Martin MJ, O'Donovan C, Magrane M, Alpi E, Antunes R *et al.* UniProt: The universal protein knowledgebase. *Nucleic Acids Res* 2017; **45**: D158–D169.

368 Weekes MP, Tomasec P, Huttlin EL, Fielding CA, Nusinow D, Stanton RJ *et al.* Quantitative temporal viromics: An approach to investigate host-pathogen interaction. *Cell* 2014; **157**: 1460–1472.

369 Hawkins PT, Stephens LR. PI3K signalling in inflammation. *Biochim Biophys Acta - Mol Cell Biol Lipids* 2015; **1851**: 882–897.

370 Kobayashi SD, Braughton KR, Whitney AR, Voyich JM, Schwan TG, Musser JM *et al.* Bacterial pathogens modulate an apoptosis differentiation program in human neutrophils. *Proc Natl Acad Sci U S A* 2003; **100**: 10948–10953.

371 Khan MA, Palaniyar N. Transcriptional firing helps to drive NETosis. *Sci Rep* 2017; **7**: 1–16.

372 Lundqvist-Gustafsson H, Norrman S, Nilsson J, Wilsson A. Involvement of p38-mitogen-activated protein kinase in Staphylococcus aureus-induced neutrophil apoptosis. *J Leukoc Biol* 2001; **70**: 642–8.

373 Borovik L, Modaff P, Waterham HR, Krentz AD, Pauli RM. Pelger-huet anomaly and a mild skeletal phenotype secondary to mutations in LBR. *Am J Med Genet Part A* 2013; **161**: 2066–2073.

374 Gravemann S, Schnipper N, Meyer H, Vaya A, Nowaczyk MJ, Rajab A *et al.* Dosage effect of zero to three functional LBR-genes in vivo and in vitro. *Nucleus* 2010; **1**: 179–189.

375 Hase M, Volker C. Direct Interaction with Nup153 Mediates Binding of Tpr to the Periphery of the Nuclear Pore Complex. *Mol Biol Cell2* 2003; **14**: 1923–1940.

376 Feng D, Nagy JA, Pyne K, Dvorak HF, Dvorak AM. Neutrophils Emigrate from Venules by a Transendothelial Cell Pathway in Response to FMLP. *J Exp Med* 1998; **187**: 903–915.

377 Hong C-W. Current Understanding in Neutrophil Differentiation and Heterogeneity. *Immune Netw* 2017; **17**: 298.

378 Blackwood RA, Hartiala KT, Kwoh EE, Transue AT, Brower RC. Unidirectional heterologous receptor desensitization between both the fMLP and C5a receptor and the IL-8 receptor. *J Leukoc Biol* 1996; **60**: 88–93.

379 Bago R, Malik N, Munson MJ, Prescott AR, Davies P, Sommer E *et al.* Characterization of VPS34-IN1 , a selective inhibitor of Vps34 , reveals that the phosphatidylinositol 3-phosphate-binding SGK3 protein kinase is a downstream target of class III phosphoinositide 3-kinase. *Biochem J* 2014; **463**: 413–427.

380 Bilanges B, Vanhaesebroeck B. Cinderella finds her shoe: the first Vps34 inhibitor uncovers a new PI3K – AGC protein kinase connection. *Biochem J* 2014; **464**: e7-10.

381 Anderson KE, Boyle KB, Davidson K, Chessa TAM, Kulkarni S, Jarvis GE *et al.* CD18-dependent activation of the neutrophil NADPH oxidase during phagocytosis of Escherichia coli or Staphylococcus aureus is regulated by class III but not class I or II PI3Ks. *Blood* 2008; **112**: 5202–5211.

382 Anderson KE, Chessa TAM, Davidson K, Henderson RB, Walker S, Tolmachova T *et al.* PtdIns3P and Rac direct the assembly of the NADPH oxidase on a novel, pre-phagosomal compartment during FcR-mediated phagocytosis in primary mouse neutrophils. *Blood* 2010; **116**: 4978–4989.

383 Sabroe I, Jones EC, Usher LR, Whyte MKB, Dower SK. Toll-Like Receptor (TLR)2 and TLR4 in Human Peripheral Blood Granulocytes: A Critical Role for Monocytes in Leukocyte Lipopolysaccharide Responses. *J Immunol* 2002; **168**: 4701–4710.

384 Skjeflo EW, Sagatun C, Dybwik K, Aam S, Urving SH, Nunn MA *et al.* Combined inhibition of complement and CD14 improved outcome in porcine polymicrobial sepsis. *Crit Care* 2015; **19**: 415.

385 Sun D, Zhang M, Liu G, Wu H, Zhu X, Zhou H *et al.* Real-time imaging of interactions of neutrophils with Cryptococcus neoformans : a crucial role of C5a-C5aR signaling. *Infect Immun* 2015; **84**: IAI.01197-15.

386 Huey R, Hugli. Characterization of a C5a receptor on human polymorphonuclear leukocytes (PMN). *J Immunol* 1985; **135**: 2063–2068.

387 Hsu WC, Yang FC, Lin CH, Hsieh SL, Chen NJ. C5L2 is required for C5a-triggered receptor internalization and ERK signaling. *Cell Signal* 2014; **26**: 1409–1419.

388 Paczkowski NJ, Finch AM, Whitmore JB, Short AJ, Wong AK, Monk PN *et al.* Pharmacological characterization of antagonists of the C5a receptor. *Br J Pharmacol* 1999; **128**: 1461–1466.

389 Ifrx INVN. InflaRx receives IND acceptance to proceed with a Phase IIb Trial with lead candidate IFX-1 in Hidradenitis Suppurativa. 2018.

390 Dutta D, Donaldson JG. Search for inhibitors of endocytosis; intended specificity and unintended consequences. *Cell Logist* 2012; **2**: 203–208.

391 Foster TJ. The *Staphylococcus aureus* 'superbug'. *J Clin Invest* 2004; **114**: 1693–96.

392 Vizcaíno JA, Deutsch EW, Wang R, Csordas A, Reisinger F, Ríos D *et al.* ProteomeXchange provides globally coordinated proteomics data submission and dissemination. *Nat Biotechnol* 2014; **32**: 223–226.

393 Deutsch EW, Csordas A, Sun Z, Jarnuczak A, Perez-Riverol Y, Ternent T *et al.* The ProteomeXchange consortium in 2017: Supporting the cultural change in proteomics public data deposition. *Nucleic Acids Res* 2017; **45**: D1100–D1106.

394 Richter E, Harms M, Ventz K, Nölker R, Fraunholz MJ, Mostertz J *et al.* Quantitative Proteomics Reveals the Dynamics of Protein Phosphorylation in Human Bronchial Epithelial Cells during Internalization, Phagosomal Escape, and Intracellular Replication of Staphylococcus aureus. *J Proteome Res* 2016; **15**: 4369–4386.

395 Ersing I, Nobre L, Wang LW, Gygi SP, Weekes MP, Gewurz BE *et al.* Resource A Temporal Proteomic Map of Epstein-Barr Virus Lytic Replication in B Cells Resource A

Temporal Proteomic Map of Epstein-Barr Virus Lytic Replication in B Cells. *CellReports* 2017; **19**: 1479–1493.

396 Greenwood EJD, Matheson NJ, Wals K, van den Boomen DJH, Antrobus R, Williamson JC *et al.* Temporal proteomic analysis of HIV infection reveals remodelling of the host phosphoproteome by lentiviral Vif variants. *Elife* 2016; **5**: 1–30.

397 Jaber N, Mohd-naim N, Wang Z, Deleon JL, Kim S, Zhong H *et al.* Vps34 regulates Rab7 and late endocytic trafficking through recruitment of the GTPase-activating protein Armus. 2016; : 4424–4435.

398 Yadav SK, Feigelson SW, Roncato F, Antman-Passig M, Shefi O, Lammerding J *et al.* Elevated nuclear lamin A is permissive for granulocyte transendothelial migration but not for motility through collagen I barriers. *J Leukoc Biol* 2018; : 1–13.

399 Wisler JW, Rockman HA, Lefkowitz RJ. Biased G protein-coupled receptor signaling: Changing the paradigm of drug discovery. *Circulation* 2018; **137**: 2315–2317.

400 Smith JS, Lefkowitz RJ, Rajagopal S. Biased signalling: From simple switches to allosteric microprocessors. *Nat Rev Drug Discov* 2018; **17**: 243–260.

401 Jamur M, Oliver C. Permeabilization of Cell Membranes. In: Oliver C, Jamur MC (eds). *Immunocytochemical Methods and Protocols*. Humana Press: New York, USA, 2010, pp 63–66.

402 Kielkowska A, Niewczas I, Anderson KE, Durrant TN, Clark J, Stephens LR *et al.* A new approach to measuring phosphoinositides in cells by mass spectrometry. *Adv Biol Regul* 2014; **54**: 131–141.

403 Walton RM. Validation of laboratory tests and methods. *Semin Avian Exot Pet Med* 2001; **10**: 59–65.

404 van der Poll T. Future of sepsis therapies. *Crit Care* 2016; **20**: 106.

405 Calfee CS, Delucchi K, Parsons PE, Thompson BT, Ware LB, Matthay MA. Subphenotypes in acute respiratory distress syndrome: Latent class analysis of data from two randomised controlled trials. *Lancet Respir Med* 2014; **2**: 611–620.

406 Famous KR, Delucchi K, Ware LB, Kangelaris KN, Liu KD, Thompson BT *et al.* Acute respiratory distress syndrome subphenotypes respond differently to randomized fluid management strategy. *Am J Respir Crit Care Med* 2017; **195**: 331–338.

407 Breitman TR, Selonick SE, Collins SJ. Induction of differentiation of the human promyelocytic leukemia cell line (HL-60) by retinoic acid. *Proc Natl Acad Sci* 1980; **77**: 2936–2940.

Chapter IX: Appendices

1. Neutrophil isolation from venous blood

Chilvers laboratory protocol

1.1. Materials

- Place following into warmer bath at 37°C
    - 6% dextran
    - 0.9% saline - also keep one Falcon tube of saline at 4°C for diluting Percoll
    - PBS +/+ (with Ca^{2+}/Mg^{2+})
    - PBS -/- (without Ca^{2+}/Mg^{2+})
- Prepare anticoagulated Falcon tubes
- Set up 50 mL BD Falcon polypropylene tubes- 40 mL blood per Falcon tube
- Put 3.8% sodium citrate (vials in fridge) into Falcon tubes
    - Use 1 mL citrate/10mL blood = 4 mL citrate/40 mL blood
- Prepare bleach solution
    - 2 bleach tablets + water

1.2. Procedure

- Collect blood with 19G butterfly and 50 mL syringes (40 mL per syringe)
- Add 40mL blood down the side of each Falcon tube; invert gently to mix
- Remember to spray each item before placing in hood
- 1^{st} spin programme 1 (20 min, 300 x g)- separates into:
- Supernatant (S/N) = platelet rich plasma (PRP), pellet = white and red cells
- Remove (pipette/Pasteur) S/N (PRP) into fresh 50 mL Falcon tubes
- Use to make platelet poor plasma (PPP) and autologous serum
- Sediment remaining cells
- Add 6% dextran down sides of tubes- add 2.5 mL dextran /10 mL cell pellet
- Then add warm saline to make up volume to 50 mL
- Mix by gently rolling tubes several times to re-suspend cells
    - Leave with caps loosely on (to let air in) for 25-40 min at room temp
- Upper layer - white cells, bottom layer = red cells
- Prepare Percoll gradients whilst waiting for sedimentation
- Once Percoll prepared, place in fridge whilst remainder of sedimentation occurring.
- Add 10 mL PRP into sterile glass vial
- Then add 220 µL of 10 mM $CaCl_2$ (do not add $CaCl_2$ first) => vortex
- Place in CO_2 incubator, leave for 30-60 min with lid of vial loose
    - Then store at 4°C or freeze
- Use remaining PRP- 2nd spin programme 2 (20 min, 1400 x g) - separates into:
    a. S/N = PPP, pellet = platelets
- Remove (pipette/Pasteur) S/N (PPP) into fresh 50 mL Falcon tubes; discard pellet (platelets)
- Sedimented cells: upper layer - white cells, bottom layer = red cells
- Remove (pipette/Pasteur) upper layer (white cells) into fresh Falcon tubes
- Discard bottom layer (red cells)
- Upper layer (white cells): 3rd spin programme 3 (5 min, 260 x g)

- (Discard S/N, use cell pellet for below)
- Make one set of gradients for each individual tube
- Make 90% Percoll
- mL Percoll + 0.5 mL Cold 0.9% saline => Vortex to mix
- Make gradients - add Percoll and PPP => Vortex
- Get white cells after 3rd spin
    - Discard (pour carefully) S/N into waste container with bleach
    - Resuspend remaining pellet by tapping tube gently
    - Pool maximum of 2 tubes of cell pellets together into 15 mL Falcon tube (use glass or plastic Pasteur not Gilson)
    - Add PPP to make up volume to 2 mL per tube of cells ("wash" old tube with required PPP then pipette into small tube)
- Underlay Percoll gradients: 42% first, then 51%
    - Use glass Pasteur with Pipette boy
    - Take all of Percoll up glass Pasteur- avoid air bubbles
    - Slide Pasteur down side of cell tube to the bottom of tube, then slowly release Percoll- avoid air bubbles
- Transfer tube carefully to centrifuge
- 4th spin programme 4 (14 min, 150 x g, 1/ \0) - layers:
    - Top (PPP/42%) interface: mononuclear cells (PBMCs)
    - Next (42%/51%) interface: polymorphonuclear cells (PMNs)
- Collect PMNs
    - Remove PPP, mononuclear cells and 42% with P1000 Gilson/Pasteur - discard
    - Collect PMNs with fresh Pasteur- put into fresh 50 mL Falcon tube
    - Discard 51% and red cell pellet
- Add remaining PPP to PMN, mix
    a. Discard S/N
    - Resuspend cells then make up volume to 50 mL with PBS -/-
    - Use these cells in PBS -/- for cytospin and haemocytometer
- From this point onwards use Cell Saver (wide bore) pipette tips
- Breathe onto haemocytometer to moisten
- Slide cover slip over until Newton's refraction (rainbow-like) rings appear
- Fill each of the two chambers with 10 µL of cells suspend in PBS -/-
- Calculate total number of cells
- Counting area of 5 x 5 large squares with total area = 1mm^2
- Depth of chamber = 0.1 mm
- Number of cells per mL = Haemocytometer count x 10000
- Total number of cells in 50 mL - Haemocytometer count x 10000 x 50
- Calculate volume of PBS +/+ required to make concentration of 5 million cells
- Label slides with pencil
- Set up into clip (bottom to top): slide, filter paper smooth side facing down towards slide, funnel
- Add 100 µL of cells suspended in PBS -/- into funnel (use Cell Saver tips)
- Spin in Cytospin3 machine: programme 1 (300 x rpm, 3 min, high acceleration)
- Remove slides and air dry for 10-15 min
- Stain slides

42%:	[0.8 mL + 40 µL] of 90% Percoll [1.0 mL + 160 µL] of PPP
51%:	[1.0 mL + 20 Ml] of 90% Percoll [0.9 mL + 80 µL] of PPP

Dimensions	Area	Volume at 0.1 mm depth
1 x 1 mm	1 mm^2	100 nL
0.25 x 0.25 mm	0.0625 mm^2	6.25 nL
0.25 x 0.20 mm	0.05 mm^2	5 nL
0.20 x 0.20 mm	0.04 mm^2	4 nL
0.05 x 0.05 mm	0.0025 mm^2	0.25 nL

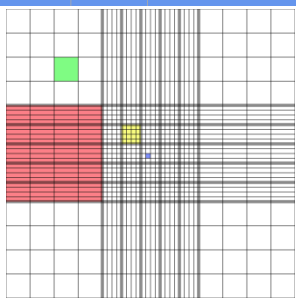

- 4 min in methanol => 1 min in orange stain => 3 min in blue stain
- Rinse with water then air dry
- When dry, mount with 1 drop of DPX then add cover slip
- Count cells under microscope for differential count
- Count 200 cells- count neutrophils, eosinophils, PBMCs, RBCs
- Cells in PBS -/-: 5th spin programme 5 (5 min, 256 x g)
    - Discard S/N
- Resuspend cells then make up volume to 50 mL with PBS +/+
- Cells now in PBS +/+: 5th spin programme 5 (5 min, 256 x g)
    - Discard S/N
- Resuspend cells
- Add volume of PBS +/+ required to make up a concentration of 5 million cells / mL
    - Cells now ready

2. PMN phagocytosis assay

Author: Alex Wood. Last revised October 2016.

2.1. Materials

- pHrodo Bioparticles (Life Technologies)
    - Red *E. coli* : P35361 (2 mg)
    - Green *E. coli*: P35366 (2mg)
    - Green zymosan: P35365 (1mg)
    - Ensure to protect Bioparticles from light at all times – work with lights off in hood + foil covering if exposed to ambient light
    - NOTE BATCH NUMBER USED IN EACH EXPERIMENT
- RPMI 1640 + 10 mM HEPES
- 2mL round-bottom Eppendorfs
- Effectors e.g.:
    - Cytochalasin D (Sigma C2618-200UL) made up to
    - C5a (R&D Systems 2037-C5)
- FACS tubes
- CellFix mix (1 :40) = 1 mL CellFix + 9 mL dH_2O + 30 mL PBS -/-
    - Keep on ice until used
- Freshly prepared neutrophils and autologous serum
    - $5x10^6$/mL in RPMI 1640 with 10 % autologous serum by volume

2.2. Procedure

- Setup and label Eppendorfs with relevant conditions. Examples below. Always include 1 and 2.
    - Neutrophils + pHrodo cold (negative)
    - Opsonised pHrodo + neutrophils (positive control)
    - pHrodo alone in HCl solution (pH = 4 as positive control)
- Opsonisation
    - Resuspend pHrodo in 2 mL phenol red-free IMDM (0.5 mg/mL zymosan, 1 mg/mL E.coli/S.aureus). Aliquot 50 uL into Eppys and store at -20 protected from light.
    - Vortex for 1 minute. Pipette required volume for experiment into separate Eppendorf. Store stock and protect from light.
    - Sonicate in Eppendorf for 10 minutes
    - Opsonise with 50 % autologous serum for 30 minutes at 37 °C in shaker/incubator
- Preparing neutrophils
    - Whilst opsonisation occurring, can incubate neutrophils with effector compounds
    - Resuspend 10^6 purified neutrophils (200 µL) in 2 mL Eppendorfs
    - Add effector compounds at relevant concentrations (e.g. 20 µL will give 1:10 dilution)
    - Place in thermomixer at 37 °C for 30 minutes
- Phagocytosis
    - Final concentration of pHrodo *S. aureus* needs to be 3 µg/mL
    - Add 0.6 µL unopsonised (neat) or 2.8 uL opsonised (diluted 1:2 in serum) pHrodo bioparticles to neutrophils as appropriate
    - Place tubes back in thermomixer at 37 °C for 30 minutes
- Quenching and transfer to FACS tubes
    - Add 400 µL cold CellFix mix to quench reaction and fix cells

    - Transfer solutions to labelled FACS tubes and place on ice to prevent further phagocytosis. Take care to resuspend cells and pipette 3 times to ensure cells not lost
    - Take FACS tubes for flow cytometry on ice
- Flow cytometry
    - Run controls first to establish stopping gates for PMNs

3. Whole blood assay of neutrophil function

Author: Alex Wood. Last revised June 2017.

3.1. Materials

- Whole blood collected in Argatroban anticoagulant 150 µg/mL. Stock tubes at -70 ˚C, 200 uL of 1500 µg/mL diluted to 2 mL with fresh blood
    - 10 mg Argatroban powder dissolved in 200 uL DMSO (vortex vigorously until dissolved)
    - Dilute the 200 uL volume to 6600 uL (add 6400 uL PBS -/-)
    - Gives concentration of 1500 µg/mL. Aliquot 200 uL aliquots into 2 mL Eppendorfs and store at -70. I then add 1.8 mL blood to 200 uL argatroban aliquot to give final concentration of 150 µg/mL.
- RPMI 1640 (phenol free) with 10 mM HEPES
- PBS -/- vehicle control
- 2 mL sterile Eppendorfs
- Combined ROS/phagocytosis indicator
    - pHrodo red Bioparticles @ 1 mg/mL for *S. aureus/E. coli* or 0.5 mg/mL for zymosan in PBS -/- (stock).
    - DHR ROS probe (stored in DMSO in -70). Dilute 1:100 in PBS -/- on day.
        - Final concentration in-assay 15 µg/mL pHrodo and 3 µM DHR
        - Prepare working solution of 150 µg/mL pHrodo and 30 µM DHR (10 X and will be diluted by 10 in-assay) and vortex.
        - These concentrations should be calculated by titrating pHrodo required for given experimental system/time point. These are appropriate for 30 minutes phagocytosis.
- Antibodies/fluorophores
    - CD16-PacBlue Clone 3G8 302021 Biolegend (0.5 uL per 100 uL stain)
    - C5aR1 PerCP/Cy5.5 S5/1 Biolegend (1 uL per 100 uL stain)

3.2. Procedure

- Whole blood (WB) collected into argatroban via butterfly.
- Prepare 96-well plate wells in triplicate – final volume **100 uL**. Include cold/compensation controls as appropriate
    - **50 uL** anticoagulated blood pre-treated as appropriate
- Add **10 uL** of 10 X phagocytosis/ROS indicator so final concentrations are 15 µg/mL and 3 µM respectively.
- Make volume up to 100 uL with RPMI 1640 with 10 mM HEPES (i.e. add **40 µL**) using multichannel pipette and pipette up and down x 5 to homogenise.
- Allow 30 minutes phagocytosis time in 5 % CO_2 and 37 ˚C in incubator.
- At end of phagocytosis time point place plate onto ice.
- Homogenise by pipetting up and down x 5, take 5 uL from each well and add to FACS tube with 100 uL stain mix. Can pool triplicates at this stage if required.
- Stain on ice in dark for 30 minutes
- Dilute final volume in each tube to 4 mL (add 3.9 mL)
- Keep on ice until analysis on Attune Nxt. Settings saved on machine.

4. Western blotting of purified human neutrophil proteins

Original by Katharine Lodge 2016, last revised August 2018 by Alex Wood.

4.1. Materials

- 1 x 2 L conical flasks, 1 x 2 L Duran bottle, 2 x 200 mL Duran bottles, 1 x 1 L measuring cylinder
- If making own gels:
    - Protogel, resolving buffer (4X) and stacking buffer
    - dH_2O
    - 10 % ammonium persulfate (APS)
    - TEMED
    - 10 or 12 well combs, 1.5 mm thickness
    - Glass plates, gel setting stands + holders
    - Ethanol
- If using pre-cast gels
    - Pre-cast gel at appropriate SDS percentage
    - Appropriate gel running buffer
- Running gels
    - Running buffer (diluted from 10 X with dH2O)
    - Running tank + lid (rounded Bio-Rad tanks) + power pack
    - Gel casette and blank gel if only running 1 sample gel (need 2 in total for current to travel through casette)
- Sample preparation (for reduced proteins)
    - 5 X Laemmli's buffer, stored in 2nd drawer Mark Ormiston's -20 in main lab, made up by Paul Upton.
    - Beta mercaptoethanol (BME, reducing agent) stored in Cat 1 lab, door of Dong's 4 degree fridge
    - Lysis buffer used to make neutrophil lysates (see protocol AW3). Currently this is simply 0.5 % SDS and 0.1 % TEAB (with 1 X HALT protease inhibitor cocktail for lysate, not required here).
    - 1.5 mL or 0.6 mL eppendorfs and pre-heat thermomixer to 95 C
    - Long-tipped gel loading pipettes
- Gel transfer to PVDF membrane
    - PVDF membrane x 1 for each blot, cut to 8 cm x 6.5 cm
    - Blotting paper x 4 for each blot, cut to 8.5 cm x 7.0 cm
    - Sandwich x 1 and sponges x 2 for each blot
    - Clean flat tub for preparing sandwiches
    - Methanol (in solvents cupboard)
    - Transfer buffer: prepare first thing and put in -20 to cool down in morning; will freeze if left in -20 for long periods. If prepared in bulk, store at 4C.
        - 3.03 g Trizma base
        - 14.4 g glycine
        - 200 mL methanol
        - 800 mL dH_2O
    - Running tank + lid (square lid) + power pack
    - Ice box full of wet ice and -20 ice pack from -20 freezer top shelf outside Cat 1 lab
- Washes, blocking and antibody staining
    - 1 L 10 X Tris buffered saline (TBS)
        - 24.2 g Trizma base
        - 80 g NaCl
        - Adjust pH to 7.6 with HCl

- TBS with 0.1 % Tween (TBS-T)
  - Make 1 L X TBS by diluting 100 mL 10 X TBS with 900 mL dH2O
  - Add 1 mL Tween 20 to 1 L. Will need to cut pipette tip as viscous
- Small plastic tubs (cleaned with ethanol)
- 5 % milk in TBS-T for blocking and antibody dilutions/staining: use 5 % milk as default unless specified by antibody manufacturer. Some use 5 % BSA instead.
  - 5 g non-fat milk diluted in 100 mL TBS-T
  - Beware that this can take time to dissolve fully, store at 4C when not in use
- Antibodies
  - Often raised in mouse or rabbit. Try to choose validated Abs, preferably in primary human neutrophils, though this is rare!
    - Usually diluted 1:1000 with blocking buffer
    - Ideally purchase a protein standard known to work with antibody from same manufacturer to test
  - Ensure we have relevant secondary (HRP-conjugated)
    - Usually diluted 1:5000 with blocking buffer
    - Goat anti-rabbit-HRP conjugate in blue secondary antibody box in small lab fridge

- Developing
  - ECL kit (stored in 4 degree lab fridge where antibodies kept
  - Xray film and cassette
  - Bin liner
  - Access to dark room and film developer (down corridor opposite Dougan lab)

4.2. Methods

- Preparing and reducing samples for loading
  - Perform Bradford protein assay (Protocol AW.4) and calculate volume of sample required to add 25 ug of protein to each well.
  - Dilute sample with lysis buffer to achieve 1 ug/uL concentration
  - Take 5 X Laemmli's buffer, add 50 uL BME (do this in fume hood in Cat 1 lab) and vortex
  - Add 20 uL sample to 5 uL Laemmli/BME.
  - Make spare/blank well mixture (for 8 wells) by adding 160 uL lysis buffer to 40 uL Laemmli/BME
  - Boil samples for 10 minutes at 95 C rotating at 300 rpm; be careful after boiling as lids can pop off
  - Spin down briefly to minimise sample loss
  - Setup gels and/or spacer in cassette, load into tank, pour running buffer into cassette and ensure no leaks, then fill tank up to relevant mark for number of gels
  - Load 10 uL PageRuler Plus ladder into first well (5 uL for pre-cast gels). Load from right to left, as this will lead to the ladder being on the left of the PVDF membrane.
  - Load 25 uL sample into each well. Space wells/ladders with a blank well in-between if numbers permit. Load all wells from right to left with sample or blank well mixture (otherwise gel will deform)
  - MAKE A NOTE OF THE CONTENTS OF EACH WELL
  - Close lid, connecting red electrode to red electrode, connect to powerpack (red to red) and run at 100 V for 10-15 minutes (stacking).
  - Transition to resolving once ladder starts to separate: 150 V for approximately 60 minutes, check at 30 and 45 minutes to ensure still running and

appropriate pace. Voltage can be adjusted depending on time available and protein of interest.
    - If not already prepared and doing Western, prepare transfer buffer now and keep in -20
    - Submerge PVDF membrane in methanol
    - Stop running when protein ladder has reached close to bottom of gel.
    - This gel can be stained using a Coomassie stain or silver stain, or transferred to PVDF/nitrocellulose membrane for Western blotting
- Transfer to PVDF membrane for western blotting
    - Prepare items specified in materials on bench (transfer buffer should be cold by now)
    - Transfer tank in ice box surrounded by ice (needs to stay cold during transfer)
    - Pour transfer buffer into tub, enough to submerge sandwich
    - Setup sandwich as follows:
    - Black side on right, sponge, 2 pieces of blotting paper
    - White on left, sponge, 2 pieces of blotting paper
    - Remove gel cassette from electrophoresis tub
    - Break seal with green gel tool, remove stacking gel and discard
    - Carefully manipulate gel onto right side (black) so that it sits on top of blotting paper
    - Using forceps, place PVDF membrane (soaked in methanol) on top of gel, ensuring all edges are covered and that there are no bubbles between PVDF and gel
    - Place left-sided blotting papers and sponge on top, close sandwich carefully making sure not to dislodge gel/membrane
    - Place sandwich in tank WITH BLACK SIDE OF SANDWICH FACING BLACK PART OF TANK
    - Place -20 ice pack in gap on other side of tank
    - Fill tank with remaining transfer buffer right to the brim
    - Place lid, connect to powerpack and run 75 V for 2 hours

- Blocking and primary antibody staining
    - Prepare TBS-T and 5 % milk/BSA solutions as in materials
    - Take sandwich out of transfer tank, carefully peel membrane off gel without dislodging and check if ladder has transferred. If not can replace and re-run
    - Place PVDF protein side up in small plastic tub. Discard gel and blotting paper
    - Add 15 mL TBS-T to tub, wash gel briefly on bench.
    - Discard TBS-T and add 5 % milk to block non-specific binding. Incubate for one hour on rocker, at room temperature
    - Prepare antibodies whilst this is occurring
    - Need 10 mL antibody solution minimal per tub/membrane
    - Remove blocking solution, add 10 mL antibody solution to each tub
    - Incubate rocking gently at 4C overnight

- Method 5: washes and secondary antibody staining
    - Remove primary antibody mixture, can keep this for future staining if necessary. Store as directed by antibody manufacturer
    - Add 15 mL TBS-T, wash on rocker at room temp for 5 minutes. **Repeat twice (3 washes in total)**
    - Prepare 10 mL secondary antibody
    - Dilute 1:5000 in 5 % milk or BSA as appropriate (add 2 uL to 10 mL)
    - Add 10 mL secondary antibody and incubate for one hour at RT on rocker
    - Wash x 3 as previously
    - Can prepare ECL solution during this time

    - Add 500 uL solution A to 500 uL solution B in 2 mL Eppendorf, vortex and protect from light

- ECL Chemiluminescence and developing blot
    - Prepare the necessary materials as above. Cut bin liner to appropriate size
    - Prepare clean flat surface on bench (gladwrap or same tub used for transfer)
    - After final wash, hold membrane with forceps, wick excess TBS-T off onto paper towel, place PVDF protein side up and add 1 mL ECL mix on top of it
    - Flip PVDF over and ensure fully coated with ECL mix. Incubate for 5 minutes protected from light
    - Wick excess ECL off, place inside bin liner close and tape in place ensuring no bubbles, close cassette
    - Take cassette and x-ray film to dark room, ensure door closed and only infrared lights on
    - Remove film, bend one corner to allow orientation and place over membrane in cassette, ensuring reproducible placement
    - Expose for 1 minute initially as test
    - Develop by feeding film into developer
    - Adjust exposure time based on band intensity from (8)
    - Can store membranes in PBS -/- in fridge for later analysis (2-3 days max)
    - Can do densitometry in Image-J for quantification

- Stripping and re-probing (optional)
    - After development of blot, can strip and re-probe using different primar/secondary antibody
    - Wash PVDF briefly in PBS -/-
    - Add 15 mL stripping buffer (from bottle above Ben's bench) in small tub and incubate rocking gently at RT for 10 minutes MAX (longer incubations risk stripping more protein from PVDF)
    - You can ensure all antibody has been stripped by re-ECLing the PVDF at this stage
    - Then block and re-probe as previous

4.3. Notes

- This protocol has been adapted as stated and modified according to protocol from Cell Signalling Technologies (worth reading anyway): https://media.cellsignal.com/www/pdfs/resources/white-papers/guide-to-successful-wb.pdf
- This is a long and complex protocol but will become easier with practice. A lot of steps have been listed for the benefit of the absolute beginner
- Be very careful not to tear the gels or membranes. Gels are considerably more fragile, and the 12 % pre-cast gels are more fragile again.
- Try to look ahead and prepare buffers/samples/equipment as this will greatly speed the process

5. Publications and presentations arising from this thesis

5.1. Publications

Wood AJT, Vassallo A, Summers C, Chilvers ER, Conway Morris A. C5a anaphylatoxin and its role in critical illness-induced organ dysfunction. European Journal of Clinical Investigation

Vassallo A, Wood AJT, Subburayalu J, Summers C, Chilvers ER. The counter-intuitive role of the neutrophil in the acute respiratory distress syndrome. British Medical Bulletin (manuscript under review October 2018).

Wood AJT, Vassallo A, Okkenhaug K, Scott J, Simpson J, Summers C, Chilvers ER, Conway Morris A. Complement protein C5a induces prolonged neutrophil dysfunction in a clinically relevant model of human bacteraemia. Thorax. 2017: 72 (Suppl. 3): A3

5.2. Conference presentations

2018 Understanding mechanisms of complement-induced neutrophil dysfunction: insights from whole blood functional assays and phosphoproteomics profiling (poster). Neutrophil 2018, Quebec City.

2017 A novel, rapid assay for assessment of multiple neutrophil functions in human whole blood (oral presentation). Young Investigator Session (winner), British Thoracic Society, London.

2017 Assessment of neutrophil functions in human whole blood (poster). Intensive Care State of the Art, Liverpool.

2016 C5a impairs neutrophil phagocytosis of clinically relevant pathogens (poster). Academy of Medical Sciences, London.

2016 Morpho-rheological characterisation of neutrophils (poster). Cambridge University Department of Medicine Research Day, Cambridge.